

Science Research Council

RHEL / R 270

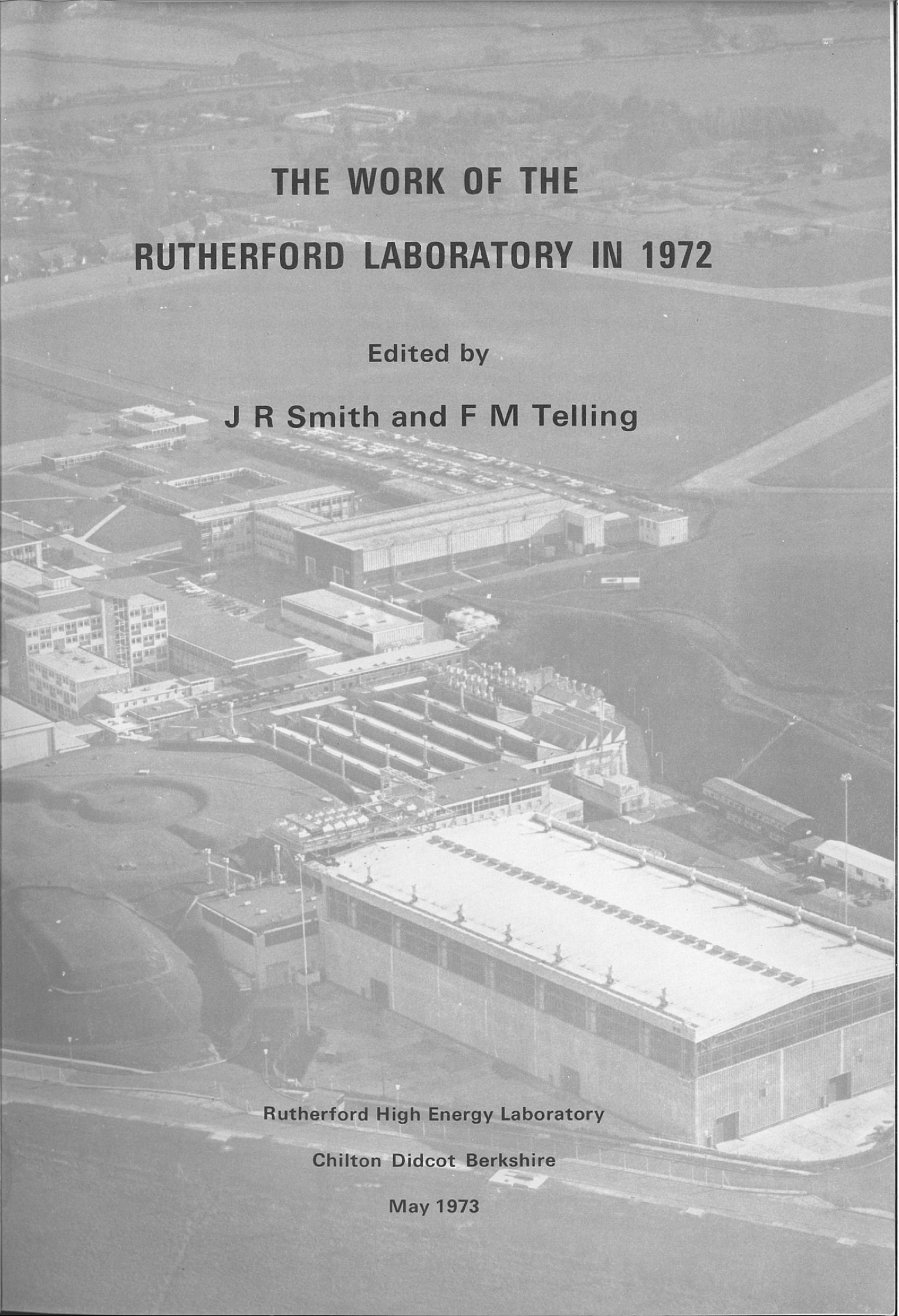
Rutherford Laboratory Report

THE WORK OF THE  
**RUTHERFORD LABORATORY**  
**1972**

© The Science Research Council 1973

"The Science Research Council does not accept any responsibility for loss or damage arising from the use of information contained in any of its reports or in any communication about its tests or investigations."

F. H. Wakelin Ltd.  
328 Witton Road, Birmingham B6 6PB



# THE WORK OF THE RUTHERFORD LABORATORY IN 1972

Edited by

J R Smith and F M Telling

Rutherford High Energy Laboratory

Chilton Didcot Berkshire

May 1973

**The Rutherford Laboratory** was established in 1957 as the first Laboratory of the National Institute for Research in Nuclear Science to build and operate for the common use by university scientists, that equipment which was required for the conduct of research in the nuclear sciences and which by its scale or cost was beyond the resources normally available to individual universities. In 1965 the Laboratory became part of the Science Research Council retaining a similar principal role.

The experimental high energy physics research programme is based on the particle accelerator Nimrod, a 7 GeV proton synchrotron in the Rutherford Laboratory, but the Laboratory also supports research carried out at international nuclear research centres, particularly at CERN in Geneva. Research is also done in theoretical physics, accelerator physics and various other branches of experimental physics which may have relevance to the long-term development of high energy physics.

The Laboratory also has a Neutron Beam Research Unit whose function is to support the community of scientists who use neutrons generated in nuclear reactors as their main research tool. The main European centre for this work is now at the Institut Laue-Langevin in Grenoble.

The research and development programmes are supported by a computing centre based on an IBM 370/195 computer which serves the requirements of the nuclear physicists and neutron beam users and also selected users in other fields.

There are 1200 staff employed by the Laboratory and about 250 University scientists associated with its scientific programme.

## Contents

	Page
LABORATORY ORGANISATION (December 1972) .. .. .	7
<b>HIGH ENERGY PHYSICS .. .. .</b>	<b>9</b>
Experiments using electronic techniques .. .. .	10
Bubble Chamber Experiments .. .. .	50
Nuclear Structure Experiments .. .. .	66
Radiological Experiments .. .. .	80
Theoretical High Energy Physics .. .. .	83
<b>ACCELERATOR OPERATIONS AND DEVELOPMENT .. .. .</b>	<b>91</b>
Operation of Nimrod .. .. .	92
Accelerator development .. .. .	98
Beam lines and associated equipment .. .. .	102
Theoretical studies on high energy accelerators .. .. .	109
<b>INSTRUMENTATION FOR HIGH ENERGY PHYSICS .. .. .</b>	<b>113</b>
1.5 metre cryogenic bubble chamber .. .. .	114
Instrumentation for counter experiments .. .. .	115
Electronic instrumentation .. .. .	121
Cryogenic targets .. .. .	122
<b>APPLIED RESEARCH .. .. .</b>	<b>125</b>
Superconducting magnet studies .. .. .	126
Superconducting r.f. separator development .. .. .	129
Polarized target development .. .. .	130
Rapid cycling bubble chamber development .. .. .	132
Experiments mounted on space satellites .. .. .	137
<b>NEUTRON BEAM RESEARCH .. .. .</b>	<b>141</b>
Development of neutron beam techniques .. .. .	143
Ultra-cold neutron gas facility .. .. .	146
Research programmes .. .. .	148
<b>COMPUTER SYSTEMS AND APPLICATIONS .. .. .</b>	<b>151</b>
Work stations and terminals .. .. .	152
Central computer system and operations .. .. .	155
Film analysis .. .. .	162
<b>TECHNICAL AND ADMINISTRATIVE SERVICES .. .. .</b>	<b>169</b>
Radiation Protection and General Safety .. .. .	170
Support services .. .. .	172
Administration and Public Relations .. .. .	174
<b>PUBLICATIONS AND LECTURES .. .. .</b>	<b>181</b>
(Publications are referenced by margin numbers throughout the Report)	
<b>BEAM LINES IN THE EXPERIMENTAL HALLS .. .. .</b>	<b>215</b>
(December 1972)	

# Laboratory Organisation (December 1972)

**DIRECTOR: G. H. STAFFORD**

## **HIGH ENERGY PHYSICS DIVISION**

Experiments in particle physics and nuclear structure physics in collaboration with university groups; nuclear electronics.

**DIVISION HEAD & DEPUTY DIRECTOR: G. MANNING**  
**DEPUTY DIVISION HEAD: J. J. THRESHER**

## **THEORY DIVISION**

Studies in theoretical particle physics

**DIVISION HEAD: R. J. N. PHILLIPS**

## **NIMROD DIVISION**

Operation and development of Nimrod (7 GeV proton synchrotron accelerator); accelerator design; experimental area management; development of beam line components and cryogenic targets; bubble chamber operations and development; radiation protection.

**DIVISION HEAD: D. A. GRAY**  
**DEPUTY DIVISION HEAD: G. N. VENN**

## **NEUTRON BEAM RESEARCH UNIT**

Support of research by universities using UK reactors and the reactor at the Institut Laue-Langevin, Grenoble; development of new instruments and techniques; study of new neutron sources; participation in experiments.

**HEAD OF UNIT: L. C. W. HOBBS**

## **APPLIED PHYSICS DIVISION**

Superconducting magnet studies; development of polarized targets; rapid cycling bubble chamber studies; superconducting power supplies and energy transfer.

**DIVISION HEAD: D. B. THOMAS**

## **COMPUTING & AUTOMATION DIVISION**

Operation and development of the central computer (IBM 370/195) and satellite computer system; computer applications for bubble chamber and spark chamber film analysis.

**DIVISION HEAD: W. WALKINSHAW**

## **ENGINEERING DIVISION**

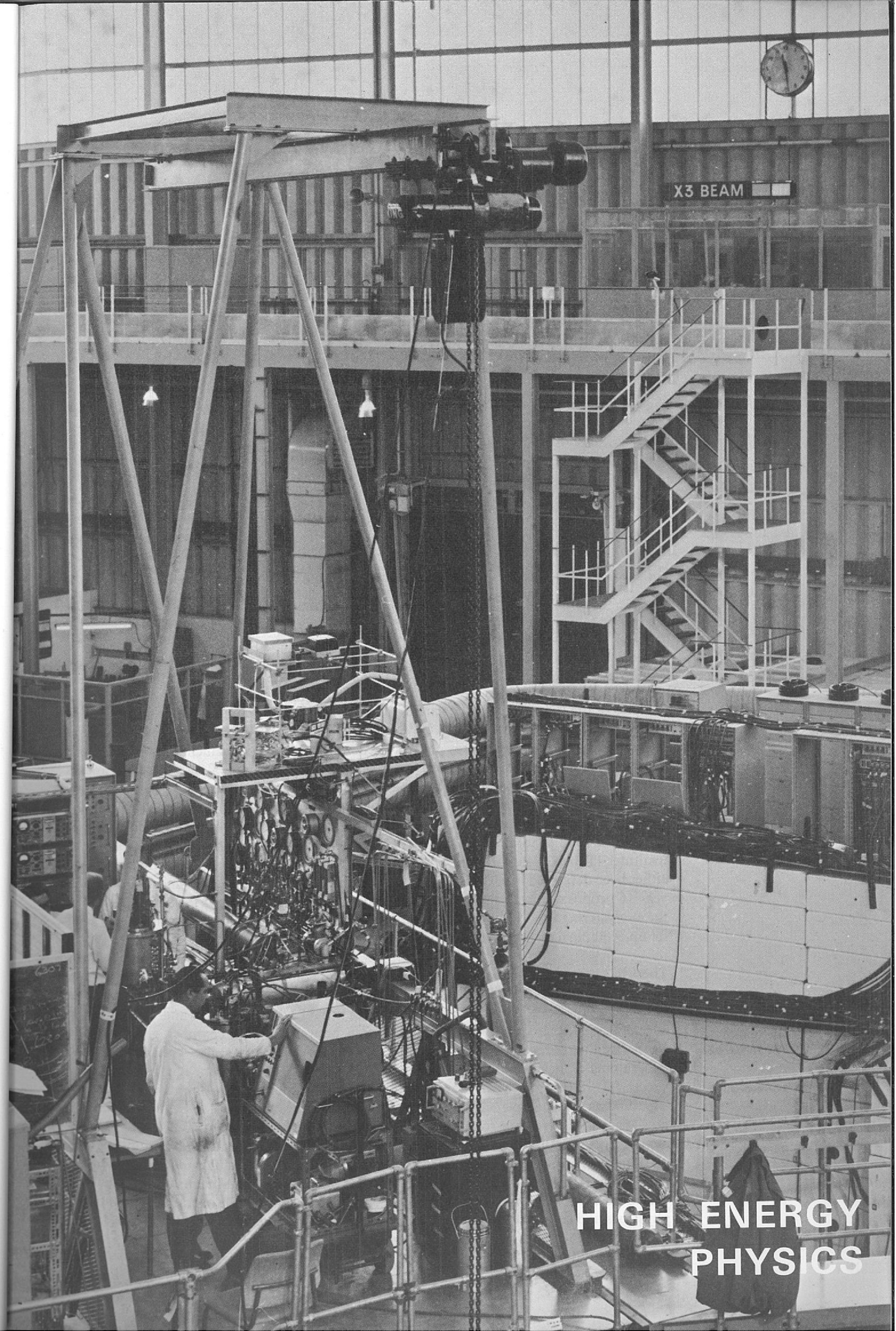
Design and manufacture of equipment for nuclear and applied physics research; department of engineering science; mechanical, electrical and building services; chemical technology; safety services.

**DIVISION HEAD & CHIEF ENGINEER: P. BOWLES**  
**DEPUTY DIVISION HEAD: G. E. SIMMONDS**

## **ADMINISTRATION DIVISION**

Personnel, finance and accounts, general and scientific administration; library, photographic, stores, transport and security services.

**DIVISION HEAD & LABORATORY SECRETARY: J. M. VALENTINE**



View of the polarized target controls, Experiment 11,  
 $\pi^9$  Beam, Hall 3 (10625).

**HIGH ENERGY  
PHYSICS**

# High Energy Physics

In spite of the reduction of funds arising from general policy changes and the decision to join the CERN SPS project ("300 GeV machine"), during 1972 an intense programme of work in experimental high energy physics has continued. The involvement of the Rutherford Laboratory in this field is indicated by considering the number of "active" experiments shown in Table 1. An experiment becomes active when it has been accepted by the Rutherford Laboratory Selection Panel and remains so until final data has been submitted for publication, at which stage it is considered to be complete. By this definition there were at the end of 1972, a total of 57 active experiments involving collaborators from some 52 institutes (Table 2). Reports on most of these experiments, are given below. Others have either been described in earlier reports or are in the early stages of development. During the year 16 proposals have been accepted, 17 experiments have advanced from data taking to the analysis stage and 12 have been completed. At the end of 1972, 4 experiments were being set up, 9 taking data and results from 24 being analysed.

There has been a continuation of the outward looking philosophy with particular emphasis on experiments at CERN and also our first involvement with the 400 GeV proton synchrotron of the National Accelerator Laboratory (NAL), Batavia, USA and the TRIUMF accelerator, British Columbia. A collaboration between bubble chamber groups at the Rutherford Laboratory and the Argonne Laboratory, USA has also been set up. The programme of expansion of activities at CERN, started about 4 years ago, has been very successful; during this year 8 experiments at CERN finished data-taking and 2 earlier experiments were completed. For many reasons it is to be expected that the level of activity now reached will remain roughly constant for the next few years. In addition to specific experiments the Rutherford Laboratory has supported the work of various committees and working parties directing their efforts towards a rapid and successful evolution of the SPS programme. During 1973 the first round of letters of intent for experiments on this machine will be called for and this will cause yet another shift of emphasis in the overall programme, as physicists and support groups begin to think about the problems of 400 GeV physics.

## Table 1

### High Energy Physics Experiments: Status of Proposals Active during 1972

Proposal No.	Title/Group	Beam/Lab	Technique			Status at 31.12.72
			EL Electronic	BC Bubble Chamber	TST Track sensitive target	
30	Differential Cross-Sections in $K^-p$ Elastic Scattering 0.85–2.2 GeV/c	K8		EL		Completed
31	Non-Leptonic Decay Parameters of $\Sigma^+$	K14		EL		Completed
33	Neutral Final State Studies	K10S		EL		Completed
36	A Study of $\pi^+p$ and $\pi^+n$ Interactions	K9		BC		Analysis
38	A proposal for a 2.3 GeV/c $K^-$ exposure in the Heavy Liquid Bubble Chamber			HLBC		Completed
40	$K^-p$ Elastic Scattering 0.45–0.85 GeV/c	K12		EL		Analysis
43	$K^+p$ $d\sigma/d\Omega$ 1.07–2.0 GeV/c Bristol/Soton/RHEL	K15		EL		Analysis
45	Test of the $\Delta S = \Delta Q$ Rule for $K^0$ Leptonic decays	K13		EL		Completed
50	Investigations of Narrow Width Mesons Produced in $\pi^-p$ Interactions	$\pi^7$		EL		Analysis
55	Polarization Effects in $\pi^+p$ Elastic Scattering	K14A		EL		Analysis
56	A proposal to study $K^+d$ Interactions in the 2 to 2.5 GeV/c range	K9		BC		Analysis
63	$K^+p$ Elastic Scattering 0.45–0.9 GeV/c	K12		EL		Completed
67	S and P Wave Amplitudes in $\pi^+p$ Elastic Scattering 80–300 MeV	CERN		EL		Completed
70	$\eta \rightarrow 3\pi$ Decay Westfield/RHEL	$\pi^8$		EL		Analysis
72	Large Angle $\mu$ Production Bristol/Cambridge/Liverpool/UCL/Westfield/RHEL	CERN ISR		EL		Data taking
73	$K^+d$ $d\sigma/d\Omega$ 0.45–0.95 GeV/c Birmingham/RHEL	K12A		EL		Analysis
74	Differential Cross-Sections in $K^+p$ Elastic Scattering 1.6–2.35 GeV/c	K8		EL		Completed
75	$\bar{p}p \rightarrow 2$ body 0.5–2.0 GeV/c QMC/DNPL/RHEL	CERN		EL		Analysis
76	$\eta \rightarrow \pi^0 e^+ e^-$ Westfield/RHEL	$\pi^8$		EL		Analysis
78	Investigation of Bremsstrahlung Anomalies	K13B		EL		Analysis
79	$\pi$ -nuclear Total Reaction Cross-Section Birmingham/Surrey/RHEL	$\pi^{10}$		EL		Completed
81	Polarization in $\pi^-p \rightarrow \pi^0 n, \eta n$ 0.6–3.5 GeV/c Glasgow/RHEL	$\pi^9$		EL		Setting-up
82	A Bubble Chamber Study of Hyperon-Nucleon Interactions	CERN		BC		Analysis and Development
83	$\pi^+p$ $d\sigma/d\Omega$ 0.6–2.0 GeV/c Bristol/RHEL	K15		EL		Data collection
84	$K^-p \rightarrow \Sigma^0 \pi^0$ 0.4–0.8 GeV/c UCL	RHEL		BC/TST		Accepted 11.11.70
85	np Interactions up to 8 GeV/c Cambridge	K9		BC		Part A—Analysis Part B—decision deferred

**Table 2**

**Institutions participating in the research programme of the Rutherford Laboratory**

AERE, Harwell	University of British Columbia, Canada
Bedford College, London	University of California
CEN, Saclay	University of Cambridge
CERN, Geneva	University of Chicago
Christie Hospital, Manchester	University of Copenhagen
Churchill Hospital, Oxford	University of Durham
Daresbury Laboratory	University of Edinburgh
Ecole Polytechnique, Paris	University of Glasgow
ETH, Zurich	University of Gothenborg
Harvard University, USA	University of Leeds
Imperial College, London	University of Liverpool
King's College, London	University of Lund
Lawrence Berkeley Laboratory, USA	University of Mainz
Queen Mary College, London	University of Oxford
Queen's University, Belfast	University of Paris-Sud
Rutger's University, USA	University of Pisa
St. Bartholomew's Hospital, London	University of Rome
SIN, Zurich	University of Southampton
Tata Institute, Bombay	University of Stockholm
Tufts University, USA	University of Surrey
University College, London	University of Sussex
University Libre de Bruxelles	University of Tel-Aviv
University of Bergen	University of Turin
University of Birmingham	University of Uppsala
University of Bologna	University of Warwick
University of Bristol	Westfield College, London

## Experiments using Electronic Techniques

The rapid improvement of experimental conditions at NAL has allowed data taking to start in the first round of experiments and it is gratifying that two groups supported by the Rutherford Laboratory are involved. Further experiments are proposed or are under consideration. Experience gained at NAL will of course be of great value in planning experiments at the CERN SPS. Conditions at the CERN Intersecting Storage Rings (ISR) have also improved to the point at which the design luminosity (interaction rate) has been reached.

At the Rutherford Laboratory's 7 GeV proton synchrotron, Nimrod, the year can be seen as a turning point. The most important single development has been the approval of the new injector project (described in the chapter on Accelerator Operations and Development). Together with the second rf accelerating cavity, to be installed early in 1973, and improvements in extraction efficiency this will result in an increase by a factor of 10 in extracted beam intensities, opening up new fields for electronic experiments. Since the start of the Nimrod high energy physics programme in 1964, the bulk of the work has been concerned with the study of strong interaction physics in the resonance region of pion-nucleon and kaon-nucleon scattering, as was discussed in the two preceding Annual Reports. It is a remarkable indication of the richness of the field and of improvements in experimental techniques that although in 1964 several accelerators of comparable energy already existed, almost all the world collection of data has been generated since then, and about half of this has come from Nimrod. There have also been important experiments in weak interaction physics (eg CP violation, stopping K decay). One can now think of this first phase of strong interaction experiments as coming to an end. They were nearly all single

scattering experiments in which differential cross-sections or asymmetries equivalent to recoiling baryon polarizations were measured. The data have contributed significantly to our overall view of  $\pi N$  and  $K N$  interactions in the range of incident momentum between about 500 and 2500 MeV/c, mainly through incorporation in analyses of data from many different sources. These show that in this region the dominant effect is the formation of "resonances". One can think of the interaction proceeding through the formation of a new particle (resonance) which then rapidly breaks up either into the same kind of particles from which it was formed (elastic scattering: Figure 1a) or into two or more particles, some or all of which may be different from the initial particles (reaction processes: Figure 1b). In contrast to this picture of particle **formation**, studies of scattering and reaction processes at much higher energies have shown that the interactions are mediated by the **exchange** of particles (Figure 1c). These two descriptions are united by the concept of duality, the discovery of which arose from the detailed study of the pion-nucleon resonances. Duality is one of the most important theoretical ideas to have been developed during the last few years. Very simply, it states that the two descriptions are equivalent. Thus the exchange of particles at very high energies and the formation of resonances at lower energies are intimately connected with each other. This connection imposes several constraints on the mathematical description of the interactions; through duality the resonance and very high energy regions are no longer independent.

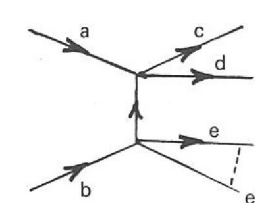
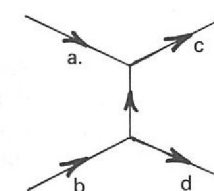
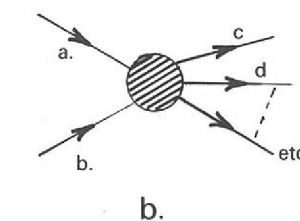
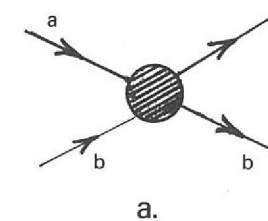


Figure 1. In each diagram, time is to be thought of as running from left to right. The letters label the various types of particle. Thus in 1c, the first diagram would describe exchange-mediated elastic scattering if  $a = c$  and  $b = d$ . In 1a, 1b, the "blobs" represent the unstable resonances described in the text.

The second phase of strong interaction experiments will be concerned broadly with several problems. Obvious examples are in the resonant region where there remain to be settled some important questions of detail, in particular the question of the existence of resonances with strangeness +1 in kaon-nucleon interactions. Another important area to be covered is the investigation of the spectrum of resonances with strangeness -2 ( $\Xi^*$ ), our knowledge of which is relatively incomplete. This is due to the requirement of high intensity  $K^-$  beams and the technical difficulty of the experiments. The intermediate region of incident momenta up to about 5 GeV/c will become accessible when the Nimrod improvement programme is complete and adequate fluxes of  $\pi$  and  $K$  mesons become available. Finally, the study of interaction channels in meson-baryon interactions, both with and without polarized targets, will provide a valuable alternative approach in both the resonance and intermediate regions. This work will require not only higher beam intensities but also further developments in polarized targets. The higher intensities will of course give greater scope for nuclear structure and weak interaction physics.

It is interesting to review briefly the programme of electronic experiments within this general framework. Figure 108 shows the layout in the experimental halls during 1972, when beam lines for most of the Nimrod-based experiments described below were still in existence. Many of these beams have now been removed (see Figure 2), creating the opportunity for a complete reorganisation of the experimental areas, which will then be available for "phase 2" physics. One possibility is the construction of a special 'chopped beam' to feed a rapid cycling vertex detector. This device, which combines electronic and bubble chamber techniques, would permit triggering biased towards chosen configurations of outgoing particles, with simultaneous observation of particle decay vertices close to their production points. It would be used first in a systematic study of  $\Xi^*$  resonances. In the short term the programme of electronic experiments will be based largely on the beam lines in Hall 3, and it is here that one can see most clearly the shift to "phase 2" physics. The measurements of  $K^+p$  elastic scattering (K15 beam line, Experiment 3) have set a new standard of completeness, consistency and precision. It is expected that they will contribute greatly to the settling of the question of the existence of  $S = +1$  resonances. Measurements of similar quality are to be made on  $K^-p$  elastic scattering when the Nimrod intensity is high enough. In Experiment 11 ( $\pi^0$ ), where measurements are being made on  $\pi^-p \rightarrow \pi^0n, \eta n$  up to 3.5 GeV/c, the higher incident momenta are already well into the intermediate region. Finally, in the proposed  $\pi 12$  beam line, studies of the process  $\pi^-p \rightarrow \Lambda^0 K^0$  will be made using a polarized target. The extra information obtained from the orientation of the decay products of the produced  $\Lambda$  particle determines the direction of the  $\Lambda$  spin. The combination of this information and the use of a polarized target gives the spin orientation in the reaction, permitting a much fuller analysis than is possible in an elastic scattering experiment such as  $\pi^-p \rightarrow \pi^-p$ . This is a good example of the increasing utilisation of polarized targets in the study of reaction processes.

*Data Handling for  
Electronic Experiments  
(ref. 44)*

The MIDAS system, in which graphics terminals connected to a DDP516 computer are used to provide event displays as an aid to the analysis of spark chamber experiments, is under continuing development. During the year, two additional terminals and a fast data link to the IBM 370/195 computer have been installed. Extensions to the operating system have been written to allow many programme development tasks to proceed in parallel with production use of the displays by experimenters. The addition of an extra 16K of core memory and a memory protection feature allow simultaneous production and software development.

As well as providing displays of digitised HPD data and events which have failed the analysis procedure, the system is increasingly being used for interactive rescue operation. Analysis of data from the CERN OMEGA magnet spectrometer (Experiment 14) and ISR Muon Experiment (Experiment 8) will begin shortly.

Three film measuring machines have been connected to the computer via CAMAC and a programme has been written to receive 'road guidance' information from several machines simultaneously. The data are written to a disk buffer store and transferred to the IBM 370/195 once a day. Scanning information on events from the ISR Muon Experiment will be dealt with in a similar way using alphanumeric display consoles.

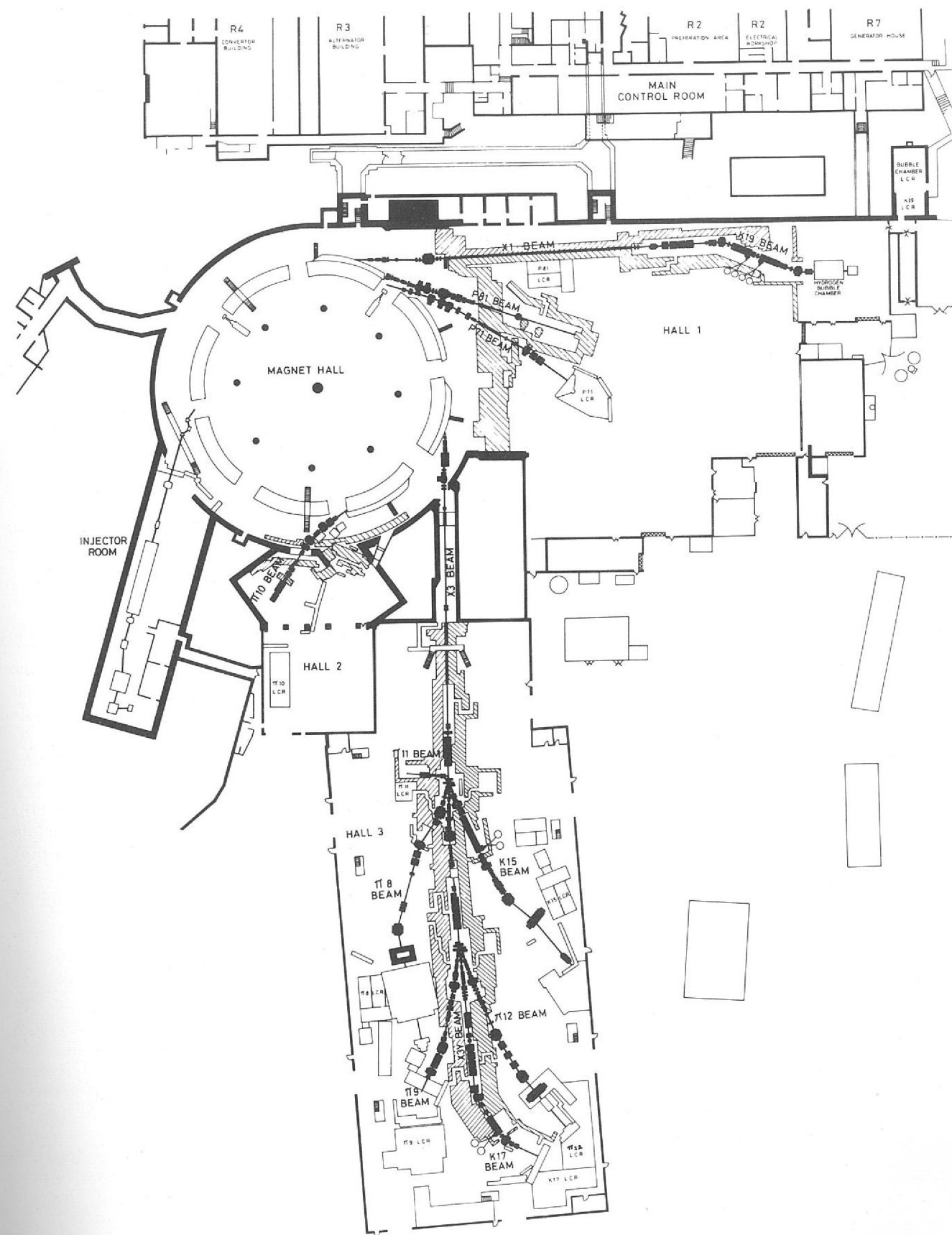


Figure 2. Planned lay-out of beam lines in the Experimental Halls for 1973 (12683)

**Table 3**

List of Experiments Using Electronic Techniques: Status Reports Follow

Expt. No.	Proposal No.	Experiment
1	30, 74	$K^+p$ and $\pi^+p$ Elastic Scattering at Incident Momenta between 1 GeV/c and 2.5 GeV/c.
2	40, 63	$K^+p$ Differential Cross-Sections in the Incident Momentum Range 0.43 to 0.94 GeV/c.
3	43	$K^+p$ Differential Cross-Sections in the Incident Momentum Range 0.7 to 1.9 GeV/c.
4	50, 99, 110	An Investigation of Narrow Width Mesons produced in $\pi^-p$ Interactions.
5	55	Polarization Effects in $\pi^+p$ Elastic Scattering.
6	67	Low Energy Pion-Nucleon Interactions
7	70, 76	Search for C-Violation in the Decay of the $\eta$ Meson.
8	72	The ISR Search for the Intermediate Boson and other Massive Particles: Particle Production Spectra.
9	73	$K^+n$ Elastic and $K^+n$ Charge Exchange Differential Cross-Sections below 1 GeV/c.
10	75	Anti-proton Proton Elastic Scattering and Two Body Annihilations.
11	81, 101	Differential Cross-Sections and Polarization Effects in the Charge Exchange Reactions $\pi^-p \rightarrow \pi^0n$ and $\pi^-p \rightarrow \eta^0n$ .
12	83, 105	Differential Cross-Section in $\pi^\pm p \rightarrow \pi^\pm p$ from 0.6 to 2.0 GeV/c.
13	87	Differential Cross-Sections and Polarization in the Reaction $\pi^- + p \rightarrow K^0 + \Lambda$ between Threshold and 1.4 GeV/c.
14	88	A Study of Neutral Bosons using a Neutron Time of Flight Trigger.
15	90	Measurement of the Polarization Parameter in $\pi^\pm p$ Backward Elastic Scattering at 6 GeV/c.
16	92	Neutral States from $K^-p$ Interactions.
17	93	Study of Non-Diffractive Production of $S = 1$ Neutral Resonances.
18	95	Coherent Production of $I = \frac{1}{2}$ States on Helium.
19	96	A Study of Inelastic Muon-Proton Scattering
20	98	The Pion Nucleon Scattering Lengths.
21	103	Polarization in the Process $\bar{p} + p \rightarrow \pi^+ + \pi^-$ .
22	107	Measurement of the P, A and R Parameters in the Backward peak of the Reaction $\pi^-p \rightarrow \Lambda K^0$ .
23	112	Investigations of Spin-Dependent Effects in High Energy Hadron-Proton Interactions
24	118	Study of the Inclusive Reactions $p+p \rightarrow p+X, n+X$ between 30 GeV/c and 400 GeV/c.

# Experiment 1

UNIVERSITY COLLEGE, LONDON  
RUTHERFORD LABORATORY

(Proposals 30, 74)

The differential cross-section for the elastic scattering of  $\pi$  and K mesons or protons has been measured for the following momentum regions:

$K^\pm p$  and  $\pi^\pm p$  Elastic Scattering at Incident Momenta Between 1 GeV/c and 2.5 GeV/c

Incident Particle	Momentum Range MeV/c	No. of Momenta	Average No. of Events/Momentum
$K^+$	1368 2259	23	6000
$K^-$	1094 1371	13	4400
$K^0$	1732 2466	19	2500
$\pi^+$	996 1352	16	6800
$\pi^-$	996 1352	16	600

The experimental work was completed in May 1970. Analysis of these data was completed during 1972 and publications are in preparation. Figure 3 shows a sample of the  $K^+$  data obtained in this experiment.

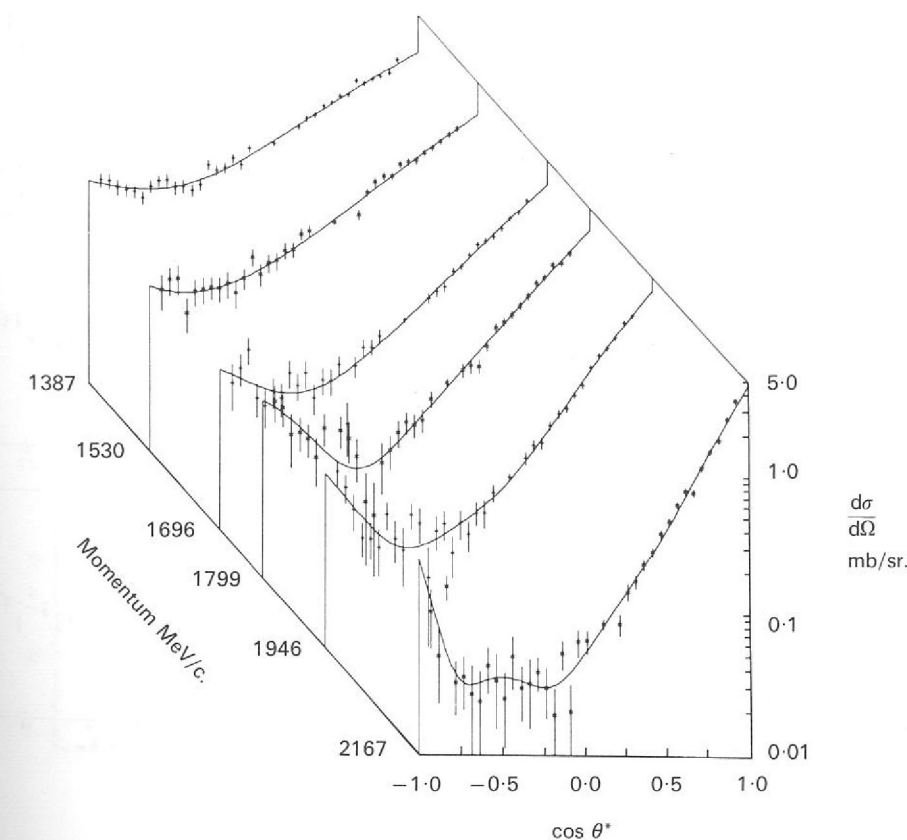


Figure 3.  $K^+p$  cross-sections obtained in Experiment 1. The solid lines are the result of a fit to the cross-sections by a series of Legendre Polynomials.

The measurements were made as part of a programme of research aimed at an improved knowledge of the baryon resonance spectrum. In the  $K^+p$  channel the interest lies, primarily, in the existence of possible "exotic"  $K^*$  resonances. The data from this experiment have been compared with the predictions of several published phase shift analyses of  $K^+p$  elastic scattering, some with resonant-like structure in the partial waves. Three solutions out of the eighteen gave a significantly better fit to the data than the rest. The best solutions were UCLC (Barber *et al.* Phys. Lett. 32B 214 (1970)), SENS  $\alpha$  and SENS  $\gamma$  (Albrow *et al.* Nucl. Phys. B30 273 (1971)). SENS  $\gamma$  has a small "resonance like loop" in the P3 wave which was not present in either SENS  $\alpha$  or UCLC solutions. None the less, it is hoped that the inclusion of the data from this experiment in a full phase shift analysis will lead to a better defined solution than has been found up to now.

The  $K^+p$  data were also found to be well represented by a model consisting of an exchange-degenerate Veneziano-type amplitude superimposed linearly on a diffractive pomeranchuk amplitude. It was found that the agreement improved with increasing incident momentum, as expected with this type of model. Work on the interpretation of the  $K^-p$  and  $\pi p$  data is in progress.

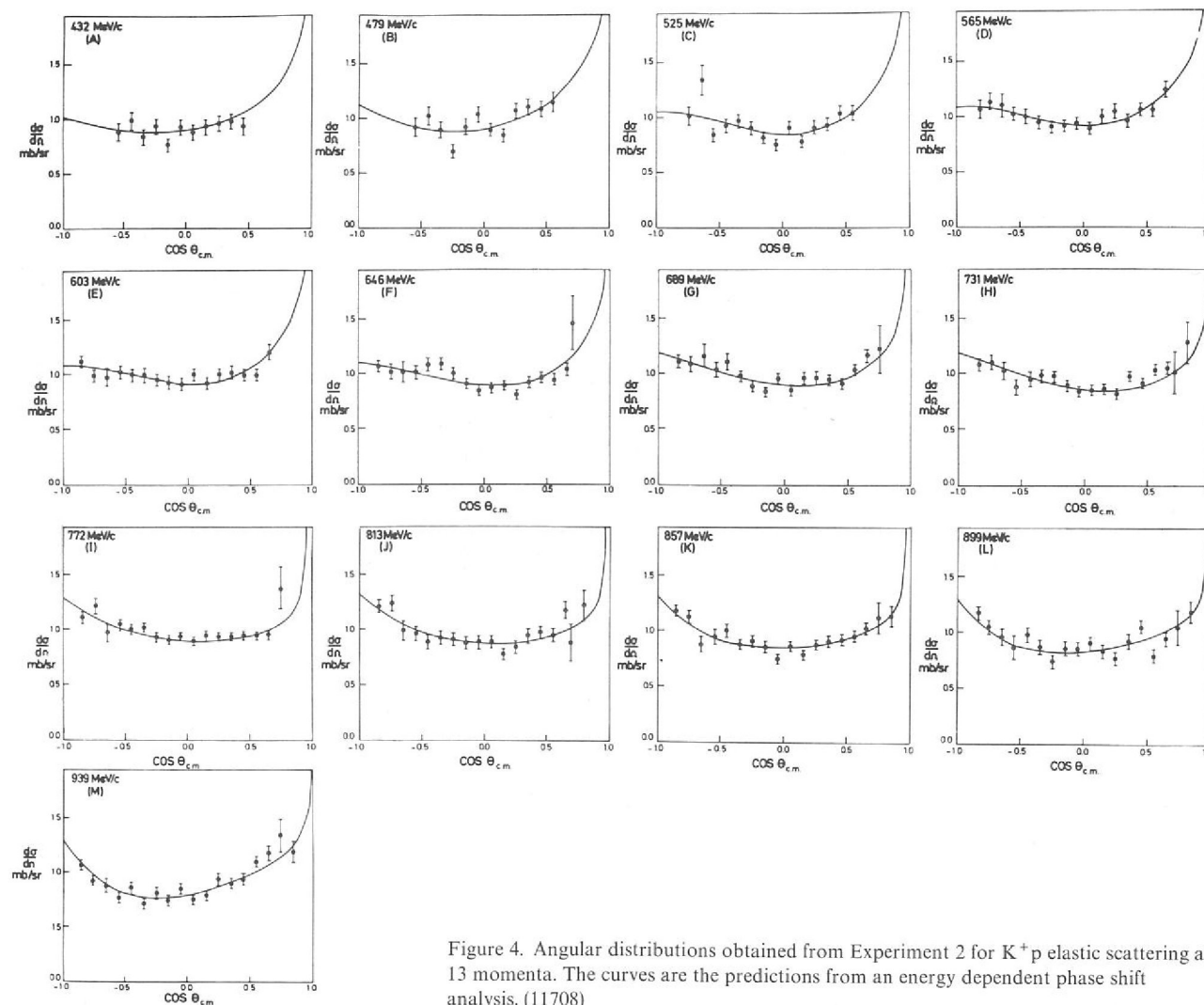


Figure 4. Angular distributions obtained from Experiment 2 for  $K^+p$  elastic scattering at 13 momenta. The curves are the predictions from an energy dependent phase shift analysis. (11708)

## Experiment 2

UNIVERSITY OF BIRMINGHAM  
RUTHERFORD LABORATORY

(Proposals 40, 63)

During the past year the analysis of the raw data for both  $K^+p$  and  $K^-p$  elastic scattering has been completed. In order to check on the absolute normalization the decays  $K \rightarrow \mu\nu$  have been reconstructed and compared with the expected rate for such decays calculated with a Monte Carlo programme. As a result of this study a normalization correction of about 12% has been applied to the differential cross-section data bringing them into much better agreement with already published elastic scattering data and with the spark chamber measurements of the Bristol-RHEL-Southampton group (Charles *et al.* 1972). The smooth behaviour of the  $K^+p$  differential cross-section as a function of momentum now seems firmly established if three total cross-section points near 0.7 GeV/c are ignored (see Figure 5) and no unusual interpretation is necessary. Indeed the results of this experiment, including the definitive Coulomb interference measurements made earlier by the group confirm that repulsive S-wave scattering dominates in this momentum range. Figure 4 shows the  $K^+p$  angular distributions and Figure 5 the elastic and total cross-sections as a function of momentum taken from this and other work. The  $K^+p$  data were presented at the XVth International Conference on High Energy Physics together with the results of an energy dependent phase shift analysis which is now being completed.

$K^\pm p$  Differential  
Cross-Sections in the  
Incident Momentum  
Range 0.43 to 0.94 GeV/c  
(ref. 127)

The  $K^-p$  differential cross-sections will shortly be available.

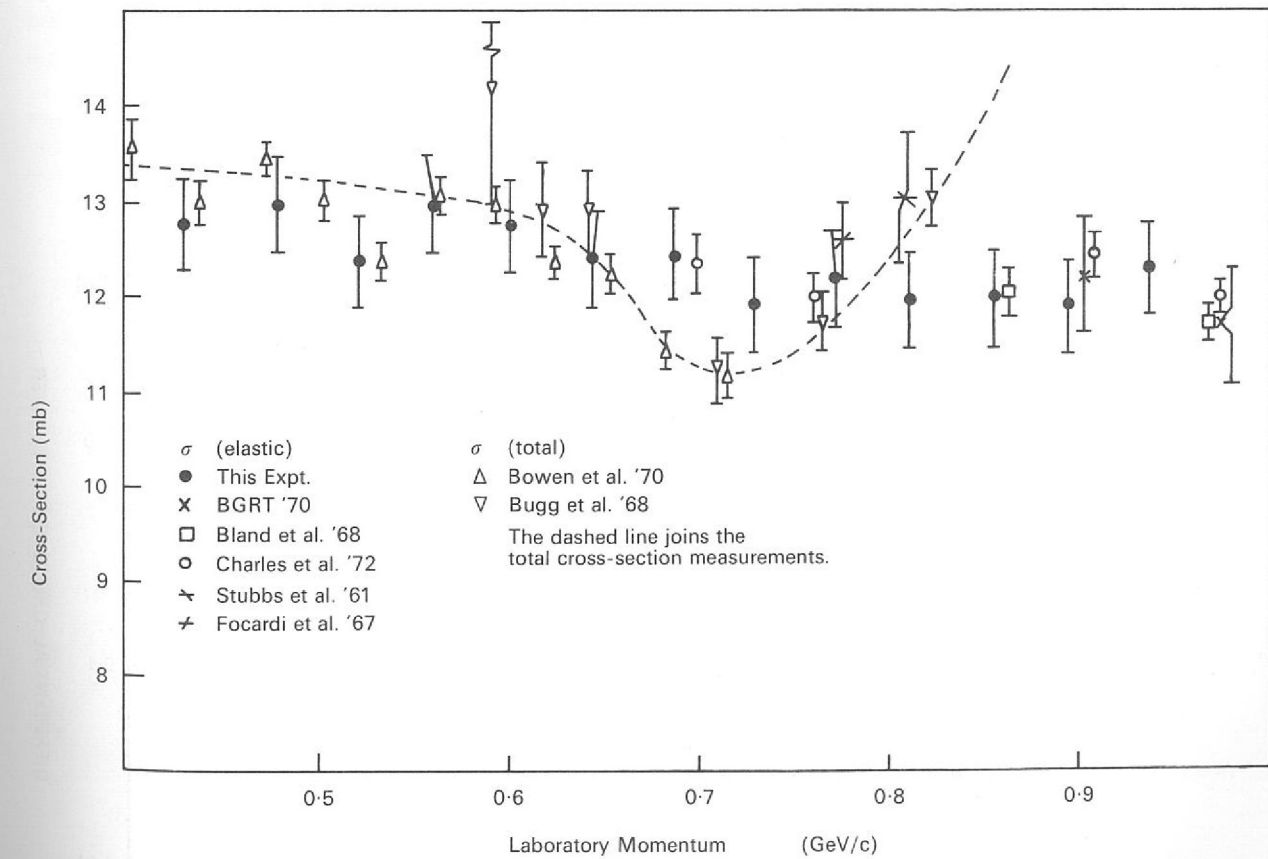


Figure 5.  $K^+p$  elastic and total cross-sections as a function of momentum taken from Experiment 2 and other experiments.

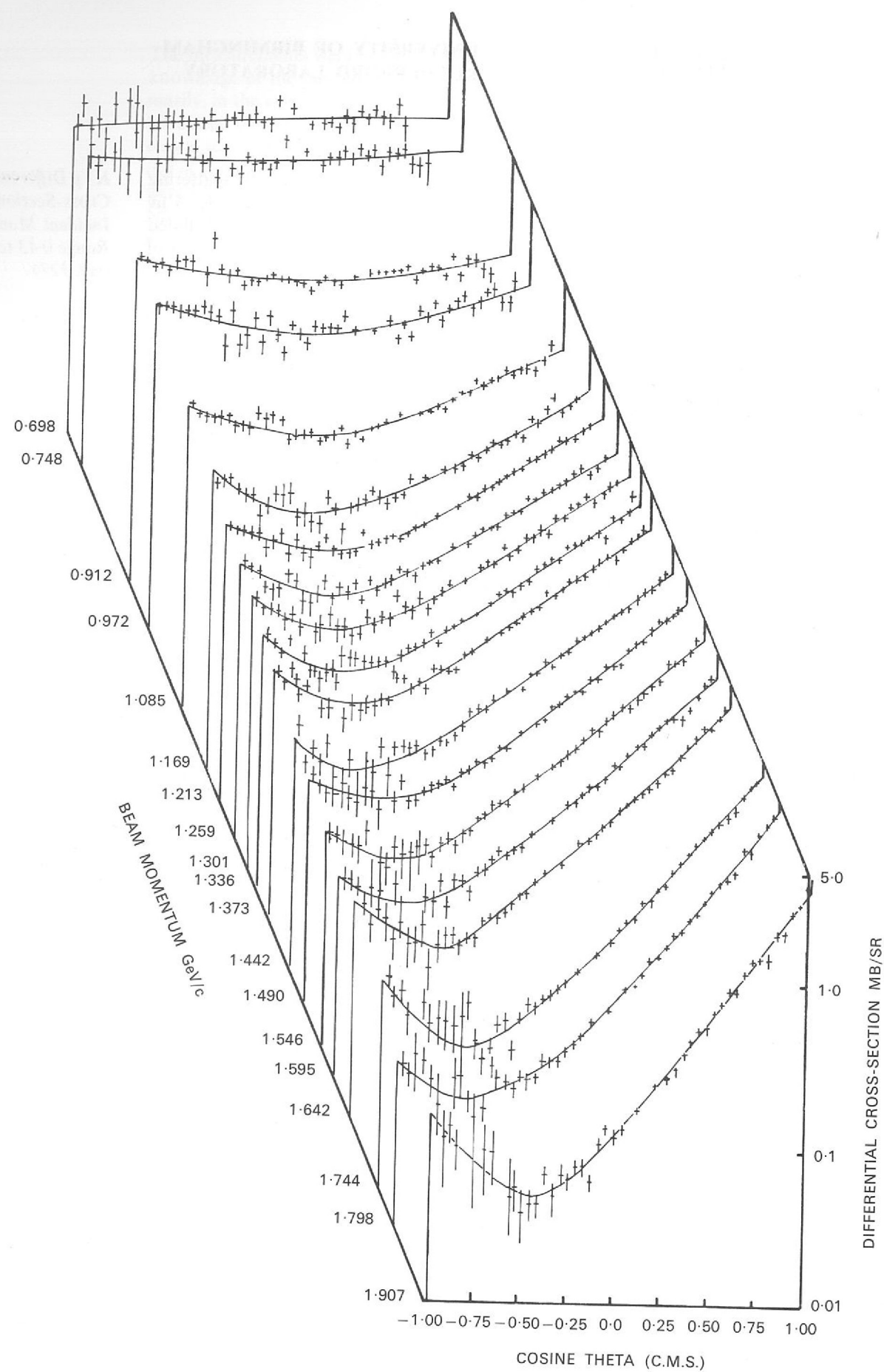


Figure 6. A complete set of differential cross-section measurements at 19 momenta for  $K^+p$  elastic scattering from Experiment 3.

## Experiment 3

(Proposal 43)

UNIVERSITY OF BRISTOL  
UNIVERSITY OF SOUTHAMPTON  
RUTHERFORD LABORATORY

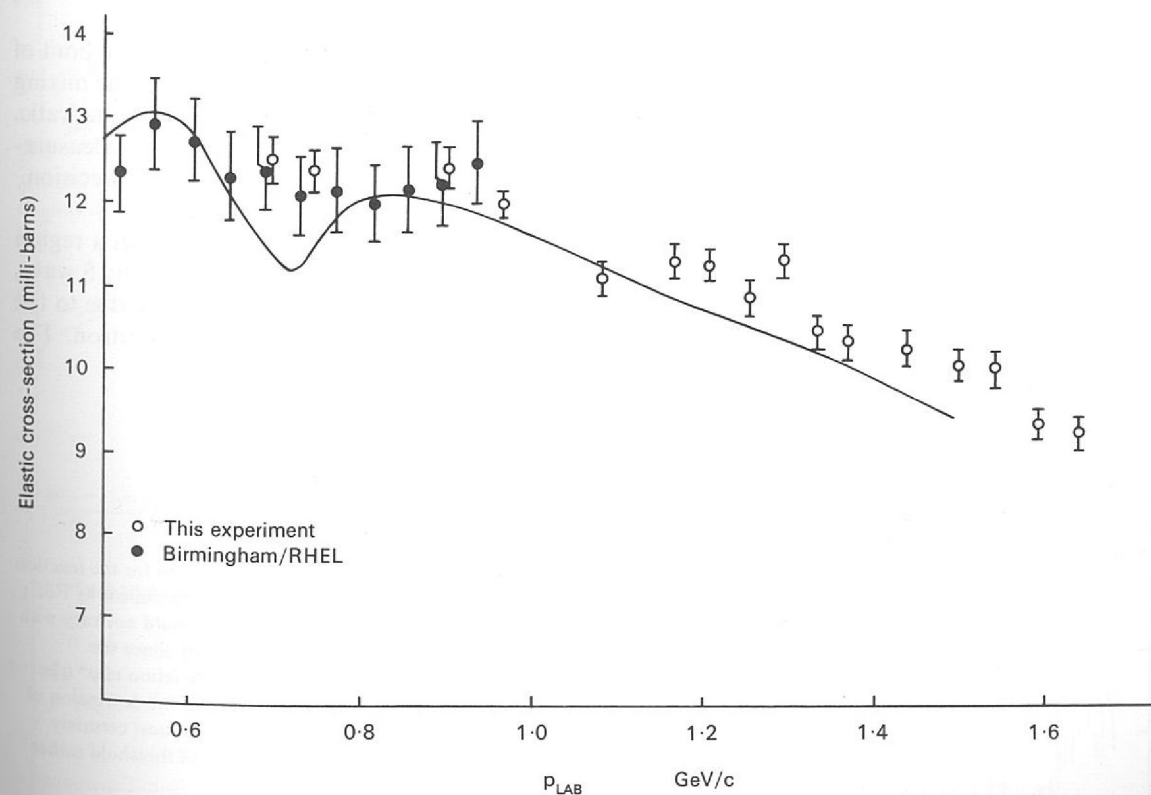
Sonic spark chambers and a spectrometer magnet were used to measure differential cross-sections for  $K^+p$  elastic scattering with good precision over a wide range of scattering angles. The experimental configuration has been described in previous annual reports. The analysis has now been completed and the results published. The complete set of differential cross-section measurements at 19 momenta are shown in Figure 6.

*$K^+p$  Differential Cross-Sections in the Incident Momentum Range 0.7 to 1.9 GeV/c (ref. 15, 80, 129, 175)*

A measurement of the total elastic cross-section at each momentum has been obtained by integration of the angular distributions of Figure 6. This measurement is believed to be accurate to better than 5% because of the good overall normalisation of the differential cross-section measurements and the wide range of scattering angles covered in the experiment. In response to a suggestion from other workers that there may be a dip in the total elastic cross-section around a momentum of 0.7 GeV/c it was decided to extend the measurements to cover this region. Data were taken during the summer at 0.70 and 0.75 GeV/c and the results presented at the Batavia Conference. These results confirmed the findings of the Birmingham-RHEL group and more recent total cross-section measurements that the cross-section varies smoothly in this region with no evidence of a dip (see Figure 7).

The differential cross-sections obtained in this experiment have been used to check the phase-shift analyses of a number of different groups. Three solutions (which are qualitatively similar) remained after this analysis. Two of the solutions contain no resonances but the third indicates a resonant  $P_3$  wave. This difficulty in finding a unique solution, which would clarify the question of the existence of a  $Z_1^*$  resonance, arises from the very weak coupling of the  $Z_1^*$  (if it exists) to the elastic channel.

Figure 7.  $K^+p$  elastic cross-sections around the momentum of 0.7 GeV/c. There is no evidence of a dip which was suggested by results of other experiments. The continuous line is a fit to previous elastic cross-section data. (Experiment 3).



## Experiment 4

IMPERIAL COLLEGE, LONDON  
UNIVERSITY OF SOUTHAMPTON

(Proposals 50, 99, 110)

*An Investigation of  
Narrow Width Mesons  
Produced in  $\pi^-p$   
Interactions  
(ref. 12, 118)*

The production of mesons in  $\pi^-p$  interactions has been studied by measuring the momentum and angle of outgoing neutrons or protons. These variables, together with the incident beam momentum, define the "missing mass" of the recoiling meson system. A novel feature of the experiment is that the missing-mass spectrum is obtained by varying the incident beam momentum. This enables the study of mesons very close to their production thresholds where very high mass resolution can be obtained.

The equipment consists of a precisely controlled and variable momentum pion beam, a hydrogen target, six neutron counters near the forward direction and, surrounding the target, an arrangement of counters differentially sensitive to both charged particles and gamma rays. During the year data have been taken on backward elastic and charge exchange scattering of  $\pi^-$  mesons, as well as the production of the narrow width meson resonances  $X^0$  and  $\omega$ .

*Backward Elastic and  
Charge Exchange  
Scattering*

Data have been taken on the reactions  $\pi^-p \rightarrow \pi^-p$  and  $\pi^-p \rightarrow \pi^0n$  at three different scattering angles near  $180^\circ$  and at 60 different incident momenta between 0.6 GeV/c and 1.1 GeV/c. Some data were also obtained on  $\eta$  production. The 1% spacing between adjacent momenta is finer than any previous data on these reactions. The high statistical precision and fine spacing of points should provide a significant test of current phase-shift analyses of these reactions. Analysis is nearing completion.

*Results on the  $X^0$  Meson  
and the Nearby Mass  
Range*

Production of the  $X^0$  meson is clearly seen and the cross-section in the region close to the threshold has been measured. However, no evidence was found for the production of any other narrow resonances in this mass region. This is contrary to the claims for two other narrow resonances which have been reported from a similar experiment at Argonne National Laboratory, USA. As a further check on the possible existence of these resonances data were taken under conditions more closely resembling those of the Argonne experiment. These data are currently being analysed.

The very high mass resolution of the apparatus was exploited to give a new upper-limit of 1.9 MeV for the width of the  $X^0$  meson. This result suggests that the formula for the mixing of the pseudo-scalar meson nonet should be linear in the masses rather than quadratic. This is an important theoretical question and to improve the accuracy of the width measurement additional data have been taken with improved resolution and statistical precision.

*Results on the  $\omega$  Meson*

The production cross-section and width of the  $\omega$  meson have been measured in a region close to threshold. While the production mechanism appears to be predominantly S wave, a depression of the cross-section is found very close to threshold which may be due to the effects of a final state interaction between the  $\omega$  decay products and the neutron. The cross-section points are shown in Figure 8.

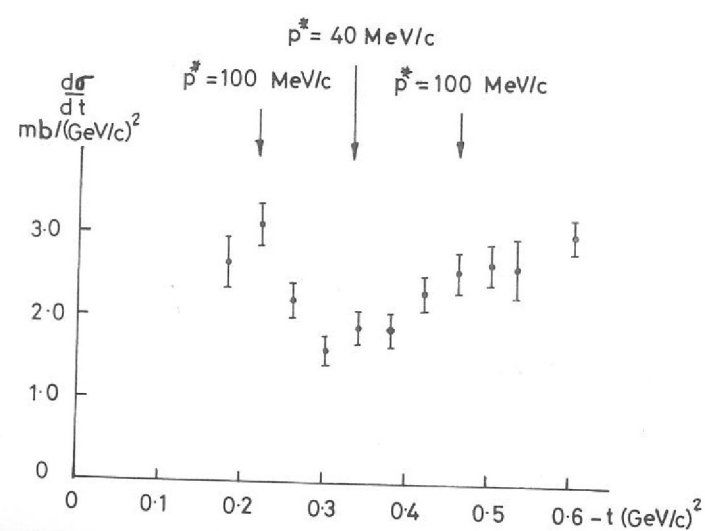


Figure 8. Differential cross-sections for the reaction  $\pi^-p \rightarrow \omega n$  close to threshold (Experiment 4). For pure S wave production  $d\sigma/dt$  should not vary with  $t$  (4-momentum transfer squared). Since the laboratory angle is fixed,  $t$  is a function of  $p^*$  (the final state c.m.s. momentum) and the depression of  $d\sigma/dt$  near  $t = 0.32$  ( $\text{GeV}/c$ )<sup>2</sup> is almost certainly due to the very close proximity of threshold rather than to a  $t$  channel effect.

## Experiment 5

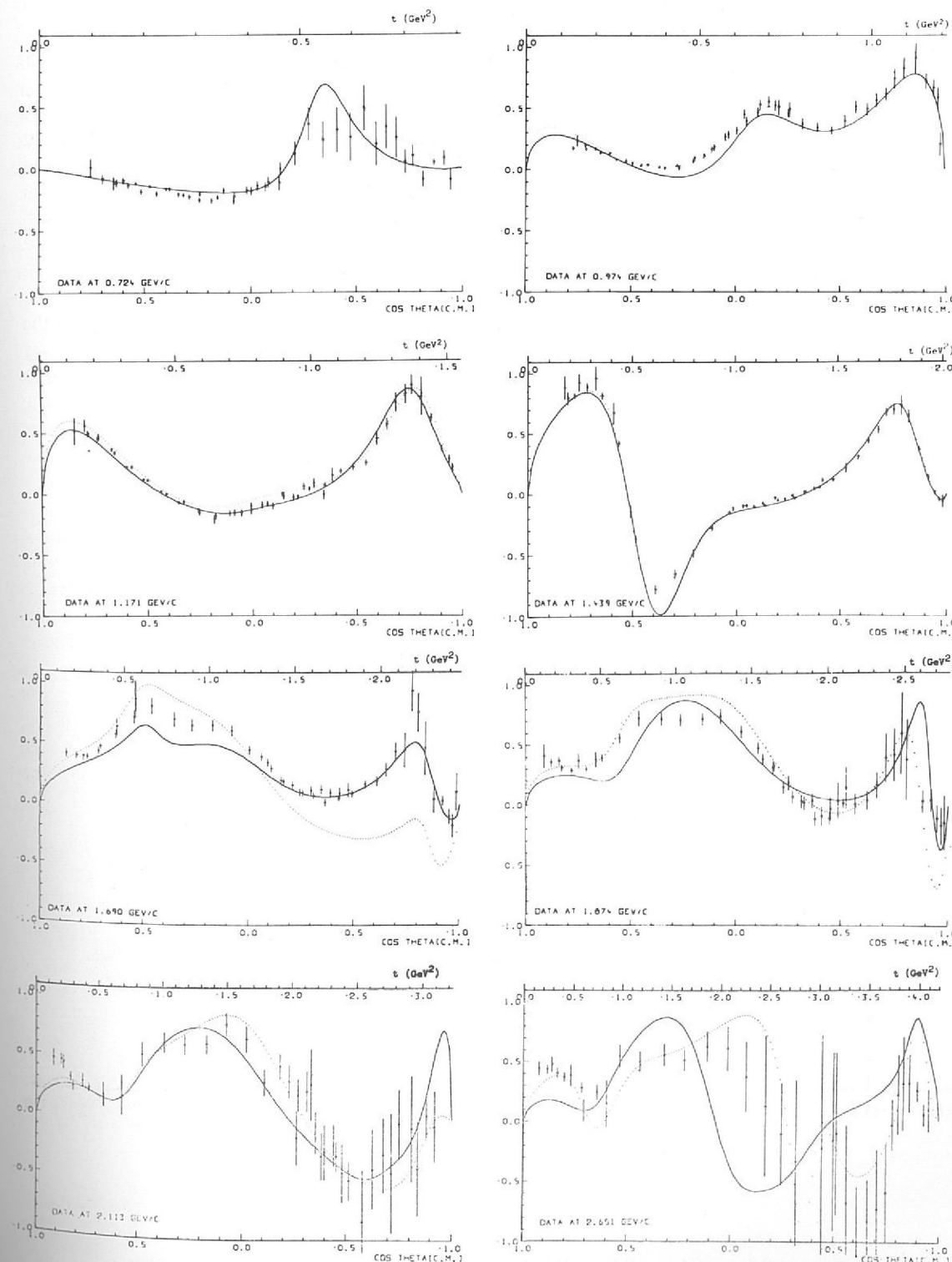
UNIVERSITY OF OXFORD  
RUTHERFORD LABORATORY

(Proposal 55)

In this experiment the polarization in  $\pi^+p$  elastic scattering has been measured in the incident momentum range from 0.6 to 2.6 GeV/c. The analysis of the data is now complete. Figure 9 shows a selection of the results which typify the precision obtained over the momentum range covered. Also shown in the figure for comparison are the predictions of various phase shift analyses.

*Polarization Effects in  
 $\pi^+p$  Elastic Scattering  
(ref. 177, 180)*

Figure 9.  $\pi^+p$  polarization data, from Experiment 5, at eight incident momenta. The predictions of two recent phase shift analyses are shown for comparison. (12566).



# Experiment 6

(Proposal 67)

UNIVERSITY OF CAMBRIDGE  
QUEEN MARY COLLEGE, LONDON  
RUTHERFORD LABORATORY

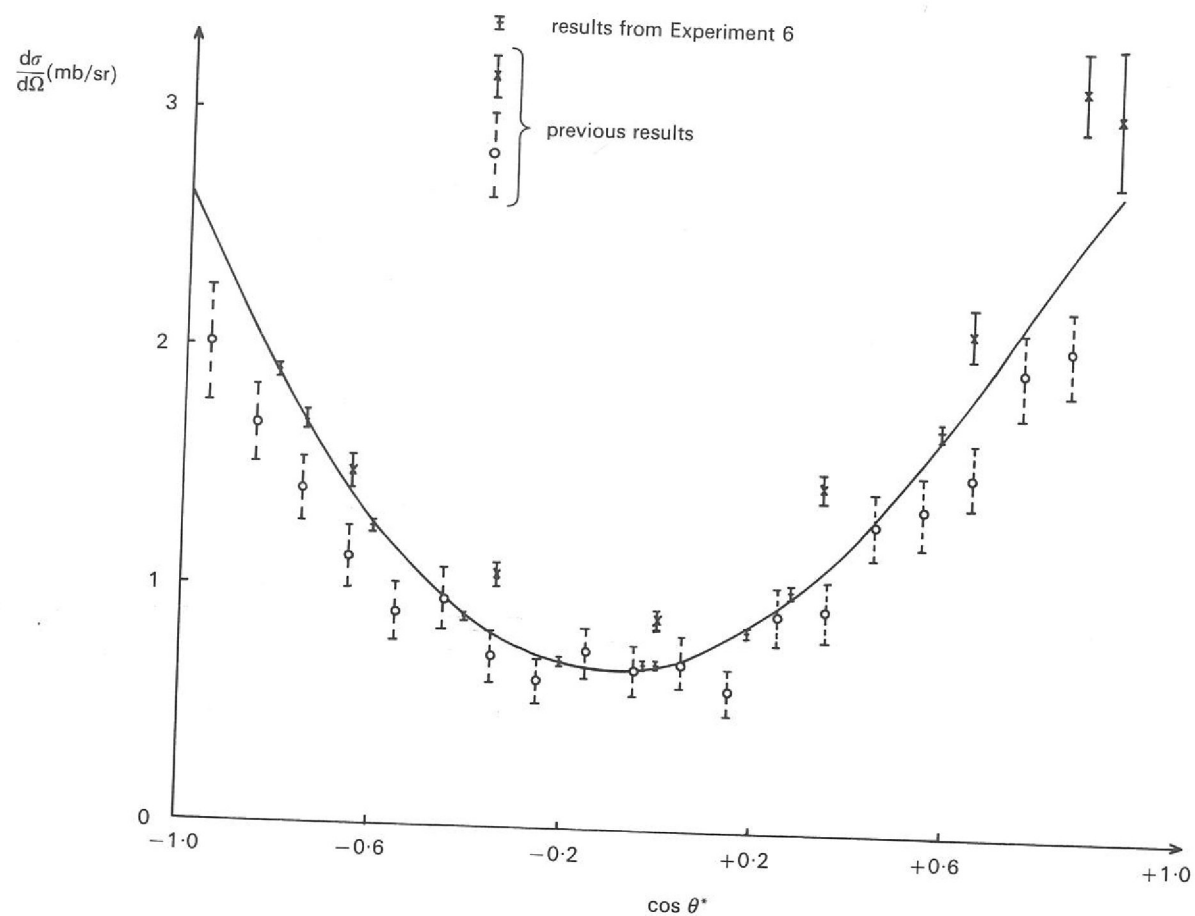
Low Energy Pion-  
Nucleon Interactions  
(ref. 116)

Angular distributions have been determined at 10 energies for each sign of incident pion between 88 and 292 MeV. A typical angular distribution is shown in Figure 10, together with results of two previous measurements. Typical errors on each point in an angular distribution are  $\pm 2\%$ ; integrated angular distributions agree well with measured total cross-sections.

Phase shifts have been determined, and show much better consistency from energy to energy than previous results. Reconstructed amplitudes have been compared with fixed  $t$  dispersion relations, as a check against systematic errors; the data satisfy these checks extremely well, and give a value for the  $\pi^-p$  coupling constant  $f^2 = 0.0791 \pm 0.0008$ .

A novel result is that the difference in the measured widths of the  $\Delta(1231)$  resonance in its  $\Delta^0$  and  $\Delta^{++}$  states is  $\Gamma(\Delta^0) - \Gamma(\Delta^{++}) = 11.5 \pm 1.5$  MeV. Of this, the Coulomb barrier accounts for  $3.5 \pm 0.5$  MeV, and the photoproduction channel  $\pi^-p \rightarrow \gamma n$  accounts for 1.1 MeV; finally, the extra phase space in the  $\pi^-p \rightarrow \pi^0 n$  channel accounts for 1.6 MeV. The origin of the outstanding  $5.3 \pm 1.5$  MeV is obscure, but may well have its origin in charge dependence of the  $\pi NN$  coupling constant.

Figure 10. The angular distribution for  $\pi^-p$  elastic scattering obtained from Experiment 6 for an incident kinetic energy of 220 MeV/c.



# Experiment 7

(Proposal 70, 76)

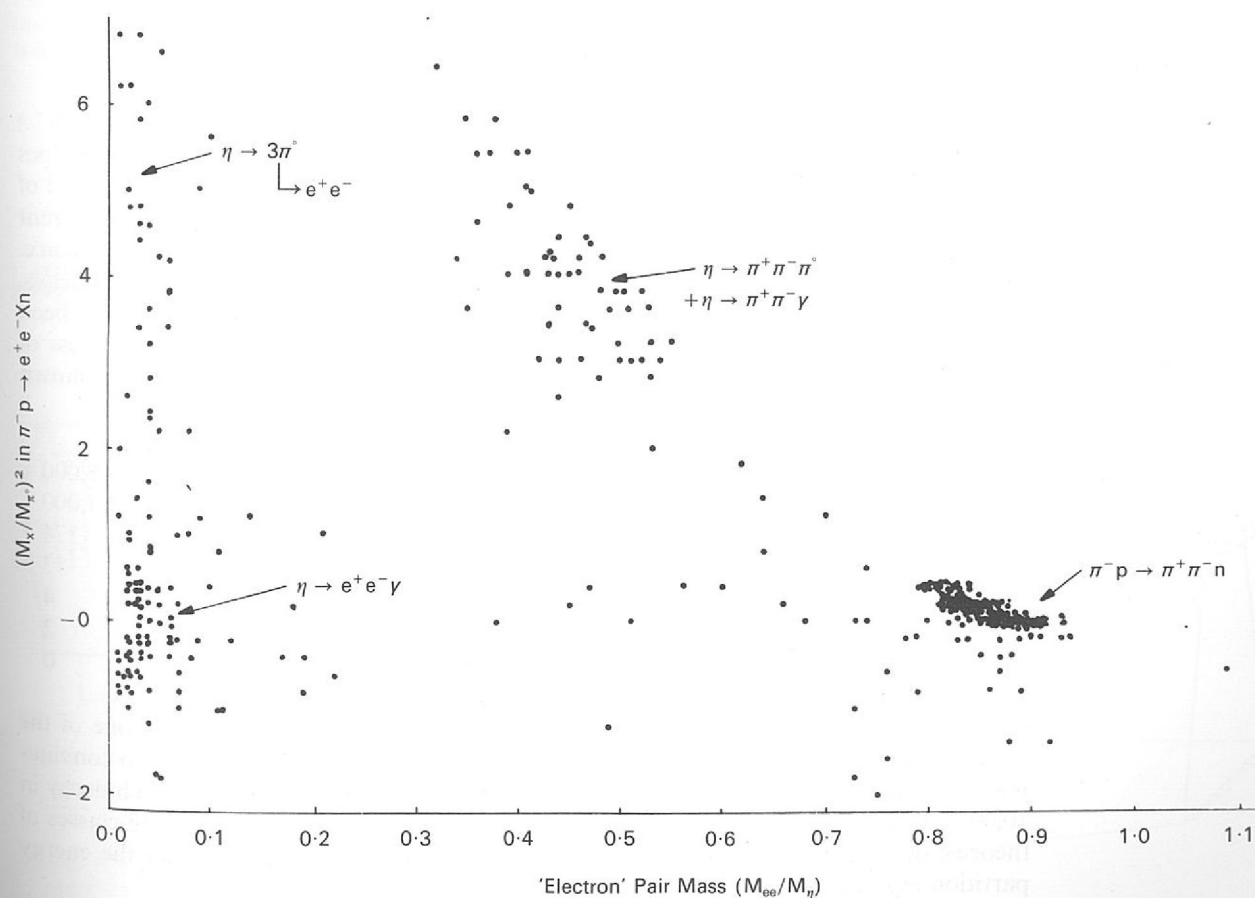
WESTFIELD COLLEGE, LONDON  
RUTHERFORD LABORATORY

Search for C-Violation in  
the Decay of the  $\eta$  Meson

Physical laws are frequently expressed in a symmetrical fashion even though perfect symmetry is rarely found in the world of our common experience. For example, naturally occurring sugar is dextrose, but the laws of chemistry are P-invariant (P for parity) and do not distinguish dextrose from laevose. In experiments, equal amounts of both can be synthesised. Similarly, particles and anti-particles are both produced in high energy physics experiments and it was at first supposed that the basic theories would be C-invariant (C for charge-conjugation, or particle-antiparticle substitution), as well as P and T (for time reversal) invariant. However, in the weak interaction, P conservation is violated: there are no right-handed neutrinos. There is still a symmetry, CP, since all anti-neutrinos are right-handed. This symmetry is violated in the decay of the  $K^0$  meson, and since all physical theories are CPT invariant, it follows that T invariance must also be violated.

These discoveries showed very clearly that the assumptions of symmetry in the theory frequently had very weak or no experimental basis. In particular C conservation in the electromagnetic interaction had no rigorous experimental verification and it was conceivable that a small C-violating term in the electromagnetic interaction could be linked with the CP-violation problem in  $K^0$  decay. The decay of the  $\eta$  meson is one of the few other processes in which such effects might be seen. Two tests are being examined in this experiment. The first test is in the decay  $\eta \rightarrow \pi^+ \pi^- \pi^0$ , where C invariance requires that on average the  $\pi^+$  receives the same fraction of the decay energy as the  $\pi^-$ . This test requires very high statistics and sophisticated analysis techniques to control systematic biases.

Figure 11. A two dimensional plot for all 374 events satisfying Cherenkov requirements (Experiment 7). The two observed charged particles are assumed to be an electron and a positron. The different reactions are indicated on the plot. (11924)



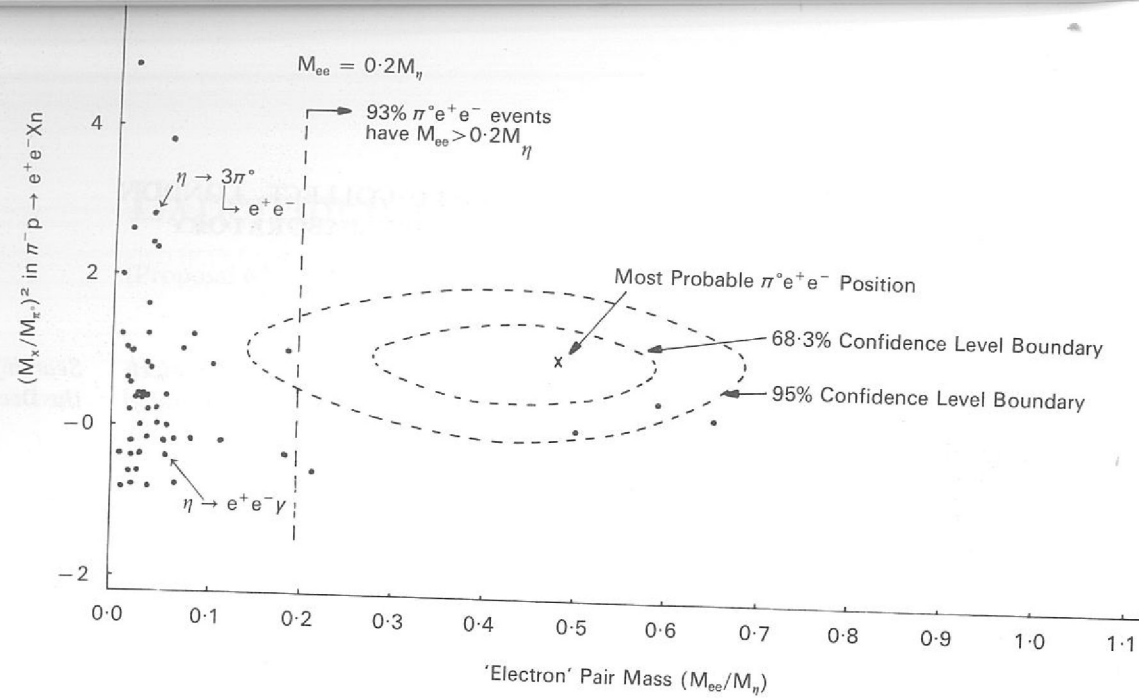


Figure 12. A plot of data of Figure 11 after cuts have been applied to remove  $\eta \rightarrow \pi^+\pi^-\pi^0$ ,  $\eta \rightarrow \pi^+\pi^-\gamma$  and  $\pi^-\pi^0 \rightarrow \pi^+\pi^-\pi^0$  events. These cuts will also remove some of the  $\eta \rightarrow e^+e^-\gamma$  and  $\eta \rightarrow \pi^0\pi^0\pi^0$  events. A cut of  $(M_{ee}/M_\eta) > 0.2$  is then applied. The dashed curves show the confidence level boundaries for events of the type  $\eta \rightarrow \pi^0e^+e^-$ . (11928).

Some 400,000 events are being analysed. First order systematic effects are cancelled by the symmetry of the apparatus and the reversal of the magnetic field. Evidence from the channel  $\pi^-\pi^0 \rightarrow \pi^+\pi^-\pi^0$  (which was accepted by our trigger), where the  $\pi^+$  and  $\pi^-$  must necessarily have the same energy in their centre of mass, shows that there is some residual systematic effect present. This effect is correlated with any asymmetry in the decay  $\eta \rightarrow \pi^+\pi^-\pi^0$ . After making the appropriate correction a preliminary result for the asymmetry is

$$A = \frac{N^+ - N^-}{N^+ + N^-} = 0.0040 \pm 0.0030$$

( $N^+$  is the number of times the  $\pi^+$  is more energetic than the  $\pi^-$ , and vice versa for  $N^-$ .) The second test is for the presence of the C-violating decay  $\eta \rightarrow \pi^0e^+e^-$ . C invariance does permit this decay to occur through two-photon exchange processes, but only at a level of less than 1 in  $10^9$  of all decays, which is well below the detection level possible in current experiments. Thus observation of an event would be evidence for C non-invariance. Previous experiments limit the occurrence of this process to less than one in 2,500  $\eta$  decays. A preliminary analysis of some 378,000 vidicon recorded spark chamber events has been made. The final analysis of nearly one million events is almost complete. The process of sifting the 378,000 events for possible  $\pi^0e^+e^-$  candidates is summarised in the Table shown below and Figures 11 and 12.

Total Events	378,000
Events with electron signal (one $\hat{C}$ counter)	31,000
Events with strong electron signal (two $\hat{C}$ counters)	374
Events surviving kinematic cuts to eliminate known background	53
Events with $m_{e^+e^-} > 0.2m_\eta$	4
Events in region which should contain 99% of genuine $\pi^0e^+e^-$ events	2
Events in region which should contain 85% of $\pi^0e^+e^-$ events	0

It can be seen that both kinematical resolution and positive identification of one of the electrons in the decay are needed in order to eliminate background processes. No convincing  $\pi^0e^+e^-$  event was found, and we are able to quote a limit of at most one such decay in 10,000  $\eta$  decays. The final result should be significantly more sensitive. In some classes of theories this test is much more sensitive to the presence of C-violation than the energy partition asymmetry in the decay  $\eta \rightarrow \pi^+\pi^-\pi^0$ .

## Experiment 8

(Proposal 72)

UNIVERSITY OF BRISTOL  
UNIVERSITY OF LIVERPOOL  
UNIVERSITY COLLEGE, LONDON  
RUTHERFORD LABORATORY  
UNIVERSITY OF BERGEN  
UNIVERSITY OF LUND  
UNIVERSITY OF COPENHAGEN  
UNIVERSITY OF STOCKHOLM  
CERN

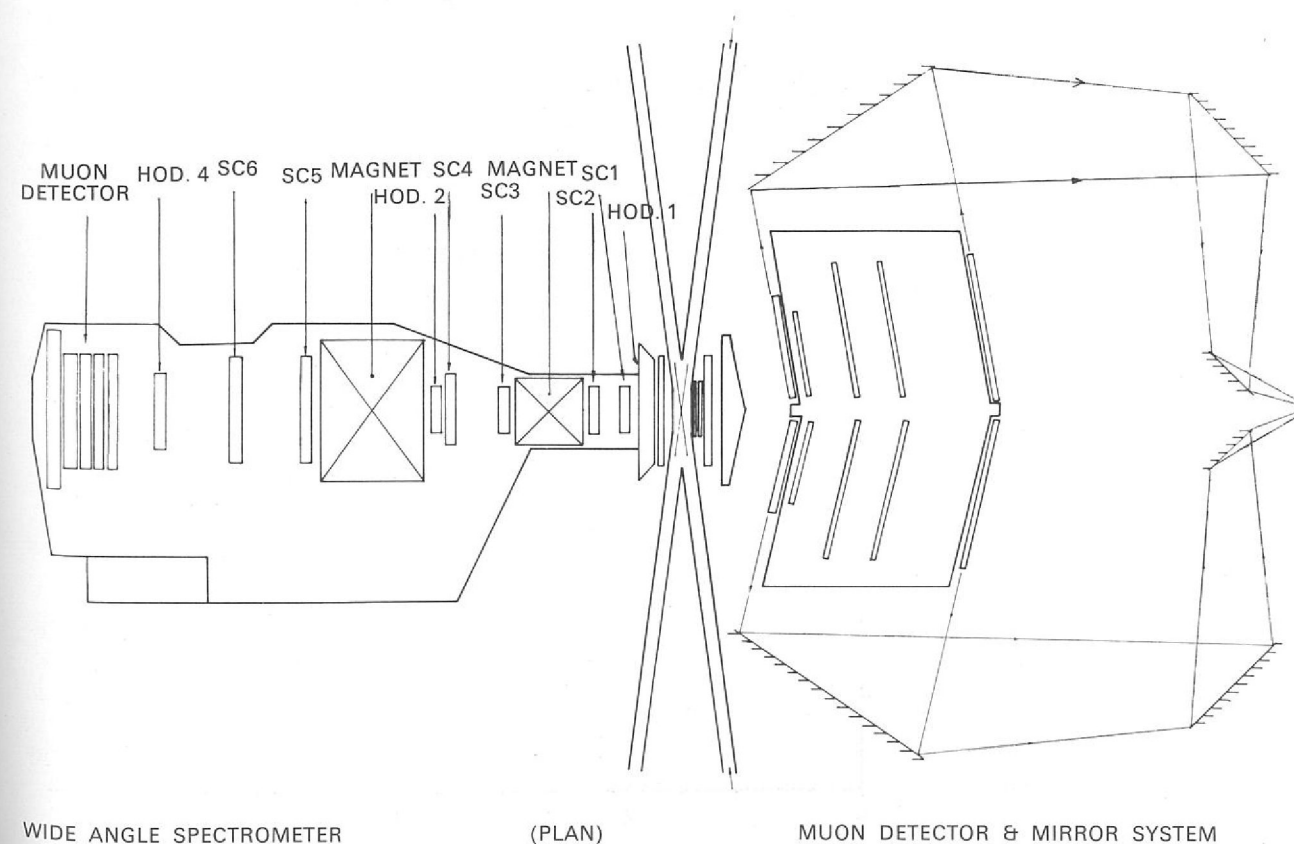
The research programme of this collaboration comprises four experiments using two major pieces of equipment, located at the CERN Intersecting Storage Ring (ISR) (see Figure 13). A large solid angle muon detector is in use to detect muons with high transverse momentum which would be evidence for the existence of the intermediate boson, and possibly also of massive photons. A wide angle spectrometer which can be placed at angles between  $30^\circ$  and  $90^\circ$  to the beam bisector is used in the following experiments:

- Measurement of the particle production spectra in the momentum range 0.1 to 1.3 GeV/c,
- Measurement of the particle production spectra in the momentum range 1.5 to 6 GeV/c, and
- A search for particles with mass greater than  $1 \text{ GeV}/c^2$ .

The **Muon detector** consists of an array of magnetised steel plates separated by scintillation counters and optical spark chambers. To trigger the spark chambers a particle (normally a muon) must have passed through  $\sim 10$  interaction lengths of material and have a momentum of at least  $1.6 \text{ GeV}/c$ . Particle co-ordinates are recorded on film which is developed, measured and analysed at the Rutherford Laboratory.

*The ISR Search for the Intermediate Boson and other massive particles: Particle Production Spectra.* (ref. 125)

Figure 13. Diagram of the apparatus of Experiment 8 situated on both sides of Intersection 2 region of the Intersecting Storage Ring facility at CERN. The wide angle spectrometer can carry a variety of detectors. It is shown here with scintillation counter hodoscopes and magnetostrictive spark chambers. (10976)



The cosmic ray background has been successfully removed from the data, while muons from mesons produced in the interaction region are removed in two ways. The first is to study the muon momentum spectrum as a function of the position of the absorber placed between the equipment and the interaction region. The second is to measure the meson production spectra using the wide angle spectrometer, and to calculate the correction for meson decay. To date 180,000 pictures have been taken and all these data have been scanned and the selected events have been measured. The analysis and Monte-Carlo programmes are in an advanced state of development.

Two papers have been submitted to international conferences on the preliminary results from ~5% of the present data. The muon momentum spectra for two positions of the absorber are shown in Figure 14. These observations agree with Monte-Carlo predictions based on the best data available on high transverse momentum meson spectra. The present upper limit for the production of single muons with momenta greater than 6 GeV/c

$$\text{is } \frac{d\sigma}{d\Omega} \leq 4 \times 10^{-33} \text{ cm}^2/\text{sr}$$

The production cross-section for muon pairs can be measured in two ways; firstly by noting the number of reconstructable two-muon events seen in the muon detector, and secondly by measuring events in which a muon is seen in the wide angle spectrometer in coincidence with a muon in the muon detector. These data are being analysed.

**The Wide Angle Spectrometer** has two modes of operation. The first is used in the measurement of low momentum particle yields, and in the search for massive particles. The second, used to measure the high momentum particle yields, is shown in Figure 15. The spectrometer arm is pivoted below the intersection region and can be rotated by remote control.

Figure 14. Muon momentum spectra for two positions of the lead absorber. (Experiment 8).

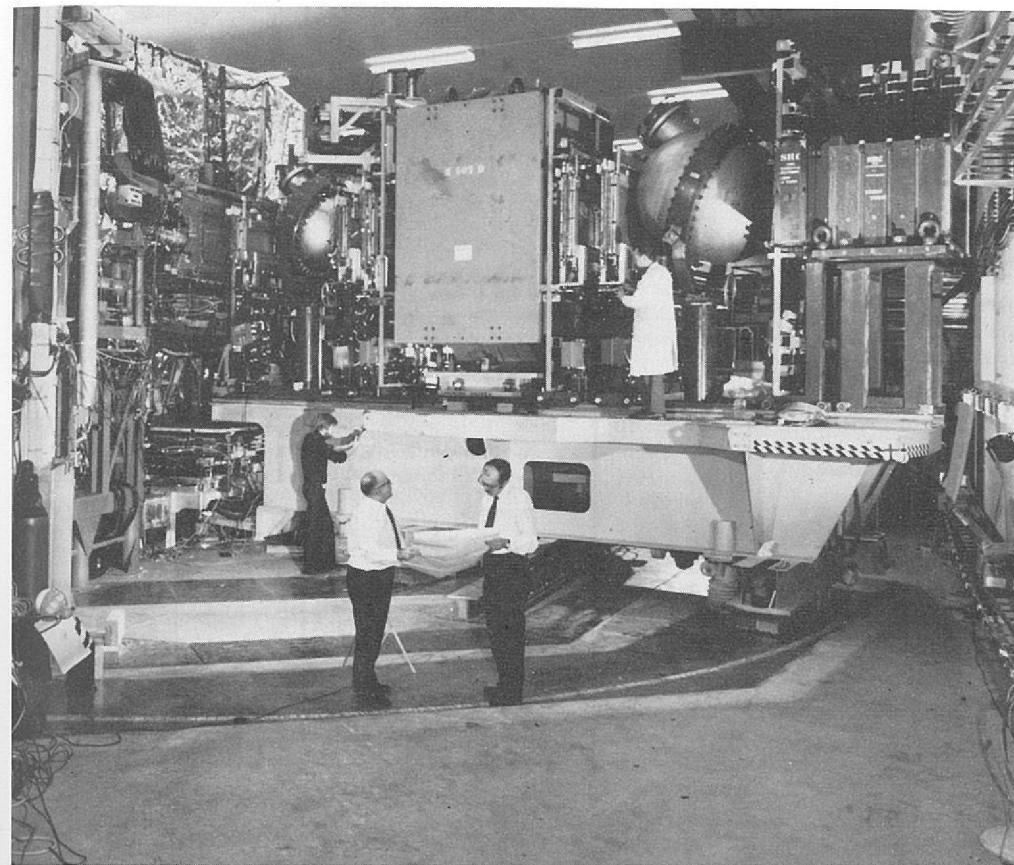
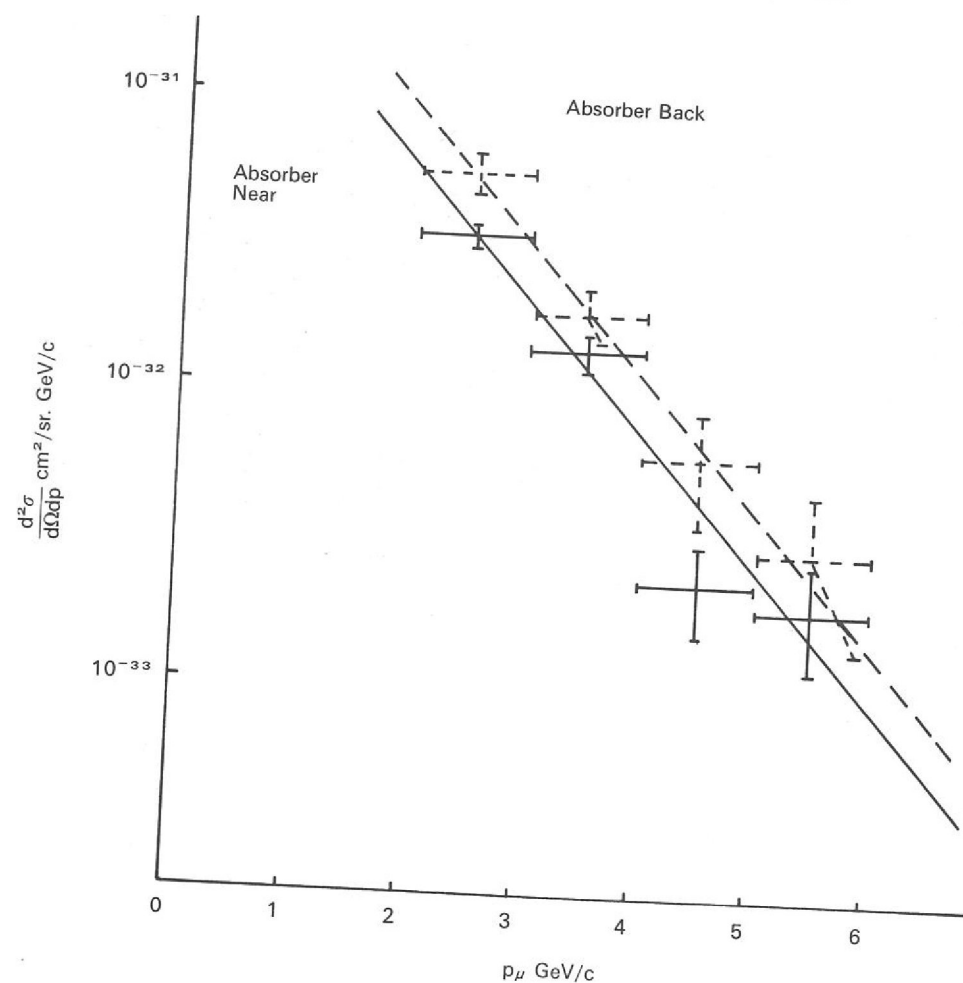


Figure 15. A view of the wide angle spectrometer (Experiment 8) in the mode for measuring high momentum particle yields. (CERN 128-12-72).

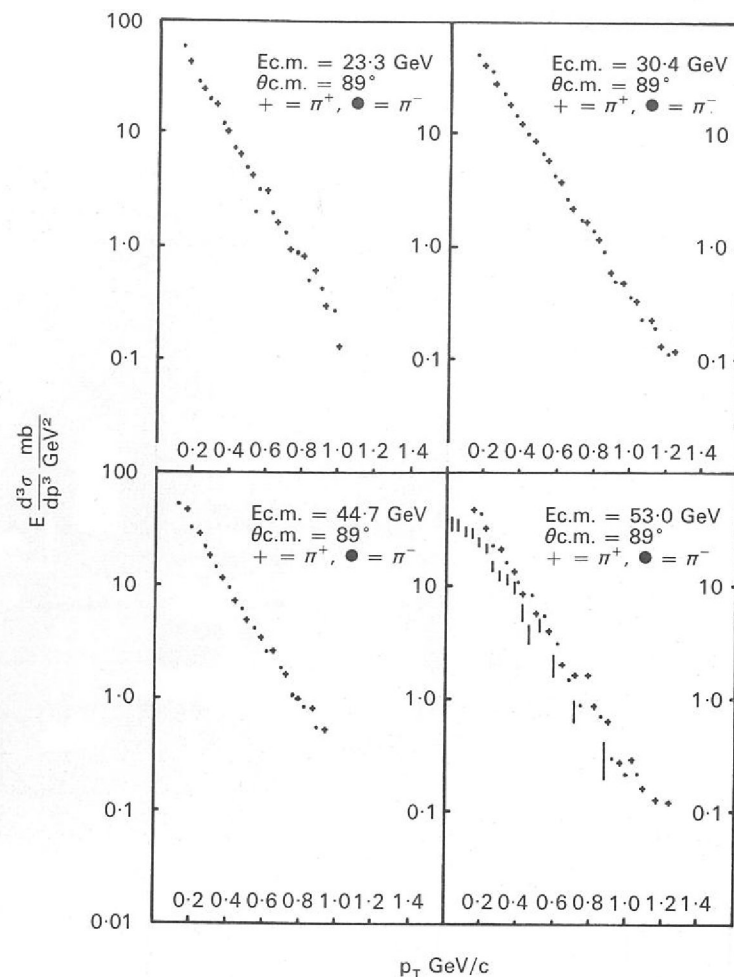
In the first configuration, two dipole magnets and six magnetostrictive wire spark chambers are used to make two independent determinations of particle momenta. Three scintillation counter hodoscopes are used to trigger the spark chambers, and to provide independent time of flight measurements to obtain particle velocities. Momentum spectra are measured for  $\pi^+$ ,  $K^+$ ,  $p^+$ ,  $d^+$  as a function of the spectrometer angle. Particles with momenta greater than 1.3 GeV/c cannot be separated by time of flight, but data on the unseparated charged particle spectra at high transverse momenta have nevertheless been taken.

To date 10 million events have been recorded on magnetic tape and analysed using the Rutherford Laboratory 370/195 computer. Two conference papers have been presented on preliminary data, and the final data are being prepared for publication.

A selection of invariant cross-sections for pion production are plotted as a function of transverse momentum in Figure 16. These plots show data taken throughout the ISR energy range, including runs at 19 GeV/c. Antiproton data taken at the same centre of mass energies show an increase in the invariant cross-section of ~40% with energy in contrast to the pion data shown, which changes only by ~10%.

Preliminary data suggest that the slopes of these momentum spectra decrease by a factor of 3 in the transverse momentum range 1 GeV/c-5 GeV/c. There is evidence from other experiments at the ISR that the  $\pi^0$  cross-sections at large values of  $p_T$  increase with increasing centre of mass energy. To investigate further these observations, the spectrometer arm has recently been changed to the high momentum mode in which particles are identified by two threshold gas Cherenkov counters, while the momentum is determined by one dipole magnet and magnetostrictive spark chambers. Test data have been taken at two centre of mass energies.

Figure 16. The invariant cross-section  $E \frac{d^3\sigma}{dp^3}$  for pions plotted as a function of the transverse momentum  $p_T$ . The scatter of the points indicates the statistical accuracy. The 19 GeV/c data are shown as vertical bars. (Experiment 8).



## Experiment 9

UNIVERSITY OF BIRMINGHAM  
RUTHERFORD LABORATORY

(Proposal 73)

*K<sup>±</sup>n Elastic and K<sup>±</sup>n Charge Exchange Differential Cross-Sections below 1 GeV/c*

This experiment is part of a systematic study of the kaon-nucleon interaction below 1 GeV/c. In this case K<sup>±</sup>n charge exchange and K<sup>±</sup>n elastic differential cross-sections are obtained by measuring the scattering of kaons in a liquid deuterium target for a number of incident momenta in the range of 430 to 940 MeV/c; the experiment will add significantly to existing data.

Data collection was completed in August with some 20 million events recorded on magnetic tape. The apparatus, which has been described in previous Annual Reports, consisted of scintillation counters, sonic spark chambers and a large spectrometer magnet.

Some π<sup>±</sup>p elastic scattering data (liquid hydrogen target) were recorded as a check on the performance of the apparatus and analysis programmes. The differential cross-sections obtained are in excellent agreement with published data (Figures 17a and 17b). K<sup>+</sup>p elastic scattering has also been measured and preliminary results are shown in Figure 17c.

A preliminary analysis has been performed on the deuterium target data. K → μν decays of the incident kaons have been extracted and their rate and angular distribution agree with those predicted from the measured incident beam rate and direction. Events have also been extracted of scatters from the deuteron (Kp(n) and Kn(p) scattering) but some problems remain for events near the limits of angular acceptance. Although these will have to be understood before final results for scattering off the neutron can be produced, a preliminary result for the charge exchange cross-section at 600 MeV/c is shown in Figure 17d.

Work has started on a phase shift analysis programme to give the I = 0 amplitudes when the final Kn results are available. These should clarify the still unsettled question of a possible exotic I = 0 resonance (Z<sub>0</sub><sup>\*</sup>) corresponding to a peak in the K<sup>+</sup>n elastic cross-section at about 750 MeV/c.

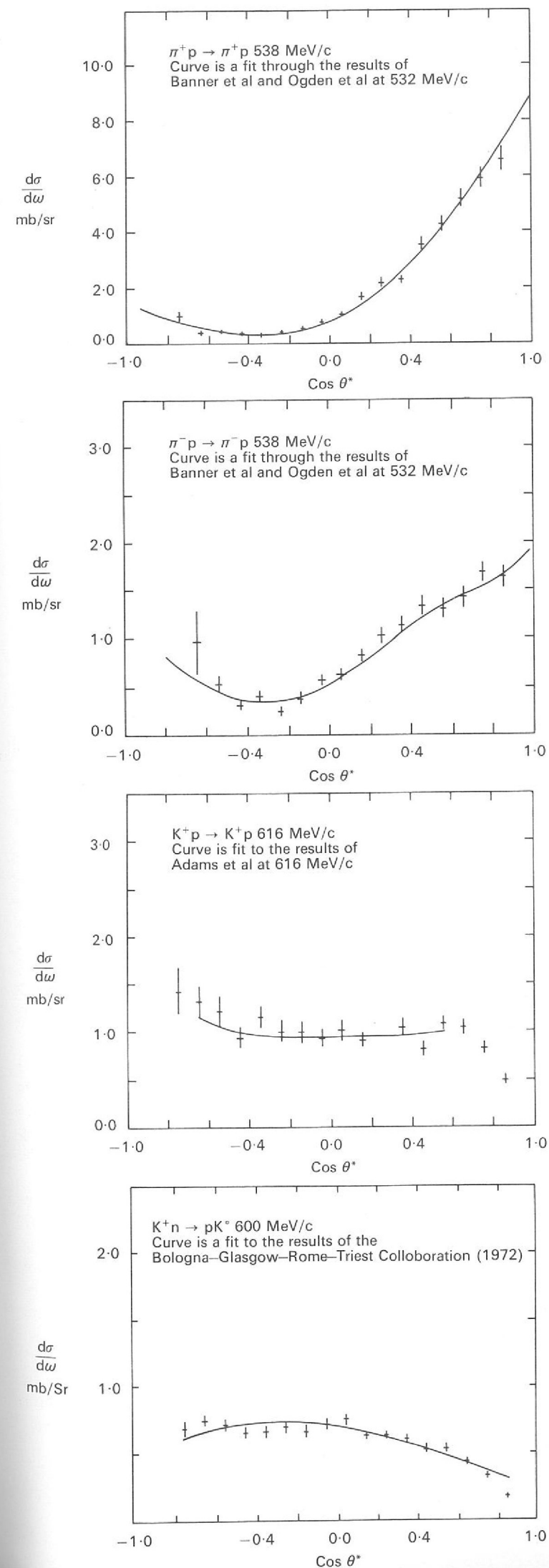


Figure 17. Differential cross-sections for π<sup>±</sup>p, K<sup>+</sup>p elastic scattering and K<sup>+</sup>n charge exchange scattering from Experiment 9.

# Experiment 10

(Proposal 75)

UNIVERSITY OF LIVERPOOL  
 QUEEN MARY COLLEGE, LONDON  
 DARESBUARY LABORATORY  
 RUTHERFORD LABORATORY

The processes:

- (a)  $\bar{p} + p \rightarrow \bar{p} + p$
- (b)  $\bar{p} + p \rightarrow \pi^- + \pi^+$
- (c)  $\bar{p} + p \rightarrow K^- + K^+$

*Antiproton-Proton  
 Elastic Scattering and  
 Two Body Annihilations  
 (ref. 74)*

have been studied using the apparatus described in the 1971 Annual Report (Experiment 10). Data-taking started in August 1971 and was completed in June 1972. Measurements were made at 21 incident antiproton momenta between 0.7 GeV/c and 2.4 GeV/c, covering a range of total energy in the centre of mass from 2.02 to 2.57 GeV/c<sup>2</sup>.

The antiproton-proton system allows the formation of meson states with masses greater than two nucleon masses. At present, the mass range covered by this experiment contains contradictory results concerning the existence of meson states. The analysis of this experiment in conjunction with the asymmetry measurement described later should permit a partial wave analysis of process (b) to be made in this energy region.

Figure 18. Differential cross-section for  $\bar{p} + p \rightarrow \bar{p} + p$  at 1.3 GeV/c incident momentum. (Preliminary data from Experiment 10).

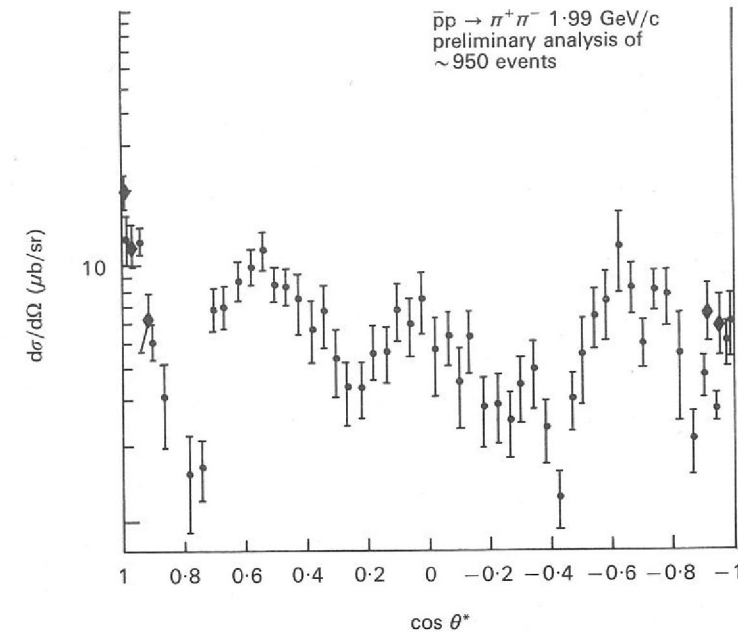
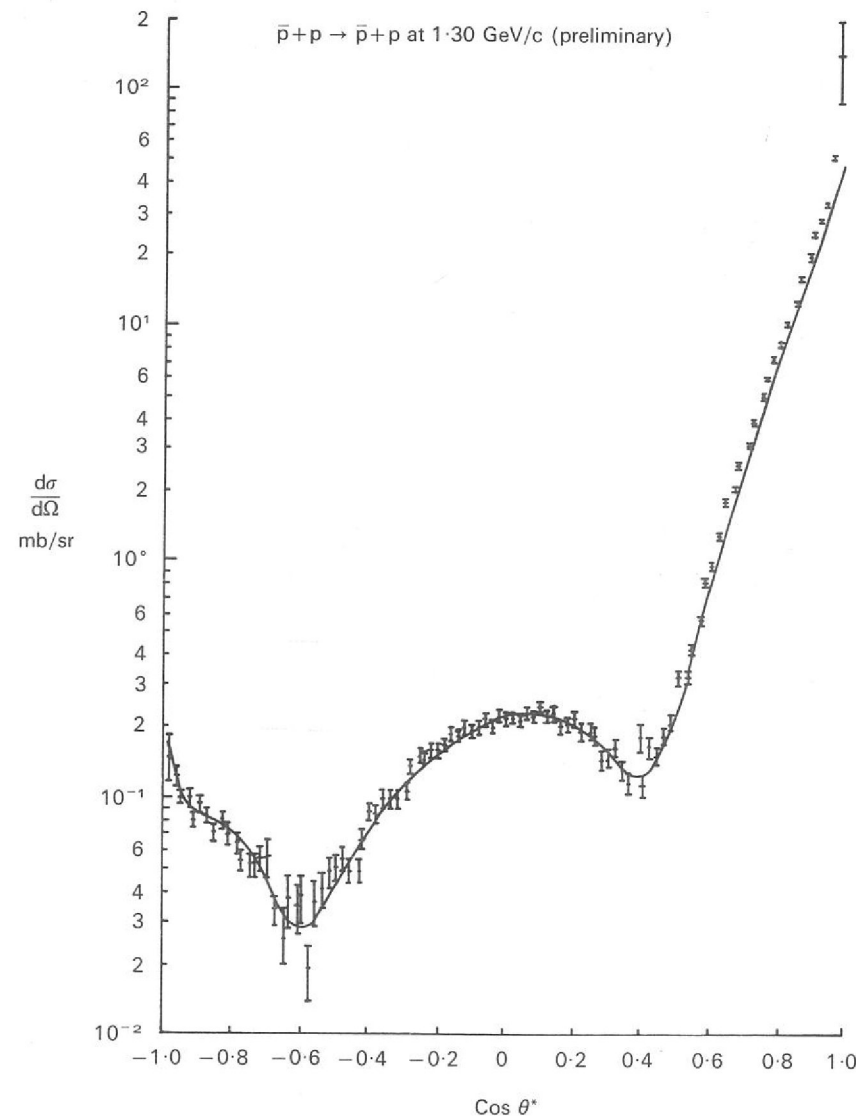
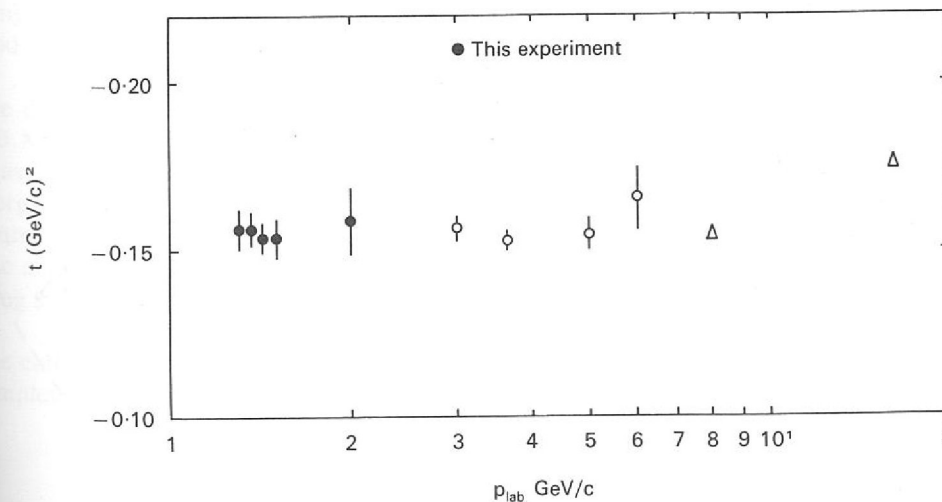


Figure 19. Differential cross-section for  $\bar{p} + p \rightarrow \pi^- + \pi^+$  at 1.99 GeV/c incident momentum. (Preliminary data from Experiment 10).

Data were recorded simultaneously for the three channels mentioned above. Of a total of  $8 \times 10^6$  events, 25% corresponded to (a) and 0.6% to (b) and (c) after broad cuts were applied to the data. The analysis of the experiment is presently in progress using the Rutherford and Daresbury Laboratories' computers. A fraction of the data was subjected to a preliminary analysis at CERN to monitor the quality of data being recorded. Figure 18 shows a differential cross-section for process (a) and Figure 19 for process (b) taken from this preliminary work. In the final angular distributions at each momentum about 40,000 events are expected for process (a), 1,500 for process (b) and 400 for (c).

The smaller fluxes of antiprotons available during parasitic operation of the beam were used to study small angle elastic proton-proton and antiproton-proton scattering. The position of the cross-over point (where the two differential cross-sections are equal) could thus be measured with the same apparatus and in the same geometry. The measured position of this cross-over point in 't' (square of the four-momentum transfer) as a function of incident momentum is shown in Figure 20 together with data available at higher incident momenta. Only a fraction of the available data from this experiment is represented.

Figure 20. Cross-over point for the elastic  $\bar{p} + p$  and  $p + p$  forward differential cross-sections versus incident momentum, for a fraction of the available data (Experiment 10).



# Experiment 11

UNIVERSITY OF WARWICK  
RUTHERFORD LABORATORY

(Proposals 81, 101)

*Differential Cross-Sections and Polarization Effects in the Charge Exchange Reactions  $\pi^- p \rightarrow \pi^0 n$  and  $\pi^- p \rightarrow \eta^0 n$ .*

In this experiment differential cross-sections and polarizations for the charge exchange reactions  $\pi^- p \rightarrow \pi^0 n$  and  $\pi^- p \rightarrow \eta^0 n$  are being measured at 30 incident momenta between 600 and 3500 MeV/c. A large number of pion-nucleon resonances are known to be formed in this momentum range and others have been suggested by current theoretical models. One of the objects of the experiment is to provide new data to be incorporated into an analysis in terms of partial wave amplitudes. From the behaviour of these amplitudes as a function of momentum of the incident pion, it is possible to obtain information on the properties of any resonant states which may be formed in the scattering process.

At present the measurements of the differential cross-sections are being made by scattering the incoming pions off a liquid hydrogen target. The experimental arrangement is shown in Figure 21. When these are complete the hydrogen target will be replaced by a polarized target and the polarizations will then be measured.

It is a characteristic of the charge exchange reaction that as the beam momentum increases from 600 MeV/c to 3500 MeV/c the differential cross-section over much of the angular region drops by more than 3 orders of magnitude. Hence, in order to achieve reasonable data taking rates, it is desirable to have detectors which cover as much of the solid angle around the target as possible and for the target itself to have a large angular access. The polarized target which is being developed for the polarization measurement enables as much as 67% of the total possible solid angle to be used.

As can be seen in Figure 22 the counter arrays surrounding the target are designed to take full advantage of this solid angle. The neutron counters consist of cells, each one metre long, filled with liquid scintillator. The neutrons are detected in these counters when they undergo nuclear collisions which yield charged secondary particles. The scintillation light from the secondary particles is detected by photomultiplier tubes.

Figure 21. Diagram of the apparatus for Experiment 11 with liquid hydrogen target installed. The latter will be replaced by a polarized target during 1973 so that polarization measurements may be made.

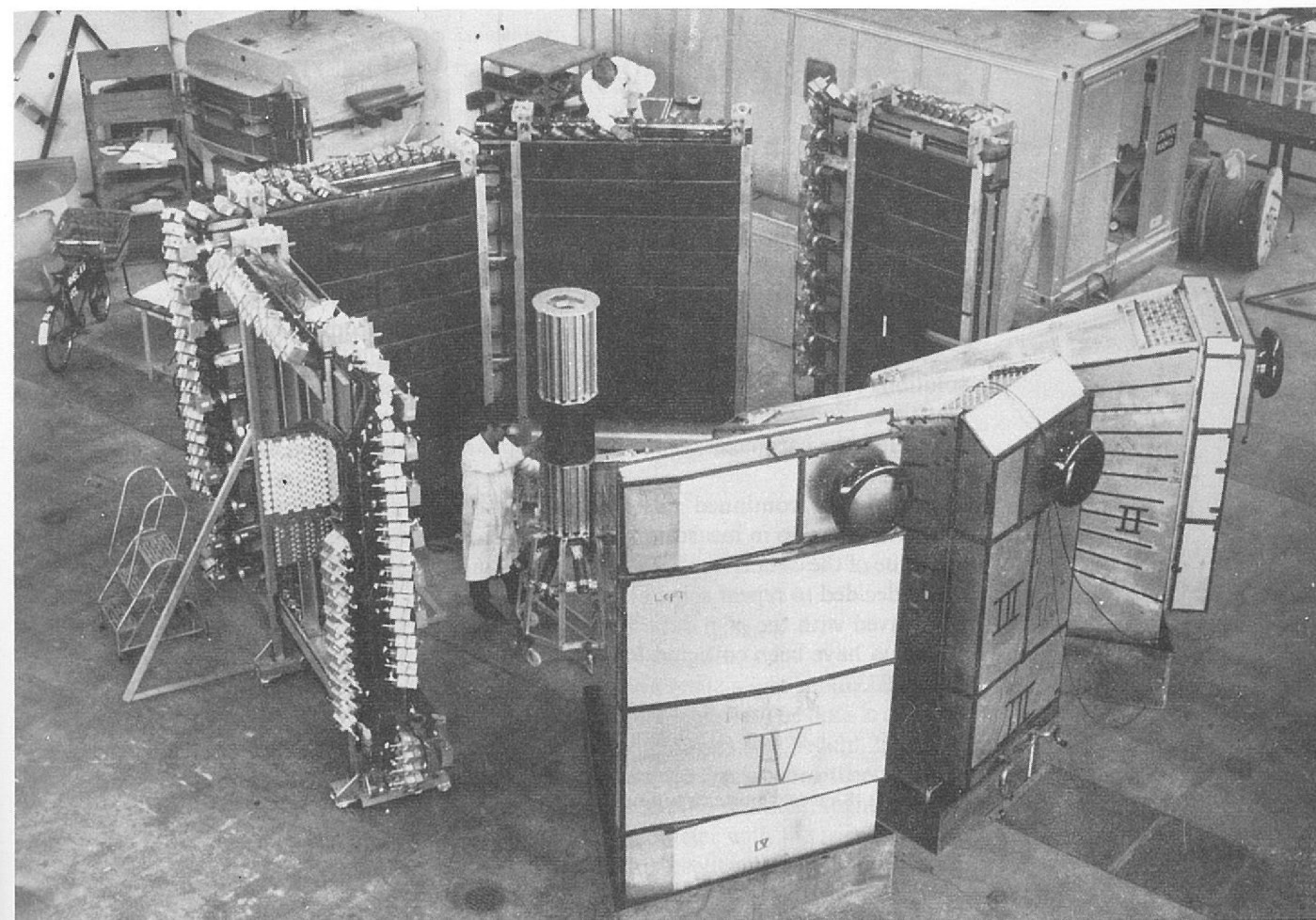
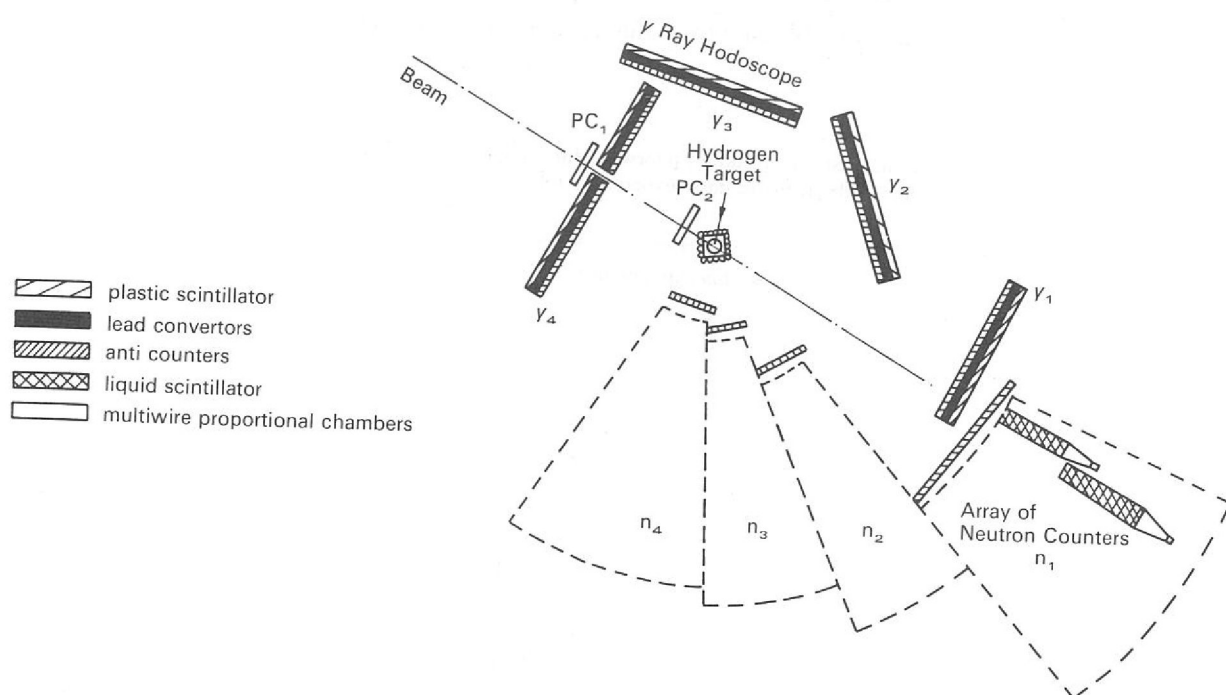


Figure 22. (Experiment 11) The gamma-ray hodoscopes and neutron counters arranged as in an exploded view around the polarized target veto counter. (11760)

The  $\pi^0$  and  $\eta^0$  mesons travel only a minute distance ( $< 10^{-4}$  cm) before decaying into two  $\gamma$ -rays. These  $\gamma$ -rays are converted by large sheets of lead to electron-positron showers. Each shower is detected in hodoscopes of plastic scintillation counters placed immediately behind the lead.

The neutrons and  $\gamma$ -rays can be detected with sufficient angular resolution to distinguish charge exchange events from neutral background processes. Plastic scintillation counters placed around the target and in front of each counter array are used to reject charged particle backgrounds.

The measurement of the differential cross-section requires a knowledge of the overall efficiency of the detectors. The efficiencies of the  $\gamma$ -ray hodoscope have been measured using photons of known energy. These photons were selected from the bremsstrahlung produced in a thin radiator bombarded by electrons present in the  $\pi^9$  beam.

The detection efficiencies of the neutron counters were determined at momenta above 600 MeV/c using neutrons scattered elastically off protons in the N4 neutral beam. A measurement of the momentum and angle of the recoil proton enables the angle and energy of the scattered neutron to be predicted. Comparison of the predicted number of neutrons with the number observed in the neutron array gives the detection efficiency. The efficiencies at momenta below 600 MeV/c were measured at the Harwell cyclotron, using a neutron beam of known intensity and energy.

The collection of differential cross-section data which is now in progress is expected to be complete by February 1973. Measurements of the polarization will then commence.

# Experiment 12

(Proposals 83, 105)

UNIVERSITY OF BRISTOL  
UNIVERSITY OF SOUTHAMPTON  
RUTHERFORD LABORATORY

Differential Cross-Sections in  $\pi^\pm p \rightarrow \pi^\pm p$  from 0.6–2.0 GeV/c (ref. 168)

This experiment uses the same beam line and apparatus as Experiment 3. The data which were taken last year, covering  $\pi^+ p$  elastic scattering at 18 incident momenta between 0.8 and 1.6 GeV/c have now been analysed and an isometric plot is shown at Figure 23. A plot of the forward point and comparison with predictions from forward dispersion relations is shown in Figure 24. The data have been used in a re-minimisation of existing phase-shift solutions together with new theoretical work from Bristol University on the higher partial wave amplitudes. The new amplitudes do not differ markedly from the earlier values but they allow the parameters of the known resonances to be defined more accurately.

The work has continued this year in extending the momentum range, increasing the statistics, and also in measuring differential cross-sections for  $\pi^- p$  elastic scattering. Since the value of the data is improved if both  $\pi^+ p$  and  $\pi^- p$  are taken under the same conditions, it was decided to repeat some of the earlier  $\pi^+ p$  work at the same time and so this is being interleaved with the  $\pi^- p$  data. So far about 25,000 elastic scattering events at each of 18 momenta have been collected for each charge. Data taking should be completed by February 1973.

Figure 23. An Isometric plot of the differential cross sections for  $\pi^+ p$  elastic scattering at 18 incident momenta between 0.8 and 1.6 GeV/c. (Experiment 12).

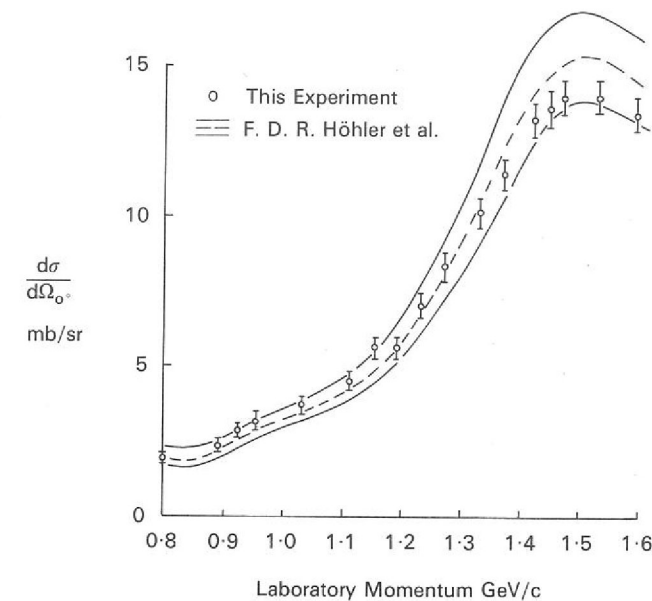
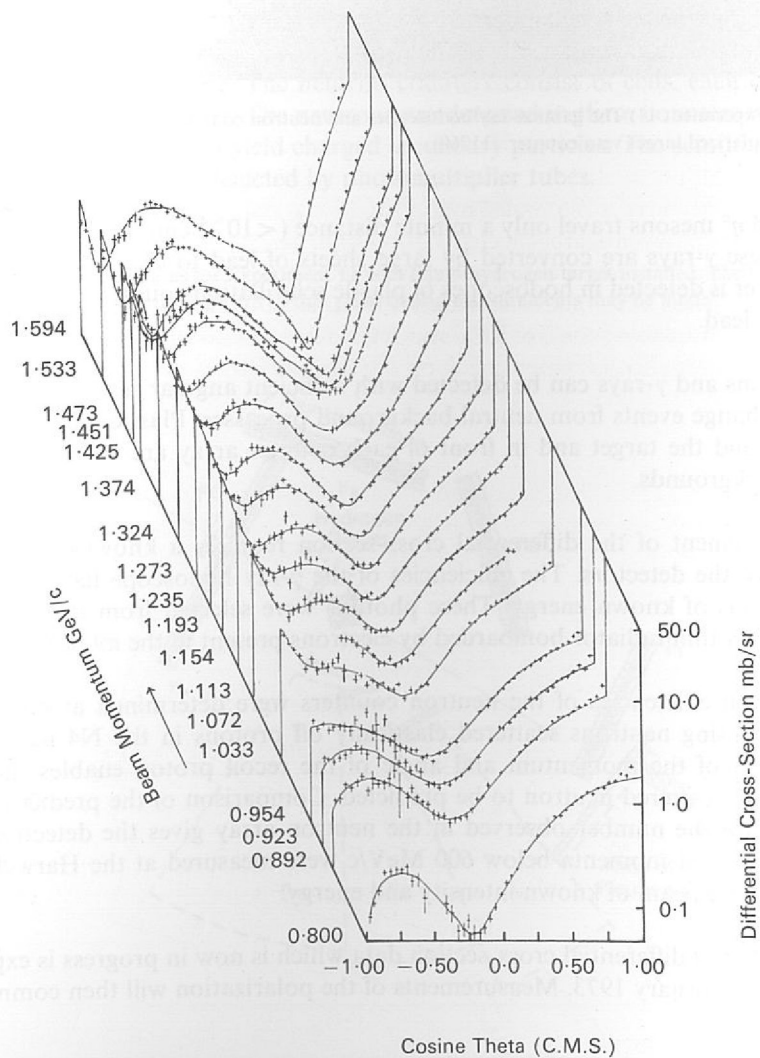
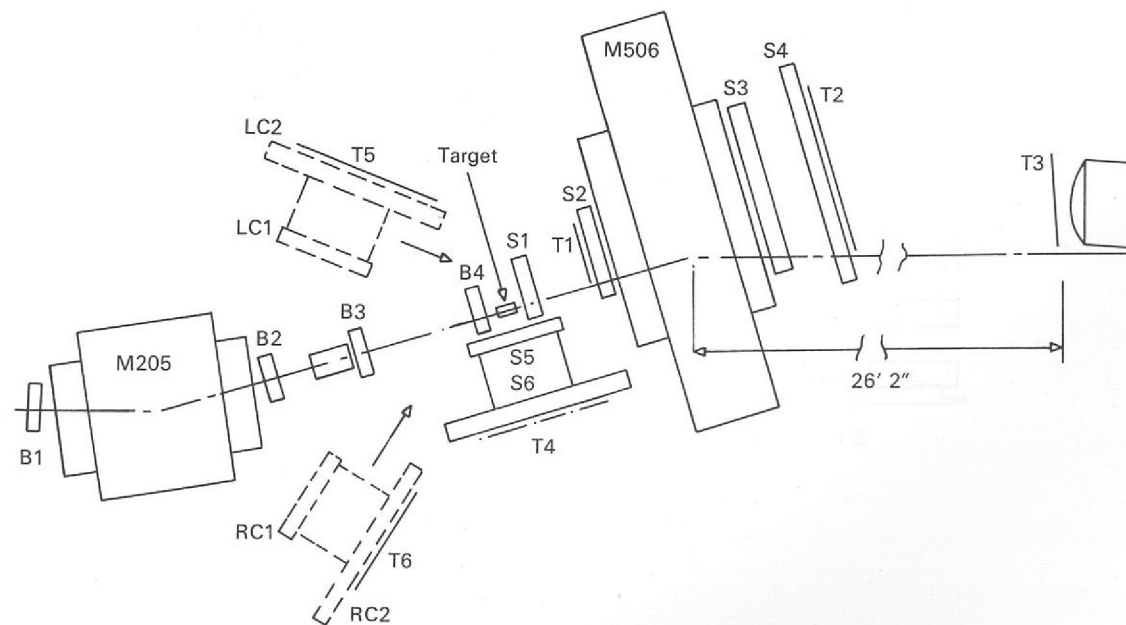


Figure 24. Forward differential cross-section from data of Experiment 12. The solid lines show the predictions of forward dispersion relations.

Since the apparatus was designed for  $K^\pm p$  elastic scattering some slight modification has been necessary to accommodate the different kinematics for  $\pi^\pm p$  data. The data is collected in three modes, each covering a different range of scattering angles (see Figure 25). In the "spectrometer mode", which covers the forward and backward region of the scattering distribution, only the forward going particle (scattered or recoil) is detected. Its momentum and direction are measured using magnet M506 as a spectrometer with the trigger counter T1 and T2 and the spark chambers S1–S4. Elastic scattering events are required to have a measured momentum within 4% of the predicted value for the observed angle. Since the  $\pi^-$  and proton have opposite charge it is necessary to run with both spectrometer magnet polarities when studying  $\pi^- p$  scattering.

In the "correlation mode" the scattered particle and the recoil proton are both detected using the trigger arrays T5 and T6 and the spark chambers LC1, LC2, RC1 and RC2. Elastic scattering events are selected during analysis by the angular correlation between incoming and scattered tracks. The remaining angular region is covered by a new configuration: the "overlap mode" in which a modified correlation arrangement is used with T4, S5 and S6 replacing the T6, RC1 and RC2 detectors. In this way we retain the advantages of the internal consistency check on our normalisation.

Figure 25. Diagram showing how the apparatus in Experiment 12 is arranged in three different modes to cover different angular ranges. The items shown dotted are in their extracted positions.



# Experiment 13

UNIVERSITY OF CAMBRIDGE  
RUTHERFORD LABORATORY

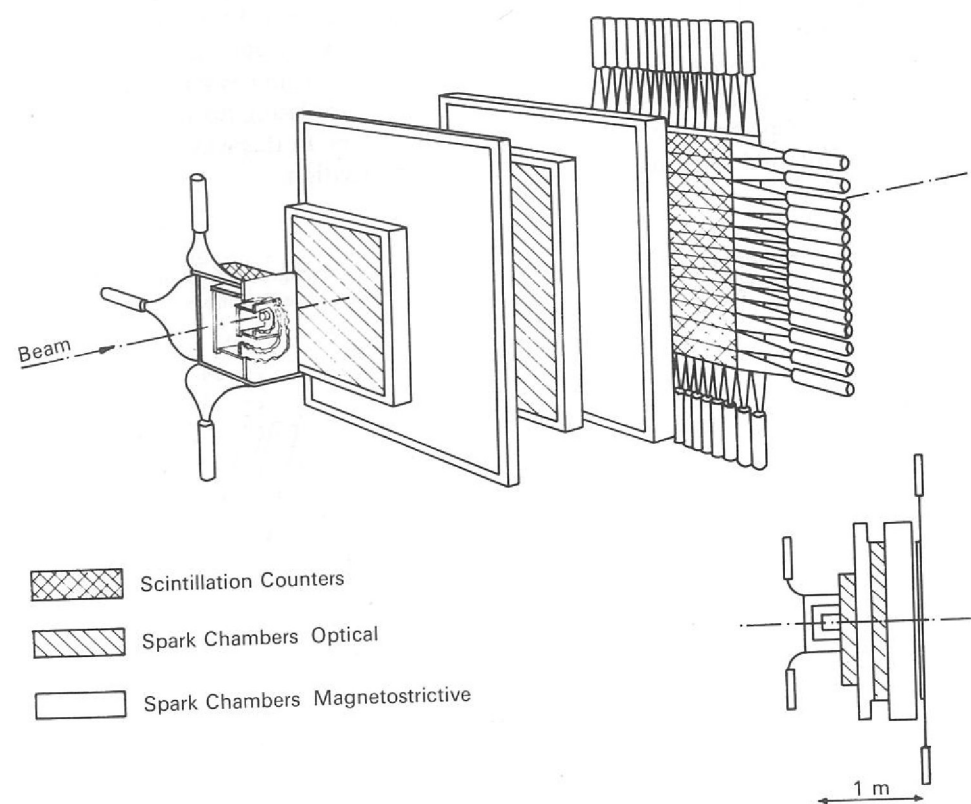
(Proposal 87)

*Differential Cross-Sections and Polarization in the Reaction  $\pi^- + p \rightarrow K^0 + \Lambda^0$  between Threshold and 1.4 GeV/c.*

The object of the experiment is to identify resonances in the  $\pi N$  system in the mass range 1600 to 1850 MeV/c<sup>2</sup> and to determine their parameters. A study of this reaction,  $\pi^- p \rightarrow K^0 \Lambda^0$ , is of particular interest for low spin resonances in this mass region since (a) the reaction is a pure isotopic spin channel, (b) high angular momentum waves are inhibited by centrifugal barriers near threshold and (c) polarization data are obtained simultaneously from the decay asymmetry in  $\Lambda^0 \rightarrow p \pi^-$ .

The detection equipment comprises spark chambers and scintillation counters controlled and monitored by a DDP 516 on-line computer. A diagrammatic view of the experiment is shown in Figure 26. The large acceptance of the apparatus allows high statistics to be obtained. Data taking was completed at the end of 1972. About 80,000 pictures were taken at each of the following momenta: 940, 980, 1020, 1040, 1100, 1160, 1220 and 1340 MeV/c. After analysis 10,000 events at each momenta are expected. The momentum measurement uncertainty for beam particles was 0.3%, allowing detailed study in the region of the  $K^0 \Sigma^0$  threshold at 1033 MeV/c where structure has been suggested in other experiments. Measurement of the film using CYCLOPS, a flying spot digitizer, has started. Analysis procedures are being established.

Figure 26. A diagrammatic view of the apparatus of Experiment 13. (8591).



# Experiment 14

WESTFIELD COLLEGE, LONDON  
UNIVERSITY OF BIRMINGHAM  
UNIVERSITY OF TEL AVIV  
RUTHERFORD LABORATORY

(Proposal 88)

The properties of neutral bosons ( $X^0$ ), produced in the processes  $\pi^- (K^-) p \rightarrow n X^0$ , are being studied through their decays.

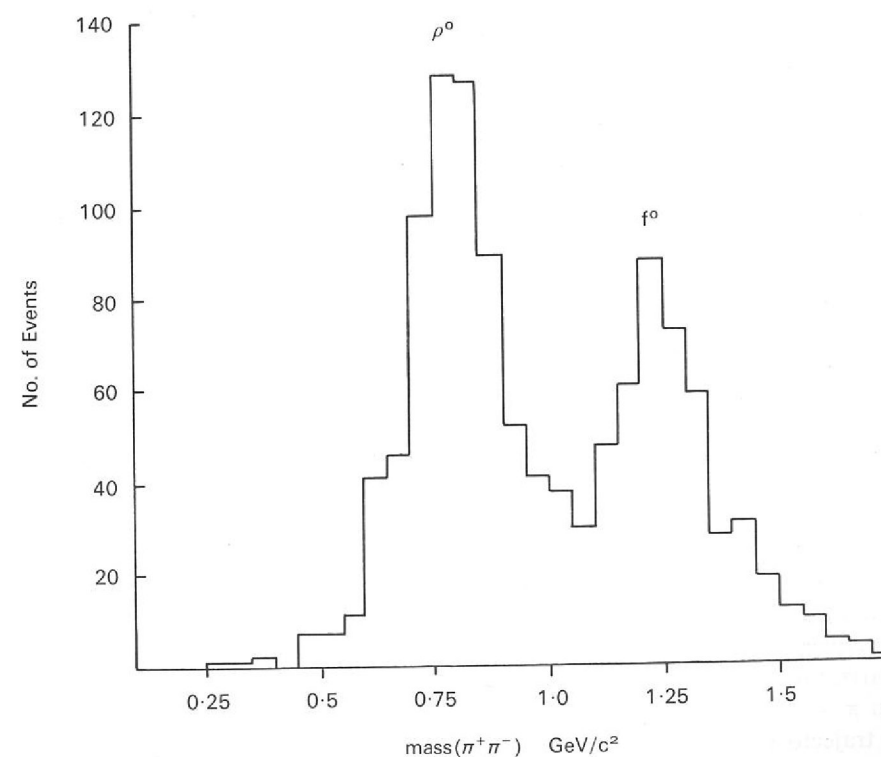
*A Study of Neutral Bosons Using a Neutron Time of Flight Trigger*

The decay products are detected in the optical spark chambers (volume 6 m<sup>3</sup>) in the field of the Omega superconducting spectrometer magnet at CERN. This has a very high detection efficiency for charged particles over almost all the solid angle about the target. The chambers are triggered by the detection of a neutron, within a preselected range of times of flight, by a large (3 m x 1.5 m) modular scintillation counter. The angle of emission of the neutron and its time of flight define the mass of the recoiling  $X^0$  to, typically, better than  $\pm 20$  MeV/c<sup>2</sup>.

After tests and calibration at RHEL and AERE, the neutron counter arrived at CERN in May 1972 ready for the start of Omega operation in June. Meanwhile, the lead-oxide vidicon cameras used for direct digital read-out of the optical chambers had been developed by the collaboration and CERN, and were installed in the experiment.

Since June the four groups using Omega, plus some parasitic users, have tuned up their experiments and the complex data handling system. This comprises a PDP-11 computer per experiment, with the Main User connected to a larger computer handling the television cameras and the beam proportional chambers, the whole linked to a computer capable of on-line analysis of a sample of data. The magnet, (currently running with only one coil and giving a central field of 1.0T) has performed well and the television camera system yielded the specified  $\pm 0.5$  mm accuracy.

Figure 27. Effective mass of  $\pi^+ \pi^-$  system in the  $\pi^+ \pi^- n$  final state showing the  $\rho^0$  and  $f^0$  peaks. (Experiment 14).



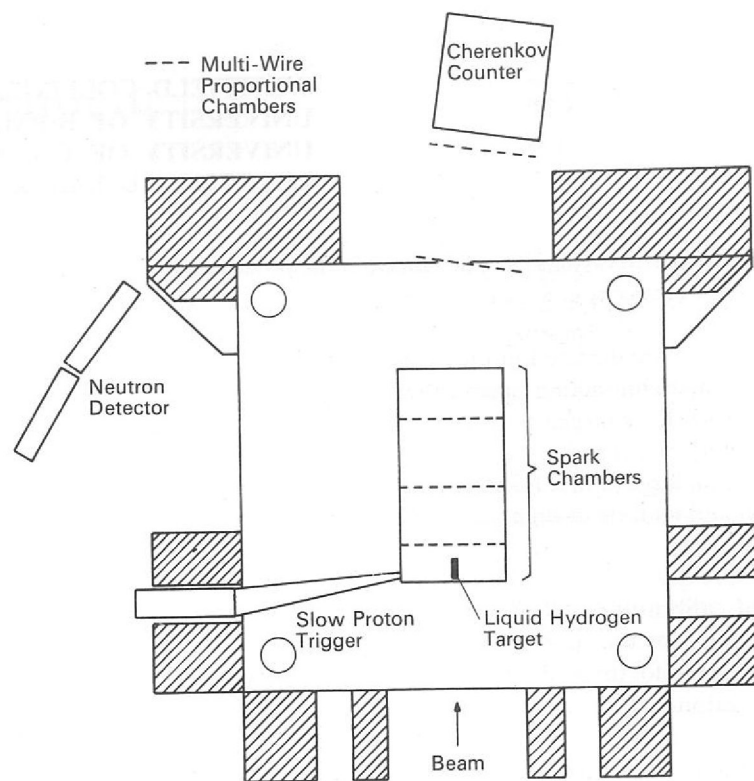


Figure 28. Diagram indicating positions of detectors for Experiment 14 in the Omega superconducting magnetic spectrometer at CERN

These preparations culminated in a 15 day shared data-taking run in October, during which this experiment took some 300,000 events with 8 GeV/c  $\pi^-$  beam, under various conditions covering the mass range 0.5 to 1.6 GeV/c<sup>2</sup> and the range  $0.015 < |t| < 0.8$  (GeV/c)<sup>2</sup>. Over 100,000 events have been through pattern recognition and geometry programmes with 2-prongs (i.e.  $n\pi^+\pi^-$ ,  $n\pi^+\pi^-\pi^0$ ) selected for special study. The decay distributions of  $\rho$ ,  $\omega$ ,  $f$  can be examined to give information on possible detection inefficiencies and biases. Figure 27 shows the  $\rho$  and  $f$  signal from a sample of the data; the agreement with published bubble chamber data is good. The RHEL kinematics programme is being converted to run on the CERN CDC 7600 computer when full kinematic fitting will be done.

## Experiment 15

(Proposal 90)

UNIVERSITY OF OXFORD  
UNIVERSITY OF PARIS-SUD  
CERN

*Measurement of the Polarization Parameter in  $\pi^+p$  Backward Elastic Scattering at 6 GeV/c (ref. 25, 181)*

This experiment was described in some detail in the 1971 Annual Report and the final results on  $\pi^+p$  scattering were presented there. The running of the experiment and the data analysis are now complete, and we present here the final  $\pi^-p$  results. The purpose of the experiment is to measure the polarization in both  $\pi^+p$  and  $\pi^-p$  elastic scattering in the backward peak region. This region is believed to be dominated by baryon exchange in the crossed ( $u$ ) channel. For  $\pi^-p$  backward scattering, the simple Regge pole model with linear trajectories predicts zero polarization, as only a single trajectory, the  $\Delta_b$ , can be exchanged. However, if cuts or other contributions are present, or if the trajectory has a term in  $\sqrt{u}$ , the polarization can be non-zero. The final  $\pi^-p$  results are shown in Figure 29, where they are compared with some of the models. The polarization is definitely non-zero, and moreover is not reproduced by the models. An interesting feature of the results is that the polarization  $P_0(u)$  in  $\pi^-p \rightarrow p\pi^-$  is very similar in magnitude and shape to  $P_0(t)$  in the reaction  $\pi^-p \rightarrow \pi^0n$ , where again only a single trajectory (albeit a meson rather than a baryon trajectory) can be exchanged.

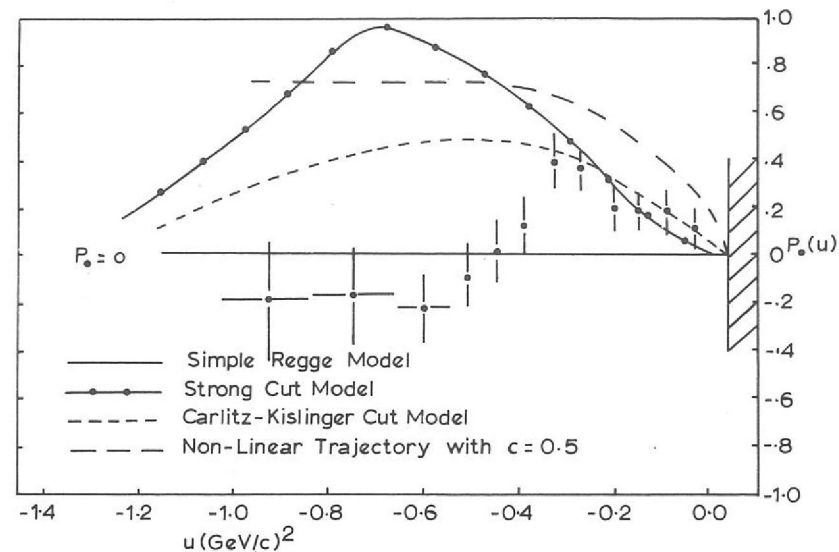


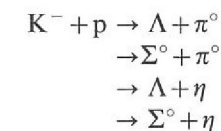
Figure 29. Measured polarization at 6 GeV/c from analysis of  $\pi^-p$  backward elastic scattering data taken in Experiment 15. Also shown are the predictions of some of the models.

## Experiment 16

UNIVERSITY OF OXFORD

(Proposal 92)

This experiment is a study of resonance states formed in  $K^-p$  interactions, in particular the reactions



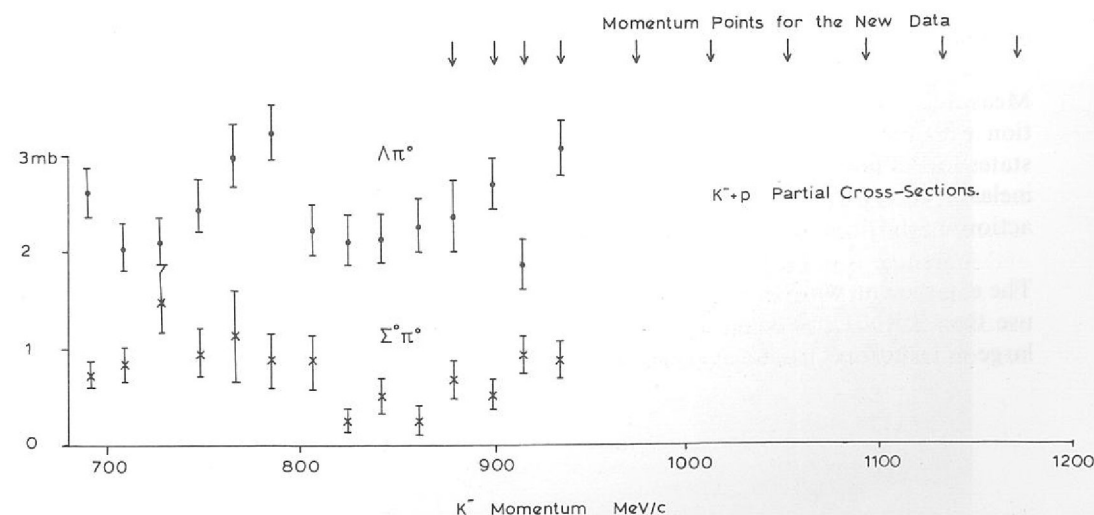
*Neutral States from  $K^-p$  Interactions (ref. 178)*

19 magneto-restrictive wire spark chambers, placed around the target to digitise the  $K^-$ ,  $\pi^-$  and  $p$  tracks, were added to an existing lay-out to give improved efficiency of data-taking and data analysis.

Data have been taken at 10 momenta, in the range 880 to 1180 MeV/c. At each momentum there are about 7 times as many events as were obtained in the earlier experiment. This greatly enhances the information in the  $\Sigma^0\eta$  threshold region and extends the phase shift analysis into the region of the D and F wave resonances up to mass 1870 MeV/c<sup>2</sup>.

Present work is directed towards an understanding of the performance of the wire spark chambers, by comparing events selected by that system with those analysed by optical spark chambers alone. This will permit normalisation of the new data. Figure 30 shows the cross-sections as obtained in the old experiment, with an indication of the range of the data.

Figure 30.  $K^-p$  partial cross-sections from early data taken in Experiment 16. The range of the new data is indicated.



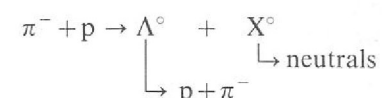
## Experiment 17

UNIVERSITY OF ROME  
RUTHERFORD LABORATORY

(Proposal 93)

*Study of Non-Diffractive  
Production of  $S = 1$   
Neutral Resonances*

The object of this experiment is to study the peripheral production of neutral  $K^*$ 's in the reaction



The experiment is designed to yield at least an order of magnitude more events than it has been possible so far and it covers, with good resolution, the mass interval from 500 to about 2000 MeV/c<sup>2</sup>. There is considerable interest at present in the question of which  $K^*$ 's are non-diffractively produced.

By a system of veto scintillation and water Cherenkov counters, slow lambdas are selected in association with neutral  $K^*$ 's. The directions of the beam pion and of the decay proton and pion are observed in a system of optical chambers and the momentum of the decay proton is measured by means of a range chamber. This information, together with the knowledge of the beam momentum, allows the determination of the mass of the missing system.

Data taking has been completed at the 2 momenta of 6.5 and 10 GeV/c and the experiment is now in the analysis stage. Digitization of the events is currently under way at the Rutherford Laboratory using HPD II. Final results are expected during 1973.

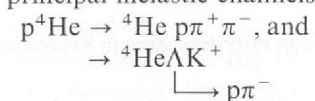
## Experiment 18

CERN  
UNIVERSITY COLLEGE, LONDON  
UNIVERSITY OF UPPSALA

(Proposal 95)

*Coherent Production of  
 $I = \frac{1}{2}$  States on Helium*

The object of this experiment is to study the elastic and inelastic scattering of 19 GeV/c protons on helium nuclei. The principal inelastic channels of interest are



in which all final-state particles are charged, but it is anticipated that data will also be obtained on channels with a single neutral particle in the final state.

Measurements of the decay distributions of the short-lived,  $I = \frac{1}{2}$  states produced in association with recoil helium nuclei are expected to provide spin-parity information on such states free of possible  $I = \frac{3}{2}$  contamination. On the other hand, comparison of elastic and inelastic data with the aid of specific models of coherent production will allow the interactions of the produced states in nuclear matter to be studied in detail.

The experiment, which is being set up in a high-energy proton beam at the CERN PS, will use the CERN/Uppsala spectrometer to detect the helium recoils and the CERN/MPI large-aperture spectrometer to measure fast forward particles from an event.

## Experiment 19

UNIVERSITY OF OXFORD  
UNIVERSITY OF CHICAGO  
HARVARD UNIVERSITY

(Proposal 96)

*A Study of Inelastic  
Muon-Proton Scattering  
at NAL (USA)*

The deep inelastic scattering of electrons on nucleons has been extensively studied at the Stanford Linear Accelerator Centre and the results are of great interest. In the deep inelastic region both the momentum transfer  $q^2$  and the mass  $W$  of the final hadronic system are large. The cross-sections are greater than expected and depend on the ratio  $q^2/W^2$  and not on  $q^2$  and  $W^2$  separately as one would expect. All attempts to interpret these experimental facts lead back to the scaling property originally predicted by Bjorken. An exciting feature of this prediction and its experimental observation is that the electric charge distribution within the proton has a point-like structure.

Muon inelastic scattering explores the same structure and this experiment aims, by using a muon beam at the National Accelerator Laboratory near Chicago, to extend the investigations in the following ways:

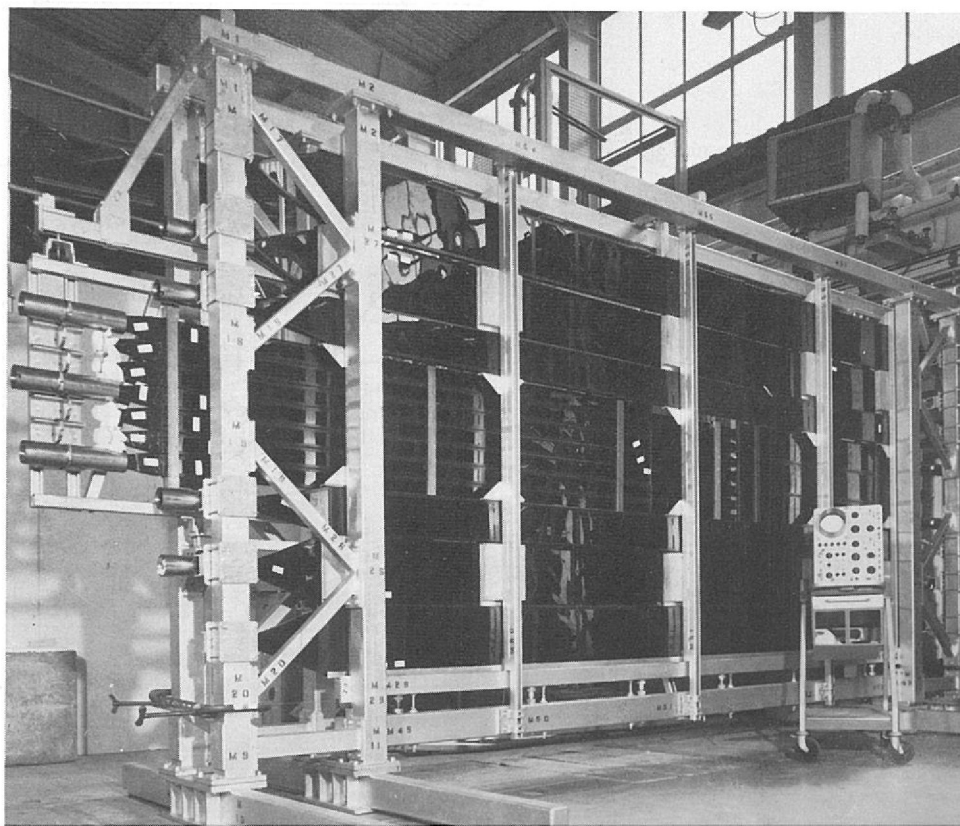
- (a) To investigate cross-sections and scaling over a very much wider range of kinematic variables.
- (b) To investigate the behaviour of the cross-sections in various channels of the hadronic recoil system.

The equipment consists of a muon beam of momentum adjustable from 50 to 200 GeV/c, a liquid hydrogen target, a large analysing magnet and various detectors for the scattered muon and the produced hadrons.

The University of Oxford, supported by the Rutherford Laboratory, has designed and built four large counter hodoscopes for the triggering system (see Figure 31), six hodoscopes for the incident beam, a gas Cherenkov beam counter and the equipment for measuring the field of the analysing magnet. All this equipment arrived at NAL in September 1972. Preliminary studies of the muon beam have been made.

In addition to providing equipment, Oxford collaborators are very actively involved in the preparation of programs to be used in a computer on-line to the experiment, and of programs to be used in the more sophisticated off-line analysis of the data obtained.

Figure 31. Photograph showing one of the scintillation counter hodoscopes in Experiment 19 used to trigger on scattered muons. The central horizontal counters detect muons scattered at small angles similarly the wider horizontal counters detect muons scattered at large angles. (11676).



## Experiment 20

(Proposal 98)

### The Pion-Nucleon Scattering Lengths

This experiment was described in detail in the 1971 Annual Report. Since then, improvements have increased the X-ray yield to 150/hour and have substantially enhanced the signal-to-noise ratio. Typical spectra from one run are shown in Figure 32. Data-taking is complete, and the data are being analysed.

The  $M_V$  photoelectric absorption edge in Bismuth has been measured using both a single crystal and a double crystal monochromator at Leicester University. The result is shown in Figure 33, together with a preliminary result from early data.

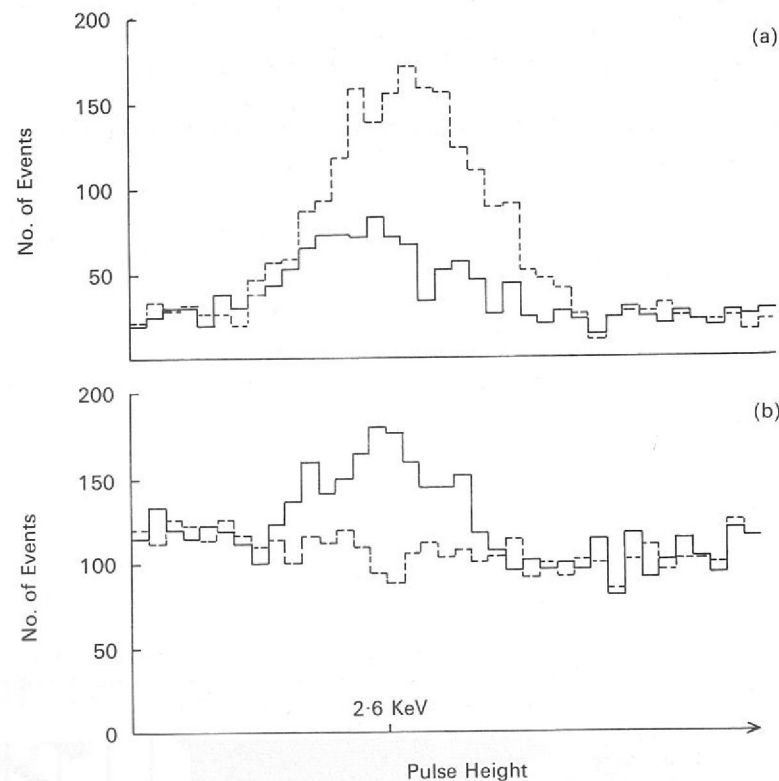


Figure 32. Typical X-ray spectra from a single run taken in Experiment 20.  
(a) The dotted histogram shows the spectrum of all K X-rays from pionic deuterium. The full lines show the  $K_{\alpha}$  spectrum remaining when a chlorine filter is inserted to remove the  $K_{\beta}$ , etc.  
(b) The full histogram shows the spectrum of the  $K_{\alpha}$  transmitted through a bismuth foil. The dotted histogram shows the background, measured by inserting a sulphur filter to absorb all X-rays.

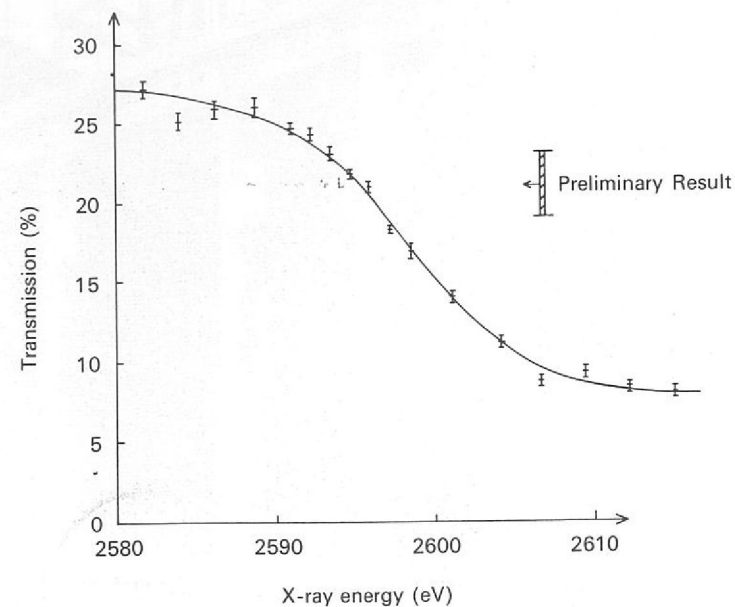


Figure 33. The  $M_V$  photoelectric absorption edge in bismuth, and the preliminary value of the transmission of  $K_{\alpha}$  pionic X-rays from deuterium.

QUEEN MARY COLLEGE, LONDON  
DARESBUURY LABORATORY  
UNIVERSITY OF BIRMINGHAM  
UNIVERSITY OF PISA  
UNIVERSITY OF MAINZ

## Experiment 21

(Proposal 103)

QUEEN MARY COLLEGE, LONDON  
DARESBUURY LABORATORY  
RUTHERFORD LABORATORY

In order to give a complete description of the reaction  $\bar{p} + p \rightarrow \pi^+ + \pi^-$ , two complex quantities known as scattering amplitudes must be specified. These amplitudes are directly related to quantities which can be measured experimentally such as the differential cross-section,  $\frac{d\sigma}{d\Omega}$  measured using a hydrogen target and the asymmetry,  $P$ , from a polarized

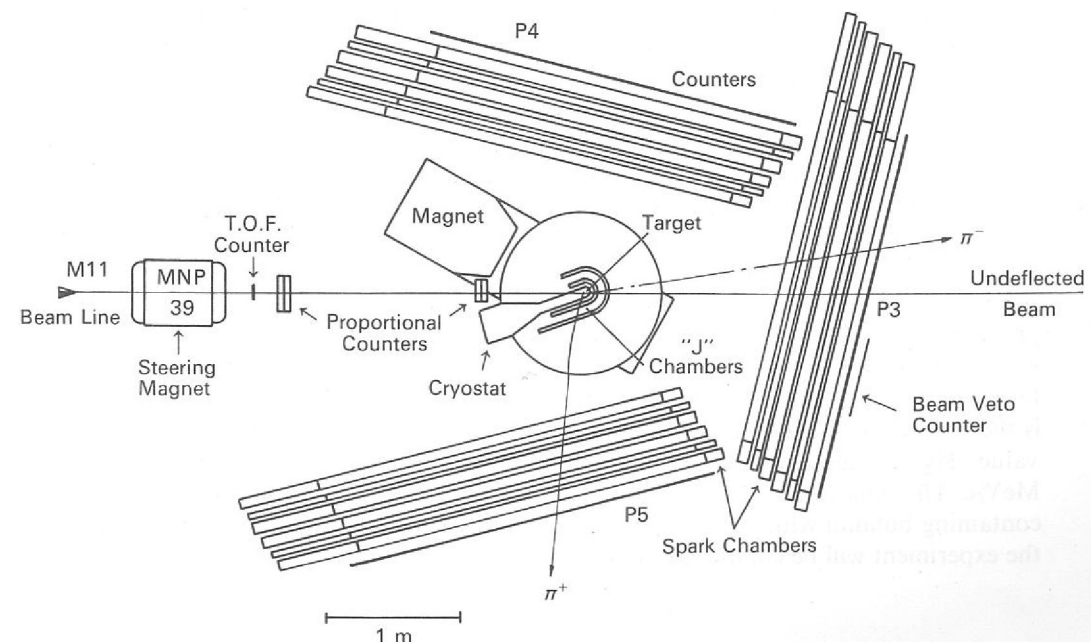
target. Measurements of  $\frac{d\sigma}{d\Omega}$  have already been made and the object of the present work is to measure  $P$  as a function of scattering angle for the process  $\bar{p} + p \rightarrow \pi^+ + \pi^-$  at incident  $\bar{p}$  momenta between 1.2 and 2.4 GeV/c. This range will cover the invariant mass region of the T and U Mesons (2190 and 2375 MeV/c<sup>2</sup> respectively).

A diagram of the apparatus is shown in Figure 34. The target consists of a cylinder of propanediol, 10 cm  $\times$  3.5 cm dia. which is placed in a magnetic field of 2.5T.

The antiprotons in the partially separated beam are selected by time-of-flight and their directions are measured by a series of multiwire proportional chambers. The trajectories of the outgoing particles are measured in cylindrical spark chambers within the magnetic field volume and in an arrangement of spark chambers placed around the polarized target magnet but outside the magnetic field region. This arrangement enables both the direction and the momentum of the outgoing particles to be determined so that a kinematic fit can be used to identify the 2-pion annihilation events. Most of the particle detection equipment

and electronics for this experiment have already been used in the  $\frac{d\sigma}{d\Omega}$  measurements. New equipment includes the polarized proton target, which has been constructed by the CERN polarized target group, the polarized target magnet (supplied by the Rutherford Laboratory), the multiwire proportional chambers and the cylindrical spark chambers. The experiment is currently being set up.

Figure 34. Diagram of the apparatus for Experiment 21. The polarized target consists of a cylinder of propanediol (100 mm  $\times$  35 mm dia.) which is situated in a 2.5T magnetic field.



Polarization in the Process  $\bar{p} + p \rightarrow \pi^+ + \pi^-$

## Experiment 22

(Proposal 107)

IMPERIAL COLLEGE, LONDON  
ETH, ZURICH  
CERN  
CEN, SACLAY

*Measurement of the P, A and R Parameters in the Backward Peak of the Reaction  $\pi^- p \rightarrow \Lambda K^0$ .*

The full determination of pseudo-scalar nucleon scattering amplitudes requires the measurement of the spin parameters P, A and R in addition to the differential cross-section. In the reaction  $\pi^- p \rightarrow \Lambda K^0$  this can be done by using a polarized target and measuring the decay angular distribution of the  $\Lambda$ , as was done in this experiment for the backward peak of the differential cross-section for this reaction, i.e. with forward going  $\Lambda$ 's, at an incident momentum of 5 GeV/c.

A 15 cm long butanol target was polarized in special pole-pieces added to the CERN-ETH Spectrometer Magnet at CERN. The average polarization was about 60%. Neutral final states were selected with a scintillation counter veto around the target and the  $p\pi^-$  decay of the  $\Lambda$  was selected with two planes of scintillation counter hodoscopes down-stream of the magnet. Optical spark chambers in the spectrometer magnet enabled the decay angles of the  $\Lambda$  to be measured. The photographs obtained have been measured on automatic measuring machines at CERN.

It is estimated that the data contain about 9,000 backward peak events on polarized protons and that this will enable us to give values of P, A and R in the range  $0 < -u < 0.8$  (GeV/c)<sup>2</sup> with errors of about  $\pm 0.1$ .

## Experiment 23

(Proposal 112)

UNIVERSITY OF OXFORD  
UNIVERSITY OF PARIS-SUD  
CERN

*Investigations of Spin Dependent Effects in High Energy Hadron-Proton Interactions at RHEL and CERN*

As a continuation of the programme of the CERN-IPN Orsay-Oxford collaboration, the group has initiated a series of experiments to study spin dependent effects in low cross-section p-p elastic scattering at large momentum transfer and in a qualitatively new area for such a study; that of hadron induced inclusive reactions. The energy region chosen for this investigation is that corresponding to an incident momentum of 8 GeV/c. This is the maximum momentum of the Nimrod proton accelerator and a momentum where high fluxes of secondary particles ( $\pi$ 's, K's) can be obtained from the CERN PS.

The first phase of this experiment is now running at CERN in an 8 GeV/c pion beam. The reaction being studied is the inclusive one,  $\pi^\pm p(\uparrow) \rightarrow \pi^\pm + \text{anything}$  where the  $\pi^\pm$  in the projectile fragmentation region is momentum analysed in a magnet spectrometer system with scintillation counter hodoscopes for trajectory determination and Cherenkov counters for particle identification. The kinematic region being covered is  $x = .2$  to  $x = .9$  where  $x$  is the ratio of the longitudinal momentum of the observed pion to its maximum possible value. The measurements are made at a fixed transverse momentum ( $P_T$ ) of  $(300 \pm 50)$  MeV/c. The polarized proton target used in the experiment is the 'standard' CERN type containing butanol with a free proton polarization of 70%. Data taking for this phase of the experiment will be completed by April 1973.

## Experiment 24

(Proposal 118)

RUTGERS UNIVERSITY, NEW JERSEY, USA  
IMPERIAL COLLEGE, LONDON

Theoretical developments in the last few years have revealed the importance of studying the single particle inclusive reaction  $a + b \rightarrow c + X$ . Here a, b, c are identified particles and X represents anything else. One of the first and simplest inclusive reactions to be measured in the new energy range at NAL is  $p + p \rightarrow p + X$ . Data on this reaction were collected in late 1972 using an internal H<sub>2</sub> jet target. By pulsing the jet target at different instants during the acceleration ramp, the above reaction was studied from  $p_{LAB} = 30$  to 200 GeV/c. At present this range is being extended to 400 GeV/c.

The H<sub>2</sub> jet target has been developed and brought to NAL by a team of Soviet physicists from the Institute of High Energy Physics at Serpukhov. The Rutgers-Imperial College experiment is run in parallel with a Soviet-American collaboration studying small angle elastic proton-proton scattering. Small modifications to the present apparatus will allow a more detailed study of  $p + p \rightarrow p + X$  as a function of s, t and  $M_x^2$  as well as a simultaneous study of reaction  $p + p \rightarrow n + X$ .

*Study of the Inclusive Reactions  $p + p \rightarrow p + X$ ,  $n + X$  between 30 GeV/c and 400 GeV/c*

## Bubble Chamber Experiments

The formulation and verification of a theory of elementary particle interactions not only requires conceptual advances but also more extensive, detailed and accurate experimental data.

The Rutherford Laboratory combined with outside Laboratories and Universities has maintained its extensive participation in many and varied bubble chamber experiments. 1972 has seen the extensive utilisation of the technical advances made during 1971 and a continued development and improvement of conventional techniques.

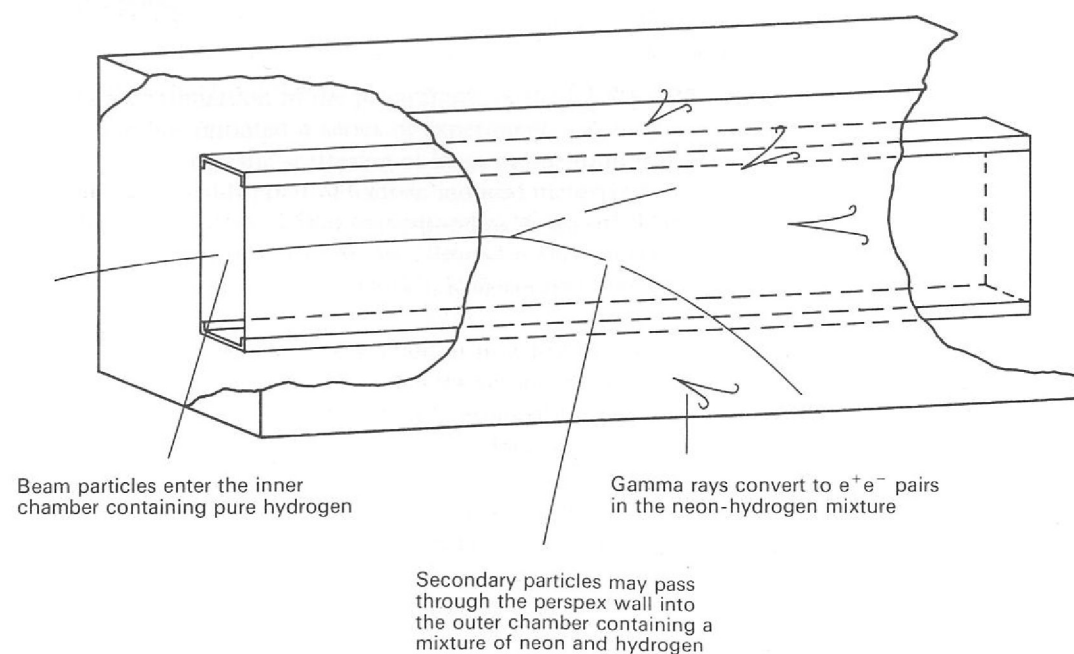
The requirement for the extension of the area over which data are available makes demands for new techniques. This demand the Rutherford Laboratory successfully met by developing the Track Sensitive Target (TST) Bubble Chamber which opened up an extensive region of physics not previously available for analysis. The demand for detailed and accurate data means higher statistics experiments. A fast and efficient film analysis processing system is in operation to handle the large volume of data involved.

### Utilisation of New Techniques

Following the important technical success of operating a track sensitive target in the 1.5 m bubble chamber in 1971 it has been extensively exploited in 1972. In addition another technical success was achieved by operating a fully transparent track sensitive target which opens the way for the full exploitation of this technique to larger chambers.

The fully transparent TST consists of a perspex walled vessel filled with liquid hydrogen which is mounted centrally inside the main bubble chamber. The chamber is filled with a liquid neon-hydrogen mixture. The arrangement is shown diagrammatically in Figure 35. The beam particles are introduced into the hydrogen region where they interact on free protons. Reaction products pass through the perspex into the neon-hydrogen mixture which has the property of a short radiation length and thus allows the efficient conversion of gamma rays into electron positron pairs.

Figure 35. Diagrammatic view of the neon-hydrogen track sensitive target inside the main bubble chamber.



1,545,000 pictures in the TST were obtained in 1972. These consisted of 1,340,000  $4 \text{ GeV/c } \pi^+p$  pictures (Experiment 32) and 205,000  $\bar{p}p$  pictures (Experiment 33). The new region made available for study by the bubble chamber consists of systems made up of a multiple number of particles with dominant electromagnetic decay modes e.g.  $\pi^0\pi^0$ ,  $\eta^0\pi^0$ ,  $\Sigma^0\pi^0$ . Some of these systems have severe quantum number constraints and are hence less complex than their charged particle counterparts. Thus there is hope that a more complete understanding of elementary particle interactions can be obtained from a study of these systems and especially from a comparison with their equivalent systems made up of charged particles.

The successful operation of the TST has opened new areas for future investigations and the preparation of these investigations has featured strongly in the work of the past year.

During 1972 a neutral  $K^0$  beam was built at CERN by a collaboration from the Rutherford Laboratory and the universities of Pisa, Bologna, Glasgow and Edinburgh. This beam was successfully run during the autumn of 1972 (Experiment 35) and constitutes the first monochromatic neutral kaon beam in Europe. This beam will allow a more precise study of some aspects of the strong interactions between neutral kaons and nucleons. The neutral kaons are obtained from the reaction  $\pi^-p \rightarrow \Lambda K^0$  produced in collisions of a high intensity pion beam with protons in a liquid hydrogen target. The photon background is kept low by selecting the neutral kaons produced at an angle of  $4^\circ$  to the direction of the pion beam.

1972 has been generally a year of increased data taking and data accumulation. For example the experiment studying  $14 \text{ GeV/c } K^-p$  interactions (Experiment 25) has now reached an exposure of 1,200,000 CERN 2 m pictures and is now the largest high energy  $K^-p$  experiment in Europe. This data accumulation is now necessary so that high energy physics can pass into a more advanced phase of investigation, which consists of more precise measurements and the study of finer detail so that current theoretical models can be refined or rejected.

In order to process the increasing amount of bubble chamber film required to supply the data for high energy physics analysis the already powerful film analysis system at the Rutherford Laboratory has been continuously developed and improved. The film analysis system consists of two sections. One is the rough digitising system supplying measurements to the automatic measuring machine (HPD) and the other is a system of two film plane measuring machines.

The rough digitising system consists of twelve measuring machines on line to an IBM 1130 computer which interfaces via a multiplexor to the peripheral units of the central computer, the IBM 370/195. These measurements then pass to the HPD for precise measurement of the events.

During 1972, the new multiplexor and 1130/370 interface have been commissioned. The next task is to commission an interface between the 1130 and a second disk drive. This will speed up response times for machine operators and also provide a permanent store of information for the 1130. Much of the effort applied to the 1130 system has been concentrated on documentation, program modifications for new experiments and on the preparation for measuring by "reduced guidance" on the HPD. As part of this preparation for the "reduced guidance" mode of HPD operation a series of test runs have recently been completed. In addition a continuing series of program modifications to improve overall systems efficiency and to increase available core storage are being made.

The second part of the film analysis system consists of two film plane measuring machines on line to a PDP8L computer. This system was set up to provide a backup to the HPD system and especially to handle events with complex topologies. It is now planned that in 1973 this system will be used to measure at least 20,000 events from the  $4 \text{ GeV/c } \pi^+p$  experiment using the track sensitive target chamber. This system has been brought into

### The Conventional Scene

### Film Analysis System (ref. 78)

production, measuring its first events during the closing weeks of 1972. A program of system development, to increase the measuring rate, will be pursued in parallel with production measuring.

#### Future plans

The Rutherford Laboratory Bubble Chamber Group look forward to experiments using the large bubble chamber BEBC at the 300 GeV/c accelerator. In preparation for this two scanning tables for handling film from BEBC have been received and during 1973 they will be incorporated in the IBM 1130 system to predigitise film for HPD measurement.

The Nimrod intensity is expected to be increased in the coming years and this will enable experiments using a rapid cycling bubble chamber technique to be performed and such experiments are under consideration.

The utilisation of the TST technique will be expanded and a proposal for a TST experiment in the 12 ft chamber at the Argonne National Laboratory in the USA has been made.

**Table 4**

List of Bubble Chamber Experiments

Expt. No.	Proposal No.	Experiment
25	109	14 GeV/c $K^-p$ Interactions.
26	108	$K^-p$ Interactions in the c.m. energy range 1775 to-1960 MeV.
27	39, 86	$\pi^+p$ Interactions in the momentum range 0.8 to 1.6 GeV/c.
28	56	$K^+d$ Interactions in the momentum range 2 to 3 GeV/c.
29	36	$\pi^+d$ Interactions at 4 GeV/c.
30	49, 82	Hyperon-proton Interactions.
31	85	n-p Interactions from 1 to 3.5 GeV/c.
32	91	$\pi^+p$ Interactions at 4 GeV/c using a neon-hydrogen track sensitive target system.
33	115	$\bar{p}p$ Interactions at 2 GeV/c using a neon-hydrogen track sensitive target system.
34	38	$K^-$ Interactions in a heavy liquid bubble chamber.
35	89	$K_L^0$ Decays and $K_L^0p$ Interactions in the momentum range 400 to 850 MeV/c.

## Experiment 25

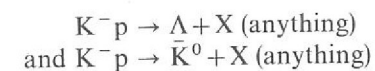
(Proposal 109)

ECOLE POLYTECHNIQUE, PARIS  
CEN SACLAY  
RUTHERFORD LABORATORY

14 GeV/c  $K^-p$   
Interactions  
(ref. 119, 131, 132, 133,  
134)

During the past year there has been a steady accumulation of data. The present statistical level is 10 events/ $\mu$ b. An additional 400,000 stereo photographs were obtained from the CERN 2 m chamber. This made the final exposure of the experiment equal to 1,200,000 stereo photographs and hence the largest high energy bubble chamber experiment in Europe.

In addition to the continuing study of two-body and quasi-two-body reactions, this year has seen the beginning of a large scale study of the inclusive data provided by the experiment. The reactions studied so far are:



This study which involved the use of the Triple Regge formalism facilitated the measurement of the effective trajectories of the  $\rho$ ,  $K^*$  and nucleon. These are shown in Figure 36. The results of these measurements suggest that the Triple Regge formalism is relevant to the description of inclusive reactions in the fragmentation regions and encourage a similar analysis at higher energy where the formalism is more strictly applicable. Also a significant polarization of the  $\Lambda$ 's with high laboratory momentum was observed and its possible correlation with other kinematic variables is being examined (see Figure 37).

Studies of the reactions:



are in progress. These will provide additional information about the exchange mechanism from the values of the spin density matrix elements of the  $\Delta^{++}$  and  $K^{*-}$  decays.

Figure 36. Effective trajectories obtained from the reactions  $K^-p \rightarrow \Lambda + X$  and  $K^-p \rightarrow \bar{K}^0 + X$  at 14.3 GeV/c. (Experiment 25).

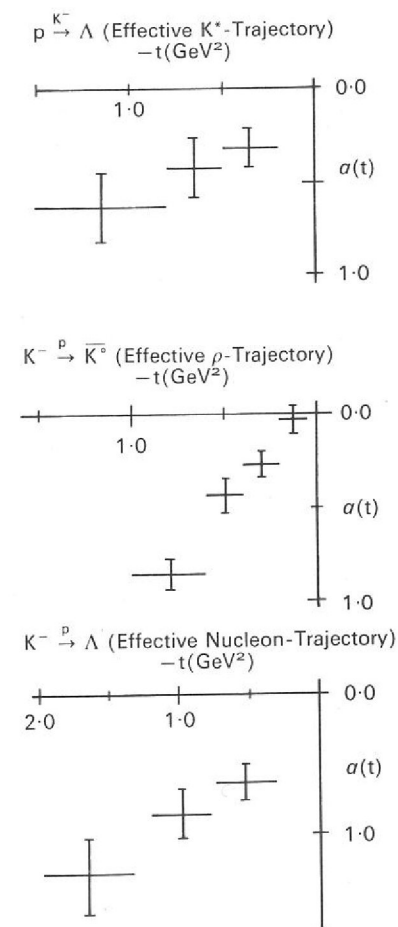
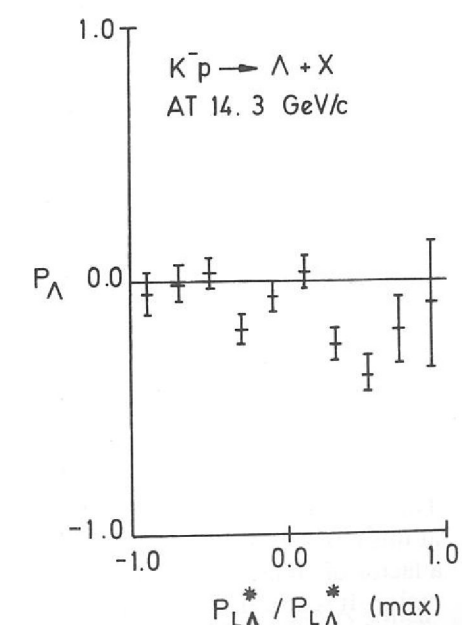


Figure 37. The  $\Lambda$  polarization as a function of  $x$  ( $x = p_{L\Lambda}^*/p_{L\Lambda}^{* \text{ (max)}}$ ) for the reaction  $K^-p \rightarrow \Lambda + X$  at 14.3 GeV/c. (Experiment 25).



## Experiment 26

IMPERIAL COLLEGE, LONDON  
RUTHERFORD LABORATORY

(Proposal 108)

*K<sup>-</sup>p Interactions in the  
Centre of Mass Energy  
Range 1775–1960 MeV*

This high statistics experiment is designed to resolve ambiguities in the partial wave analysis of the  $K^-p$  system in the centre of mass energy range from 1775 to 1960 MeV.

415,000 pictures were taken in the 2m Bubble Chamber at CERN at 11 beam momenta ranging from 1.0 to 1.4 GeV/c. The number of events at each momentum together with the number of events/ $\mu\text{b}$  are as follows:

Beam Momentum	1.00	1.04	1.08	1.12	1.16	1.20	1.24	1.28	1.32	1.36	1.40	Total
Number of Events	25731	24510	42240	39388	40212	43985	40778	50724	51403	53248	67264	479483
Number of Events/ $\mu\text{b}$	0.70	0.63	1.02	1.03	1.14	1.36	1.30	1.83	1.86	1.99	2.62	15.48

The total number of events/ $\mu\text{b}$  together with the ones from previous experiments in the same energy range are summarised below.

Momentum Interval	Number of Events/ $\mu\text{b}$	Experiment
1.00–1.40 GeV/c	15.48	This Experiment
0.777–1.226 GeV/c	3.32	CERN, Heidelberg, Saclay
1.263–1.843 GeV/c	8.03	Collège de France, Rutherford, Saclay
0.821–1.694 GeV/c	11.12	Lawrence Berkeley Laboratory

All the first measurements are now complete and remeasurements are under way. The analysis of events on data summary tapes has already started. As an example of the data we show in Figure 38 the missing mass squared to the  $\Lambda$  for events with a visible  $\Lambda$  and no charged prongs at the production vertex. The  $\pi^0$  and  $\eta^0$  peaks are clearly discernible together with the reflection at large masses of the  $\Sigma(1385)$  produced in the reaction  $K^-p \rightarrow \Sigma(1385) + \pi^0$ .

$\downarrow \Lambda\pi^0$

*K<sup>-</sup>p Interactions in the  
Centre of Mass Energy  
Range 1740–1800 MeV*

As an extension to this experiment, 310,000 pictures have been taken in the CERN 2 m Hydrogen Bubble Chamber, at four incident  $K^-$  momenta between 0.92 GeV/c and 1.04 GeV/c. The number of pictures taken at each beam momentum is shown below.

Beam Momentum	No. of Pictures
0.92 GeV/c	41K
0.96 GeV/c	32K
1.00 GeV/c	213K
1.04 GeV/c	24K

The extra pictures at 1.04 GeV/c were taken to increase the comparatively lower statistics at this momentum in the earlier exposure. The number of pictures at 1.0 GeV/c constitutes a factor of 10 increase in statistics, compared with earlier experiments around this energy region. It is hoped that such an increase in statistics will help reduce the number of ambiguous solutions in partial wave analyses of different channels, and thus provide anchor points for the energy continuation of partial wave solutions.

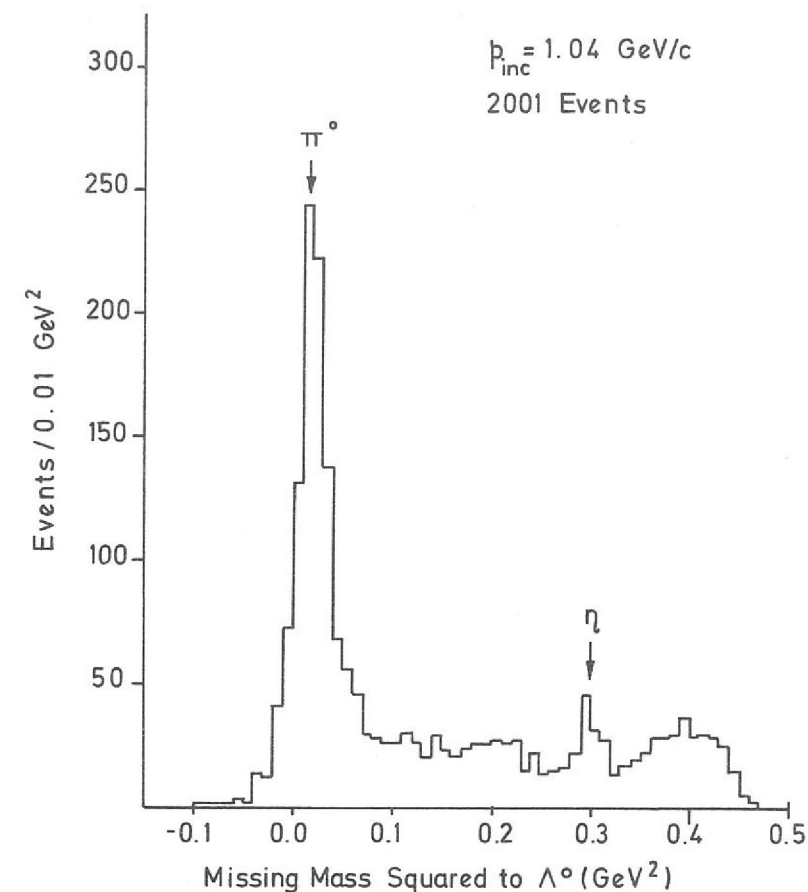


Figure 38. The missing mass squared in the reaction  $K^-p \rightarrow \Lambda + \text{missing mass}$ . (Experiment 26).

## Experiment 27

UNIVERSITY OF CAMBRIDGE  
IMPERIAL COLLEGE, LONDON  
WESTFIELD COLLEGE, LONDON

(Proposals 39, 86)

A systematic study of the  $\pi^+p$  interaction in the mass range 1500 to 1930 MeV is being undertaken using film from the 80 cm and 1.5 m hydrogen bubble chambers exposed at the Rutherford Laboratory.

**0.9 to 1.05 GeV/c.** In this experiment, film at 0.9, 0.95, 1.0 and 1.05 GeV/c has been analysed by Imperial College and Westfield College. A paper describing the single pion production channels has been published. Isobar-model studies using the joint Dalitz plot distributions for  $\pi^+\pi^0p$  and  $\pi^+\pi^+n$  have been continued. The results are in broad agreement with inelasticities from the latest elastic phase shift analyses. A paper presenting the results of this investigation is in preparation.

We are presently extending the above analysis to include all of the four variables which describe the three-body final state, and also developing an independent analysis using a different angular momentum formalism.

*$\pi^+p$  Interactions in the  
Range 0.8–1.6 GeV/c  
(ref. 4, 106)*

**1.1 to 1.5 GeV/c.** Data summary tapes now exist for all of the film at 1.1 and 1.2 GeV/c, and for part of the film at 1.3, 1.4, 1.45 and 1.5 GeV/c, containing about 40,000 events in total. A small amount of film taken at 1.55 and 1.6 GeV/c will not be processed, as the limited number of events prevents the detailed analyses that are underway at the other momenta. Dalitz plot fitting of the  $\pi\pi N$  channels has been carried out at 1.1 and 1.2 GeV/c and the results will be included in the paper mentioned above. In the elastic channel, our backward cross-sections continue to be lower than those reported by some counter groups. A study of the  $\pi-\pi$  interaction in the  $\pi\pi N$  channels is underway at the higher momenta.

**0.80 to 1.25 GeV/c.** This exposure includes film at 0.80, 0.85, 1.15 and 1.25 GeV/c. Much of the film has proved impossible to measure on the HPD automatic measuring system, and is now measured conventionally. Incomplete data summary tapes exist at 1.15 and 1.25 GeV/c.

## Experiment 28

IMPERIAL COLLEGE, LONDON  
WESTFIELD COLLEGE, LONDON

(Proposal 56)

*K<sup>+</sup>d Interactions in the  
2-3 GeV/c Region  
(ref. 23, 92, 104, 105,  
107, 170, 174, 183)*

About 750,000 frames have been taken with the deuterium filled 1.5 metre bubble chamber at Nimrod. This film is being measured on the Imperial College HPD. The further analysis of  $K^+$  hydrogen interactions in the range 2.1 to 2.7 GeV/c of a previous pilot exposure has been incorporated in this experiment.

The channel  $K^+p(n) \rightarrow K^{*+}p(n)$  has been studied in deuterium. The data confirm the variation of the  $K^*$  production angular distribution with centre of mass energy observed with a hydrogen filling in the bubble chamber. Preliminary results indicate a similar effect in the channel  $K^+n(p) \rightarrow K^{*+}n(p)$ . The general production and decay of these  $K^*$ 's produced without charge exchange indicate that  $\omega^0$  exchange is dominant. However the charge exchange production  $K^+n \rightarrow K^{*0}p$  goes by  $\pi$  exchange, and a simple OPE model gives good fits to the differential cross-section and the  $\rho_{00}$  and  $\rho_{10}$  density matrix elements.

The production amplitudes for  $K^*$  have been separated into  $I = 0$  and  $I = 1$  S-channel components; the angular distribution of the pure  $I_s = 0$  state is more sharply peaked forwards than the mixed isospin  $K^{*0}$  production.

A partial wave analysis of  $K\pi$  scattering has been started using the channel  $K^+n(p) \rightarrow K^+\pi^-p(p)$ . Using a sample of about 4000 events, results indicate that the S wave  $\delta_{\frac{3}{2}}$  phase shift approaches  $90^\circ$  at about 1 GeV and then remains constant up to about 1.3 GeV. This result is not sensitive to the  $\delta_{\frac{3}{2}}$  phases.

Among the coherent events, with a deuteron in the final state, a possible  $d^*$ , not associated with a  $K^*$ , is visible in the final state  $K^0\pi^+d$  and is being studied further.

The charge exchange between  $K^+$  and neutrons  $K^+n(p) \rightarrow K^0p(p)$  has been studied. Some evidence of a minor structure in the  $t$  distribution is seen, consistent with an earlier experiment at 2.3 GeV/c.

Various Regge model fits to this and other data have been made. Recent cut models involving different phases for cut and pole contributions ( $\rho$  and  $A_2$  poles are sufficient) are successful in predicting all measured  $\pi N$  cross-sections and polarizations. However they yield a cross-section for  $K^+N$  charge exchange at low energies only one half of that measured. Traditional pole models (e.g. Rarita-Schwartzschild) give good fits, but require an ill-established  $\rho'$  trajectory.

Less than half of the film has so far been processed. The remainder should be completed within the next year.

## Experiment 29

UNIVERSITY OF BIRMINGHAM  
UNIVERSITY OF DURHAM  
RUTHERFORD LABORATORY

(Proposal 36)

The purpose of this experiment is to study neutral boson states  $B^0$  produced in the reaction  $\pi^+d \rightarrow ppB^0$ .

*The Study of 4 GeV/c  
 $\pi^+d$  Interactions*

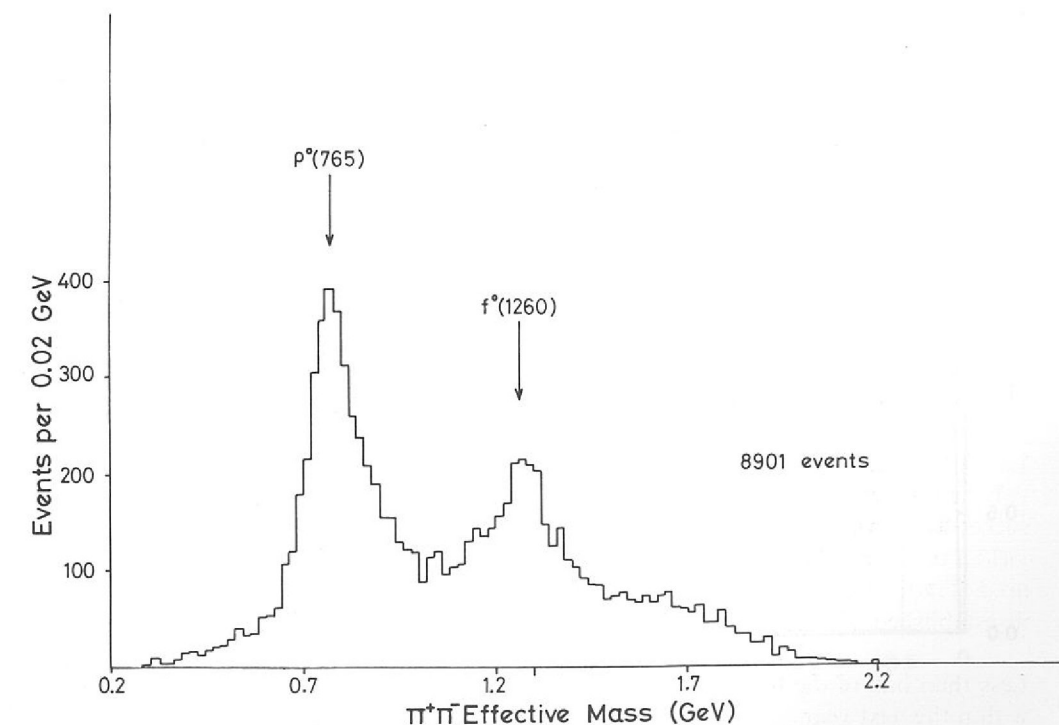
In 1970, 420,000 pictures were taken in the CERN 2 m bubble chamber using the U5 r.f. separated beam. A further 315,000 pictures were taken in December 1972 utilising the same experimental set-up.

The scanning and digitising of 90% of the first part of the film has been completed for most topologies. The events have been measured on HPD's both at the Rutherford Laboratory and at Birmingham, and a data summary tape containing about 180,000 events of all topologies is expected to be completed by the end of January 1973.

The analysis of the data from the first part of the film is in progress, the first topic to be studied in detail being the mechanisms involved in the production of the resonances  $\rho^0(765)$  and  $f^0(1260)$ . The  $\pi^+\pi^-$  effective mass distribution of a sample of the data, as shown in Figure 39, exhibits clear peaks due to the production of these resonances. The increased statistics available from the second part of the experiment should also enable the  $\rho-\omega$  interference to be studied.

In addition, new techniques for the separation of different production processes within the same final state are being applied to the experimental data.

Figure 39. The  $\pi^+\pi^-$  invariant mass distribution from the reaction  $\pi^+d \rightarrow \pi^+\pi^-pp$  at 4 GeV/c. (Experiment 29).



# Experiment 30

UNIVERSITY OF CAMBRIDGE

(Proposals 49, 82)

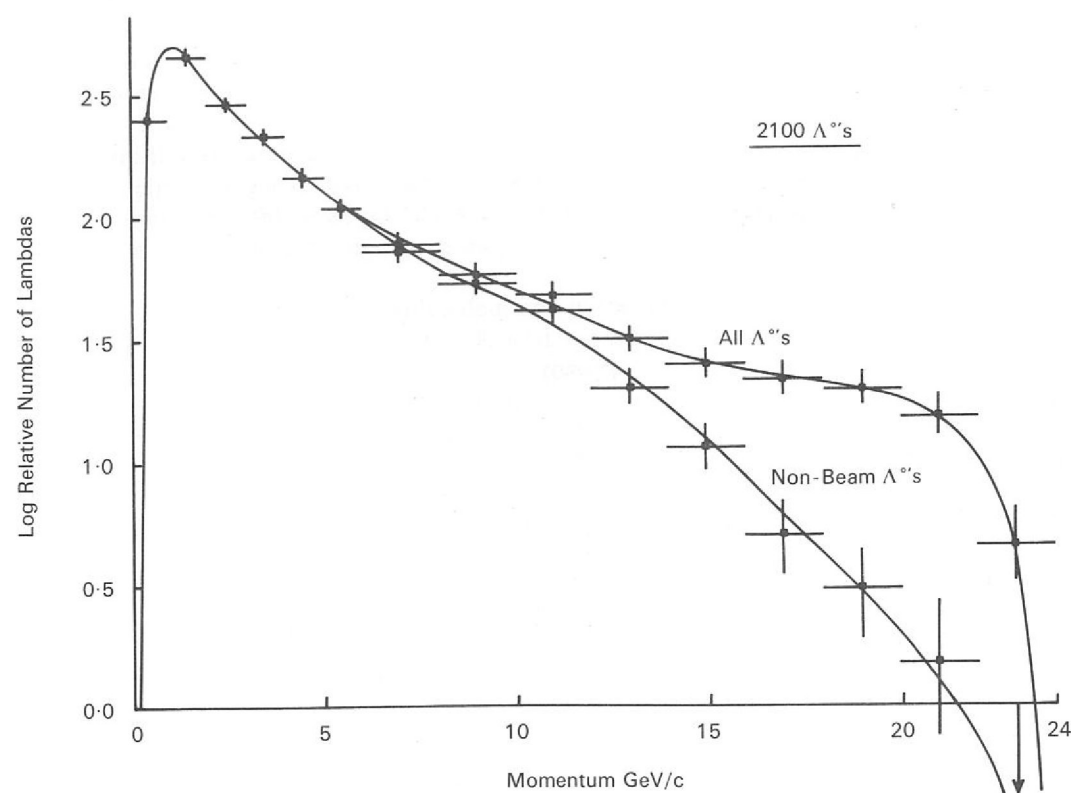
*Hyperon-Proton Interactions*  
(ref. 16, 17)

About half the 290,000 pictures taken in the CERN 2 m bubble chamber during 1971 have been scanned for  $\Lambda^0$  decays. Scanning criteria have been evolved to minimise the contamination of the  $\Lambda^0$  events by electron-positron pairs. Currently some 10,500  $V^0$  events have been measured and the momentum spectrum of a sample of fitted  $\Lambda^0$ 's is shown in Figure 40. The enrichment of the spectrum by high momentum  $\Lambda^0$ 's originating in the target is clearly visible. The shape and normalisation of the spectrum is in good agreement with the Hagedorn-Ranft model.

The second phase of the analysis, the search for  $\Lambda p$  interactions, is now under way. Preliminary results indicate that there will be several hundred such events in each of the momentum ranges 0-5, 5-10, 10-15 and > 15 GeV/c.

As a separate experiment an analysis of the 3-prong neutron stars on the film is being conducted. In this way it is intended to study the reaction  $np \rightarrow pp\pi^-$  at beam momenta up to 24 GeV/c.

Figure 40. The momentum spectrum of  $\Lambda$ 's in the hyperon beam. (Experiment 30).



# Experiment 31

UNIVERSITY OF CAMBRIDGE

(Proposal 85)

52K three-prong neutron proton interactions in hydrogen have been measured, divided equally between Sweepnik and the Clara manual system; all have been processed and the necessary remeasurement of 8% of the events is in hand. An ionisation scan to distinguish between the final states will be completed by March 1973.

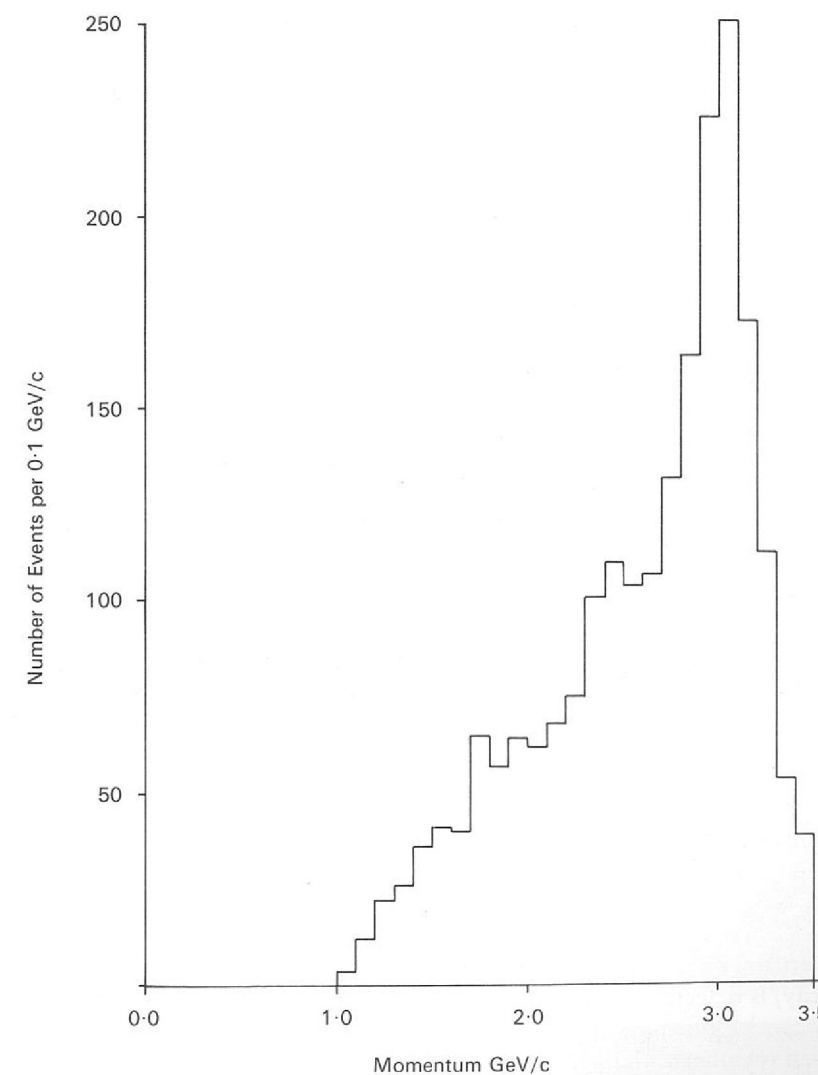
*n-p Interactions from 1 to 3.5 GeV/c.*

Preliminary data from 8K events are now available.

The numbers of events found in each channel are as follows:

$np \rightarrow$	(a) $pp\pi^-$	34%
	(b) $pp\pi^-\pi^0$	9%
	(c) $np\pi^+\pi^-$	56%
	(d) $nn\pi^+\pi^+\pi^-$	$\geq 1\%$
	(e) $pp\pi^+\pi^-\pi^-$	$\leq 1\%$
	(f) $\Sigma^-pK^+$	$\sim 0.03\%$ (2 events)

Figure 41. The momentum spectrum of the neutron beam for  $pp\pi^-$  events. (Experiment 31).



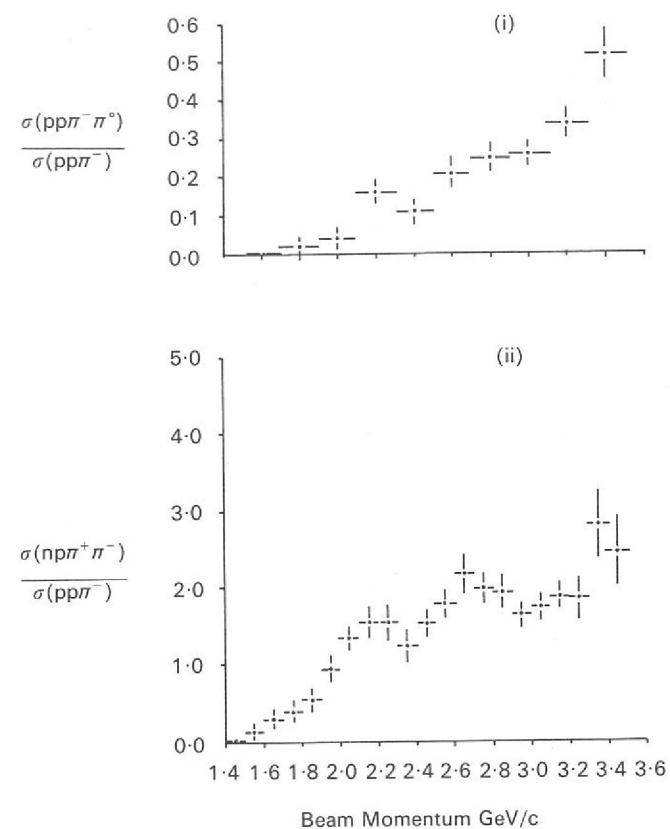


Figure 42. (i) The cross-section for  $pp\pi^-\pi^0$  events relative to the  $pp\pi^-$  channel, (ii) The cross-section for  $np\pi^+\pi^-$  events relative to the  $pp\pi^-$  channel. (Experiment 31).

The percentages relate to 6,200 events which reconstructed correctly within a narrow fiducial volume. Channel (d) consists of events which failed to fit other hypotheses and were identified by ionisation. The number for channel (e) was estimated from the number of five prongs found. The momentum spectrum of events in channel (a) is shown in Figure 41. As a neutral beam was used only relative cross-sections can be calculated. Those for channels (b) and (c) relative to channel (a) are shown in Figures 42 (i) and (ii).

Reactions (a) and (c) are both dominated by  $\Delta(1236)$  production. Crude estimates indicate that one third of the events in channel (c) are the result of the reaction  $np \rightarrow \Delta^-\Delta^{++}$ . It is not yet clear if the interaction  $NN \rightarrow N^*(1470)N$  followed by  $N^* \rightarrow N\pi$  or  $N\pi\pi$  contributes to these reactions.

## Experiment 32

(Proposal 91)

LAWRENCE BERKELEY LABORATORY  
UNIVERSITY OF TURIN  
RUTHERFORD LABORATORY

4 GeV/c  $\pi^+p$  in the  
Track Sensitive Target  
in the 1.5m Bubble  
Chamber

This experiment is the first using the new technique of a Track Sensitive Target and is designed to provide data on the channel



Interest is centred on events in which at least one  $\pi^0$  (two paired gamma rays from the  $\pi^0 \rightarrow \gamma\gamma$  decay) is detected and preferably both (i.e. four gammas). Given this information the channel can be kinematically fitted and the  $\pi^+\pi^0$  angular and energy correlations can be determined together with the  $\Delta^{++}$  decay to  $p\pi^+$ .

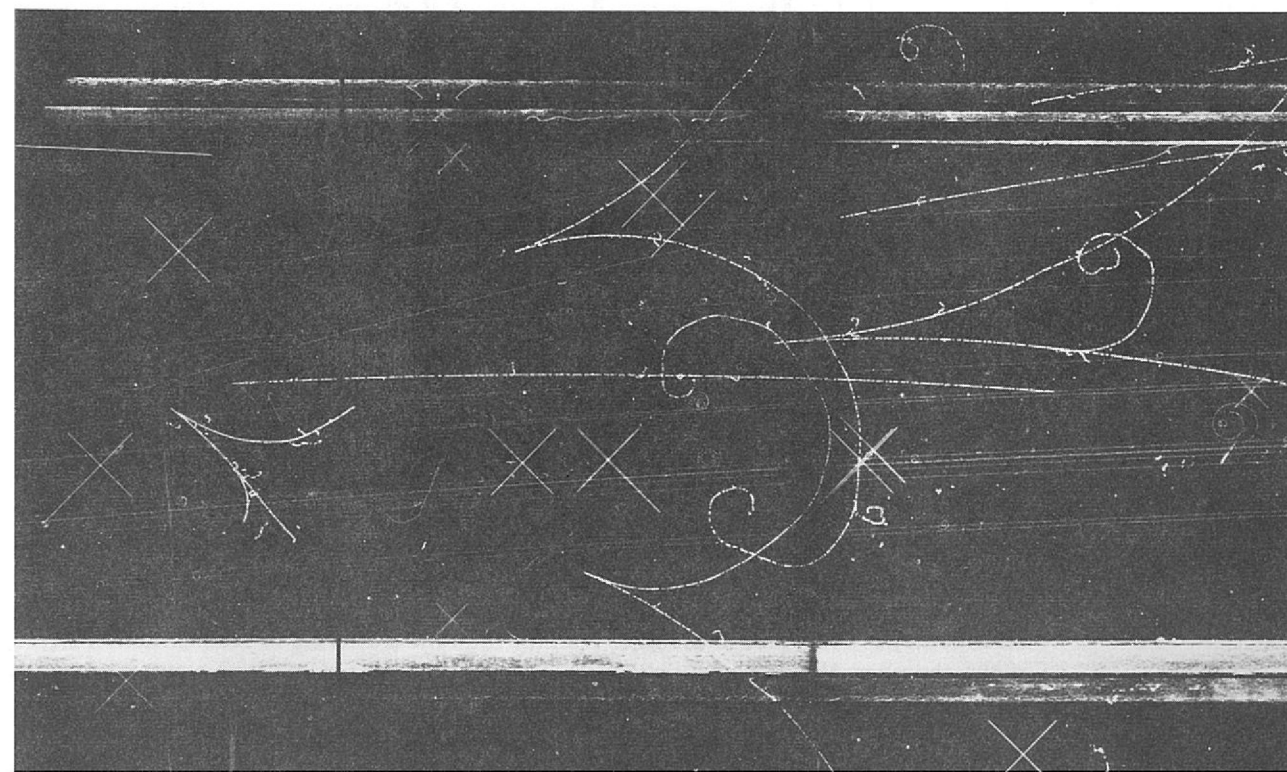
Two target designs were employed for data taking for this experiment. Approximately 800,000 pictures were taken in a metal framed target having useful dimensions 4.5 cm deep  $\times$  33.5 cm high  $\times$  140 cm long. Because of the metal frame the regions of the chamber beyond this height i.e. not seen through the target, cannot be used. A second target fabricated entirely of perspex was therefore employed for the remaining 520,000 pictures of the run. This target has dimensions 4.5 cm deep  $\times$  25 cm high  $\times$  140 cm long, however the effective chamber height remains at 44.5 cm defined by the main chamber windows (see the section on Bubble Chamber Operations).

The pictures taken were as follows:

No. of Pictures	Neon Concentration and radiation length ( $X_0$ )	Target in use
220,000	73 mole % (46 cm)	Metal Frame
606,000	77 mole % (40.5 cm)	" "
516,000	80 mole % (37 cm)	Perspex
Total;	1,342,000	

Figure 43 shows an event from the perspex target run. The two prong production vertex in hydrogen has four associated gamma rays and the event is therefore a candidate for the  $\Delta^{++}\pi^0\pi^0$  channel. The secondary charged tracks have gaps as the particles pass through the 6 mm perspex walls of the target. The tracks in the hydrogen have small bubbles and high bubble density whilst in the neon the bubbles are larger and of relatively low density. It is therefore quite obvious which liquid the track is in. This is a considerable aid to scanning. The electron positron pairs are clearly seen in the neon and point very well to the production vertex.

Figure 43. A candidate for the reaction  $\pi^+p \rightarrow \Delta^{++}\pi^0\pi^0$  in the track sensitive target. All four gamma rays from the two  $\pi^0$ 's convert to  $e^+e^-$  pairs in the neon-hydrogen mixture. (Experiment 32).



## Experiment 33

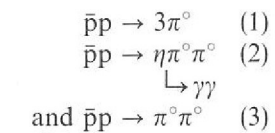
TATA INSTITUTE, BOMBAY

(Proposal 115)

The aim of this experiment is to analyse  $\bar{p}p$  annihilations at 2 GeV/c with an emphasis on the final states which are inaccessible with conventional bubble chambers. These final states are those consisting of two or more neutral pions. This experiment will also give more accurate results on the final states with one neutral pion. Nearly 50% of the annihilation cross-section consists of these multiple neutral pion final states and hence their measurement will contribute important and more complete information to the study of the  $\bar{p}p$  annihilation process.

*2 GeV/c  $\bar{p}p$  Interactions  
in a Neon Hydrogen  
Track Sensitive Target*

Examples of reactions which are of particular interest are:



In reactions (1) and (2) there are no dipion systems possible with odd isospin, spin or C-parity and hence this reaction is simpler than its charged pion counterpart. In particular no  $\rho^0$ -meson production is possible. Reaction (3) will provide an important comparison with the charged dipion annihilation process, particularly concerning the c.m. angular distribution as a means of investigating S-channel resonance effects reported in this region.

200,000 pictures with about 4  $\bar{p}$ 's per picture were taken in the autumn of 1972. This experiment is the first antiproton experiment run at Nimrod.

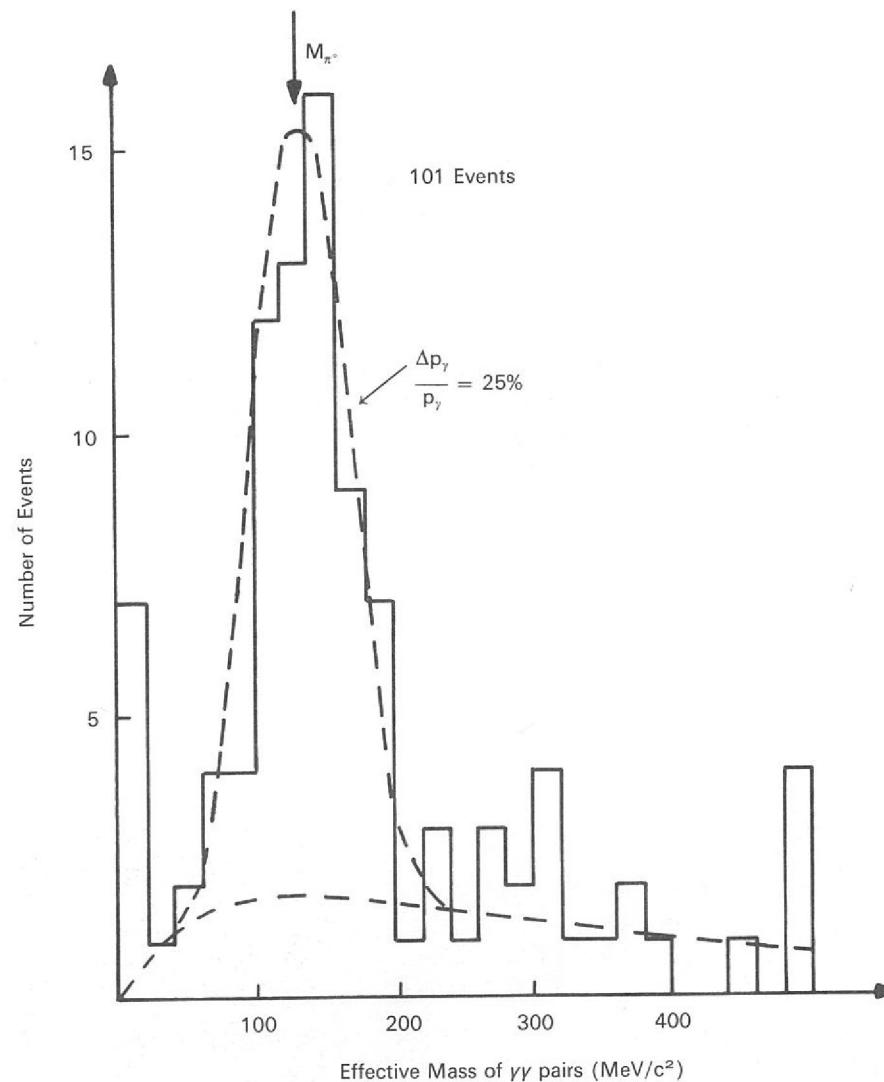


Figure 44. Preliminary measurements on a sample of film from the track sensitive target. (Experiment 32).

Analysis is under way, the pictures being scanned for events with two or more gamma rays converted. Figure 44 shows the results of preliminary measurements made on a sample of the film from the metal frame target. Clearly there is no difficulty in resolving the  $\pi^0$  signal from the unpaired gamma background. These measurements were made on the Rutherford Laboratory image plane digitisers and the resolution of the  $\pi^0$  mass reflects the accuracy of these machines rather than the multiple scattering or reconstruction errors in the chamber. However a suitably modified geometrical reconstruction program exists and accurate measurements are now in progress.

## Experiment 34

FREE UNIVERSITY OF BRUSSELS  
CERN  
TUFTS UNIVERSITY, USA  
UNIVERSITY COLLEGE, LONDON

(Proposal 38)

640,000 pictures have been analysed from an exposure of the 1.4 m Rutherford Laboratory Heavy Liquid Bubble Chamber to a 2.2 GeV/c  $K^-$  beam from Nimrod. The chamber liquid was a propane-freon mixture with a radiation length of 30 cm. The probability of converting a  $\gamma$ -ray from a  $\pi^0$  decay was about 55%.

*K^- Interaction in a  
Heavy Liquid Bubble  
Chamber  
(ref. 8, 9, 48, 69)*

The masses and lifetimes of the  $\Xi^0$  and  $\Xi^-$  have been measured and the  $\Lambda-\gamma$ ,  $\Lambda-\Lambda$  and  $\Lambda-p$  final states have been studied.

The  $\Lambda-\gamma$  final state yielded no evidence of new radiative decays, in particular the  $Y^*(1327)$  was not found.

$\Xi^0$ 's and  $\Xi^-$ 's, produced with an associated  $K^+$  or  $K^0$ , were selected by a double scan of all the film. After cuts on the  $\Xi^0$  lengths to remove background, 62 events with two detected  $\gamma$ -rays and 170 with one  $\gamma$ -ray remained. These 62  $\Xi^0$ 's and an additional 831  $\Xi^-$ 's were used to determine their lifetimes and masses. For the  $\Xi^0$  mass determination, only  $\Xi^0$  events with 2 observed  $\gamma$ 's were used. Their lifetimes agreed with results from other techniques and with the predictions of the  $\Delta I = \frac{1}{2}$  rule. The results are summarised as follows:

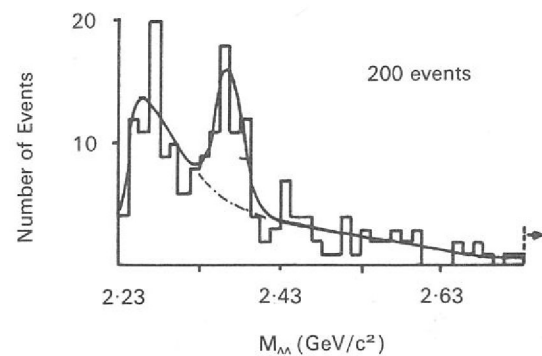
	Lifetime in p sec.	Mass in MeV/c <sup>2</sup>
$\Xi^0$	$290^{+32}_{-27}$	$1315.2 \pm 0.9$
$\Xi^-$	$173^{+8}_{-7}$	$1321.1 \pm 0.4$

The mass difference,  $m_{\Xi^-} - m_{\Xi^0}$ , was measured to be  $5.9 \pm 1.0$  MeV/c<sup>2</sup>, in agreement with the prediction of Coleman and Glashow.

400 events with two  $\Lambda^0$ 's in the final state yielded an unexplained mass peak at  $2367 \pm 4$  MeV/c<sup>2</sup>. This is the first observation of this enhancement which could be a  $\Lambda$ - $\Lambda$  resonance; the result is shown in Figure 45.

A small portion of the film was used to study  $\Lambda p$  systems produced in  $K^-$ -nucleus interactions. No significant signals in the  $\Lambda$ - $p$  effective mass distribution were detected in disagreement with a previous result.

Figure 45. Histogram of the  $\Lambda\Lambda$  invariant mass for events with charge balance and no long protons. The fitted curve is a combination of a polynomial and a gaussian centred at 2.367 GeV/c<sup>2</sup>. (Experiment 34).



## Experiment 35

(Proposal 89)

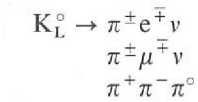
UNIVERSITY OF BOLOGNA  
UNIVERSITY OF EDINBURGH  
UNIVERSITY OF GLASGOW  
UNIVERSITY OF PISA  
RUTHERFORD LABORATORY

An exposure of 520K pictures to a  $K_L^0$  beam in the 2 m chamber at CERN was taken in October and November of this year. The  $K_L^0$  beam was formed by means of associated production on a hydrogen target ( $\pi^- p$ ) about 8 m upstream from the chamber. Six discrete momenta were taken covering the  $K^0$  momentum region 550-800 MeV/c. The lowest of these momenta being in the mono-energetic region, and the other five in the dichromatic region.

*Parameters of the  $\tau$  and Semi-Leptonic Decays of the  $K_L^0$ ;  $K_L^0 p$  Interactions in the Range 400-850 MeV/c*

Scanning and measuring of the film has started at all the laboratories. The quality of the film is good, there being on the average one visible  $V^0$  per 5 pictures, the  $\gamma$  ray background being negligible, and the neutron background of approximately 20 knock-on protons per picture not causing much difficulty in finding or measuring the wanted ( $V^0$ ) events.

The weak interaction part of the experiment is concerned with the elucidation of the mechanisms responsible for the decays:



A knowledge of the beam momentum allows the avoidance of the kinematic ambiguity which has beset previous investigations.

Of particular interest in the strong interactions is the reaction  $K_L^0 + p \rightarrow \Sigma^0 + \pi^+$ . There is some previous evidence for  $I = 1, S = -1$  baryon states with large branching ratios into  $\Sigma\pi$ . The channel is more amenable to study using a neutral rather than negative K beam.

## Nuclear Structure Experiments

The distribution of nucleons in the nucleus has been a topic of considerable interest for many years. For the proton distribution, which has been studied for a wide range of nuclei through the electromagnetic interaction from measurements of elastic electron scattering and X-ray emission from muonic atoms, reliable information is now available for the transition region of the nucleus in which the density falls from 90% to 10% of the average central value.

Comparable measurements for neutron distributions must be carried out with strongly interacting probes but these then interact with both the protons and the neutrons in the nucleus. An additional problem is that the particle-nucleus interaction is not well understood so that there are additional uncertainties in the interpretation of hadronic-nucleus interaction data in terms of nuclear sizes.

Interest in the neutron distribution is augmented by the fact that for medium-weight and heavy nuclei the number of neutrons  $N$  is larger than the number of protons  $Z$ . Simple single-particle model calculations suggest that for a heavy nucleus such as lead the neutrons could extend beyond the protons by 0.3 to 0.4 fm, thus forming a "neutron halo". More sophisticated shell-model calculations using Hartree-Fock techniques, however, reduce this difference to between 0.1 and 0.2 fm. Alternatively it can be argued that because the neutrons are required to counterbalance the long-range Coulomb repulsion and because the interaction between unlike particles is greater than that between like particles the neutrons and protons will tend to have similar spatial distributions. It is therefore of great interest to determine as accurately as possible the parameters of the neutron density distribution.

The first experiment below describes a high accuracy measurement of the reaction cross-sections for positive and negative pions on nuclei to gain information about neutron density distributions. A detailed theoretical analysis of the experimental results has been made and shows that in heavy nuclei the neutrons have the same r.m.s. radius as the protons to within  $\pm 0.1$  fm. The apparatus for this experiment has also been modified to allow total cross-sections for pions on light nuclei to be measured over a wide momentum range. Here the interest is in a study of the basic pion-nucleus interaction. The results for Carbon have been interpreted in terms of the distortion of the incident pion wave by the electrostatic Coulomb field of the nucleus. They have also been compared with the predictions of a number of models for the pion-nucleus interaction. Further analysis of the data is in progress. A similar experiment has been carried out by a collaboration of University physicists using the CERN synchrocyclotron. At the present there appears to be some discrepancy between the results from the two experiments and this is being investigated. This same collaborative group has also carried out measurements of differential cross-sections for pion-deuteron scattering and the production of pions from nuclei where the residual nucleus is left in either its ground state or a bound excited state.

The study of exotic atoms, in which an atomic electron has been replaced by a heavier negatively charged particle, is by now a well established topic in nuclear structure physics. For example extensive investigations of nuclear charge distributions have been made through measurements of the X-rays emitted by  $\mu$ -mesic atoms, whilst similar investigations for  $\pi$ -mesic atoms have given information about the low energy meson-nucleus interaction. It had originally been hoped that corresponding studies of K-mesic atoms would yield information about the distribution of matter in the outer region of the nucleus. Unfortunately this hope has not so far been realised due to problems in understanding the basic low energy kaon-nucleus interaction, however during 1973 a stopping K-meson beam is to be set up on Nimrod and the preparations for an experiment using this beam to study the kaon-nucleus interaction by the observation of nuclear  $\gamma$ -rays are described in Experiment 38.

The Laboratory continues to support several other University groups, as well as the one mentioned above, working in intermediate energy nuclear physics and using accelerators at CERN and AERE, Harwell. Included this year is a report on the preparations for a collaborative experiment to be carried out using the TRIUMF accelerator at the University of British Columbia in Vancouver, Canada. This novel accelerator, which will produce high intensity beams of 500 MeV  $H^-$  ions, is due to come into operation towards the end of 1973. It is hoped that the experiment will start to use beam time in the middle of 1974.

A programme of work is continuing on the AERE synchrocyclotron to study the few-nucleon system. The aim is to provide data to assist in an understanding of how nucleons interact in the environment of complex nuclei. In particular the nuclear three-body problem is being studied, with particular reference to the off-energy-shell component of the nucleon force. For most of the work a slow-spill neutron beam, produced from an internal beryllium target which was specially developed, is being used. This programme is being conducted as a collaboration between AERE and groups from several universities. The first two experiments of the programme, measurements of the differential cross-section for n-p and n-d elastic scattering at 130 MeV, have been completed, and were described in last years report. Some subsequent experiments are described in this report.

In the lower energy region the Kings College group have continued their studies of elastic and inelastic scattering using alpha-particle and helion beams from the Variable Energy Cyclotron at AERE, Harwell. This work has also been extended to studies of two-step processes in nuclear reactions and the description of inelastic scattering in terms of microscopic theories of the nucleus.

**Table 5**

### Nuclear Structure Experiments

Exp. No.	Experiment	Location	Status
36	Reaction cross-sections for pions on nuclei	$\pi$ 10 beam Nimrod	Completed
37	Total cross-sections for $\pi$ mesons on light nuclei	$\pi$ 10 beam Nimrod	Analysis
38	Experiments with stopping kaons	K17 beam Nimrod	Preparation
39	Studies of n-p scattering between 250 and 450 MeV	TRIUMF $H^-$ Cyclotron Vancouver	Preparation
40	n-p bremsstrahlung near 130 MeV	AERE Synchrocyclotron	Analysis
41	n-d break-up between 50 and 150 MeV	AERE Synchrocyclotron	Analysis
42	Elastic scattering of polarized neutrons from deuterium	AERE Synchrocyclotron	Data taking and Analysis
43	n-p capture between 40 and 140 MeV	AERE Synchrocyclotron	Preparation
44	Scattering studies with helion and alpha beams	AERE Variable Energy Cyclotron	Analysis
45	Investigation of two step processes in nuclear reactions	AERE Variable Energy Cyclotron, Oxford University Tandem	Analysis
46	Pion-deuteron scattering	CERN Synchrocyclotron	Completed
47	$\pi^\pm$ -nucleus total cross-sections	CERN Synchrocyclotron	Data taking and analysis
48	Measurements of pion production from nuclei	CERN Synchrocyclotron	Completed

## Experiment 36

UNIVERSITY OF BIRMINGHAM  
UNIVERSITY OF SURREY  
RUTHERFORD LABORATORY

Reaction Cross-Sections  
for Pions on Nuclei  
(ref. 1)

There is considerable interest in the density distribution of neutrons in heavy nuclei and a variety of attempts have been made to determine the parameters of the radial distribution. One of the earliest experiments with this objective in mind was performed almost 20 years ago and consisted of a measurement of the ratio of reaction cross-section for  $\pi^-$  and  $\pi^+$  mesons on Lead. By a simple analysis it was shown that the radial parameters of the density distributions for neutrons and protons must be very similar. The present experiment was aimed at improving on the accuracy of the earlier work and at considerably extending the range of elements and momenta measured.

The method used in the present experiment is based on the fact that at certain momenta around 1 GeV/c  $\pi^-$  mesons interact more strongly with protons than with neutrons whilst  $\pi^+$  mesons interact more strongly with neutrons than with protons. As a result the ratio of reaction cross-sections for  $\pi^-$  and  $\pi^+$  mesons incident on a nucleus will depend on the relative distribution of neutrons and protons. Since the proton distribution is considered to be known, a measurement of the ratio of the reaction cross-sections for incident  $\pi^-$  and  $\pi^+$  mesons yields information on the neutron distribution.

Data taking for the experiment was completed at the end of 1971 and the experimental arrangement was described in last years annual report. Measurements were made for the nuclei C, Al, Ca, Ni, Sn, Ho and Pb at momenta of 0.71, 0.84, 1.00, 1.36, 1.58 and 2.00 GeV/c and all the data have now been analysed. At 1.36 and 1.58 GeV/c the Fermi-averaged  $\pi^+$  and  $\pi^-$ -nucleon total cross-sections are equal so that the calculated ratio of  $\pi^-$  to  $\pi^+$  reaction cross-sections is independent of the neutron density distribution assumed. Excellent agreement is obtained between the measured experimental values and those calculated theoretically.

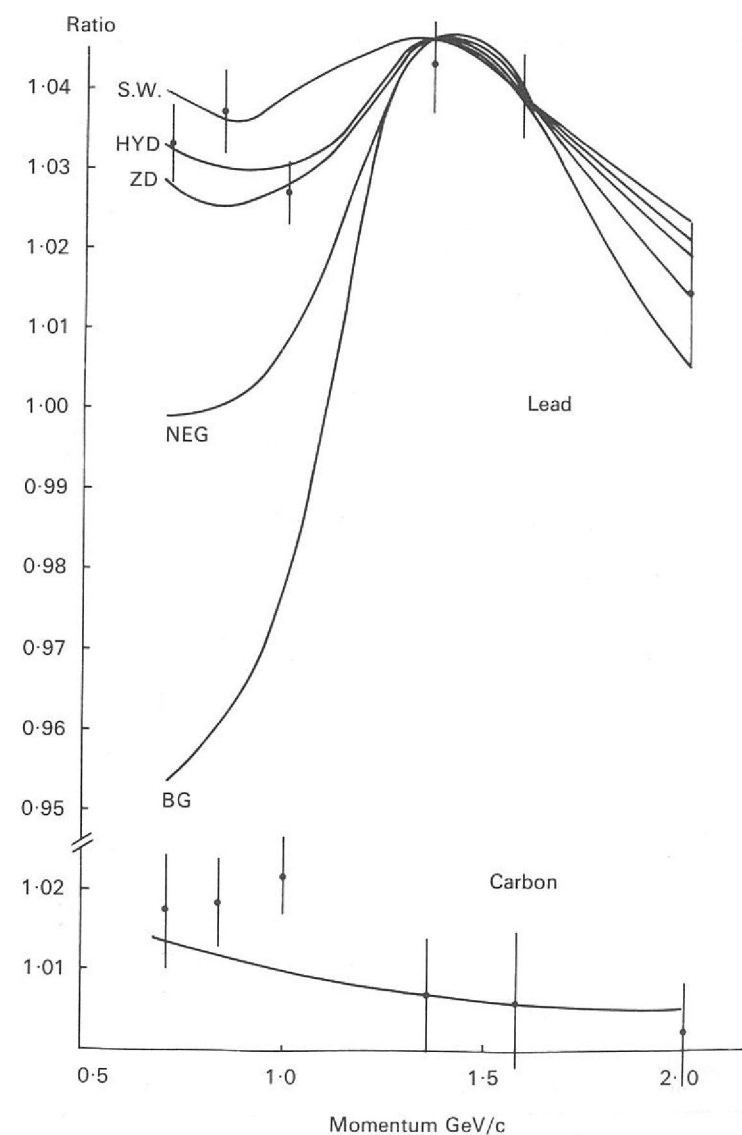
The results have been analysed in terms of neutron distributions in collaboration with theorists at the University of Surrey. Studies have been made of the correct wave equation to be used to describe the pion - nucleus interaction, the effects of Fermi-motion of the nucleons in the nucleus and of nuclear correlations and effects due to the angular dependence of the pion-nucleon scattering amplitudes.

As an example of the results obtained from this experiment the values of the  $\pi^-/\pi^+$  ratio for Carbon and Lead as a function of momentum are plotted in Figure 46 and compared with the results of calculations for a variety of neutron distributions. The results for Carbon are compared in the figure with the predictions for a harmonic oscillator density distribution with the same geometry parameters used for both protons and neutrons and are seen to be in good agreement with the theoretical predictions. For the Lead nucleus, the results are compared with the predictions of several different models. The curve labelled S W was obtained using identical Saxon-Woods forms for both the neutrons and protons. The parameters of the proton distribution were derived from fits to electron scattering data. The curve HYD was obtained using the predicted neutron distribution from a hydrodynamical model calculation. The curves ZD and BG were derived using density distributions obtained from the single particle model. Finally the curve labelled NEG was obtained using the density distributions from the Hartree-Fock nuclear matter calculations of Negele. Good agreement for momenta of 1 GeV/c and below is obtained with the curves SW, HYD and ZD which are all derived from models which give very similar neutron and proton distributions. The results do not agree with the distributions calculated by Negele which predict a difference of 0.23 fm between the r.m.s. radii of the neutrons and protons. No agreement at all below 1 GeV/c is obtained for the curve BG where the difference between the neutron and proton r.m.s. radii is large (0.62 fm).

In an attempt to interpret the data in a more direct and quantitative way the results have been compared with calculations where the parameters of the neutron distribution were varied systematically. Both proton and neutron distributions were assumed to have a Saxon-Woods form and the parameters for the protons were then fixed at the values obtained from analyses of electron scattering data. The corresponding parameters for the neutrons were then varied systematically. It was found that the r.m.s. radius of the neutron distribution is a quantity which is well defined by a measurement of the ratio of  $\pi^-/\pi^+$  reaction cross-sections. The value obtained at 0.84 GeV/c is  $5.42 \pm 0.11$  fm for the r.m.s. radius of the neutron distribution. Similar analyses of the data at 0.71 and 1.0 GeV/c gives values of  $5.47 \pm 0.11$  fm and  $5.55 \pm 0.16$  fm respectively. The mean of all three values is  $5.47 \pm 0.07$  fm. This result is to be compared with the values for the proton distribution of  $5.42 \pm 0.07$  fm from electron scattering and of  $5.43 \pm 0.02$  fm from  $\mu$ -mesic atom data.

To summarise, the results of the experiment seem to provide clear evidence that the radial parameters of the neutron and proton distributions in heavy nuclei must be very similar. Further details and the results for other nuclei are to be given in a paper describing the experiment and its theoretical analysis.

Figure 46. Ratio of  $\pi^-$  to  $\pi^+$  reaction cross-sections on Lead and Carbon as a function of the momentum of the incident meson. The theoretical curves are identified in the text. (Experiment 36). (11746).



# Experiment 37

UNIVERSITY OF SURREY  
UNIVERSITY OF BIRMINGHAM  
RUTHERFORD LABORATORY

Total Cross-Sections for  
 $\pi$  Mesons on Light  
Nuclei from 0.18 to  
1 GeV/c  
(ref. 81)

Recently there has been a great deal of experimental and theoretical work on the scattering of  $\pi$  mesons by light nuclei, particularly at momenta in the region of the (3,3) resonance for the pion-nucleon system. The data, principally measurements of the differential scattering cross-section, have been analysed in a number of ways using either an optical potential, Glauber scattering theory or a dispersion relation approach. Accurate total cross-sections have only been measured for  $\pi^-$  mesons on Carbon over a limited momentum range and there is a clear interest in extending these measurements to other momenta and target nuclei.

Using essentially the same apparatus as that used for the pion-nucleus reaction cross-section experiment, measurements have been made of total cross-sections for  $\pi^+$  and  $\pi^-$  mesons on  ${}^6\text{Li}$ ,  ${}^7\text{Li}$ ,  ${}^9\text{Be}$  and  ${}^{12}\text{C}$  at 14 different momenta between 179 and 983 MeV/c and for  ${}^{16}\text{O}$  at 6 momenta between 179 and 340 MeV/c. Analysis of the raw experimental data to give total cross-section values is almost complete.

Figure 47. Total cross-sections for  $\pi^-$  and  $\pi^+$  mesons on  ${}^{12}\text{C}$ . (Experiment 37).

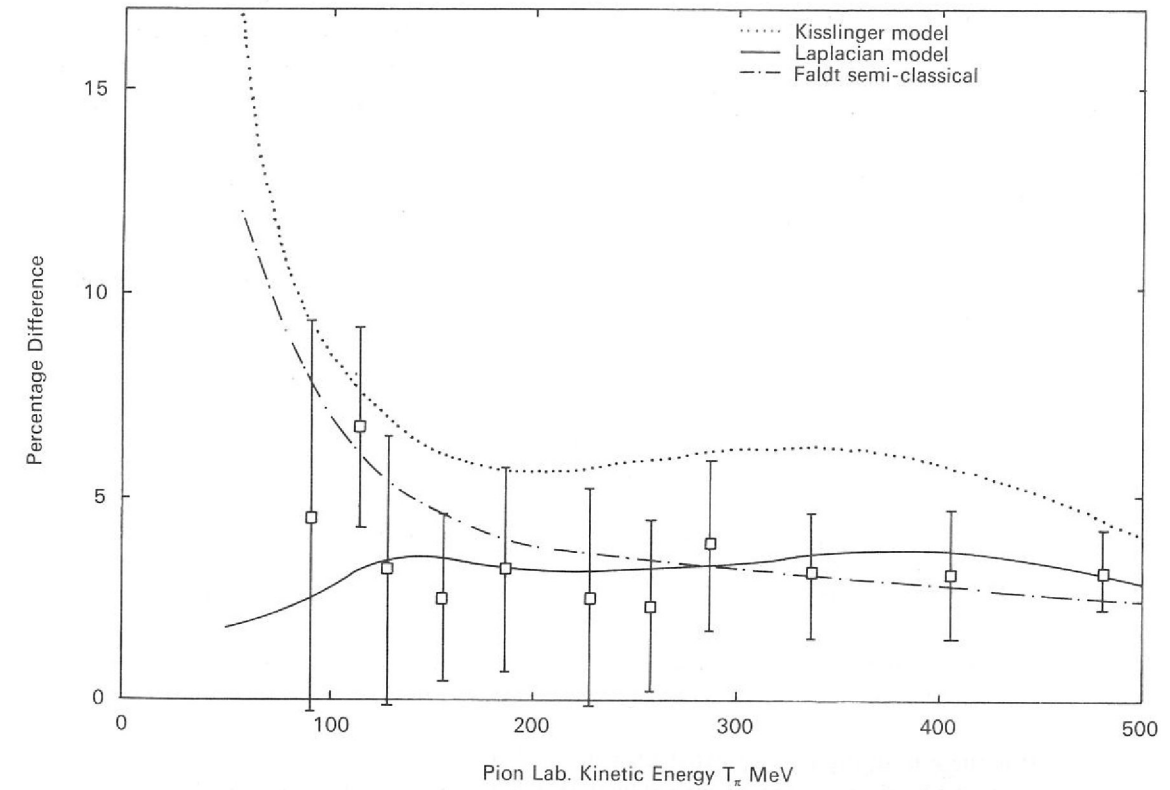
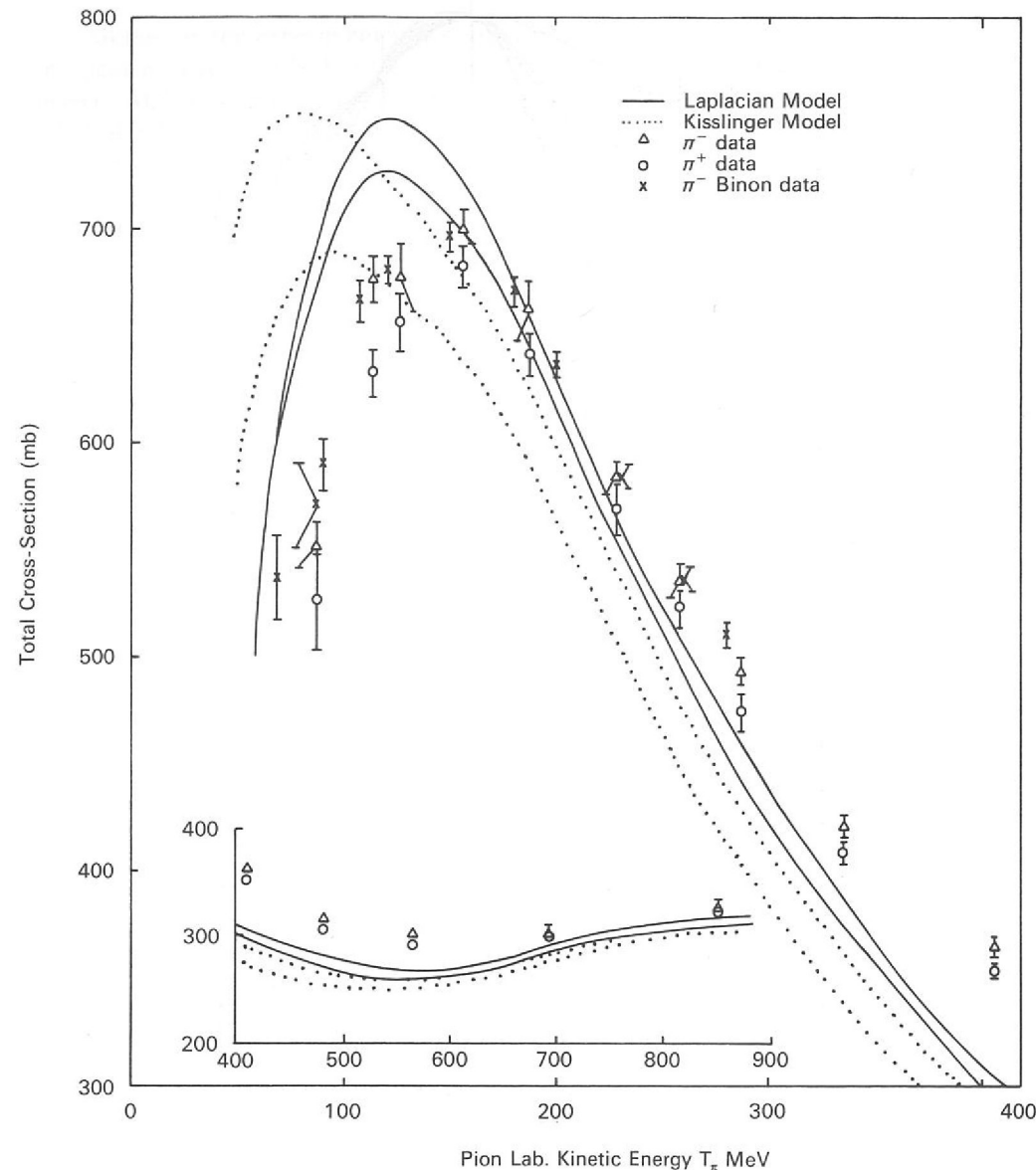


Figure 48. The percentage difference between the total cross-sections for  $\pi^-$  and  $\pi^+$  mesons on Carbon (shown in Figure 47). The  $\pi^-$  cross-section is the greater of the two. (Experiment 37).

The total cross-sections obtained in this experiment for  $\pi^+$  and  $\pi^-$  mesons on Carbon are shown in Figure 47. As can be seen the  $\pi^-$ -C cross-sections agree well with previous measurements. There have been no previous measurements of  $\pi^+$ -C total cross-sections. The predictions of optical model calculations using Kisslinger and Laplacian potentials are also shown. For these calculations the forward scattering amplitudes in the pion-nucleon system were averaged over the momentum distribution of the nucleons in the nucleus. The Laplacian model gives better agreement with the data of the present experiment than the Kisslinger model. This difference in the predictions of the two models appears to be related to different assumptions as to the behaviour of the off-shell pion-nucleon scattering amplitudes.

The measured cross-sections for positively and negatively charged pions on nuclei such as Carbon, which have zero isospin, can differ from each other and from the strong interaction cross-section due to the distortion of the incident pion wave-function by the Coulomb field of the nucleus. This distortion has the effect that the total cross-section for negatively charged particles is increased and for positive particles is decreased.

The relative difference between the  $\pi^-$  and  $\pi^+$  total cross-section for Carbon is plotted as a function of incident momentum in Figure 48. The results are compared with a semi-classical calculation and the predictions of the optical model using Laplacian and Kisslinger type potentials. Within the accuracy of the results the simple semi-classical calculation gives agreement with the measured differences. The predictions of the optical model calculations at low energies depend on the form of the potential and a better overall fit is obtained with the Laplacian model. This model also gives better agreement with the absolute values of the total cross-section.

Analysis of the results for the other nuclei is in progress.

## Experiment 38

UNIVERSITY OF BIRMINGHAM  
UNIVERSITY OF SURREY  
RUTHERFORD LABORATORY

*Experiments with  
Stopping Kaons*

The existence and qualitative features of K-mesic atoms are now well established. Several observations of X-ray spectra from kaons stopping in a number of targets have been reported in the literature and measurements of the strong interaction widths and shifts have been obtained. In order to obtain nuclear structure information from this data, it is necessary to know the kaon-nucleus interaction at low energies. Possibly this could be calculated from a knowledge of the low energy kaon-nucleon scattering parameters. However the calculation is considerably complicated by the presence of the  $Y_0^*(1405)$  resonance just below threshold in the  $K^- - p$  channel.

It has been suggested that the observation of nuclear  $\gamma$ -rays following capture of the kaon by the nucleus could give additional information about the interaction. For example suppose that the kaon interacts solely with one nucleon in the nucleus and that the residual nucleus does not break up, any  $\gamma$ -ray which is then emitted will be characteristic of that nucleus and will label the absorption as having taken place on either a proton or a neutron. Alternatively nuclear clusters may be emitted following the interaction and then the residual  $\gamma$ -rays can be used to identify the type of cluster involved. Some evidence for the existence of nuclear  $\gamma$ -rays following kaon capture exists but there has been no systematic study of the topic.

It is the aim of the present experiment to measure the spectra of  $\gamma$ -rays emitted when the kaon of a K-mesic atom is absorbed by the nucleus. If possible the  $\gamma$ -rays will be measured in coincidence with atomic X-rays to ensure that the capture occurred from orbit and not in flight. The X-ray energy spectra, measured in high resolution, will also be observed at the same time.

A stopping K-meson beam for these experiments has been designed and is to be installed on Nimrod in Hall 3 during 1973. The X3 extracted proton beam will be extended to give a third target station. Kaons produced in the forward direction will then be separated from the pions using an electrostatic separator, slowed down in a degrader and particle identification system and brought to rest in the target to be studied. Solid state detectors will be used measure the energy spectra of the X-rays and  $\gamma$ -rays and a NaI crystal used to detect X-rays for the X-ray,  $\gamma$ -ray coincidence work.

At the end of 1972 the design of the beam line had been completed and the main items of experimental equipment specified. The Cerenkov counters have been tested and  $\gamma$ -rays associated with stopping pions have been detected under conditions that are somewhat worse than those anticipated for the kaon beam.

## Experiment 39

BEDFORD COLLEGE, LONDON  
AERE, HARWELL  
UNIVERSITY OF SURREY  
QUEEN MARY COLLEGE, LONDON  
UNIVERSITY OF BRITISH COLUMBIA

*Studies on n-p Elastic  
Scattering between 250  
and 450 MeV  
(ref. 120)*

There is a paucity of data for neutron-proton scattering between energies of 250 and 450 MeV due mainly to the lack of suitable neutron beams. Hence there is a very inadequate knowledge of the  $I = 0$  phase shifts necessary for a complete understanding of the nucleon-nucleon interaction. With the imminent operation of several high intensity accelerators in the few hundred MeV region such beams will become available. A collaboration has been set up between several British Universities and physicists at TRIUMF, the 500 MeV  $H^-$  machine at the University of British Columbia. A programme of experiments is envisaged to include the differential cross-sections, polarization and triple-scattering parameters, the latter being funded by the Rutherford Laboratory (Proposal 104).

The extracted polarized proton beam from TRIUMF will be directed on to a liquid deuterium target. A resulting mono-kinetic polarized neutron beam at  $8^\circ$  to the incident proton beam will impinge on a liquid hydrogen target. A superconducting solenoid, as well as unconventional dipole magnets, will be used for spin precession. For the triple-scattering experiment, protons will be detected in a polarimeter consisting of a proportional chamber array and a carbon scatterer, and the neutrons in a large but conventional plastic scintillator assembly. At present the equipment is being designed, shipment to TRIUMF is planned for January 1974, with a view to taking beam from the summer of 1974.

## Experiment 40

QUEEN MARY COLLEGE, LONDON  
UNIVERSITY OF CALIFORNIA  
KINGS COLLEGE, LONDON  
AERE, HARWELL  
RUTHERFORD LABORATORY

The reaction  $n + p \rightarrow n + p + \gamma$  is sensitive to off-energy-shell effects in the nucleon-nucleon interaction. The experimental technique is to observe neutrons and protons in coincidence at non-conjugate angles. Data taking is complete and about 40% of the data has been analysed. Results were presented at the International Conference on Few Particle Problems in the Nuclear Interaction at Los Angeles in August 1972, in the form of double differential cross-sections as a function of neutron-proton opening angle. The data can be compared with the independent theoretical calculations of McGuire and Brown which were performed at 135 MeV in anticipation of this experiment. In these calculations the n-p elastic phase shifts are extrapolated off the energy-shell in the mathematically most convenient manner, as no conceptual guide lines exist. It is found that the measured cross-sections are in good agreement with those predicted, as also is the variation of the cross-section with opening angle. The analysis of the remainder of the data is in progress.

*n-p Bremsstrahlung  
Near 130 MeV  
(ref. 121)*

## Experiment 41

KINGS COLLEGE, LONDON  
BEDFORD COLLEGE, LONDON  
QUEEN MARY COLLEGE, LONDON  
UNIVERSITY OF CALIFORNIA  
AERE, HARWELL

Data taking has been concluded on a kinematically complete experiment on the  $d(n, np)n$  reaction, over a range of incident neutron energies from 50 to 150 MeV. Neutrons and protons were detected in coincidence at a total of 50 pairs of angles, selected so as to favour three final state processes; (a) the n-n final state interaction, (b) the n-p final state interaction, and (c) n-p quasi-free scattering. The analysis of the data is underway and will yield absolute cross-sections for these final state processes.

*n-d Break-up Between  
50 and 150 MeV  
(ref. 123, 176.)*

With the help of a modified form of the Watson-Migdal theory an accurate value for the n-n scattering length has been extracted from the data,  $a_{nn} = 17.1 \pm 0.8$  fm, and was presented at the Los Angeles Conference in August 1972. The existence of data from a variety of kinematic conditions should do much to indicate the reliability of this method, in particular the importance of the proximity of the spectator particle process. Similarly the range of neutron energies should indicate the extent of the validity of the impulse approximation, and the applicability of two stage processes in the final state interaction. It is hoped that cross-sections for the n-d bremsstrahlung reaction can also be obtained from the data.

## Experiment 42

QUEEN MARY COLLEGE, LONDON  
KINGS COLLEGE, LONDON  
BEDFORD COLLEGE, LONDON  
AERE, HARWELL

Elastic Scattering of  
Polarized Neutrons from  
Deuterium

A polarized neutron beam with energies between 20 and 120 MeV has been produced at 45° from an aluminium target using the AERE synchrocyclotron time-of-flight system. The beam polarization has been measured by studying Schwinger scattering at 1° off a uranium target. Preliminary data has shown it to be compatible with that of an earlier experiment. Data taking is virtually complete, and will yield information on the polarization in the quasi free n-p process as well as the n-d process. Our main region of interest in this experiment is that around 110° centre-of-mass angle, where the cross-section falls to a sharp minimum. Here there exist serious discrepancies between theory and experiment for both the n-d and p-d systems. From a calibration run using a hydrogen target we hope also to obtain more accurate information on the free n-p system to compare with our quasi-free results.

## Experiment 43

UNIVERSITY OF BIRMINGHAM  
AERE, HARWELL  
UNIVERSITY OF SURREY  
UNIVERSITY OF SUSSEX

n-p Capture Between  
40 and 140 MeV

There is a long-standing discrepancy between the experimentally observed and theoretically predicted values for the thermal neutron capture cross-section on hydrogen of about 10%. It was felt that a study of the capture process at higher energies might shed fresh light on the problem. Consequently we have devised a comprehensive programme of experiments to measure the observables of the capture reaction between 40 and 140 MeV on the AERE synchrocyclotron. The first experiment, a measurement of the total cross-section and angular distribution as a function of energy, has recently been approved.

Neutrons from the slow-spill beam will be incident on a solid hydrogen target. Such a target is necessary since it must be thin (~1 cm) to allow the deuterons to escape, hence even the thinnest windows of a conventional liquid target would provide an unacceptably large background. The design and construction of the target is being performed by the Rutherford Laboratory, following the pioneering work of Jarvis and Shah at Harwell. Final tests on the target are currently in progress. The deuterons are emitted into a forward cone of  $\pm 7\frac{1}{2}^\circ$  and will be swept out of the neutron beam by a magnet so that the full angular range can be studied. They will be distinguished from break-up protons by a combination of time-of-flight, total energy and dE/dx measurements, with the assistance of a  $\gamma$ -ray coincidence from lead-glass counters in the kinematically difficult regions. Installation of the equipment is in progress and it is hoped to take preliminary data in January 1973.

## Experiment 44

KINGS COLLEGE, LONDON

Scattering Studies with  
Helion and Alpha Beams  
(ref. 45, 46, 146)

The study of elastic and inelastic scattering of helions and alphas using the Harwell Variable Energy Cyclotron has continued. The analysis of 53.4 MeV helion elastic scattering from  $^{56}\text{Fe}$  demonstrated the need for a surface form of imaginary potential as well as a small spin-orbit term in the optical potential. Discrete potential ambiguities characterized by volume integrals per particle pair of the real potential ( $J_{RS}/A_p A_T$ , where  $A_p$  and  $A_T$  are the mass numbers of the projectile and target nuclei respectively) were observed with values of 330 and 440  $\text{MeV}\cdot\text{fm}^3$ . This prompted an analysis of a range of data in this mass region at

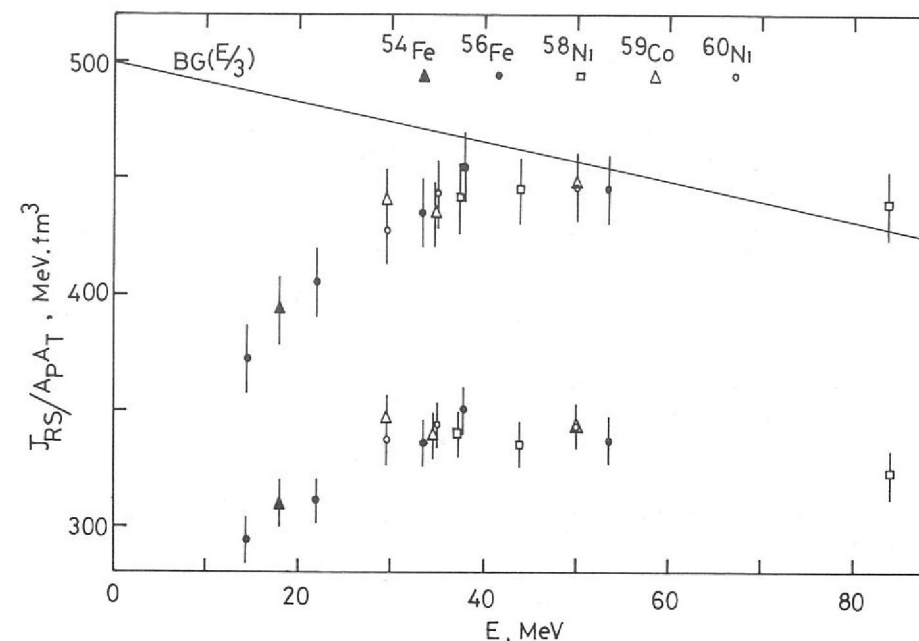
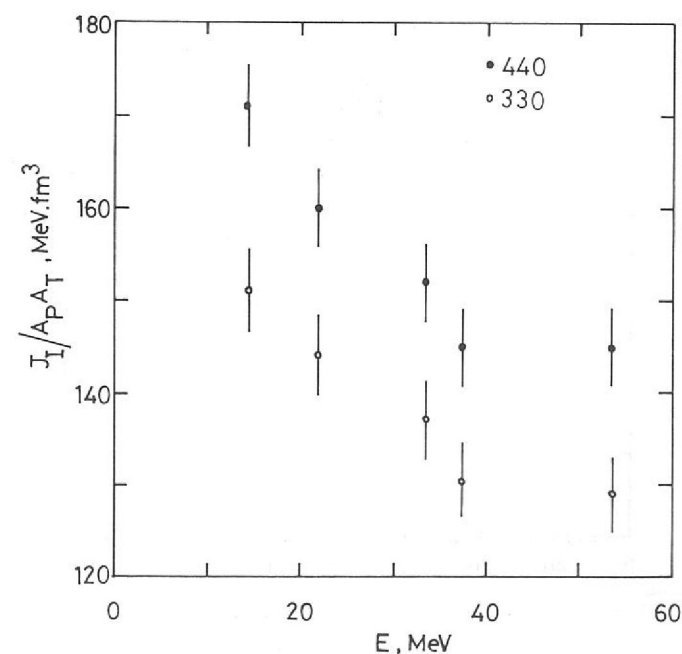


Figure 49. Energy variation of the volume integral per particle pair for the real part of the helion optical potential. (Experiment 44). (12721).

energies from 14 to 83.4 MeV. Using mean geometry parameters and a fixed spin orbit term for all data sets, the behaviour of the volume integrals for the real potentials were calculated for the two discrete ambiguities. These are shown in Figure 49 and compared with the volume integral for nucleons incident on  $A_T = 56$  at one third of the helion energy, calculated from the parameters of Becchetti and Greenlees. At helion energies higher than 35 MeV the values for the 440  $\text{MeV}\cdot\text{fm}^3$  ambiguity are close to this line.

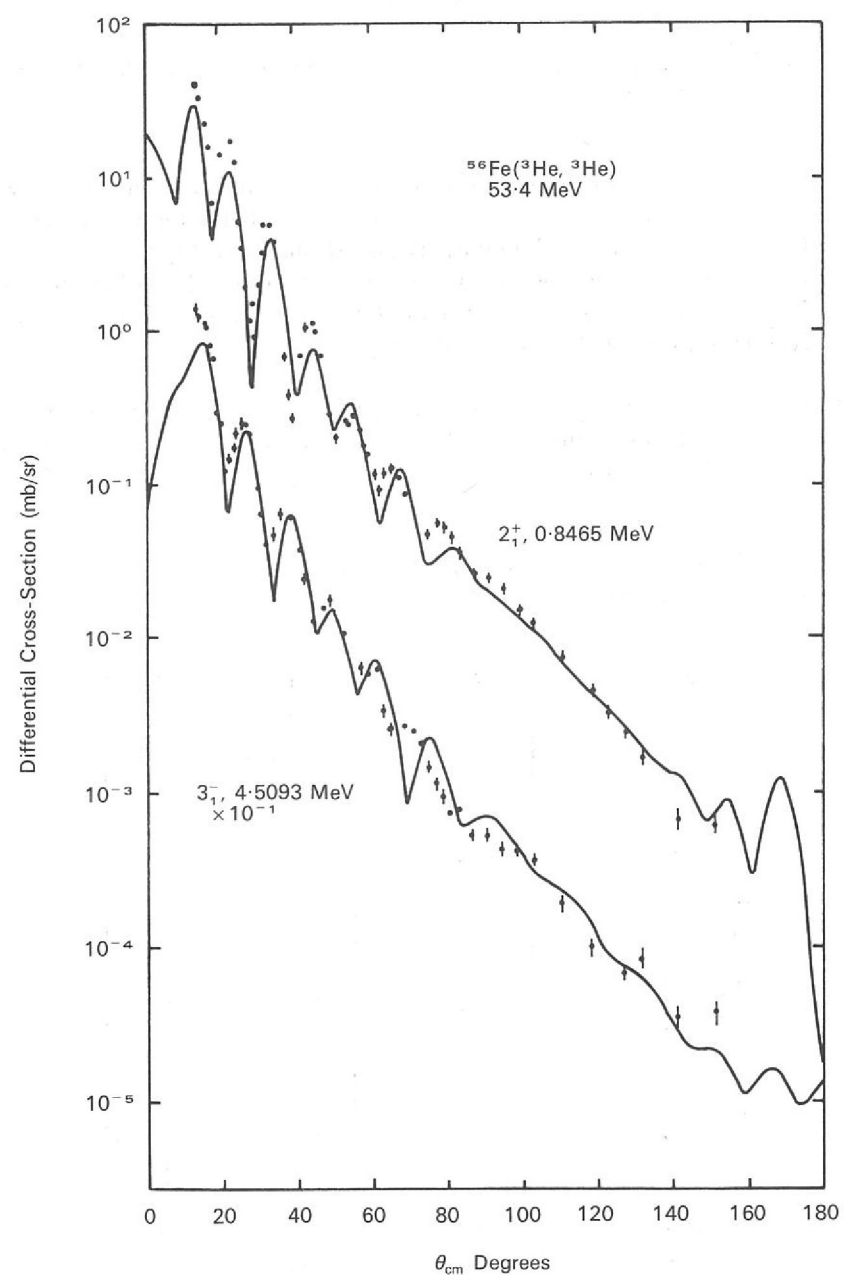
Figure 50 shows the volume integral per particle pair of the imaginary potential for  $^{56}\text{Fe}$  as a function of energy, for both ambiguities. The smooth decrease with increasing energy is probably due to collective effects.

Figure 50. Energy variation of the volume integral per particle pair for the imaginary potential of  $^{56}\text{Fe}$ . (Experiment 44). (12720).



The inelastic data taken at 33 and 53.4 MeV on  $^{56}\text{Fe}$  have been analysed using both DWBA and SCA forms of the collective vibrational model. The DWBA fits to the first  $2^+$  and  $3^-$  states using a complex form factor are shown in Figure 51. Evidence that the  $2^+$  state contains components of both one and two phonon excitations has been observed. The SCA analysis shows a preference for the lower discrete ambiguity in the optical potential as has some recent measurements of Fulmer et al at Oak Ridge at 71 MeV. Further helion scattering measurements have been made on  $^{56}\text{Fe}$  at 83 MeV and are being analysed. The data taken includes the helion elastic and inelastic scattering and the  $(h, \alpha)$  reaction for which measurement of the outgoing alpha channel at the appropriate energy has also been made. These data should show up the energy dependent characteristics of the reactions and the limitations of the current models.

Figure 51. DWBA fits to the differential cross-sections of the first  $2^+$  and  $3^-$  states of  $^{56}\text{Fe}$ . (Experiment 44).



## Experiment 45

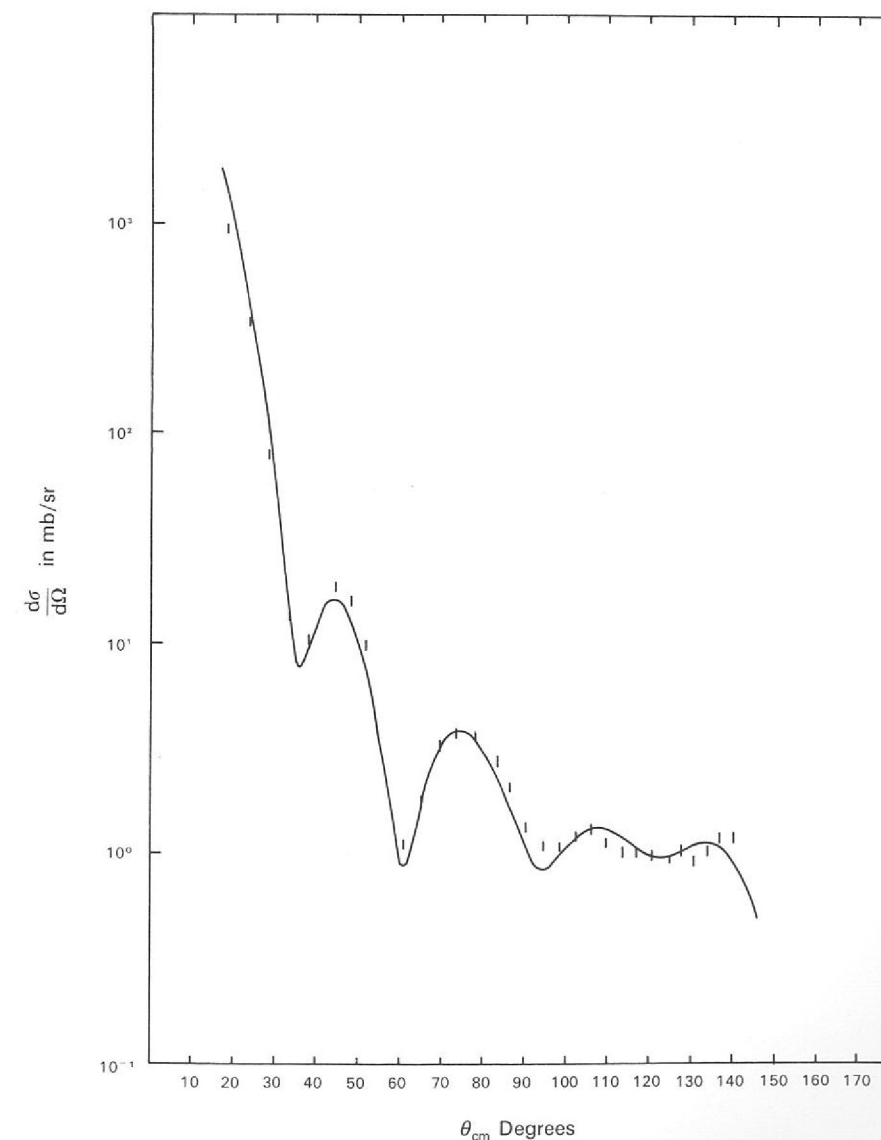
KINGS COLLEGE, LONDON  
QUEENS UNIVERSITY, BELFAST

Work has continued on the set of elastic and inelastic scattering cross-section measurements for  $^3\text{He}$  and  $\alpha$  projectiles off  $^{11}\text{B}$  and isotopes of Mg at several energies using the Harwell VEC and Oxford Tandem accelerators. This programme is now almost finished and its results together with existing data in the literature provide complete sets of scattering and one particle transfer cross-section data for the study of two step pickup processes in the reaction  $^{26}\text{Mg}(^3\text{He}, \alpha)^{25}\text{Mg}$  at 15.0 and 33.0 MeV and  $^{12}\text{C}(d, \text{He}^3)^{11}\text{B}$  at 28 and 50 MeV.

*Investigation of Two-Step Processes in Nuclear Reactions and of Microscopic Theories of Inelastic Scattering*

The eventual aim is to analyse the scattering data with an SCA program and then apply the coupled channels two-step stripping code developed at Oxford to the particle transfer cross-section. Both microscopic and collective models are to be employed for the inelastic scattering. At present the analysis is at a preliminary state and only optical model fits to the elastic data have been completed. The excellent quality of the fits is typified by the results for  $^{11}\text{B}(^3\text{He}, ^3\text{He})^{11}\text{B}$  at 17.5 MeV shown in Figure 52.

Figure 52. The elastic cross-section for  $^{11}\text{B}(^3\text{He}, ^3\text{He})^{11}\text{B}$  at 17.5 MeV. The solid curve is the optical model fit. (Experiment 45).



An analysis has been started of the inelastic data with an SCA program using the rotational model to describe the excited states involved. There is an interesting qualitative feature in the  $^{11}\text{B}$  results, namely the extraordinary extent of the violation of the K selection rules for the 2.14 and 5.04 levels. This contrasts sharply with inelastic results for  $^{25}\text{Mg}$  where the K selection rule greatly reduces the cross-sections for scattering to the first two excited states. The difference is probably connected with the greater inter-band mixing expected for  $^{11}\text{B}$  where  $K = \frac{1}{2}$  and  $K = \frac{3}{2}$  levels of the same spin lie close together.

In the last annual report we described initial results obtained with a new simple microscopic model of inelastic scattering from collective nuclei. This model used as its basis a deformed nuclear density rather than the deformed optical potential usually employed. The calculations reported last year were for the real inelastic form factor. The model has now been extended to predict the inelastic imaginary form factor.

Our approach is based on the 'frivolous model', which in its usual form gives the imaginary optical potential of a spherical nucleus. We have generalized it to collective nuclei and obtained three straightforward contributions to the inelastic imaginary form factor which arise from the dependence of the nuclear density, Fermi momentum and the real optical potential on the angle between the radius vector and the nuclear symmetry axis.

A completely new and qualitatively different contribution has also been discovered to arise from the anisotropic momentum distribution in a deformed nucleus. A technique for calculating this effect has been developed, it is found to give rise to a new type of deformed imaginary potential which depends on the angle between the direction of the momentum vector of the scattered particle and the nuclear symmetry axis.

## Experiment 46

UNIVERSITY OF OXFORD  
CERN, GENEVA  
UNIVERSITY OF GOTHENBURG  
SIN, ZURICH  
UNIVERSITY COLLEGE, LONDON

*Pion-Deuteron  
Scattering*

At or above 0.7 GeV/c the Glauber formalism seems to be almost perfect for  $\pi$ -d scattering and even at 0.4 GeV/c the prediction for  $\pi$ - $^{16}\text{O}$  scattering is extremely good. A measurement of  $\pi^+$ -d elastic scattering at 370 MeV/c, and for backward angles down to 240 MeV/c, was undertaken to establish the limit of validity of the formalism. At 370 MeV/c the Glauber prediction is never more than 20 or 30% away from the experimental measurements even for cross-sections below 100  $\mu\text{b}/\text{sr}$ , but as the incident momentum is decreased towards the 3-3 resonance the discrepancy increases to a factor of two. A paper describing this work has been prepared for publication.

## Experiment 47

UNIVERSITY OF OXFORD  
CERN, GENEVA  
UNIVERSITY OF GOTHENBURG  
SIN, ZURICH  
UNIVERSITY COLLEGE, LONDON

Originally the intention was to measure the total cross-sections of certain odd mass nuclei,  $^7\text{Li}$  and  $^9\text{Be}$ , for  $\pi^+$  and  $\pi^-$  over the (3,3) resonance to establish the  $\pi$ -nucleus coupling constant using dispersion relations. In fact much of the effort has gone into investigating the difference between  $\pi^+$  and  $\pi^-$  cross-sections for the  $N = Z$  nuclei  $^4\text{He}$ ,  $^6\text{Li}$ ,  $^{12}\text{C}$  and  $^{32}\text{S}$ . The raw data exhibits a difference of about 15% at 200 MeV/c decreasing to about zero at 300 MeV/c and above. It is difficult to account for the difference, and particularly the large energy dependence and small Z dependence, in terms of known Coulomb effects.

$\pi^\pm$  - Nucleus Total  
Cross-Sections

For the odd mass nuclei, there may be a sizeable discrepancy between the  $\pi^\pm$  total cross-sections and the "elastic" charge exchange cross-sections which are simply related by isospin. Finally, it appears that the  $\pi$ -nucleus (i.e.  $^7\text{Li}$  and  $^9\text{Be}$ ) coupling constants are about a factor of three smaller than the  $\pi$ -nucleon coupling constant, contrary to prediction.

## Experiment 48

UNIVERSITY OF OXFORD  
CERN, GENEVA  
UNIVERSITY OF GOTHENBURG  
SIN, ZURICH  
UNIVERSITY COLLEGE, LONDON

Measurements on the production of pions in the forward direction by 600 MeV protons leaving bound nuclear states have been completed and published.

The main features observed were:

- The reactions  $^3\text{He}(p, \pi^+)^4\text{He}$  and  $^4\text{He}(p, \pi^+)^5\text{He}$  have similar cross-sections of  $\sim 20 \mu\text{b}/\text{sr}$  despite the enormous difference in binding energy for the last neutron. It seems likely that the magnitude of the cross-sections can be understood in terms of a modification of Mandelstam's theory for  $pp \rightarrow d \pi^+$  without invoking any extraordinary nuclear momentum distribution.
- The comparison of  $^9\text{Be}(p, \pi^+)^{10}\text{Be}$  and the mirror reaction  $^9\text{Be}(p, \pi^-)^{10}\text{C}$  indicated a non-zero cross-section for  $\pi^-$  production but one about two orders of magnitude smaller than for  $\pi^+$  production. Again this is explicable (but complicated) in the language of Mandelstam, but not in terms of "free nucleons" or of "proton stripping".

*Measurements of Pion  
Production from Nuclei  
(ref. 48, 59)*

# Radiological Experiments

ST BARTHOLOMEW HOSPITAL  
 MEDICAL COLLEGE, LONDON  
 CHRISTIE HOSPITAL, MANCHESTER\*  
 CHURCHILL HOSPITAL, OXFORD  
 UNIVERSITY OF LEEDS  
 RUTHERFORD LABORATORY

\*Group recently moved to The Institute of  
 Radiotherapy, Belvidere Hospital, Glasgow.

$\pi$ 11 Radiological Beam  
 Line  
 (ref. 154, 155, 156, 157)

The  $\pi$ 11 beam has been used extensively by outside groups. When run with prime user status, the dose rate in excess of 1 rad/minute makes this beam the most intense  $\pi^-$  irradiation facility in the world.

Interest is centred on the expected advantages  $\pi^-$  beams have over  $\gamma$  and X rays for radiotherapy. In contrast to  $\gamma$  rays,  $\pi^-$  mesons of a definite low momentum have a well defined range, at the end of which they deposit most of their energy. Further, when stopped they are absorbed by an atomic nucleus of the target material, and the heavily ionizing products cause local damage not readily repaired by living cells. This is so even when the absence of oxygen reduces the production of free radicals, a serious drawback in the use of  $\gamma$  rays in blood-starved cancer tissue.

The experiments performed have sought to confirm these predictions and to understand the physical properties of the beam, e.g. lepton content and secondaries. The main limitations have been a relatively small spot size (2 cm useful diameter) and a dose rate which is only 10% of the minimum required for therapy.

Of the various dosimetric studies made, a distribution obtained using LiF<sup>7</sup> microrods is shown in Figure 53. This material has the property of thermoluminescence, i.e. when heated it emits light proportional to the radiation it has received. As the radiation quality is not constant with depth the isodose plot has been normalised as a function of depth to an ion chamber measurement.

Figure 53. Isodose plot of the  $\pi^-$  beam in perspex. Typically only the middle of the beam, which is of uniform density, can be used. The low peak to plateau rise of 1.5 is mainly due to the wide momentum acceptance.

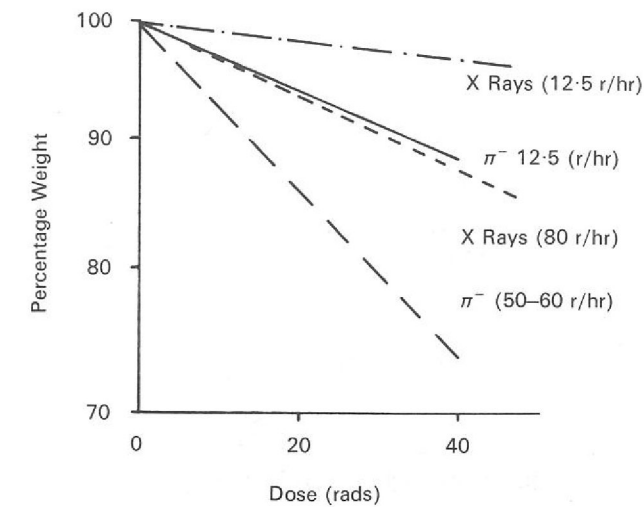
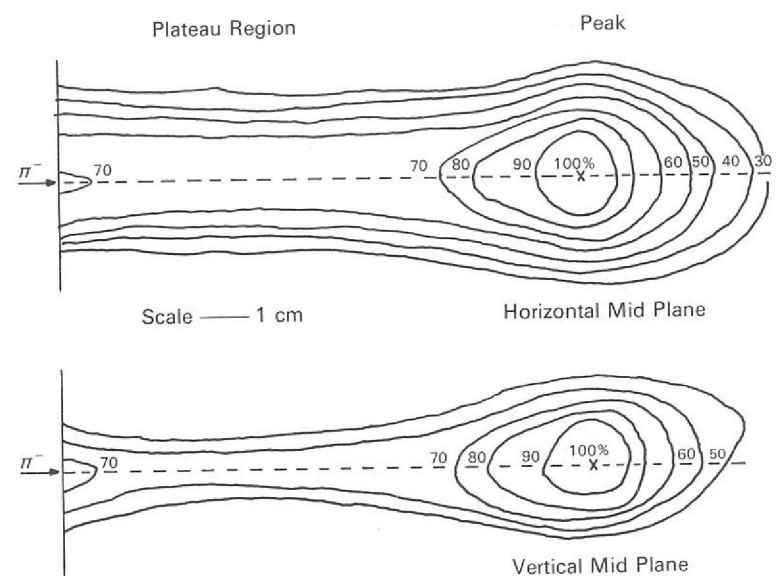


Figure 54. Effect of  $\pi^-$  mesons and X-rays on mouse thymus weight. No statistically significant difference was observed between  $\pi^-$  peak and plateau positions, so the results have been combined. Note the strong dose rate effect and the greater biological effectiveness of the  $\pi^-$  mesons.

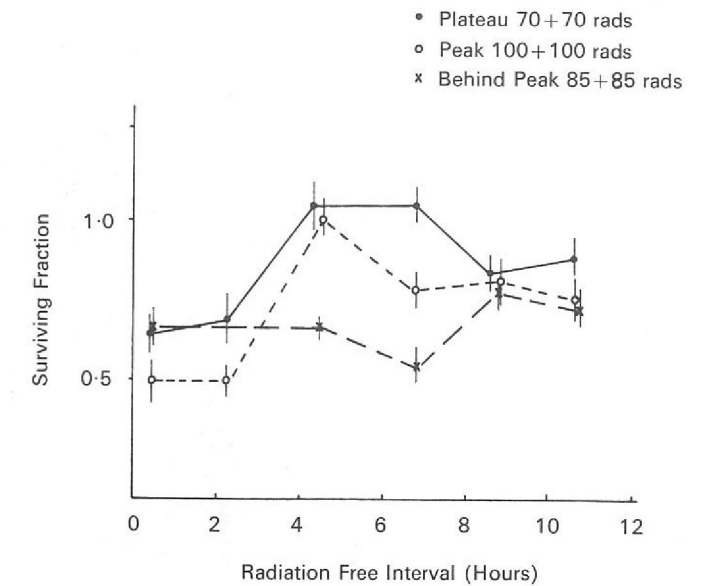


Figure 55. Effect of split  $\pi^-$  irradiations on He La cancer cells. In front of, and at the ionization peak, the surviving cells are able to undergo some repair, whereas just behind the peak little recovery is seen.

The St Bartholomew's College group have been concerned with animal experiments. The thymus gland of young mice showed a very strong dose rate dependence, one of the factors being cell mobility in the animal (see Figure 54).

The 'colony forming unit' of mice marrow (haemopoietic) cells provides the unexpected result that these sensitive structures are no more sensitive to  $\pi^-$  radiation than to  $\gamma$  rays or electrons. This has been confirmed for younger mice in a second experiment. The technique used was to irradiate a suspension of cells and to inject these into immunologically suppressed hosts where the number of colonies that grew in the spleen was scored.

The same group has also exposed a suspension of cultured human cancer cells to study the effect of both single and split doses at different depths (see Figure 55).

A similar system was exposed by the Christie Hospital group. In this case the cells were frozen at liquid N<sub>2</sub> temperatures causing radiation effects to be stored at low dose rates, the damage to the cells occurring as if there were a massive instantaneous dose. The effect of  $\pi^-$  mesons at the peak of the ionization depth distribution is shown in Figure 56. It is seen that it lies between that of X-rays and 14 MeV neutrons. (Neutrons, like  $\gamma$  and X rays, produce their maximum effect near the skin). The behaviour away from the peak is presently under investigation.

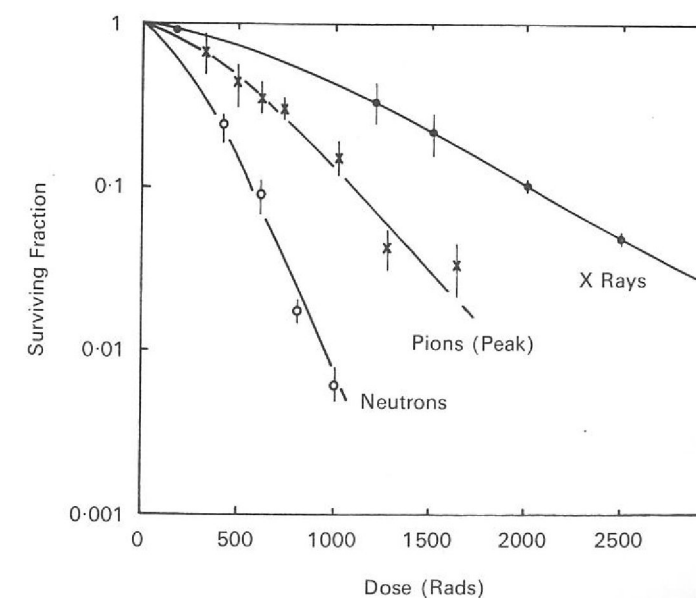


Figure 56. Effect of irradiating He La cells at  $-196^\circ\text{C}$ . A comparison with Figure 55 shows that less dose is required at room temperatures to produce a given effect. This is known to be due in part to radio-resistance caused by chemicals added to reduce cell damage during the freezing process.

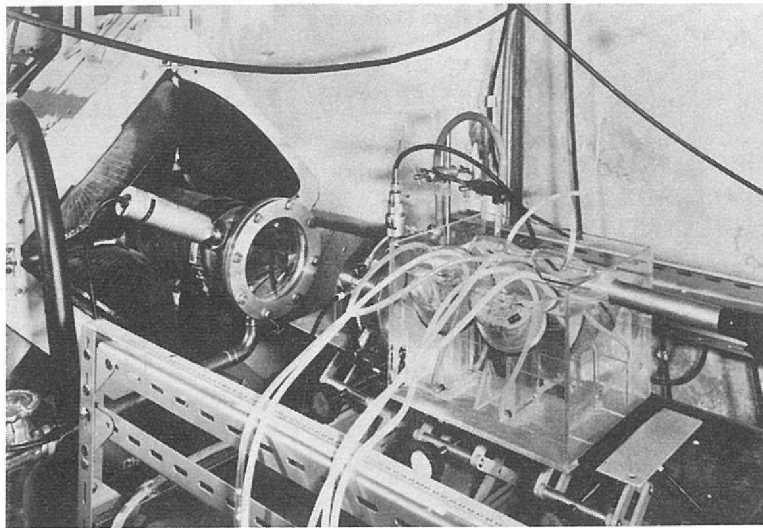
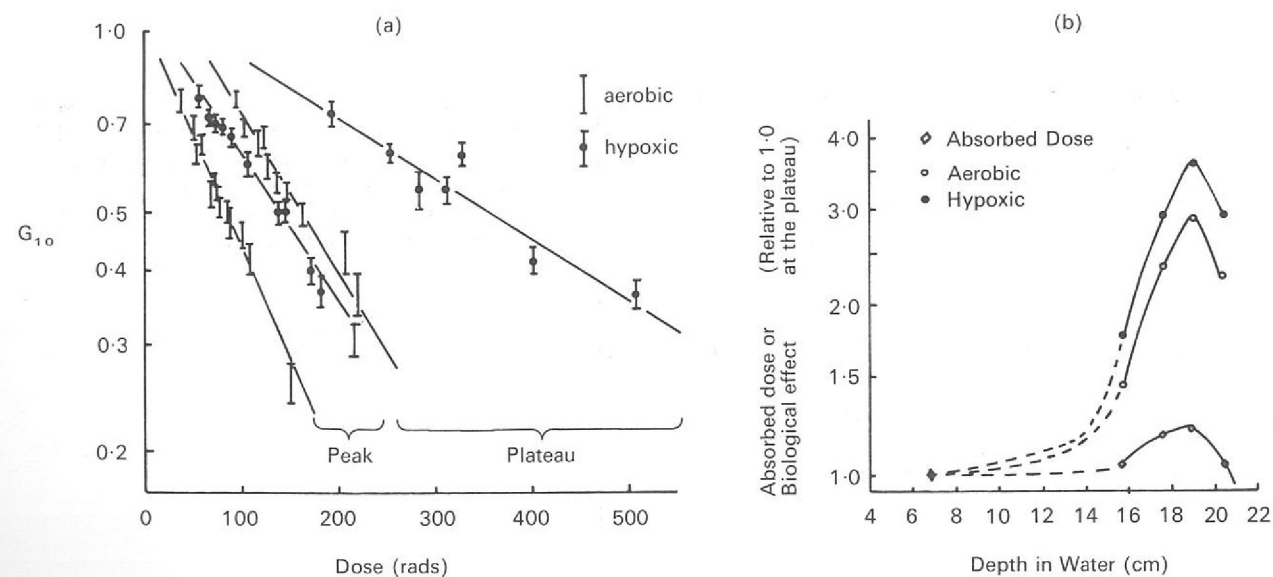


Figure 57. View of the experimental rig for exposing bean roots. In the water tank bean roots were irradiated at various depths along the beam direction at a temperature of 5°C. At each depth half the beans were made hypoxic by flushing with pure nitrogen. (9262).

The Churchill Hospital group have irradiated broad beans (*Vicia faba*). This system is a standard, having been exposed to many different fields, in particular Raju has exposed it to a  $\pi$  beam (peak only) at Berkeley Synchrocyclotron, California. Only the tips of the roots are sensitive and so two groups of 12–15 beans could be irradiated within the confines of the beam spot. The groups were in separated compartments, one of which was kept oxygen free. The beans were irradiated at 5°C where the cell cycle is halted and sublethal damage is repaired relatively slowly. Figure 57 is a photo of the apparatus, the results are given in Figure 58. The beam has a momentum spread of 13% full width at half maximum, comparable to the spread required for therapy, but it can be seen that even so the biological effect is well enhanced deep in the target material, especially for hypoxic cells.

Figure 58 (a and b). Bean root response to  $\pi^-$  mesons as a function of dose and depth. Damage to the roots is measured in terms of the relative growth during 10 days after irradiation ( $G_{10}$ ). The points on figure (b) were obtained from figure (a) and other data at different depths.



## Theoretical High Energy Physics

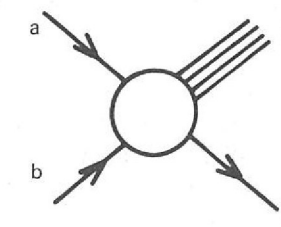
The Theory Division has been active in a wide range of investigations. The area of most intense activity, however, has been multiparticle production and inclusive reactions; since many aspects of this work are still new and unfamiliar, it is described below at some length. Other work is summarized more briefly thereafter.

In collisions at the high energies recently made available at the Batavia accelerator in the USA (400 GeV) and the Intersecting Storage Rings (ISR) at CERN, Geneva (2000 GeV), particles are profusely produced. The average charged multiplicity is about 10, while events with as many as 25 charged particles in the final state are commonly observed. Because of this, recent studies of such collisions emphasize the so-called inclusive approach, in which one measures and studies the production cross-section and momentum distributions of only some of the final particles, without specifying in general how many particles are actually produced. The reason for this shift of emphasis is partly technical, since inclusive cross-sections are easier to measure and save the experimenter from the almost impossible task of kinematically fitting high multiplicity events. Also, theoretically the inclusive approach is seen to be more natural for a system with many particles, in much the same way that in describing a liquid, it is more appropriate to consider quantities such as the density and the correlation functions without specifying in each case the exact number of liquid molecules involved.

The first quantity to study in the inclusive approach is the single particle distribution; for example, in the collision of two particles  $a$  and  $b$ , we study the distribution of particles of type  $c$  in the final state. We denote the reaction by:  $a+b \rightarrow c+X$  where  $X$  represents the 'missing' particles which are not detected by the apparatus. (See Figure 59). The single-particle distribution for type  $c$  particles is defined as  $\rho_1 = \frac{1}{\sigma_T} E_c \frac{d^3\sigma}{dp_c^3}$  where  $\frac{d^3\sigma}{dp_c^3}$  is the differential cross-section for finding a particle  $c$  with momentum  $p_c$  (and energy  $E_c$ ) in the final state; and  $\sigma_T$  is the total cross-section for  $a$ - $b$  collisions. Soon after the ISR came into operation, it was found that for  $\rho_1$ , the scaling law conjectured by Feynman and Yang was at least approximately correct. This states that the density  $\rho_1$  when considered as a function of the transverse momentum  $p_T$  and the scaled c.m. longitudinal momentum,  $x = 2p_L^*/\sqrt{s}$ , becomes independent of the incoming c.m. energy  $\sqrt{s}$  when  $s$  is sufficiently large. In other words,  $\rho_1(x, p_T, s)$  approaches a finite limit when  $s \rightarrow \infty$ .

*Multiparticle Production and Inclusive Reactions*

Figure 59. An inclusive reaction.



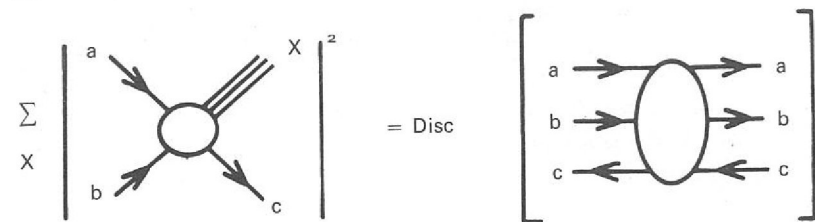


Figure 60. A representation of Mueller's optical theorem.

Once this scaling law is established, the interest immediately turns to a number of questions associated with it. How is the scaling limit approached? At what energy and under what conditions is it expected to be valid to a certain accuracy? How does the approach to scaling depend on the quantum numbers of the incoming and emitted particles? What is the shape of the density  $\rho_1$  and how is it related in one reaction to another? What dynamical mechanisms can lead to these properties? And what implications has this new knowledge on the understanding of other subjects? Attempts to answer these questions constitute a very active field of research, in which the Rutherford Laboratory is playing a significant role.

An approach to most of the questions raised above is facilitated by a generalisation of the optical theorem, first emphasized by Mueller, which relates inclusive cross-sections  $a + b \rightarrow c + X$  to forward elastic amplitudes of multiparticle collisions  $a + b + \bar{c} \rightarrow a + b + \bar{c}$ . (Figure 60). This allows inclusive cross-sections to be expressed in terms of singularities in the complex angular momentum plane, which dominate the asymptotic behaviour of scattering amplitudes. In this language, the scaling limit of inclusive cross-sections is simply the term in the Regge expansion due to the Pomanchuk singularity. The approach to the scaling limit is then governed by the non-leading singularities associated with the meson exchanges  $\rho, f, \omega, A_2$ . For emitted particles with small momenta in the rest frame of either the target or the projectile (the so-called fragmentation region with  $x \neq 0$ ) it follows that the density  $\rho_1(x, p_T, s)$  should approach the scaling limit approximately as  $s^{-\frac{1}{2}}$ . In addition, the usual criteria for the validity of Regge expansions in general help to delineate the domain of validity for the scaling limit.

The extension of the same ideas to particles with small momenta in the c.m. system (the so-called central region with  $x \simeq 0$ ) is not entirely straightforward, because of strong threshold effects which are found to persist up to very high energies (1000 GeV) in this case. Nevertheless, for the differences of cross-sections between particles and antiparticles, similar laws for the approach to scaling still apply. These predictions have since found support in the ISR data.

The size of the non-scaling terms in inclusive cross-sections depends on the Regge couplings which in turn depend on the quantum numbers of the particles involved. Now already from two-body phenomenology, certain so-called exchange degeneracy relations between Regge couplings are known to exist. In the language of the optical theorem, they imply similar relations among inclusive cross-sections for different incoming and emitted particles. Early applications of these ideas to the fragmentation regions led to predictions that for certain reactions, the non-scaling terms should approximately cancel, resulting in 'early scaling'. When extended to the central region, the relations became weaker because of the threshold effects mentioned above. Nonetheless, one still obtains useful predictions of the dependence of cross-sections on the quantum numbers of the incoming and emitted particles, which agree with existing experiments.

The Regge expansion discussed so far is an asymptotic expansion valid only for large  $s$ . Indeed, for the reaction  $a + b \rightarrow c + X$ , the scaled longitudinal momentum  $x$  of particle  $c$  is expressible as  $x = 1 - M^2/s$  where  $M^2$  is the missing mass squared of the undetected system  $X$ . When  $s$  becomes small for fixed  $x$ ,  $M^2$  becomes small also. One may then see prominent resonance structures in the system  $X$ , which are certainly not accounted for by the smooth asymptotic Regge expansion. Nevertheless, it was proposed, by analogy to the so-called dual property of two-body amplitudes, that the Regge expansion still represents in the resonance region a semi-local average of the actual cross-section. This statement is mathematically formulated in relations known as finite mass sum rules, which are based on the analyticity of scattering amplitudes and are close analogues of the finite energy sum rules of two-body collisions. It has been tested directly against experiment and found to be well-satisfied.

One very important conjecture concerning Regge couplings is that they factorise. When applied to inclusive cross-sections via the optical theorem, this leads to a large number of relations between the densities  $\rho_1$  from different reactions. Thus for example, from the factorisation of Pomeron couplings, one predicts that the distributions of  $\pi^-$  with small momenta in the laboratory are identical for  $pp, K^+p$  and  $\pi^+p$  collisions. Further, the factorisation of the couplings of other Regge poles implies simple relations between these distributions and those from collisions of e.g.  $K^-p, \pi^-p$  and  $\gamma p$ . In case of experiments with polarized targets, beams or emitted particles, most of the predictions of factorisation can be extended to the distributions in spins also. A series of careful tests have been carried out to check such predictions against data. One concludes that within existing experimental accuracy, such predictions are indeed valid. These constitute the most powerful tests of factorisation ever attempted. If their conclusion is confirmed by further experiment, it cannot fail to have important repercussions elsewhere. Although factorisation is strictly valid only at high energies, its predictions are still expected to hold in a semi-local sense in the low energy resonance region because of the duality arguments given above. This expectation is also found to be supported by experiment.

Next we turn to the shape of inclusive spectra, say for the reaction  $a + b \rightarrow c + X$ . For this one has a good description only in the additional limit when  $x \simeq \pm 1$ , or equivalent when  $s/M^2$  is large. In this limit, one can make a further asymptotic expansion in terms of the Regge singularities occurring in the  $b\bar{c}$  channel, leading to the so-called triple-Regge formula, which reduces the inclusive spectrum to a small number of parameters. The early work in checking this formula against experiment was done elsewhere, but the careful analysis later performed at the Rutherford Laboratory clarified some important points, concerning in particular the triple-Pomeron vertex of great theoretical interest and the kinematical dependence on the masses of particles involved. The latter point has since been further confirmed by the data of the local bubble chamber group. In addition, the analysis verifies in a specific example the connection of inclusive spectra to total cross-sections via a Chew-Low extrapolation and suggests models of how inclusive spectra are likely to depend on the polarization of the target.

In view of the close connection between the properties of inclusive spectra and the dynamics of hadrons in general, this new knowledge necessarily has important consequences elsewhere. A particularly impressive example of these consequences is obtained in the application of the triple-Regge formula just described via duality to quasi-two-body reactions. Again for the inclusive reaction:  $a + b \rightarrow c + X$ , the triple-Regge formula gives the shape of the inclusive spectrum (as a function of  $s$  and the missing mass  $M^2$ ) in terms of a few parameters such as the intercepts of Regge poles exchanged. The formula is originally valid only when both  $s/M^2$  and  $M^2$  are large, but can be extended semi-locally to the low  $M^2$  region by means of duality. Now when  $M^2$  is small, one sees resonances in the missing mass system  $X$ ; the inclusive cross-section is just made up of the cross-sections for the quasi-two-body production of such resonances. These last therefore must satisfy certain constraints imposed by the semi-local validity of the triple-Regge formula. As a result, one can predict the dependence on the resonance mass of quasi-two-body production cross-sections of resonances, and also how this dependence should change as the production angle varies.

Moreover, this mass dependence is seen to differ in a marked fashion from one production mechanism to another (e.g. whether  $\rho$ -exchange or  $\pi$ -exchange). All these predictions were immediately verified by the available data. Some of these effects were known already, but this is the first time that a systematic understanding has been achieved, summarising a sizeable body of experimental facts in terms of only a few parameters.

The successful application of the triple-Regge formula quoted above immediately led to others. Notice that the basic ideas in the previous example are not new, having already been made familiar in the two-body collisions. What is new is the recognition that in the triple-Regge expansion of  $a + b \rightarrow c + X$ , the expansion coefficients can conveniently be considered as the total cross-sections for the scattering between a particle and a pseudo-particle  $\bar{bc}$ , the latter being a 'Reggeon' continued off-mass-shell. By applying to particle-Reggeon scattering the familiar ideas of semi-local duality, one obtains the new results. The mass of the 'Reggeon' is  $\sqrt{t}$ , i.e. the momentum transfer between the particles  $b$  and  $c$ , and its quantum numbers are those of the system  $\bar{bc}$ . It is the greater freedom in varying both the mass and the quantum numbers of the 'Reggeon' pseudo-target which is being exploited here to yield the new information.

Obviously, exploitations of this powerful tool do not stop here. Three other examples of its use are worth quoting:

(i) A long-standing problem in hadron collisions concerns the dual properties of baryon-antibaryon scattering. It has been argued here that in contrast to the usual case, nonexotic resonances in the direct channel should be dual to exotic exchanges. The trouble with this statement is that it can not be checked experimentally with actual baryon-antibaryon scattering, the physical threshold for this being so high that direct channel resonances cannot readily be measured. However, when one of the baryons is taken off-shell by exploiting the technique just explained, this difficulty is removed. Indeed, an analysis in this direction gives for the first time empirical support for the dual property of the baryon-antibaryon system claimed above.

(ii) As far as we know, the Pomeron singularity does not exhibit itself as a genuine particle and therefore cannot easily be studied directly. None the less, its significance in hadron dynamics cannot be ignored and any information concerning its properties is of vital importance. Now by using the technique detailed above, one has a means of studying the forward elastic particle-Pomeron amplitude for any small value of the Pomeron mass  $\sqrt{t}$ . In particular, one such study reveals some interesting experimental evidence for the existence of an abnormal dual component which, in contrast to the normal components in particle-particle scattering, has diffractively produced resonances dual to Pomeron exchange.

(iii) Second order corrections to Regge pole models occur as cuts in the complex angular momentum plane, whose magnitudes are governed by the particle-Reggeon amplitudes described above. Using existing data on inclusive reactions, one can therefore set an upper limit on the size of cut corrections in certain processes. The limit so far established, though insufficiently stringent for practical purposes because of large experimental errors, has shown the way for further developments.

Thus research during the last year has provided a lot of information on the properties of inclusive cross-sections. However, one is still in the dark on a more fundamental question, namely: what are the dynamical mechanisms of particle productions which possess these properties? Present answers are very preliminary and centre on two production mechanisms, called diffraction and multi-peripheralism. The first produces particles by the formation of two heavy objects (fireballs) with constant cross-sections, followed by their subsequent decay. The second is typically an independent emission of particles. Examination of their implications for inclusive spectra led to the conclusion that their differences cannot easily be recognised at energies much below 100 GeV. At higher energies, although the two mechanisms still give similar predictions for the energy dependence of the total

cross-section and the average multiplicity, they differ markedly in the way in which the cross-section  $\sigma_n$  is distributed among the various multiplicities  $n$ . Using the latest data on  $\sigma_n$  including those from Serpukhov and Batavia, a series of careful analyses has established that neither diffraction nor multiperipheralism is by itself consistent with experiment. However, a simple combination of the two mechanisms can yield a very good description of all existing knowledge of  $\sigma_n$ . Moreover, the extrapolation of such a 'two-component model' gives interesting predictions at the highest ISR energy. Much of these results have since been confirmed by independent analyses at other laboratories.

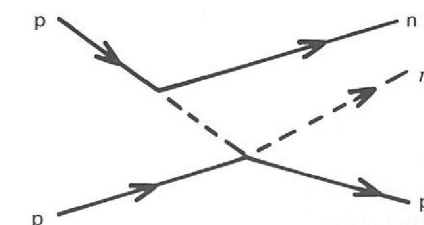
In addition to the original work described above, several review papers on multiparticle reactions have been produced, representing invited contributions to conferences and summer school lectures.

Diffractive processes  $a + b \rightarrow a' + b'$  are those in which only vacuum quantum numbers are exchanged, so that  $a'$  and  $b'$  have the same charge, isospin, G-parity, strangeness, etc. as  $a$  and  $b$ . Elastic scattering is an example; it receives contributions from other exchange mechanisms too, but at high energy the latter becomes unimportant and diffraction dominates.

Elastic pp scattering can now be measured to ultra-high energy at the ISR. The differential cross-section has some remarkable properties: the exponential slope of  $d\sigma/dt$  increases with energy ("shrinking"); there is a small but significant break in the slope at  $t = -0.1 \text{ GeV}^2$ ; and a minimum develops near  $t = -1.2 \text{ GeV}^2$  at ISR energies. Elastic  $\bar{p}p$  scattering is expected to share the same behaviour asymptotically, but up to 40 GeV/c there is no sign of shrinking—rather the opposite. Several studies of these data have been made. The pp shrinking can be ascribed to an effective Pomeron Regge pole, and the slope break can be quantitatively described by a separate peripheral component, associated with some class of peripheral inelastic processes. Changes in the pp shrinking, and sub-asymptotic differences between pp and  $\bar{p}p$  can be described by normal Regge pole exchanges. The minimum in  $d\sigma/dt(pp)$  can have various explanations: in this connection it will be interesting to examine the energy-dependence of  $d\sigma/dt$  at fixed  $t$ , since some suggested interference mechanisms can cause  $d\sigma/dt$  to rise with increasing energy, in a limited region. There is great interest in the origin of certain low-mass enhancements, observed in the spectrum of particles  $X$  in diffraction-like processes  $a + b \rightarrow a + X$ . In  $pp \rightarrow pn\pi^+$ , for example, an enhancement is seen in the  $n\pi^+$  distribution near mass 1400 MeV. Is this a genuine  $N^*(1400)$  resonance, or just a kinematical effect? (A similar question applies to the  $A_1(1070)$  enhancement in the  $\pi\rho$  distribution, seen in  $\pi N \rightarrow \pi\rho N$ .) A suggested kinematical origin is the Deck mechanism, in which the incident  $p$  dissociates virtually into  $n\pi^+$  and the  $\pi^+$  component scatters elastically from the target. (Figure 61.) This mechanism certainly gives an enhancement near threshold in the  $n\pi^+$  mass distribution, and other observed characteristics such as strong forward peaking of the resulting  $n\pi^+$  production; it has therefore been quite widely accepted. A recent more careful study, however, has shown a serious defect in this explanation. A crucial ingredient is the exchange of a virtual pion, giving strong dependence on momentum transfer at the  $p \rightarrow n$  vertex: this same ingredient also predicts a strong angular dependence within the  $n\pi^+$  system—which is simply not present, when the data are analyzed to extract it.

*Diffractive Processes*  
(ref. 13, 14, 30, 31, 33, 49, 56, 58, 61, 79, 85, 88, 89, 90, 91, 98, 114, 124, 135, 150, 153)

Figure 61. Deck mechanism for  $pp \rightarrow pn\pi^+$ .



*Analysis of  $\pi N$  and  $\bar{K} N$  Scattering, through Phase Shifts, Dispersion Relations and Duality.* (ref. 15, 28, 29, 52, 53, 54, 83, 84, 87, 97, 130, 206)

Low energy  $\pi N$  scattering has provided many valuable insights in the recent past. Systematic phase shift analyses of data have established the form of the scattering amplitude, which immediately gives information about the spectrum of excited nucleon states: information about other physical processes can also be gained, by exploiting analyticity. Some examples of the latter approach are the use of partial wave dispersion relations to learn about low-energy  $\pi-\pi$  scattering and to place constraints on high-energy  $\pi N \rightarrow N\pi$  backward scattering parameters. Another example is the use of finite energy sum rules to study Regge pole exchanges in high-energy forward  $\pi N$  scattering. A related approach, using duality, is to infer high-energy mechanisms directly from average properties of phase-shift solutions. A study along these lines found evidence that the diffractive contributions are mainly central, in impact parameter, whereas the Regge exchange contributions to imaginary parts are mostly peripheral. An analysis of the  $\pi N$  charge-exchange mechanism at momentum transfers up to  $t = -2.5 \text{ GeV}^2$ , where high-energy data are rather incomplete, confirms the FESR study above; the helicity-flip amplitude is found to behave just like a simple  $\rho$  Regge pole term, in contradiction to theories that predict strong absorptive corrections.

There is much to be gained by extending such studies to  $\bar{K} N$  and  $\bar{K} N$  scattering. These systems are described by the same invariant amplitudes but experimentally the  $K^- p$  interaction shows many resonances whereas the  $K^+ p$  interaction is almost structureless. Understanding this in terms of the form of the amplitudes will give greater insight into the ideas of duality, which relate the resonances to Regge exchanges. Comparing the  $\pi N$  and  $\bar{K} N$  amplitudes will also give greater understanding of the dynamical aspects of SU(3) symmetry. First one must extract scattering amplitudes from  $K^\pm p$  scattering data.

In collaboration with the Bristol-RHEL-Southampton experimental group the analysis of their  $K^+ p$  data was extended to investigate the movement of complex zeros of the scattering amplitudes to help with the choice between various possible amplitudes. The data have now reached the stage that only two basic types of solution exist below 2 GeV/c —one where the s-channel spin flip amplitude is almost real as preferred by duality and the other where this amplitude is almost imaginary. An experimental measurement of the sign of one of the spin rotation parameters would be enough to distinguish between these two situations.

In the case of  $K^- p$  scattering, most data below 1 GeV/c come from low statistics bubble chamber experiments. A coupled-channel analysis in the range 400 to 1200 MeV/c has confirmed many branching ratios and suggested a new resonance required by the quark model as well as providing evidence against some other possible resonances.

Another problem concerns the very low energy  $\bar{K} N$  amplitudes and their form below threshold. This knowledge is essential for extracting the  $\Sigma$  and  $\Lambda$  coupling constants as well as for studying the related problem of the coupling of the  $Y_0^*(1405)$  to the  $\bar{K} N$  channel. The analysis is very involved due to Coulomb and mass difference effects in the various channels but detailed investigation has given a better guide to the errors on our present knowledge of the amplitudes as well as indicating where new experiments would be most useful.

An essential part of all these analyses is the close contact between experimenters and theorists, influencing both the work in progress and the choice of new experiments. To review progress in the field of  $\bar{K} N$  and  $\bar{K} N$  physics a three day meeting was arranged at Cosensers House bringing together over 40 experimenters and theorists. Many useful discussions resulted and it became clear where new experiments were most needed.

*Weak and Electromagnetic Interactions* (ref. 42, 43, 94, 95, 96)

There has recently been great interest in a class of model, originally suggested by Salam and Weinberg, which aims at unifying the weak and electromagnetic interactions. It has long been known that the quantum of the electromagnetic interaction, the photon, is associated with gauge invariance of the second kind corresponding to charge conservation. In the unified type of theory the quanta associated with the weak interactions, the intermediate vector bosons, together with the photon are identified as gauge fields correspond-

ing to a more general symmetry postulated for the world. The differences between the electromagnetic and weak interactions are then described by a mechanism known as spontaneous breakdown of the gauge symmetry, which allows the intermediate vector boson to acquire a mass.

Interest in these theories has been revived because they have recently been shown to be renormalisable. Present phenomenological theories of the weak interactions, involving only the observed charged currents, violate unitarity when continued to very high energies. However renormalisable theories avoid unitarity violation by cancellation of the conventional term with either new heavy leptons or neutral currents or a combination of the two. It is of great interest to look for such hitherto unobserved objects. An analysis suggests that some effects of the neutral currents in these theories should be experimentally observable in the reactions  $e^+e^- \rightarrow \mu^+\mu^-$  and  $\mu p \rightarrow \mu + \text{anything}$  at centre of mass energies of the order of 200 GeV.

In extending these theories to hadrons, there are difficulties in reconciling the symmetry (SU(3)) preferred by the hadrons with that postulated for the leptons. In one approach a new quark is introduced and the hadronic symmetry extended to SU(4) but this leads to difficulties in interpreting the hadronic spectrum. A more promising approach uses three quark triplets which can naturally be classified in the leptonic symmetry while still generating the conventional SU(3) hadronic states.

Both of the above approaches need new "charmed" hadronic states, that play an important part in cancelling unobserved  $\Delta S = 1$  neutral currents induced by higher order processes. However this cancellation requirement puts an upper limit on the mass of the charmed states; since they should be observable with the new generation of accelerators, they seem to provide the best test of this type of model.

Calculation of other higher order effects is also very interesting with a renormalisable theory. In the proton-neutron mass difference calculation there is hope that the theoretical divergence arising from the exchange of a photon may be cancelled by contributions from the exchange of intermediate vector bosons.

Almost all detailed empirical information on  $\pi\pi$  scattering comes from analysis of dipion production reactions,  $\pi N \rightarrow \pi\pi N$  etc., with physical  $\pi\pi$  scattering given by the one-pion exchange signal extrapolated to the pion pole. The general procedure is standard but there are a number of different ways to implement it. One possibility is, before extrapolating, to make an amplitude analysis of the production process. This enables the potentially one pion exchange part to be isolated, besides giving information of interest in its own right. At present, lacking polarization information, it is not possible to make a model independent analysis, so the data have to be eked out with plausible assumptions. A start has been made by analyzing data on S and P wave dipion production in the reaction  $\pi^- p \rightarrow \pi^+ \pi^- n$  at 15 GeV/c.

A soft-core two-nucleon potential was fitted to two-nucleon data (scattering lengths, elastic scattering phase shifts for  $J \leq 5$ , deuteron constants) up to 400 MeV. The potential has central, spin-orbit, tensor and total angular momentum dependent terms, and gives a good description of the data, with  $\chi^2/n = 1.6$ .

Many-body theory based on the concept of a reaction matrix for finite nuclei has been used to calculate the ground state properties of  $\text{He}^4$ . A new method, which gives accurate solutions to the reaction matrix equations, has been developed and it has been shown that it can be applied to any double magic nucleus. The binding energy, the proton and neutron densities, the form factor and the mean square radius have been computed for  $\text{He}^4$  for three different soft core potentials. The results depend strongly on the structure of the two-nucleon potential for  $^3S_1$  and  $^3D_1$  states. A satisfactory result has been obtained for a potential which is relatively weak in these states.

*Dipion Production and  $\pi\pi$  Scattering* (ref. 32, 51, 152)

*Nucleon-Nucleon Potential and Nuclear Ground State Properties* (ref. 100, 102)

The main control room for Nimrod (HL 39719)

# ACCELERATOR OPERATIONS AND DEVELOPMENT

# Accelerator Operations and Development

## OPERATION OF NIMROD

(ref. 194, 195, 196, 197)

Nimrod, the 7GeV proton synchrotron accelerator, has had a very successful year of operation. Records have been set for the number of hours used for high energy physics, for the operational efficiency during time scheduled for high energy physics, for the number of protons accelerated and for the number of machine pulses.

The accelerator was run from late February until the end of the year. The annual shutdown due to start in December has been put back to mid-February 1973 to allow phasing-in of the work on the new injector which has now been approved and which is described later.

The accelerator has been operated in 3-week cycles. The major portion of each cycle, usually about 17 days, being devoted to high energy physics research, with the remainder accounted for by accelerator development, maintenance and start-up time.

The operations record is summarised as follows:

High Energy Physics Research	Hours
Scheduled time	5962
Good beam time	5398

ie beam on for a record 90.5% of scheduled physics research time.

The remainder of the year is accounted for as under:	Hours
Machine Physics and start-up	1,218
Routine maintenance and minor modifications at 3-weekly intervals	395
Main shut-down for major modifications and maintenance in January and February	754
National electricity supply emergency in February	348
Christmas holiday	107

The total number of protons accelerated during the year, in excess of  $22 \times 10^{18}$ , is about 26% higher than that achieved in 1971 and is a new high, as is the number of machine pulses with beam at  $8.26 \times 10^6$ .

As recorded above, the national electricity supply emergency curtailed the operation of Nimrod in the first two cycles in February. Nimrod was shut down on 11 February in order to conserve power, interrupting the programme of accelerator development work and delaying the start of HEP research. Nimrod started up again on 26 February, with limited operation possible at 4 GeV/c from 27 February. The electricity supply situation further improved and Nimrod was restored to the normal operating parameters of 8 GeV/c at 22 pulses per minute from 2 March.

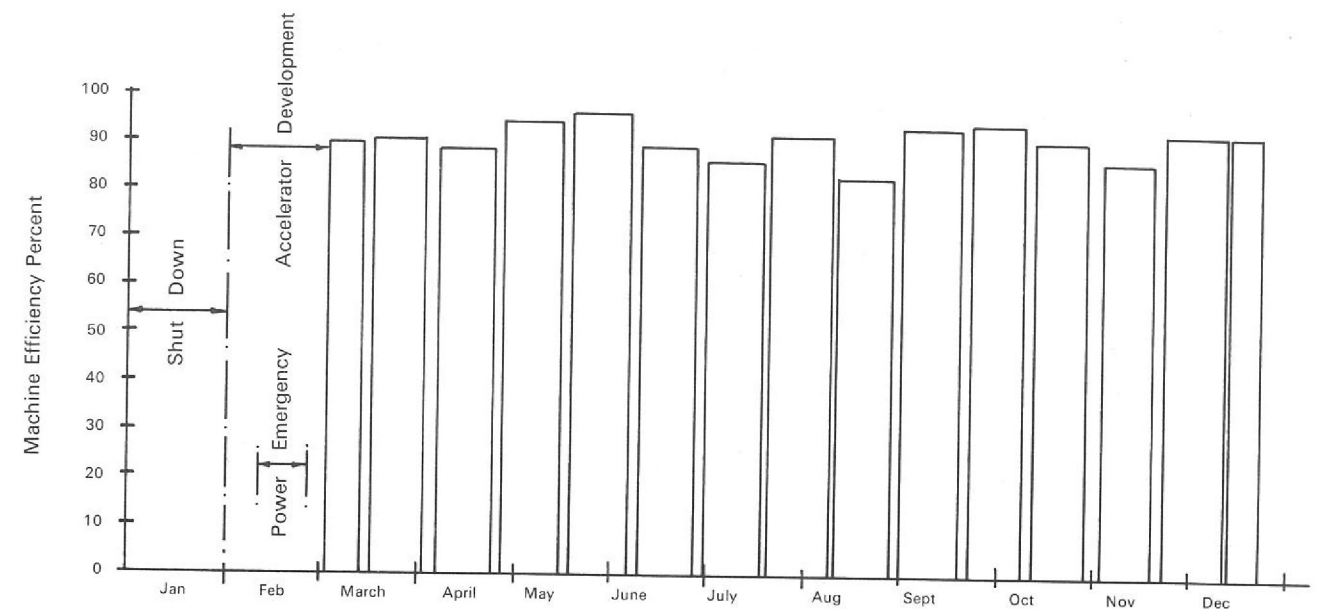


Figure 62. Nimrod operating efficiency during scheduled HEP research time, during 1972.

### Table 6

#### Nimrod Operations 1972

Date	Hours		Clock	Shut-down	Maint	HEP Research					Machine Physics and Development				
	From	To				Sched.	Beam On	Set-Up	Exp. Off	Nimrod Off	Nimrod Avail.	Sched.	Beam On	Exp. Off	Nimrod Off
Jan 1	Mar 31	2183-00	1101-08	13-68	595-30	537-48		2-38	55-44	539-86	472-94	298-03	35-03	139-88	333-06
Apr 1	Jun 30	2184-00	0-40	127-65	1734-93	1594-56		1-75	138-62	1596-31	321-02	205-32	15-66	100-04	220-98
Jul 1	Sep 30	2208-00		99-61	1971-22	1755-27	9-63	1-68	204-64	1756-95	137-17	85-13	11-90	40-14	97-03
Oct 1	Dec 31	2209-00	107-50	154-42	1660-40	1510-89	18-20	2-06	129-25	1512-95	286-68	138-05	20-83	127-80	158-88
Totals		8784-00	1208-98	395-36	5961-85	5398-20	27-83	7-87	527-95	5406-07	1217-81	726-53	83-42	407-86	809-95
Percent Clock Time		100-00	13-77	4-50	67-87	61-45					13-86				
Percent HEP Scheduled Time					100-00	90-55	0-47	0-13	8-85	90-68					
Percent MP Scheduled Time											100-00	59-66	6-85	33-49	66-51

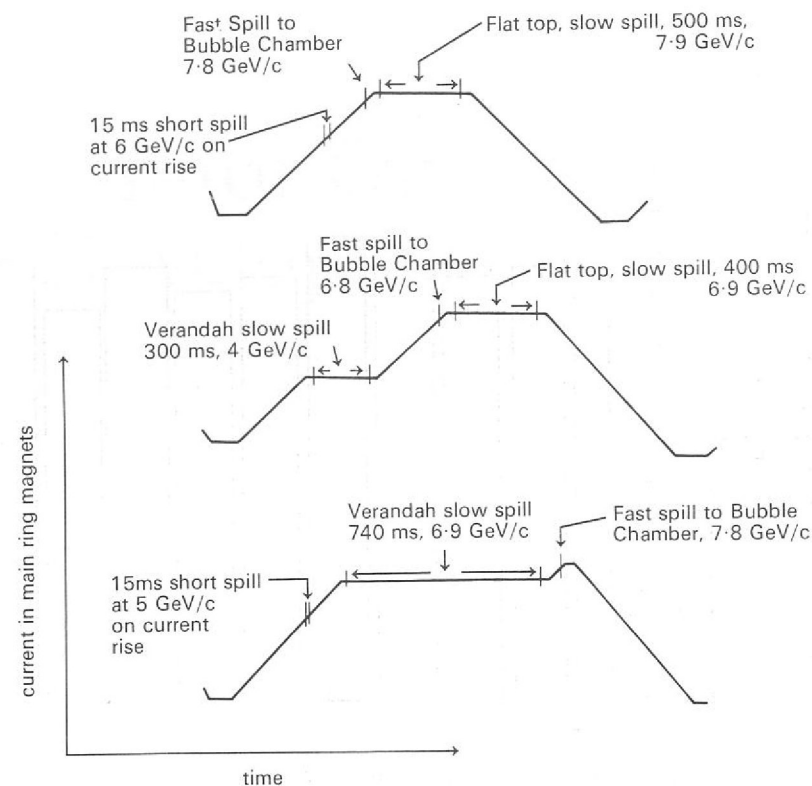


Figure 63. Beam spill conditions used during the year.

The pattern of utilization for HEP research was similar to that followed in 1971. On a number of occasions, dictated by user requirements, "verandah" operation in different modes was employed. Figure 63 showing beam spill in relation to the Nimrod magnet current waveform illustrate some of the patterns used during the year.

For the whole of the year Nimrod has operated without an injection platform. Injection was accomplished at a dB/dt of about 1.8 T/s instead of 1.0 T/s which had previously been the norm. This, together with the introduction of a simplified injection timing system involving fewer variables, has given more stable operating conditions.

A new field measurement trigger system using an electron-spin resonance probe, instead of the more conventional peaking strip previously employed, was commissioned early in the year and has proved very reliable in operation.

The computer control and data acquisition system in the Main Control Room is in extensive use to monitor the Nimrod beams and to assist with the control of the external beam lines. The programs most frequently used are a) GRAF—for plotting diagnostic data versus time or the current in a beam line magnet, b) NIXI—for displaying diagnostic data on nixie tube displays, c) STAT—for recalling from the disc and printing out a log of the circulating beam during the previous 24 hours and d) PRNT—for printing a log of selected diagnostic data averaged over several pulses and repeated every n minutes. Other programs exist e.g. for control of magnets. A hard-copy unit has been added to the display system.

A set of interactive display programs has been written. These are based on a root program which is called by pushing a button on the control desk. The resultant computer interrupt causes any current program to be ended or suspended, the root program to be loaded into core and a list of optional programs to be displayed. Across the face of the television monitor, which repeats the display on the main control room desk, are 7 horizontal and 8 vertical infra-red light beams. The program names displayed by the root program are at the intersection of some of these beams and when an operator points his finger at one of them a pair of light beams are intercepted. This causes the appropriate program to be called and a set of options to be displayed. An option can then be selected by pointing a finger at one of the option names. These options perform functions such as a) displaying a list of beam line magnet currents, or pole face winding currents or diagnostic data, b) printing out the

above type of data, c) updating data tables on the disc, or d) returning to the root program or ending the root program. There is, therefore, a 'tree' structure of programs and options which can all be run without the use of the computer teletype. The various branches of the tree can be accessed in any logical order.

X1/K9, the fast spill extracted proton beam which services the 1.5 metre cryogenic bubble chamber was available throughout the year. A new 'thin-septum' energy loss extraction system replaced the 'thick-septum' system for the X1/X2 extracted proton beams in February 1972. This new system has performed very well since then with X1 extraction efficiencies equalling that of the X3 thin septum system (commissioned mid 1970). The extraction efficiency on X2 was adequate but not as good as X1 and X3. Thus X2 is unlikely to be used to provide extracted beams in the future.

A digital position control system, on the X3 plunging mechanism, was commissioned at the start of 1972 and has performed well since then. Positional re-setting accuracy of the 'IN' position of the kicker magnet is better than  $\pm 0.5$  mm, pulse to pulse. The plunged 'IN' position is set either by computer instruction, or alternatively, by manual operation of digi-switches in the main control room. This system replaces an analogue type control system.

A 900 kW static power supply was commissioned in February 1972. This power supply, together with regulators which supply current in a pulsed mode to the two plunged kicker magnets (for X1/X2 and X3/X3X extracted proton beams), worked well right from its inception. Particularly noteworthy is the fact that the X1/X2 regulator switches the current level of about 7000 amps (for X1) to 5000 amps (for X2) in less than 20 milliseconds with a reproducibility, pulse to pulse, of better than  $\pm 0.02\%$ . This permits extraction of a fast-spill beam into X1, at the end of current rise, for the 1.5 metre cryogenic bubble chamber, followed by extraction of a slow spill beam into X2 on flat top for the counter experiments in Experimental Hall 1, in the same machine burst. The system also provides, in the same machine burst, current for the X3 kicker magnet which supplies beams to counter experiments in Experimental Hall 3, on current rise. The relative positions of X2 and X3 in the spill mode may also be reversed.

The extracted proton beams X2 and X3/X3X are mutually exclusive for data taking on flat-top, thus the mode of operation has been to run one system on flat-top for data and the other on current rise at a lower momentum for tuning and setting-up purposes. About 5% of the circulating beam goes to current rise users, with the spill being about 15 milliseconds in duration. Flat-top spills have varied between 400 and 800 milliseconds according to demand. There was an increased emphasis during the latter half of the year on the longer spill times with the flat-top set at around 950 milliseconds.

Secondary beams off the extracted proton beams X2 and X3/X3X were:

X2 — K12A and K13C  
 X3 —  $\pi 8$ ,  $\pi 11$  and K15  
 X3X —  $\pi 9$  and N4

Scattered out beams  $\pi 7$ ,  $\pi 10$ , P71 and K10S, operating from machine internal targets, were in use during 1972, as required, sharing beam with the flat top or verandah extracted proton beams every pulse.

Faults causing large amounts of lost beam time were few this year. The largest individual items in terms of lost time were extraction system components. In one instance a failure of a magnet was caused by the non-operation of a protection system; another involved a coolant water leak, to a magnet. A scored shaft on a plunging mechanism caused vacuum problems and had to be replaced.

A water leak on a poleface winding system saturated part of the main winding on one magnet octant. This required a lengthy drying out period.

External Beams  
 (ref. 210, 234)

Fault Analysis

There was a period of several weeks when Nimrod's circulating beam intensity dropped from the normal figure of  $2.7 \times 10^{12}$  to approximately  $2.0 \times 10^{12}$  protons per pulse. This fault, whilst it did not interrupt the experimental programme to any large extent, proved very difficult to diagnose. However the beam intensity returned to normal on substitution of an earthy winding by a good one on a pole face winding pancake of the field gradient correction system for low field.

**Polythene Closure Plate.** The replacement of the older thick septum extraction system for X1/X2 by the more efficient thin septum system has reduced the radiation dose to two components of the machine which were especially susceptible to radiation damage. The polythene closure plate of Octant 7, which had received 20 Mrads since the start-up of Nimrod, exhibited numerous cracks due to radiation in combination with oxygen and was replaced during the shutdown. Other closure plates will require replacement during 1973; in the long-term the polythene will be replaced by a more radiation-resistant material.

**Pole Face Winding Water Pipes.** The second component requiring replacement was the system of nylon cooling pipes in Straight 7 which was changed to a system of nylon-coated copper pipe. Other components of the machine are known to be able to withstand much larger radiation doses than the closure plates or the nylon pipes and do not give rise to concern.

**Table 7**

**Analysis of Nimrod Off Time during Scheduled Operating Time for 1972**

Total Scheduled Operating Time (Physics Research and Machine Physics)		7179.66 hours	
Total Off Time (detailed below)		935.81 hours	
	Beam Time Lost Hours	% of Scheduled Op Time	% of Nimrod Off Time
<b>1. Faults and Routine Inspections</b>			
*Extraction Systems	(192.61)		
(a) Plunging Mechanisms	91.94	1.28	9.83
(b) Magnets	83.32	1.16	8.90
(c) Power Supplies	17.35	0.24	1.85
*Vacuum Systems	191.46	2.67	20.46
Synchrotron RF/Beam Control/TV/ Diagnostics	76.22	1.06	8.15
Injector	75.46	1.05	8.06
Coolant Systems	71.68	1.00	7.66
Nimrod Magnet Power Supply	(50.76)		
(a) Converter Plant	45.49	0.63	4.86
(b) Ripple Filter Plant	4.44	0.06	0.47
(c) Rotating Plant	0.83	0.01	0.09
Nimrod Magnet	32.00	0.45	3.42
Targets and Target Mechanisms	24.73	0.35	2.64
Inflector System	23.97	0.33	2.56
Pole Face Winding Systems	12.90	0.18	1.38
Miscellaneous	56.20	0.78	6.01
<b>2. Other Reasons</b>			
Start-up	120.76	1.68	12.90
Public Electricity Supply	7.06	0.10	0.76
<b>Totals</b>	<b>935.81</b>	<b>13.03</b>	<b>100.00</b>

\* Figures for Vacuum and Extraction Systems include routine inspection time.



Figure 64. Fitting a new polythene closure plate to the vacuum tank of Nimrod (see opposite) : (12511).

### THE MAGNET RING POWER SUPPLY AND ANCILLARY PLANT

The magnet has been pulsed throughout the year using both motor-alternator-flywheel sets and the complete converter plant. The overall performance of the rotating plant has continued to be very satisfactory.

The mercury-arc converter plant has operated very reliably, with a negligible arc-back rate.

The ripple filter installations have given good service throughout the year. As a result of tests carried out in February 1972 subsequent pulsing of the magnet has been carried out without an injection platform. During the year several programmes have included an intermediate platform (verandah).

Operational statistics are as follows:

Machine running time	7002 hrs
Machine pulsing time	6772 hrs
Total pulses	$9.03 \times 10^6$
Total pulses with a verandah	$0.93 \times 10^6$

The total number of pulses produced is the highest so far for any year of operation. The number of pulses with a verandah is also an annual record.

This was re-installed during the 1971-72 shut-down following completion of the repair programme described in the 1971 Report. The results of the Dielectric Loss Analysis tests carried out on the rotor before and after rewinding indicate that the original insulation had suffered degradation typical of dry aged insulation with a low level of contamination and a significant void content. However, no reliable estimate of the life expectancy could be deduced.

As a result of further modifications and improvement which are just being completed it is expected that the problem of high brush temperature, (which can lead to extremely rapid brush wear) will be finally resolved.

New flywheels, each with an integrally forged half-shaft to eliminate the original bolted and keyed construction between the flywheel and its corresponding alternator, were installed during the 1971-72 shut-down. Their subsequent performance has been entirely trouble free. The original flywheels have been dismantled and all slots and keyways subjected to magnetic particle crack detection. Both flywheels have been treated with preservative and are now in long-term storage.

No 1 Drive Motor

Drive Motor Brushgear

Flywheels

#### Machine Spares

Two bearing pedestals, each complete with a bearing for a nominal 508 mm diameter journal, have been received. These are suitable for use at the alternator and flywheel locations. A spare laminated pole rotor is in long term storage. The second laminated pole rotor and an alternator stator are stored in a humidity controlled enclosure. Spare induction motor stator coils and winding materials have been received to replace those supplied to the manufacturer for the repair of No 2 Drive Motor stator in 1971. Two spare sets of special vacuum remelted steel Vee coil support bolts are on order, one set will be installed in No 1 alternator rotor during the 1973 shut-down to replace the present ones which will have completed approximately  $27 \times 10^6$  pulses out of their nominal useful life of  $30 \times 10^6$  pulses.

#### Master Timer

Further modifications have been carried out on the verandah section of the existing timer to remove the arc-through alarm which hitherto had been present when a verandah programme was being carried out. The new master timer has been the subject of further development during the year and is now undergoing final tests prior to its installation which is planned for the shut-down early in 1973.

#### Grid Control Equipment

A complete set of spare units for the new type of converter grid control equipment has been manufactured. All operational units have given good service throughout the year.

#### Ripple Filters

All systems have operated satisfactorily throughout the year. During the 1971-72 shut-down, new pre-charge power units were installed on the static ripple filters. These enable the filters to be operated during the flat-top periods at all energies, whereas the previous units only allowed operation over a limited range. An interlock scheme between the static ripple filter and the converter grid control gear has been installed, the object being to prevent malfunctioning of the converter plant when the static ripple filter is operational. Apart from changing the type of relay used in the interlock, operation has been virtually trouble-free.

#### Ancillary Plant

**Heat Exchangers.** The programme of inspection and remedial action on all major heat exchangers as mentioned in the 1971 Report was completed during the 1971-72 shut-down.

**Water Chillers.** The new 100 ton refrigerator has been received and installation is virtually complete. Commissioning tests are to begin shortly. The capacity of the chilled chromate tank, originally 13,640 litres, has been doubled to cope with this extra refrigeration capacity.

**Demineralised Water Systems.** A spare 112 kW (150 h.p.) pump has been installed and commissioned on the No. 1 Experimental Area circuit.

### ACCELERATOR DEVELOPMENT

#### Second Harmonic RF System

The design of the second r.f. system for Nimrod and the initial stage of the development programme has been described in the 1971 Annual Report. The accelerating structure complete with the r.f. amplifier and control system was assembled in a test area in November 1972 to undergo a series of tests prior to installation and commissioning during the Nimrod shut-down due to start in February 1973.

Much of the testing of the r.f. amplifier, bias supply and ferrite loaded resonators was carried out under closely simulated conditions using a full-sized model cavity. The bias loop incorporating a 2000 A transistor bank regulator was developed using measurements at full power under swept conditions to the point where phase errors were held to within two degrees. The automatic level control system was proved and finally a simulated phase locked system was tried to establish the feasibility of holding the phase of the harmonic field to within a few degrees of the required relationship with the main r.f. cavity.

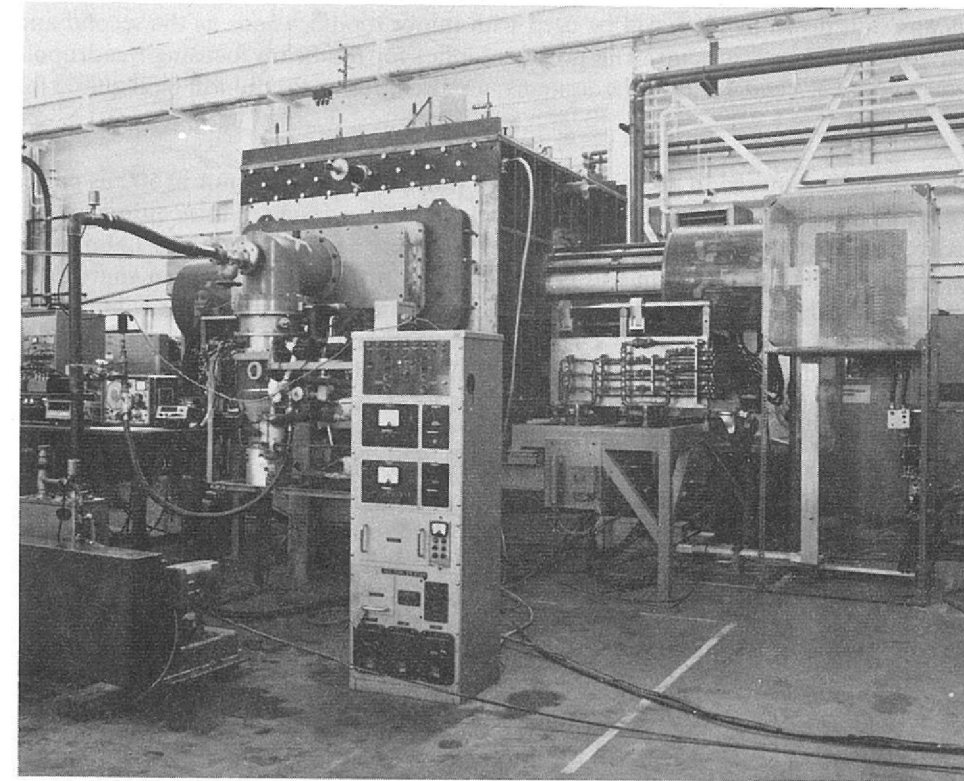


Figure 65. The second harmonic r.f. system undergoing tests (12476).

Following manufacture and vacuum testing of the steel straight section box, the bias windings, drift tube and resonators were installed for the final tests.

The performance of the system so far has proved very close to that of the model. The contacts, insulation and r.f. shielding of the final design are all within specification and the difficult vacuum sealing of the r.f. and water cooled d.c. conductors through the resonator windows has shown no signs of leaking.

The ferrite has proved to be well within specification and the required r.f. voltage levels on the drift tube are attained at about 60% of the ferrite power rating. Magneto-strictive effects in the ferrite led to mechanical/electrical resonances in the bias loop but these have now been overcome.

Reference was made in the 1971 Annual Report to a proposal to increase the intensity of extracted beams to  $10^{13}$  protons per pulse by providing a new injector which would increase the injection energy from its present value of 15 MeV to 70 MeV. Work on the design has continued during the year.

Financial approval to proceed with the new injector was received at the end of December 1972, and the aim now is to have the new injector ready for commissioning in April 1975.

To provide an extracted beam intensity of  $10^{13}$  protons per pulse the estimated current required from the injector is between 50 and 75 mA with a pulse length of 500  $\mu$ s. The new injector will be an Alvarez type of linear accelerator consisting of four r.f. cavities. The design of the first and fourth cavities is based on the corresponding parts of the injector in use on the 200 GeV accelerator at the National Accelerator Laboratory in the USA. Tanks 2 and 3 of the Proton Linac (PLA) which has been stored at the Rutherford Laboratory

*A 70 MeV Injector  
for Nimrod  
(ref. 215, 216, 248, 249,  
271-273, 283, 290, 294,  
295, 308, 312-319)*

since it was shut down in 1969, will be used with minor modifications as the second and third cavities of the new injector. The power supplies for the beam focusing quadrupole magnets in tanks 2, 3 and 4 will be d.c. systems; a pulsed power supply will be required for tank 1.

The pre-injector is required to produce a 665 keV proton beam of 200 mA in 500  $\mu$ s pulses for injection into the first cavity of the linear accelerator. The design of this equipment will be based on the results of development work which was carried out at the Laboratory during 1968-69. The proton beam will be produced by a duoplasmatron ion source and focused by a single electrostatic lens into a d.c. accelerating column. The column will operate at a potential gradient of 1.6 kV/mm which is three times that of the present pre-injector on Nimrod. With this value of gradient the expansion of the beam under space charge is not excessive and the structure should not be seriously affected by sparking. This will allow a storage condenser of high capacitance to be connected to the column to assist in stabilising the EHT voltage against the pulsed beam loading. The loading will be particularly severe in this pre-injector compared with other high current machines because of the unusually long pulse length. Electronic pulse stabilisation of the EHT voltage will also be provided. The EHT supply to the accelerating column will be from a commercial Cockcroft-Walton set similar to that at present in use on the 15 MeV Injector.

The r.f. system is designed to operate at a frequency of 202.5 MHz with a pulse length of 700  $\mu$ s, a repetition rate of 1 pulse per second and a peak power output of  $4 \times 4$  MW. The power for each of the four accelerating cavities will be derived from a master oscillator and common power amplifier stages up to a power level of 20 kW. At this level the power is divided to feed four two-stage high power amplifiers which are loop-coupled to each of the four cavities.

The 70 MeV beam will be transferred from the fourth r.f. cavity to Nimrod by a quadrupole triplet focusing channel and an achromatic inflector system. The inflector system has unequal contrary angular deflections at its input and output with quadrupole triplet lenses between the deflections to correct the momentum dispersion. For maximum radial acceptance the final element of the system is electrostatic with a 1 mm septum and an operating field of 5.75 kV/mm. At 70 MeV the sagitta of this element is so small that it must be immediately preceded by a magnetically shielded septum magnet.

Figure 66. The lay-out of the 70 MeV injector for Nimrod (12830).

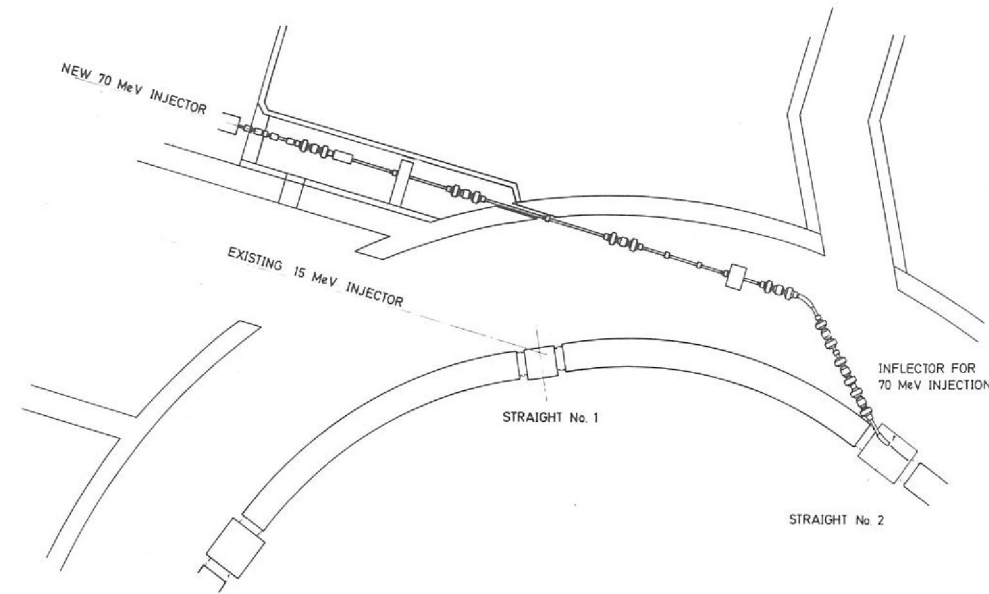
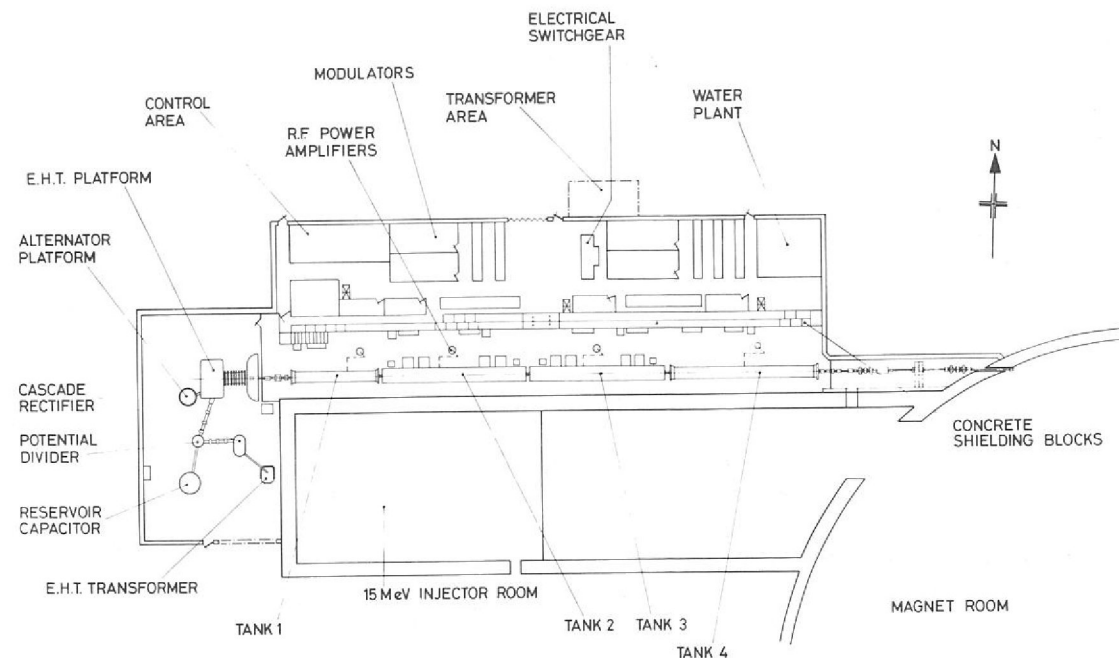


Figure 67. The lay-out of the inflector for the 70 MeV injector (12829).

A debuncher cavity is used in the transfer line. The r.f. power to the cavity has a programmed rate of change of phase so that the momentum of the beam in the transfer line may be linearly ramped by about 1 MeV during the injection interval. This allows a stationary equilibrium orbit to be maintained just inside the inflector septum so that the radial acceptance can be largely filled with particles having small amplitude betatron oscillations and is similar to the system used successfully in Nimrod with the present injector.

Where possible quadrupoles from the old PLA will be used and the debuncher-ramp cavity will be an ex-PLA unit.

It is intended that for some time Nimrod will operate with both the 70 MeV or 15 MeV injectors available. Since both beams are inflected at substantially the same machine radius in Nimrod it is necessary to remove or park the inflector system not being used. To park the 15 MeV inflector use will be made of the radial adjustment which was built into it. With some minor modifications this adjustment, which is external to the vacuum system, can withdraw the 15 MeV components sufficiently to clear the 70 MeV circulating beam. The reverse situation of enabling the 15 MeV beam to be injected will be dealt with by removing the 70 MeV inflector from its straight section hence saving the cost of a complicated parking system. (The components are larger than their 15 MeV counterparts.) In any case a rapid removal rig must be provided to remove the inflector for servicing purposes from the high level of radiation which is expected to build up in this straight section.

The building for the new injector will abut on to the existing 15 MeV injector building. The beam will be transported into the Nimrod Magnet Room via a tunnel and a hole in the wall of the magnet room. The earth mounding will be removed from the roof and sides of the existing injector building together with sufficient of the magnet room earth mounding to enable the tunnel to be constructed. Some of the magnet room earth mounding is essential for radiation shielding purposes and must be replaced, hence an earth retaining wall is required and this will form one end of the new injector building.

The accelerator tanks will be mounted on a piled foundation separate from the rest of the building to minimise effects due to settlement.

Protection from radiation will be provided by close packing of concrete blocks around the accelerator tanks.

## BEAM LINES AND ASSOCIATED EQUIPMENT

### Beam Line Installation

Most of the beam lines during early 1972 were at the final commissioning or data taking stage. Preparatory work was undertaken on equipment for the new beam lines  $\pi 12$ , K17, K19 and P81 due to be installed in early 1973 (see Figure 68).

In Hall 1, K10S and K12 were dismantled during the Autumn and in December work started on the dismantling of K9. In Hall 2, the control room for  $\pi 10$  was fitted with a re-designed air conditioning and ventilation system. The X3 Blockhouse in Hall 3 was also fitted with a ventilation system and beam line N4 was dismantled.

### K9 Beam Line Operation

During the year the K9 beam line has provided beams of particles for the hydrogen bubble chamber as follows:

- 1.1 GeV/c  $\pi^-$
- 4.0 GeV/c  $\pi^+$
- 2.0 GeV/c  $\bar{p}$
- 0.85 GeV/c p

The first three of these were used for normal physics experiments. The low momentum proton beam was used for measuring the neon hydrogen concentration ratio in the chamber liquid by a method independent of the usual thermal conductivity gas analysis. The low momentum protons stop in the chamber liquid and their range gives a measure of the density of the matter through which they pass. Adding a known amount of absorber in the form of metal bars in front of the chamber and measuring the resulting change of the range provides an absolute calibration.

The 2.0 GeV/c antiproton experiment was carried out at very short notice for the Tata Institute of Bombay. The yield of antiprotons at the end of the beam line was found to be as predicted from the measurements made in 1971 but unfortunately it was only possible to guide about 30% of them through the very narrow chamber entrance window that was fitted at that time. 200,000 pictures were taken.

The computer control system has continued to be developed during the year and is widely used both during setting up and for monitoring the beam during normal operation. It has enabled changes to be made that would not have been contemplated previously. The flexibility of the interpretive software has allowed modifications to be inserted swiftly into the programs as the users request them, and new programs can be written to suit the demands of the moment. During the year a visual display terminal has been added to the computer to replace the conventional teletype. The advantage of such a device is that quite long explanatory messages can be given to help the unfamiliar user.

### Electrostatic Separators

**Operations.** Five separators have been in operation in Nimrod beam lines during 1972. Two have been withdrawn after the successful completion of the K10S and K12A experiments. Of the remaining separators, two are of the flattened tube grid type. Operating experience is indicating that these separators are quicker to condition, more robust, need less attention and may ultimately give a superior performance.

The separator withdrawn from K10S was of the original type of construction with stainless steel plate electrodes for both anode and cathode; towards the end of its operating life, it was operating with an electrode gap field of 4.86 kV/mm at a gap setting of 150 mm.

The K12A separator was of the later glass cathode type. This separator ran at 5 kV/mm at a gap setting of 100 mm with no operational difficulties.

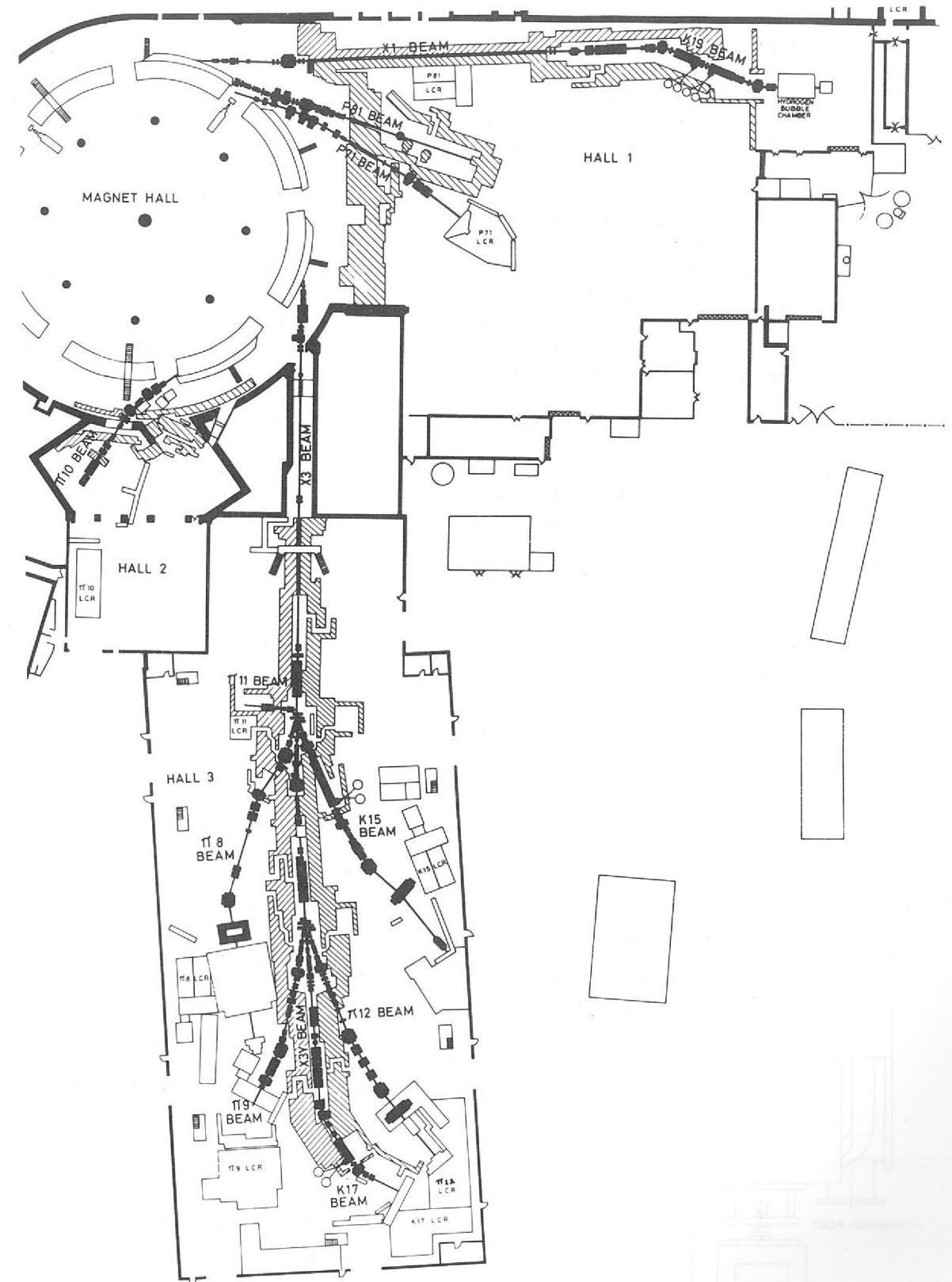


Figure 68. The beam line lay-out in the experimental halls planned for early 1973 (12683).

**Flattened Tube Grid Electrode Separators.** The first operational separator of this type is the two tank separator of the K9 beam line. This operates with the polarity reversed where the lower grid electrode is the cathode. Initially, this separator was run at 5 kV/mm with a gap setting of 100 mm and was not capable of sustaining a gap field much higher than 5.5 kV/mm. However, the field has now been raised to 6 kV/mm with a spark rate of less than eight sparks per hour by adopting a high pressure conditioning technique developed for use with the second two tank grid separator used in the K15 beam line.

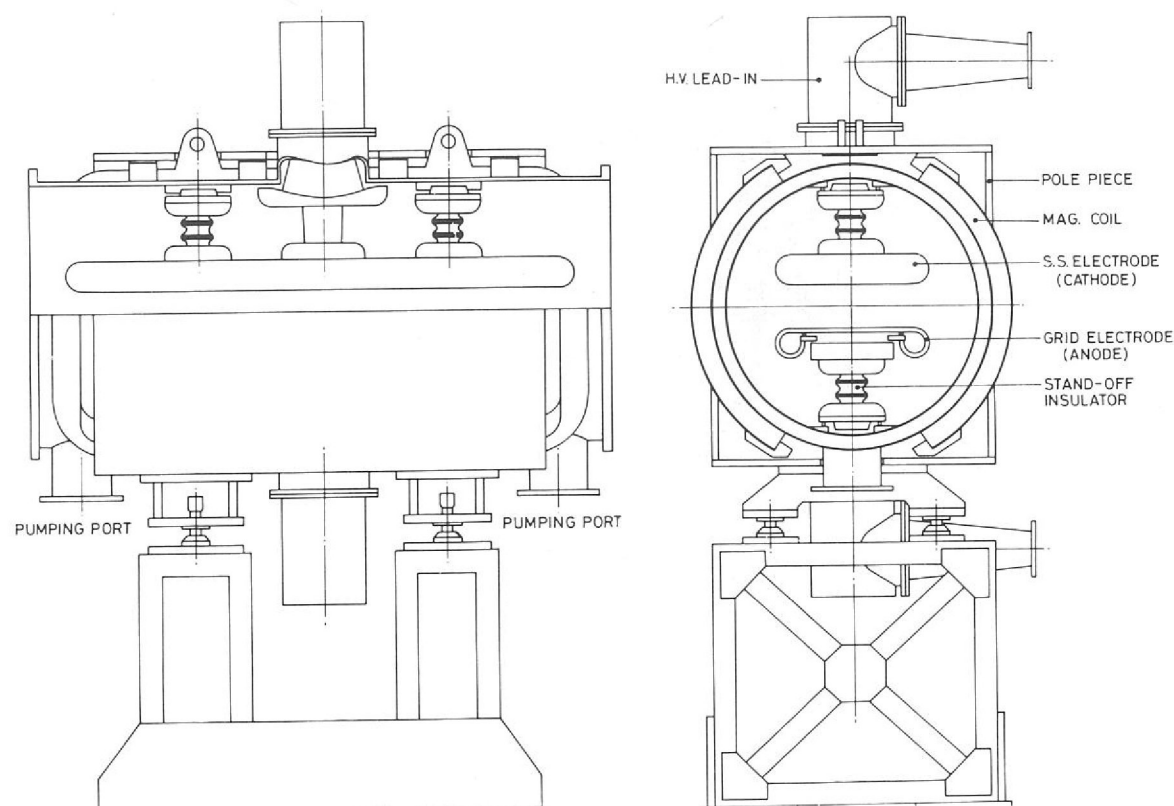
During the initial conditioning stages of the K15 separator it was found that by running the EHT power supplies without regulation and with the separator tank at low pressure, 1 mA of electrode current could be constantly drawn with a considerable reduction in low pressure conditioning time. In addition a technique was developed whereby, during the high pressure conditioning sequence, the tank pressure was gradually reduced while the electrode voltages were kept at some value higher than the normal operating level. The combination of these two techniques enabled the separator to be brought into operation within a few weeks. The latest operational features for this separator are as follows:

Electric Field	6 kV/mm
Gap	100 mm
Conditioning Time	8 hours
Time interval between conditioning	> 500 hours
Spark Rate	1 per 12 hours

These values are still improving.

It was found that the conditioning times and separator performance were unaffected by the removal of the liquid nitrogen cold trap. In consequence, the cold traps on all the operational separators have been removed without noticeable deterioration in performance.

Figure 69. Design for a short tank electrostatic separator (12754).



**Present Work.** This is concentrated on building and testing three new single tank separators for use on the K19 and K17 beam lines planned to be installed early in 1973.

One of the main changes made to these new separators is the standardisation of the stress shields. Previously, different electrode gap settings have required different sizes and contours of stress shields. The new standardised shields enable the electrode gap to be varied from 150 mm down to 80 mm without the need to change the shields.

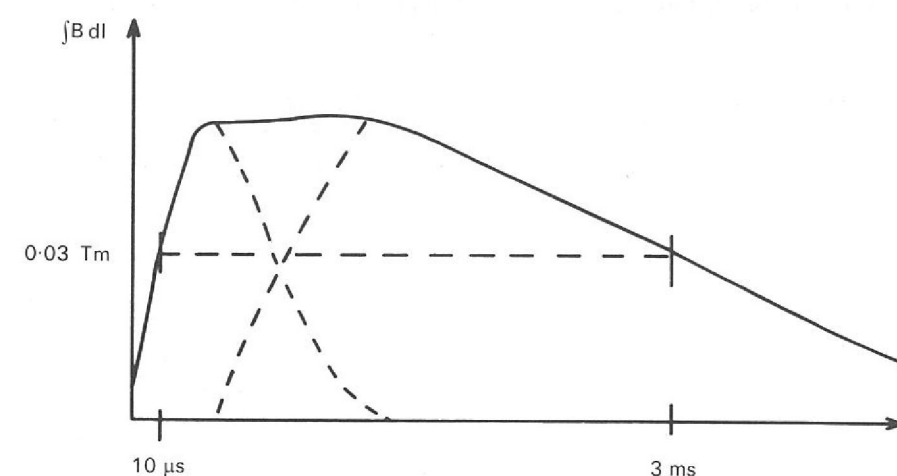
**Future Work.** Because of the need to keep beam line components as short as possible, especially in low momentum K meson beams, a new separator with as short a tank as practicable but still giving approximately 2 metres electrode length has been investigated. The lead-in end box has been dispensed with and a right angled lead-in has been manufactured and is currently under development to enable the EHT cables to be brought in to the tank at the top and bottom centres. The tank will be a hollow cylinder with axis along the particle beam; no stress shields will be required around the electrode. The coils for producing the magnetic field component of the separator will cover the full length of the vacuum tank.

To combine fast risetime with long hold-off and relatively high pulsed bending power the K19 shutter magnet will comprise two separately energised air-cored coils. The first gives the fast rise, with a trailing edge matched to the rise of the second, slower, coil whose fall-time is sufficiently long to provide the necessary pulse length. When traversing the correctly synchronised system, the beam experiences an integrated field as shown in Figure 70.

*Tandem Shutter Magnet  
for K19*

Risetime to 0.03 Tm is achieved in 10  $\mu$ s, after which the field overswings the minimum requirement by no more than 5% before finally drooping again to this value after a further 3 ms. Both 200 mm diameter air-cored coils are energised by capacitor discharge conducted by ignitrons.

Figure 70. The tandem shutter magnet waveform.



*Concrete Insulated Magnets*  
(ref. 35)

The first successful concrete insulated magnet to be built is now in service at the Daresbury Laboratory. A second magnet built by industry to our techniques, a quadrupole, has been in service for a year at DESY Hamburg, where it replaced a resin-glass insulated magnet which had been destroyed by intense radiation. There has been no detectable deterioration in the concrete insulation after a similar period of radiation.

A further concrete insulated magnet is being constructed for use in a Nimrod beam line, where it will save a conventional quadrupole from severe radiation damage.

*Ultra Thin Septum Magnets*  
(ref. 137, 228)

A test magnet with a 1.5 mm thick by 20 mm high septum has been tested and gave satisfactory results. This was built with a copper septum brazed to transverse stainless steel cooling tubes connected to a stainless steel manifold. A second thinner septum is being constructed with copper transverse cooling tubes connected to a stainless steel manifold. Studies show that the magnetic effect of the small current flowing in the manifold can be corrected with a counter current flowing in a parallel conductor adjacent to the manifold.

*High Field Magnets for Pulsed Beam Lines*  
(ref. 233)

Drawing on experience gained during the  $\Lambda^0$  hyperon experiment in 1971 a new set of pulsed magnets has been developed to provide a pulsed beam line for  $\Sigma^-$  hyperon experiments in bubble chambers.

Four series-connected air-coils, conducting 100–120 kA pulses of current derived from capacitor discharge, will be mounted in a very short beam line. The primary protons interact in a 100 mm long tungsten target sited at the first magnet. Two dipole magnets reach a peak 12 to 15 Tesla during their 1 ms pulses, and permit the later selection, at a slit bounded by depleted uranium, of only those negative secondaries having momentum in the range 16 to 20 GeV/c. Such a beam is therefore enriched in the heavier particles, such as  $\Sigma^-$ , having rejected most of the predominating negative pions. Arranged as a doublet, two quadrupoles, having gradients in the range 250 to 550 T/m, focus the secondary beam at the centre of the slit in the V-plane, permitting the capture of a much larger spread in divergence.

Figure 72 shows an 8-turn 200 mm long pulsed dipole magnet designed to withstand the enormous pulsed forces (up to 160 tonnes) generated on a coil side. Water cooling of the coil and stainless-steel components contribute to long life. To date a coil of this type has survived 55,000 pulses before failure; recent strengthening should extend this to 200,000 pulses.

The quadrupole construction is very simple, consisting essentially of four conductors arranged along the surface of a beam-axial cylinder. A test version gave 550 T/m along 500 mm, but with the useful aperture limited to 20 mm. At this strength, the focal length for a 20 GeV/c beam is about 500 mm.

Figure 71. Schematic of a pulsed beam line for  $\Sigma^-$  hyperons.

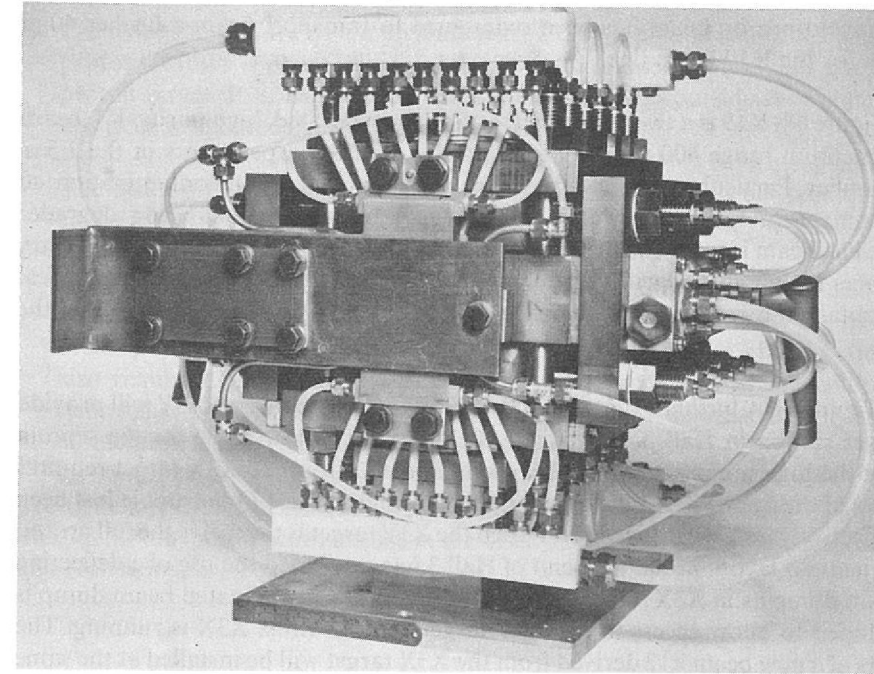
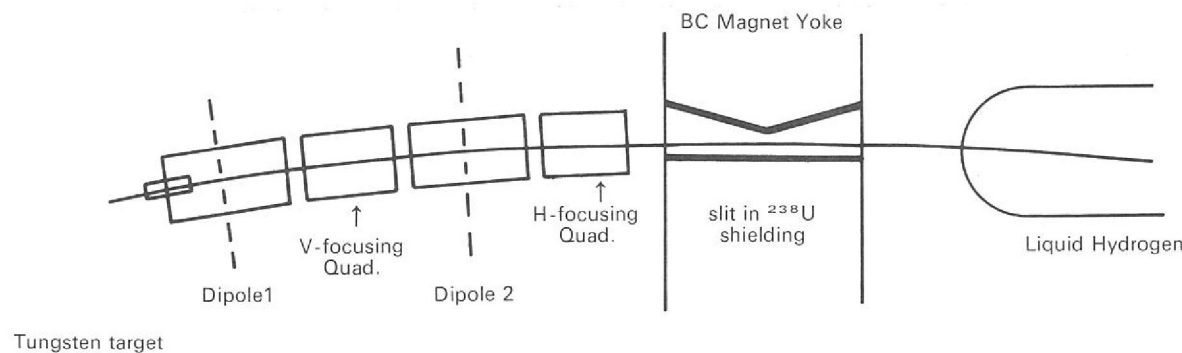


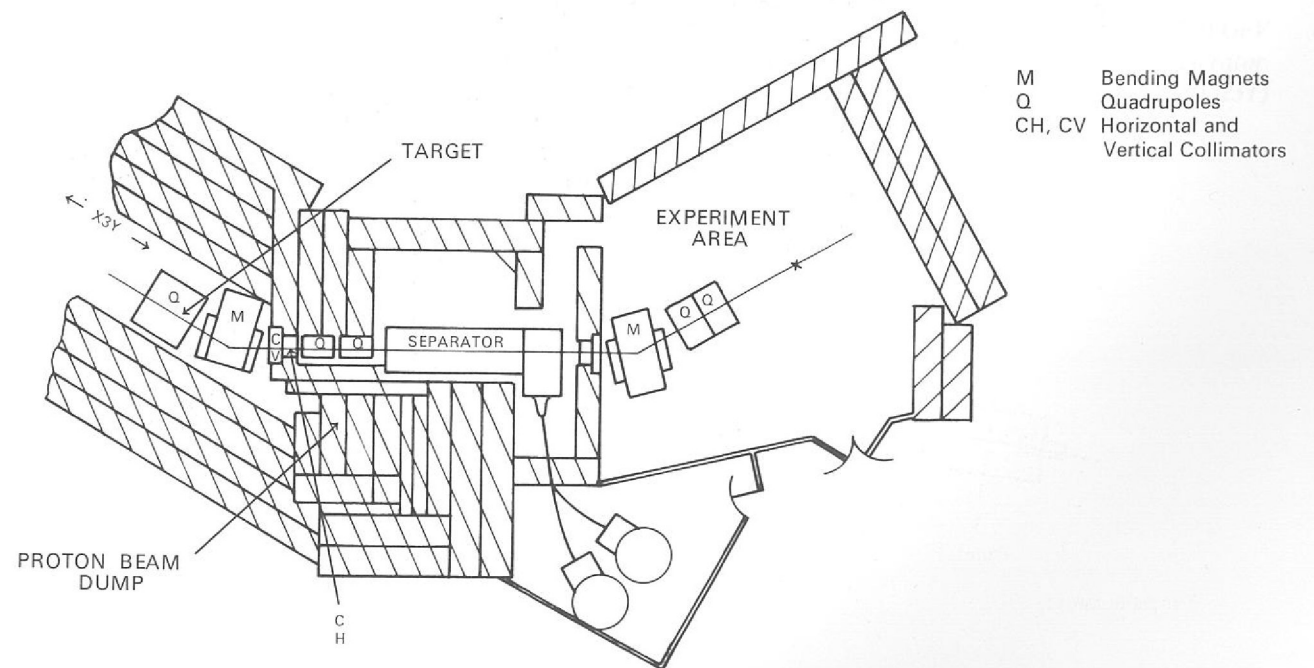
Figure 72. A pulsed dipole magnet: view of the current lead end (12479).

Designs for new beams to be built in the February 1973 shut-down have been produced. A general layout showing the experimental areas in 1973 is shown in Figure 68. This arrangement will allow simultaneous running of all beam lines installed at Nimrod.

*Beam Design*

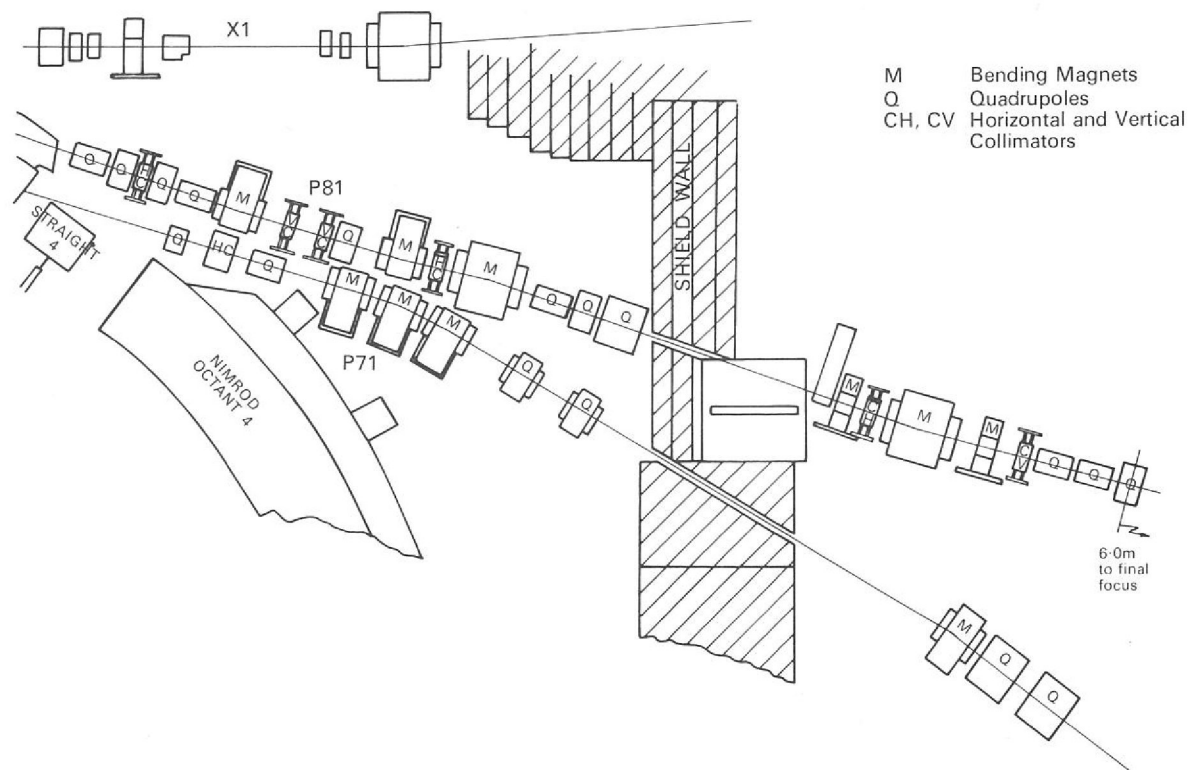
1. K17: (See Figure 73) A 600 MeV/c electrostatically separated  $K^-$  beam for use in conjunction with an energy loss degrader, to provide 'stopping' kaons for nuclear structure studies using X-rays from K-mesic atoms. The beam has an acceptance of  $20 \text{ msr } \% \Delta p/p$  and should deliver  $3000 K^-/10^{12}$  protons at the X3Y target, with a contamination of  $10\pi^-$  to  $1K^-$ .

Figure 73. K17 beam line (Hall 3).



2. The X1 extracted proton beam has been redesigned to transport beam a further 40 m to the target for the K19 beam line.
3. K19: (See Figure 68) K19 is a two stage electrostatically separated, high purity,  $K^-$  beam for the momentum range 600 to 800 MeV/c, to be used for experiments in the 1.5 m Bubble Chamber. Particular emphasis has been placed on low muon contamination, so that the momentum range below 600 MeV/c may be investigated using degrader techniques. The beam is to be constructed with a  $1.5^\circ$  downward tilt to allow a low entry to the chamber magnetic field without including separate vertical steering. Final vertical steering is obtained by rotation of the final horizontal bending magnet M110 about the beam axis.
4. X3Y: (See Figure 68) A further extension of the X3 beam line, known as X3Y will provide a third target station in Hall 3, to feed the K17 beam. The low angle for the septum magnets for the high momentum pion beams  $\pi_9$  and  $\pi_{12}$  from the X3X target requires modification of the final X3X Quadrupole Quartet. A fifth type 1 Quadrupole has been added, to effectively pull back this quartet when the X3Y target is to receive the full proton intensity. The tight layout at the west end of Hall 3 has precluded the use of a deflecting magnet beam dump as in X3X; a movable 20 ton hydraulically actuated beam dump is being developed to allow access to the X3Y target station whilst X3X is running. The components of a new beam  $\pi_{12}$  derived from the X3X target will be installed at the same time as X3Y.

Figure 74. P81 beam line (Hall 1).



5. P81: (See Figure 74) P81 is a high intensity 8 GeV/c proton beam, designed to deliver  $10^9$  protons within a phase area of  $7.5 \times 7.5$  (mm mrad) $^2$  at a 5 mm diameter polarized proton target. It is also required that the halo (beam outside the wanted emittance) is less than  $10^4$  protons/cm $^2$ .

The beam uses protons extracted from Nimrod by 'peeling-off' part of the normal X3 spill within the machine, hence allowing simultaneous running with Hall 3 experiments.

The design was required to include as high a dispersion as possible within the directional constraints of the initial ejection direction from Nimrod and the use of the present X2 access port through the main shield wall. The careful choice of collimator position was also required such that the halo which will be produced at the collimators may be removed either by 'scraping' with further collimators downstream or be lost due to its momentum loss in passage through the collimator jaw.

Design effort is being contributed to beams for the 300 GeV accelerator at CERN. Design studies for a hyperon beam for use in the West experimental area and an electron beam for the North area are being made.

Beams at CERN

## THEORETICAL STUDIES ON HIGH ENERGY ACCELERATORS

Continuation of the work, reported last year, in collaboration with our partners in the GESSS collaboration (Karlsruhe, Saclay and CERN) has led to the investigation of a number of the problems of incorporating superconducting dipole and quadrupole magnets in large diameter proton synchrotrons. This work is being collated as a GESSS report which will be published in 1973.

The 300 GeV Advisory Machine Committee consisting of representatives from national accelerator laboratories in Europe has sponsored two study periods at CERN. Several machine theorists from the Rutherford Laboratory contributed to a Spring Study in Accelerator Theory held at CERN in April 1972. Following on from this study they have been involved with CERN in reviewing the requirement for correction elements in the CERN 300 GeV machine and in deciding the optimum working point on the Q-diagram for the accelerator.

1000 GeV  
Superconducting  
Synchrotron  
(ref. 255, 262)

CERN 300 GeV  
Accelerator  
(ref. 230, 231)

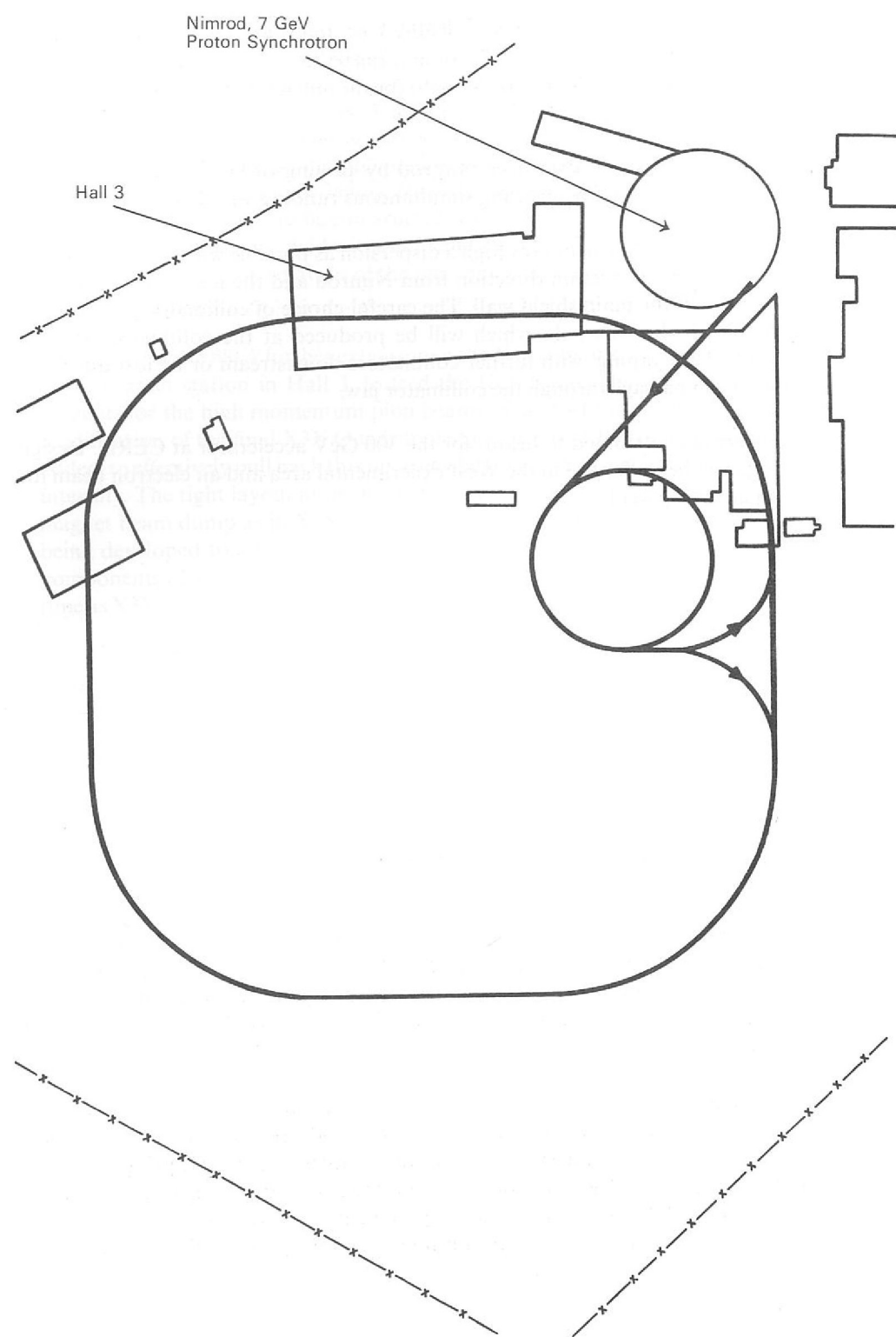


Figure 75. The relationship of the envisaged electron-proton intersecting complex (EPIC) to the existing Laboratory facilities.

Arising out of work by a joint Daresbury-Rutherford Laboratories working party to review possible new accelerators for the UK, a study has been made of machines capable of making colliding beams of high energy electrons, positrons and protons to provide very large energies measured in the centre of momentum frame of reference. The problem is to provide sufficiently intense beams of particles with sufficiently small areas so that the collision rate is high enough for particular interactions to be studied. A complex of three accelerating rings (EPIC) has been studied with beam momenta and total energies shown below:

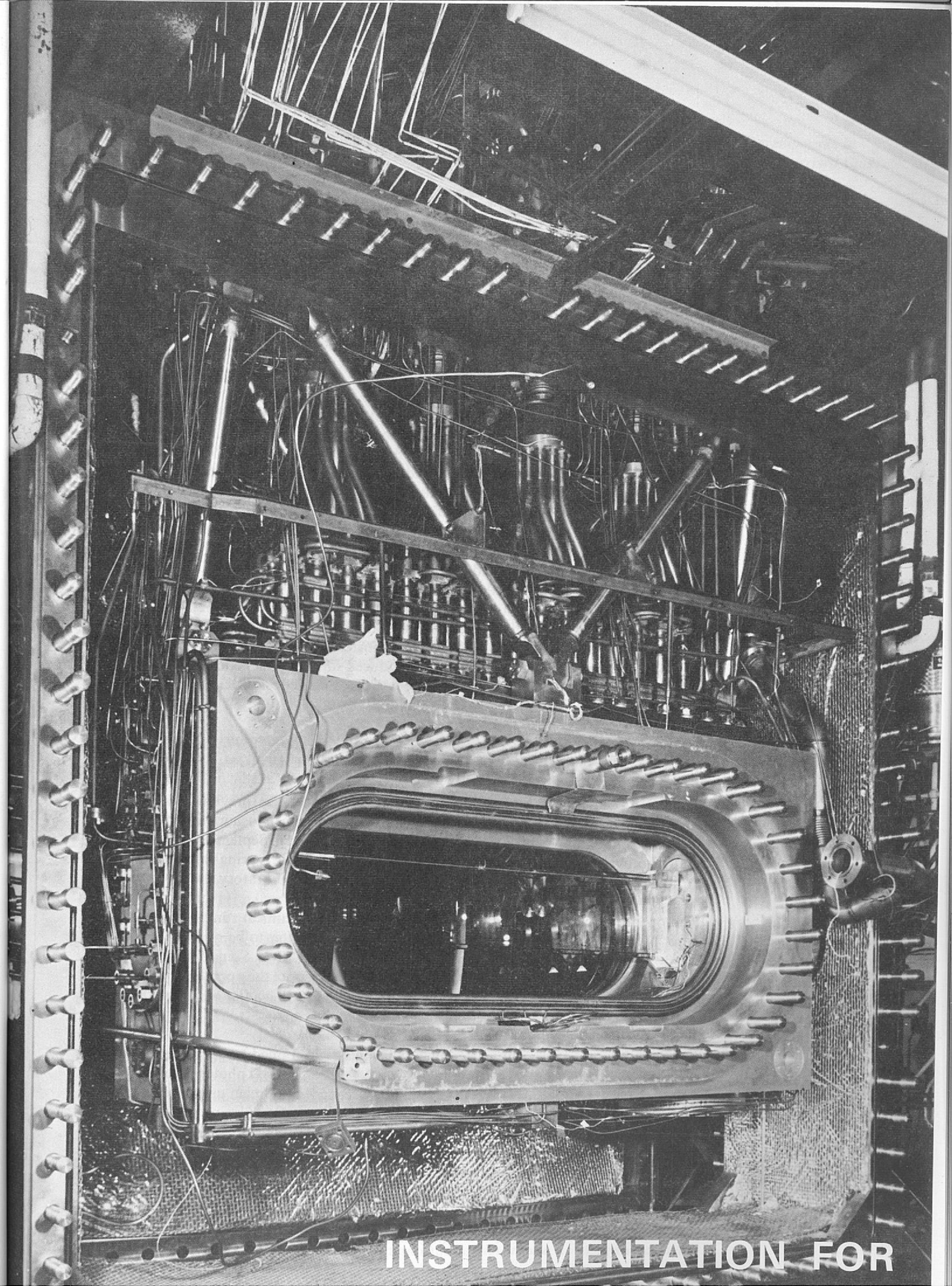
*Electron-Proton  
Intersecting Complex  
(EPIC)  
(ref. 67, 193, 252, 268,  
284-288)*

Beam Momenta (GeV/c)			Centre of Momentum Energy (GeV)
Electrons	Positrons	Protons	
8.5	8.5		17
8.5		60	45
	8.5	60	45
		28 + 46	70
8.5 + 8.5			17

Two of the rings would be conventional and would accelerate and store electrons or positrons, the third would be made from superconducting magnets and would accelerate protons. The straight sections and interaction regions would be common to the two rings being used at the time. A common booster machine would be used to fill both rings in use. The particles would be formed into 4 short bunches in each ring to increase the effective interaction rate.

This complex would make use of much equipment and many buildings already in existence and looks so promising that further study will be made of the capability of doing physics with such machines and of the problems of beam dynamics and accelerator equipment required.

View of the 1.5 m Cryogenic Bubble Chamber body showing the installed track sensitive target (12319).



**INSTRUMENTATION FOR**

# Instrumentation for High Energy Physics

Advance in our knowledge of fundamental particles is almost invariably preceded by the development of some new technique, or some new instrument to detect exotic particles, or, currently, to meet the requirements for observing particles at very high energies. The story of particle physics is full of this continuing dialogue between new technology and new information about the basic constituents of matter which then makes new demands on technology. Two examples are: particle accelerators designed to reach higher energy thresholds (the discovery of anti-matter, the anti-proton, was made in this way) and bubble chambers which have had a universal application, but were particularly vital in the discovery of short-lived particles and the resonant states of particles. A new advance in bubble chamber technology has been the recent operation of a track sensitive target system inside another bubble chamber, a sort of double bubble chamber, for experiment. This enables a new area of particle physics to be studied involving interactions where neutral particles, particularly gamma rays, are produced. This is reported below and elsewhere (Experiments 32, 33). Other instruments and detectors produced for experiments during the year and general development work on detectors are described in the rest of this chapter.

## 1.5 METRE CRYOGENIC BUBBLE CHAMBER OPERATION

(ref. 3, 19, 225, 239, 321, 323)

This year has seen the successful culmination of the work in previous years on track sensitive target (TST) operation. The first ever physics experiment using a hydrogen TST in a chamber containing a neon-hydrogen mixture was completed in September; over 1.5 million data photographs have now been taken using this technique. During this period the first anti-proton experiment to be carried out at the Rutherford Laboratory was also completed.

The operation of the chamber started in March with a technical run using a 50 mol % neon-hydrogen mixture to enable the design of a photon filter to be optimised. This filter was to be used in a Rutherford Laboratory experiment at CERN. Some 5,000 photographs were taken. Further technical running took place to investigate the operating conditions for higher neon concentrations in the neon-hydrogen mixture. The aim of these experiments was to improve the gamma detection efficiency of the chamber.

The first physics experiment started in July using a rigid framed target with two different mixtures, 73 and 77 mol % neon in hydrogen. A total of 826,000 photographs were taken using a 4 GeV/c  $\pi^+$  beam. This was followed by a second experiment using the same target, and a total of 205,000 photographs using a 2 GeV/c anti-proton beam were taken. Upon completion of these experiments, an all plastic target constructed at CERN was fitted into the chamber. This target was successfully operated with two different mixtures (80 and 82 mol % neon in hydrogen) and a further 515,000 photographs were taken using the 4 GeV/c  $\pi^+$  beam. During the year it was possible to operate the chamber for periods of over four months, without any deterioration in photographic quality. This is due to the increased use of gas analysers, both on- and off-line to continuously monitor all gas systems for nitrogen, oxygen, air and water vapour impurities.

Improvements have been made to the computer control of the bubble chamber. A digital voltmeter (DVM) and signal multiplexer have been added which allow a further 63 signals to be monitored by the computer. The DVM gives a very flexible input system since the range is set by the computer and resolution can be  $1\mu\text{V}$ . Signal conditioning amplifiers are unnecessary and the DVM can be used for thermocouples. The 'ready' rate is about 8 channels/second which makes it unsuitable for taking data associated with the chamber cycle.

The major improvement to the computerised instrumentation has been the addition of an alpha-numeric display of up to 16 chamber parameters, each continuously monitored. The interface for the display which uses a standard 625 line TV monitor was built at the Rutherford Laboratory.

During data taking operation of the bubble chamber the expanded pressure and the beam timing are stored in histogram form by the computer and typed out at the end of each roll of exposed film. Thus a close check on chamber conditions is possible.

The data processed by the computer can never be more precise than the transducer through which it is obtained. A transducer drive unit has recently been installed and this, together with unbonded strain gauge pressure transducers, provides more reliable signals than previously. The unit uses a carrier signal to power the transducers and has very good drift and noise rejection characteristics. The same system is also used for strain gauges attached to the target for monitoring its inflation and measuring peak strain.

The Vacuum Coating Plant has continued to be used for applying anti-reflection coatings to the optical surfaces of the bubble chamber. A double layer coating has been used on both surfaces of the plexiglas sides of the track sensitive targets. The first layer of the coating is conducting, to prevent static charges which tend to cause a build up of solid contamination on the surface of the plexiglas. A modified version of this coating but with a lower resistance was developed and evaporated on to mylar sheets for experimental spark chambers which required optically transparent conducting surfaces.

Contract work has been undertaken for an outside customer who required a matched pair of neutral density filters with a linear density gradient over a length of 300 mm, as well as a number of uniform filters. The evaporating technique and rotating shutter required to produce these filters was developed during the year.

## INSTRUMENTATION FOR COUNTER EXPERIMENTS

An experiment (Proposal 100, Table 1) is currently being set up at CERN by the Rutherford Laboratory and other collaborators to study the reaction  $\pi^+p \rightarrow K^+\Sigma^+$  and its line reversed reaction  $K^-p \rightarrow \pi^-\Sigma^+$  at 10 GeV/c using the same apparatus. These particular final states can be identified mainly by detecting the  $K^+$  or  $\pi^-$ . Apparatus specially developed for this experiment is described below.

The Cerenkov counter shown in section in Figure 76 is part of the system for detecting the  $K^+$  and  $\pi^-$  particles. It consists of a cylindrical pressure vessel of 1.27 m diameter, with a length of 1.78 m and wall thickness of 75 mm, made of aluminium alloy, containing Freon gas operating up to a maximum pressure of  $830\text{ kNm}^{-2}$  (120 psi). The cylinder is mounted with its axis horizontal. Particles enter the counter through an aluminium entry port 2.5 mm thick, 0.25 m high and extending for 1.2 m along the length of the cylinder. The exit port is 9.5 mm thick. The experiment will require to detect forward scattered particles close to the target, as a consequence the non-interacting particles in the incident beam will also pass through the counter. To prevent the Cerenkov radiation created by these particles being detected, they will be channelled through the counter in a thin-walled tube as indicated in the figure.

*Developments in  
Computerised Control*

*Treatment of Optical  
Surfaces*

*Pressurised Gas  
Cerenkov Counter*

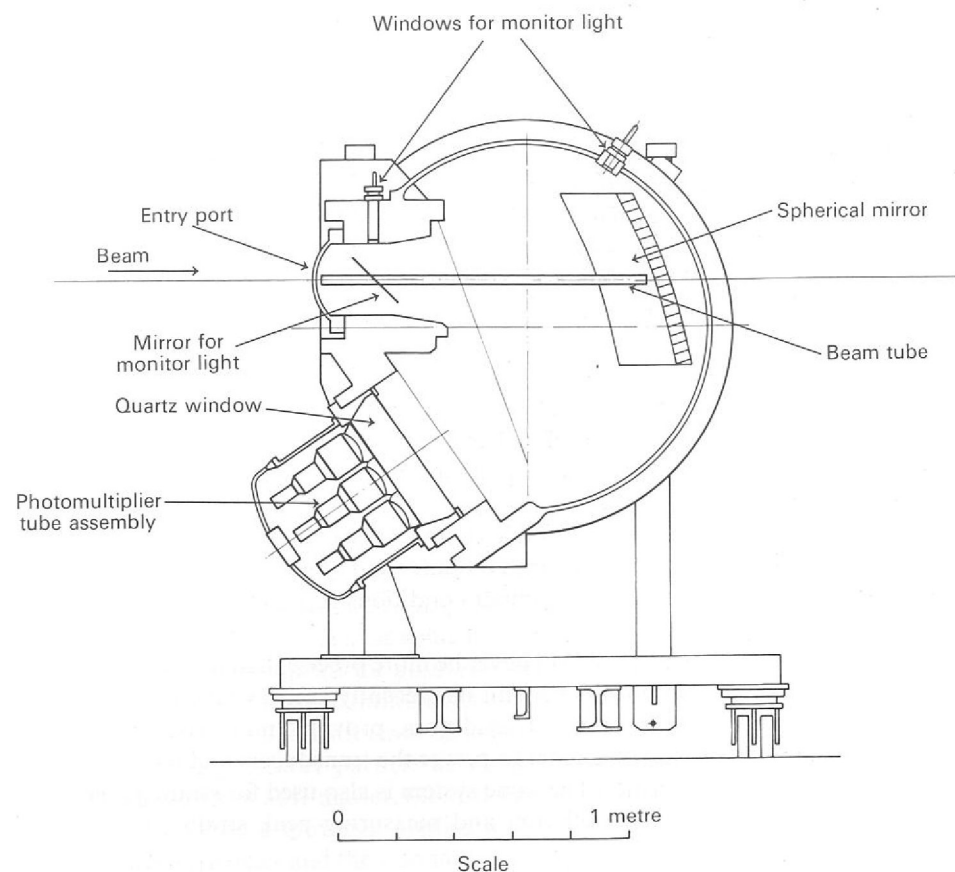


Figure 76. Section through the gas Cerenkov counter.

The Cerenkov radiation emitted by the scattered particles is reflected by a concave mirror, 1.5 m long by 0.6 m high with a radius of curvature of 1.65 m mounted within the vessel, on to a bank of seven photomultiplier tubes through a synthetic quartz window 0.5 m diameter and 120 mm thick. The mirror is of low mass ( $< 1 \text{ gm/cm}^2$ ) to minimise interactions with the on-going scattered particles which pass through the mirror. The performance of the chamber is monitored by using a gallium phosphide diode light source. Light from this single source is channelled to small windows on the vessel by fibre optic guides.

*Atmospheric Pressure Cerenkov Counter*

A second Cerenkov counter for this experiment will detect  $\pi$  mesons either from the decay of the  $K^+$  mesons or direct from interactions and hence identify the reactions more precisely. This counter covers a large area of 4.2 m wide by 2.2 m high and contains 14 concave mirrors of 0.6 m by 0.5 m and radius of curvature of 1.5 m each viewed by a photomultiplier and matching light collecting cone.

*Wire Spark Chambers with Capacitive Read-out (ref. 20, 213)*

Wire spark chambers with capacitive read-out are to be used in the detection system for the line reversed reactions experiment. Three sizes of chamber, 1.1 m  $\times$  0.3 m, 2.0 m  $\times$  1.0 m and 2.3 m  $\times$  0.6 m are being produced. There is a 1 mm gap between the wires forming each plane. Figure 77 shows a prototype 1.1 m  $\times$  0.3 m chamber with the read-out printed circuit board above it. Wires are placed at  $0^\circ$ ,  $15^\circ$  or  $30^\circ$  to the vertical for different wire planes.

The complete system of spark chambers for this experiment will have approximately 90,000 wires each with an individual read-out circuit comprising a capacitor and diode. High quality printed circuit boards are used, with track widths and track to track spacing of the order of 0.2 mm. The flexible connectors between chamber and read-out boards can be seen in the figure.

The introduction of the capacitor read-out system for the spark chambers described above has required the development of an EHT charging unit capable of recharging the capacitors within 10 ms. Prototype units have been tested to the required specification of 30 mA output current at up to 15 kV d.c. and manufacture of a complete set of such units is under way.

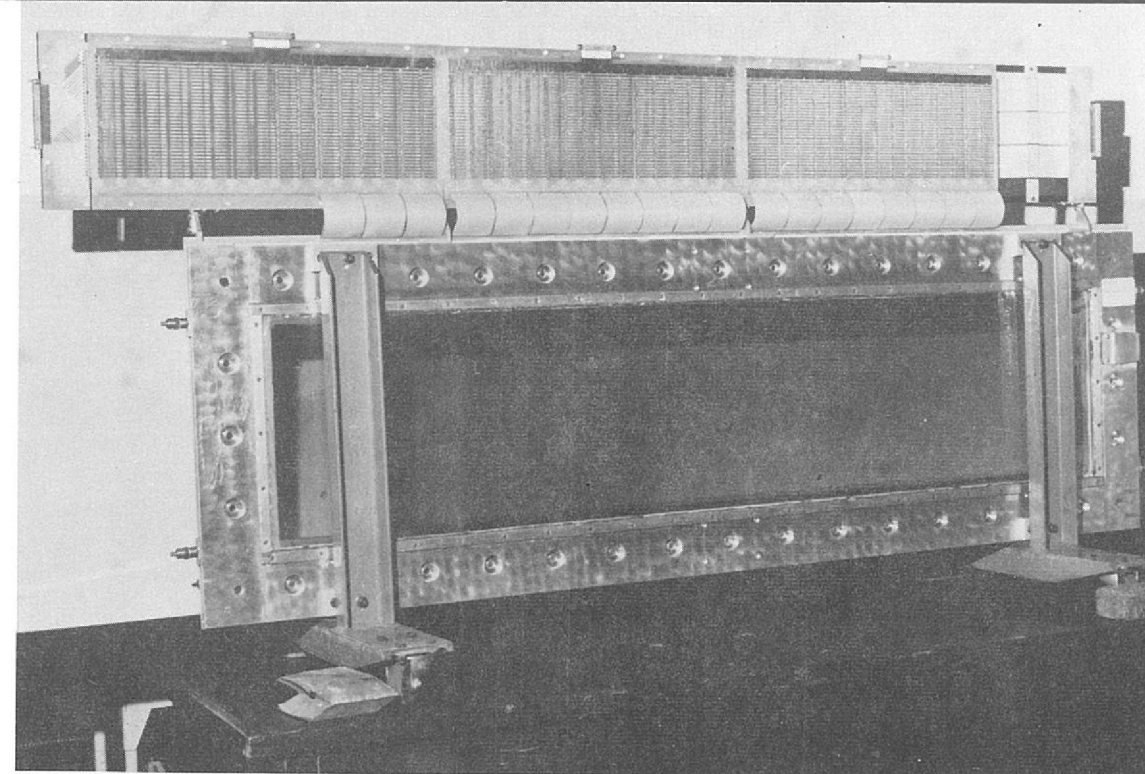
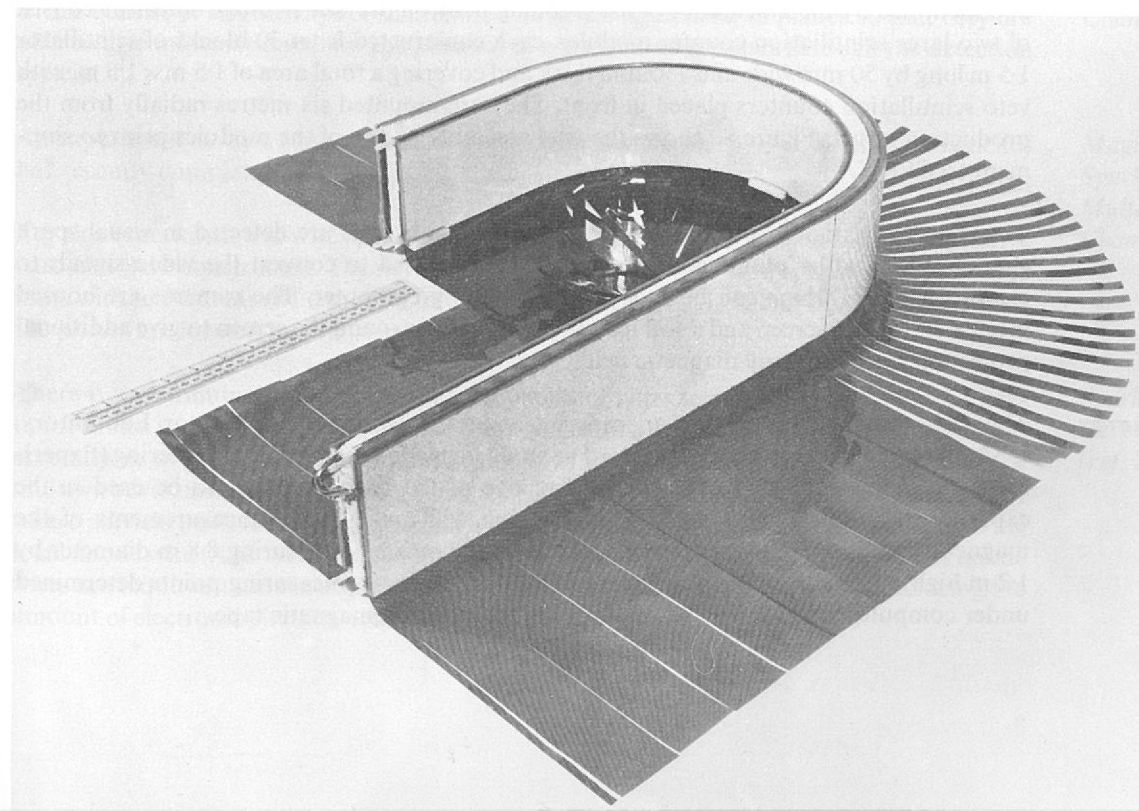


Figure 77. A prototype wire spark chamber with capacitive read-out (12024).

An experiment to measure polarization in the process  $\bar{p} + p \rightarrow \pi^+ + \pi^-$  (Experiment 21) will shortly commence data taking at CERN. Much of the equipment for this experiment was used in the experiment to measure differential cross-sections for  $\bar{p} + p$  annihilation to two body final states (Experiment 10). For the polarization experiment, a polarized target (supplied by CERN) is located in a 2.5 tesla magnetic field. The target is surrounded by "J" shaped wire spark chambers (Figure 78). These are two low mass double gap spark chambers to detect scattered charged particles immediately on exit from the polarized target. The chambers contain 2300 wires (actually copper tracks at 1.5 mm pitch on a specially developed printed circuit board) each with capacitive read-out circuits. Above and below these wire chambers are scintillation counters to veto interactions where particles emerge from the target and travel in the direction of the magnet pole pieces. An overall view of the apparatus for this experiment during the setting-up and testing phase is shown in Figure 79.

*Apparatus for  $\bar{p}p$  Polarization Measurements*

Figure 78. The 'J' shaped wire spark chambers used with a polarized target (Experiment 21): (12498).



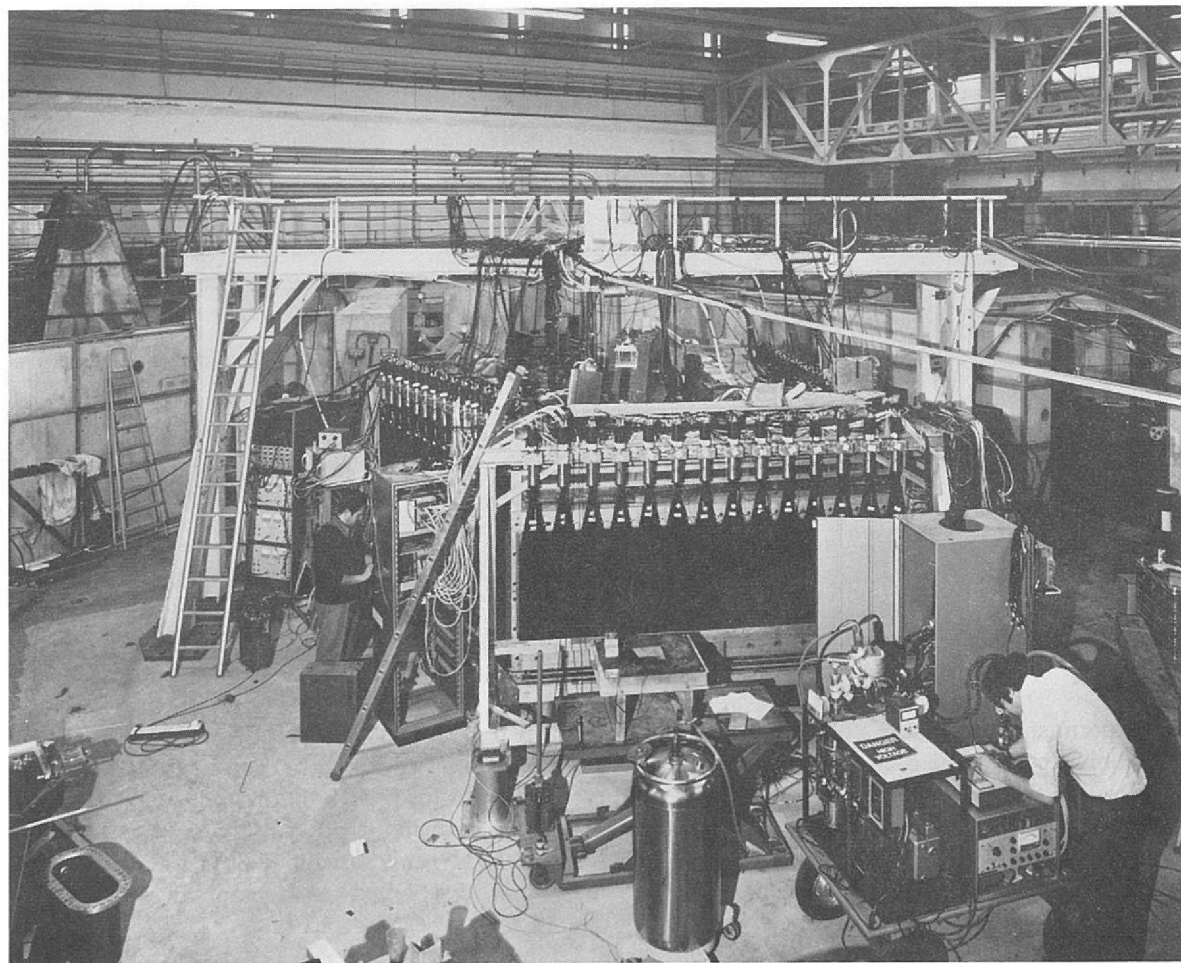


Figure 79. A view of the apparatus for the  $\bar{p}p$  polarization experiment (CERN X153-11-72).

*Apparatus for the Omega Spectrometer*

An experiment is currently being undertaken at CERN to study the properties of neutral bosons or meson resonances (Experiment 14) using the large volume magnet spectrometer (Omega). These resonances ( $X^0$ ) are produced in the reactions  $\pi^- p \rightarrow nX^0$  and  $K^- p \rightarrow nX^0$ , and identified by the kinematics of the recoiling neutron (n). The neutron detectors consist of two large scintillation counter modules, each constructed from 30 blocks of scintillator 1.5 m long by 50 mm wide and 150 mm thick and covering a total area of 1.5 m  $\times$  1.5 m, with veto scintillation counters placed in front. They are mounted six metres radially from the production target. Figure 80 shows the trial assembly of one of the modules prior to shipment to CERN.

The charged particles from the decays of the neutral bosons are detected in visual spark chambers viewed by plumbicon cameras. These are used to convert the video signals to electrical signals which can be processed directly by computer. The cameras are housed inside a mu-metal screen and a soft iron shield is placed around the screen to give additional protection from the stray magnetic fields.

*Magnetic Field Survey Machine (ref. 307)*

The Laboratory is supporting an experiment at the National Accelerator Laboratory, USA involving the University of Oxford to study inelastic muon-proton scattering (Experiment 19). A machine to survey the field of one of the large magnets, to be used in the experiment, has been developed. This machine will make 60,000 measurements of the magnetic field in three planes in the pole gap of the magnet (measuring 8.8 m diameter by 1.2 m high), with automatic positioning of the Hall probe at measuring points determined under computer control. The field values are recorded on magnetic tape.

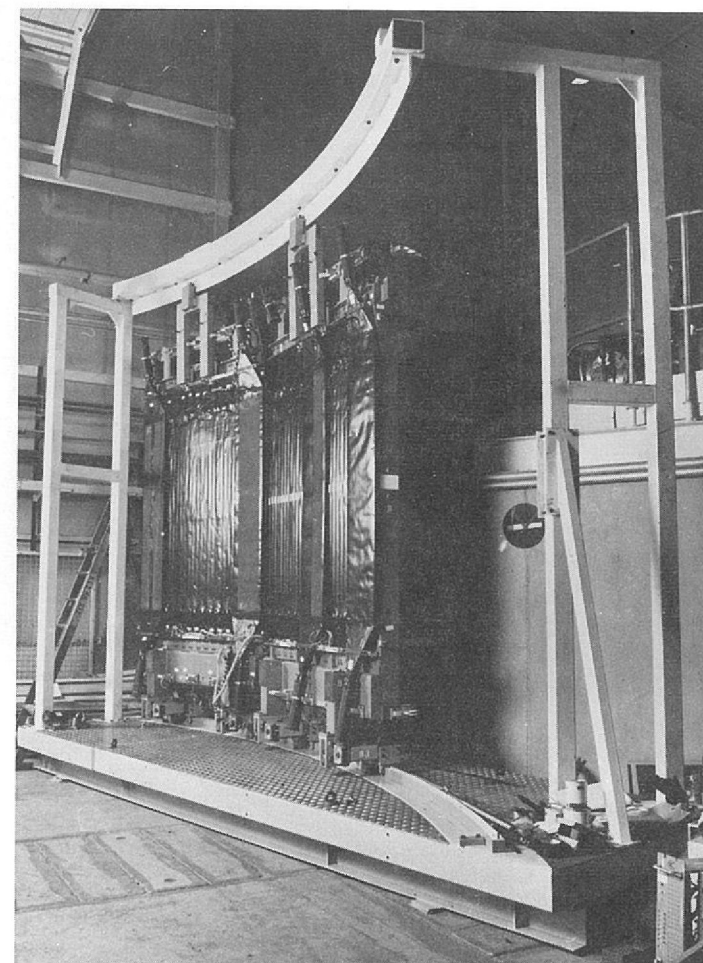


Figure 80. A large scintillation counter module for the Omega spectrometer experiment (11273).

Several hodoscope counters have been constructed for the muon scattering experiment. These consist of large arrays of scintillation counters assembled in planes so that they are able to give information about the position of a particle as it passes through the detection system.

An experiment studying the associated production reaction  $\pi^- p \rightarrow \Lambda^0 K^0$  (Experiment 13) has recently completed the data taking stage.

For this experiment five wire spark chambers of size 1.6 m by 1.6 m with magneto-strictive read-out were constructed. The detection system also included two optical spark chamber units with active areas of 1.6 m  $\times$  1.6 m, each having ten gaps of 1 cm; for this type of chamber the planes are formed by thin sheets of aluminium foil.

There is a continuing programme of development of particle detectors in two main directions, firstly to improve the efficiency of data collection (time and spatial resolution) and secondly in evolving new techniques required at very high energies. A small prototype multiwire drift chamber is currently being tested. This is a type of proportional wire chamber where particle track location is based on a measurement of the drift time of electrons to the local anode wire (A H Walenta et al, Nuc Inst & Methods 92 (1971) 373). Many fewer anode wires are required than for the conventional proportional wire chamber, thus reducing the amount of electronic circuitry required and the space resolution is improved.

*Large Hodoscope Counters*

*Magneto-strictive Wire Spark Chambers and Multi-Gap Optical Chambers*

*Spark Chamber Development (ref. 235)*

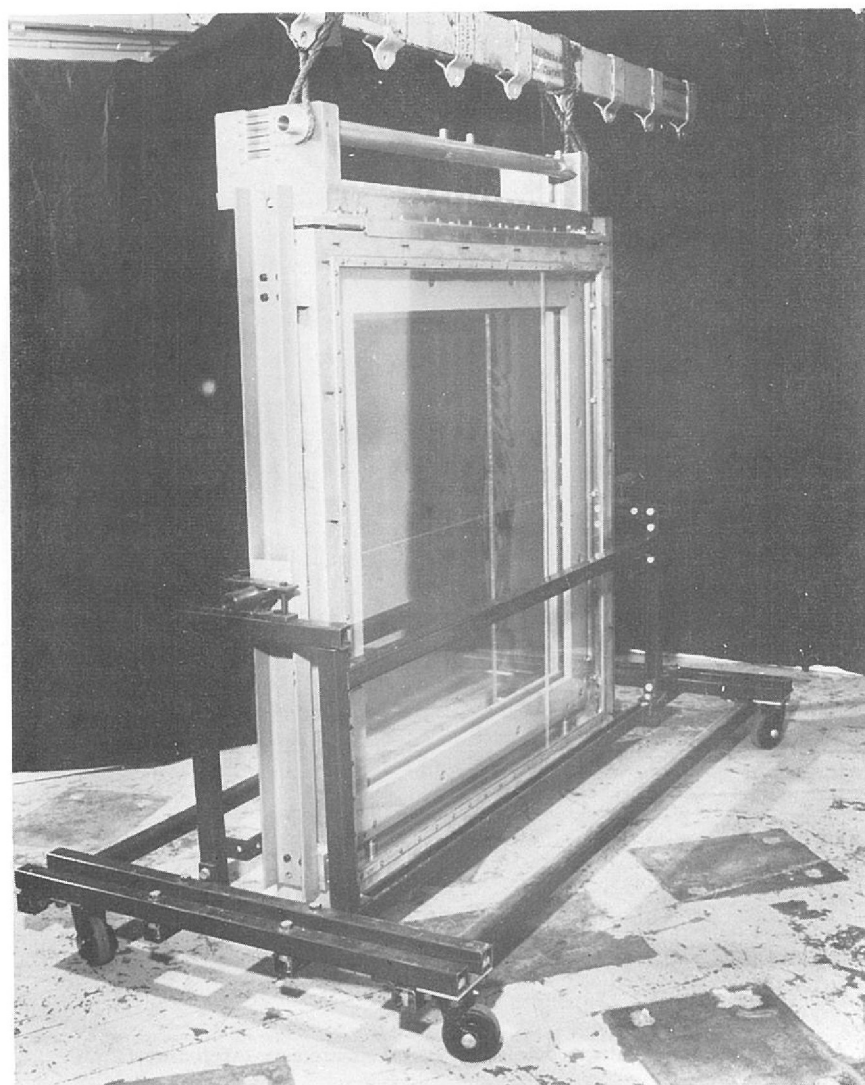


Figure 81. Assembly of a large (100 cm x 100 cm) multi wire proportional chamber (11774).

Developments for conventional multiwire proportional counters have included work on delay line read-out systems and protection systems in the high voltage supply and gas mixture supply. These latter two minimise damage and pollution in a counter when voltage breakdown occurs in the chamber or there is a failure in the gas supply. A sophisticated gas supply rig has been evolved for these counters with very precise gas mixture and gas pressure controls.

Several different sizes of multiwire proportional chambers have been constructed ranging in size from 10 cm x 10 cm to 100 cm x 100 cm active area with wire spacings of 1 mm and 2 mm respectively. Improvements have been made in the construction of chamber frames and in the method of obtaining uniform wire tension and monitoring wire tension during assembly (by measuring the natural frequency of vibration of the wire), and finally, the simple process of cleaning wires prior to winding on to the chamber frames. All of these improvements lead to standardisation and high efficiency in the operation of these particle detectors and hence ultimately affect the accuracy of the experiments.

## ELECTRONIC INSTRUMENTATION

Six plumbicon cameras and associated control units have been commissioned for the Omega spectrometer at CERN. The reliability and stability of the whole equipment under operational conditions has been very good. Measurements on fiducial lights indicate a short term (hourly) drift of about 1 digit, equivalent to 1 part in 8000. Over several days there is a cyclic wander of less than 10 digits. Our understanding of systematic distortions is not yet sufficient for this 1 digit accuracy to be obtained for particle tracks in the spark chambers. An outstanding problem is the apparent shift in spark position with spark intensity. The usual methods of centre finding do not appear to be satisfactory and further developments are underway to improve this situation.

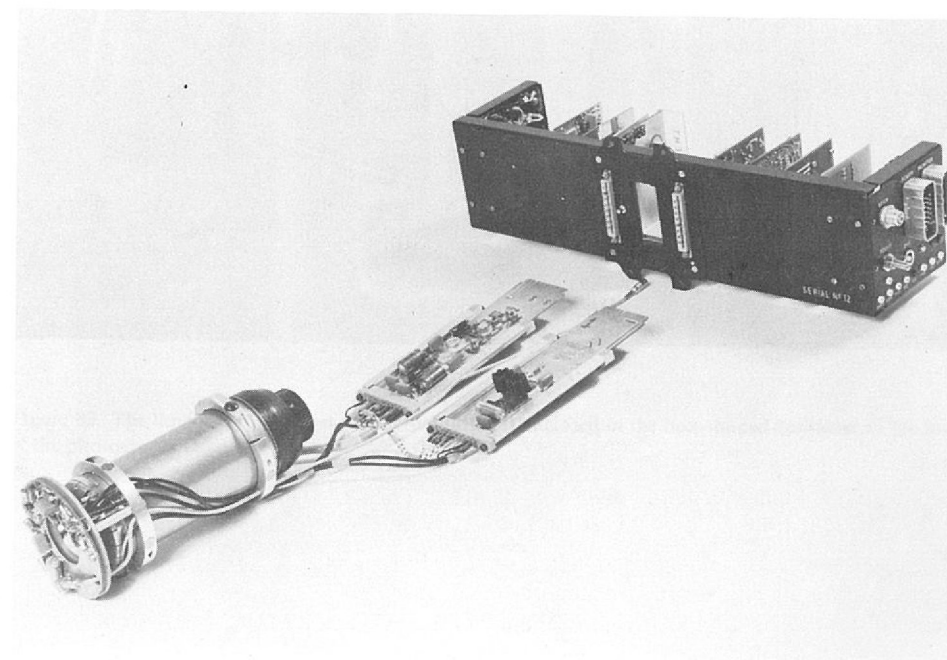
*A TV Camera Read-Out System for Omega*

The changes in experimental technique rely on a balance between, on the one hand the development of detectors and their associated data acquisition techniques, and on the other, the available computing power. Consideration has been given to ways in which increased computing power can be brought nearer to the data acquisition phase of an experiment. The emerging concept is that of dedicated parallel processors. These may be conventional general purpose computers or high-speed fixed-program hardware assemblies. Work has been concentrated on a special purpose computation unit likely to have wide application, a polynomial evaluator. Such a module could be useful in three different areas. First for the correction of systematic errors in a detector, for example the TV camera read-out system. Second for the evaluation of empirical polynomials such as may be used for calculating particle paths through magnetic fields. Third for the approximate evaluation of analytic functions.

*High Speed Computing*

A prototype has been constructed and tested. It uses a 16 bit fixed point multiplier and will maintain an accuracy of one bit under most circumstances. The computation time is  $(1 + 0.4N)$  microseconds for a polynomial of order  $N$ . To this must be added the access time of the host computer. A second model will be used in an experiment at CERN in order to assess more practically the effectiveness of the basic idea.

Figure 82. Components of a TV camera for spark position read-out. These are housed inside a magnetic screen (12539).



## CRYOGENIC TARGETS

### *Liquid Hydrogen Targets*

Six liquid hydrogen targets were operational during 1972. Four of these were of the modern refrigerator type and two of the older reservoir type. As a result of operational experience on the new refrigerated target system, several improvements have been made resulting in high operational efficiency. Among these modifications were improved low temperature pipe connections to minimise cold leaks. The electrical controls have been modified to allow the system to be automatically restarted after loss of mains power.

### *Solid Hydrogen Target*

A new target system is being developed at the Rutherford Laboratory for an AERE Cyclotron experiment. The requirement is for a target of solid hydrogen of 3 cm x 1 cm cross section by 7 cm high to be suspended in the path of a 70 to 150 MeV neutron beam. The solid hydrogen is produced in a mould and then extended into the beam path by a hydraulically activated plunger. The mould is suspended beneath a vapour cooled radiation shield liquid helium reservoir which provides the refrigeration for the target and the whole unit is enclosed in a vacuum vessel.

### *Liquid Oxygen Target*

For the first time at the Rutherford Laboratory a liquid oxygen target was designed, manufactured and operated successfully for an experiment on the  $\pi$ -nucleus total cross-section on the  $\pi 10$  beam line. The target system was one in which a known volume of oxygen gas was liquefied in a cryostat using liquid nitrogen as refrigerant. The liquid nitrogen was contained in an automatically filled reservoir through which a copper liquefying coil passed. Great care was taken to ensure the scrupulous cleanliness of all items coming into contact with oxygen. The complete project took only 5 weeks from conception to operation in the beam line.

### *Gas Analysis Service*

A gas analysis unit has been set up to give a quick turn round of sample analysis to the Bubble Chamber and Cryogenic target sections. This unit has greatly improved the purging and operation of cryogenic equipment. The analysis instrument is a commercial Gas Chromatograph with helium ionization detectors capable of detecting impurities from samples to an accuracy of better than 1 part per million.

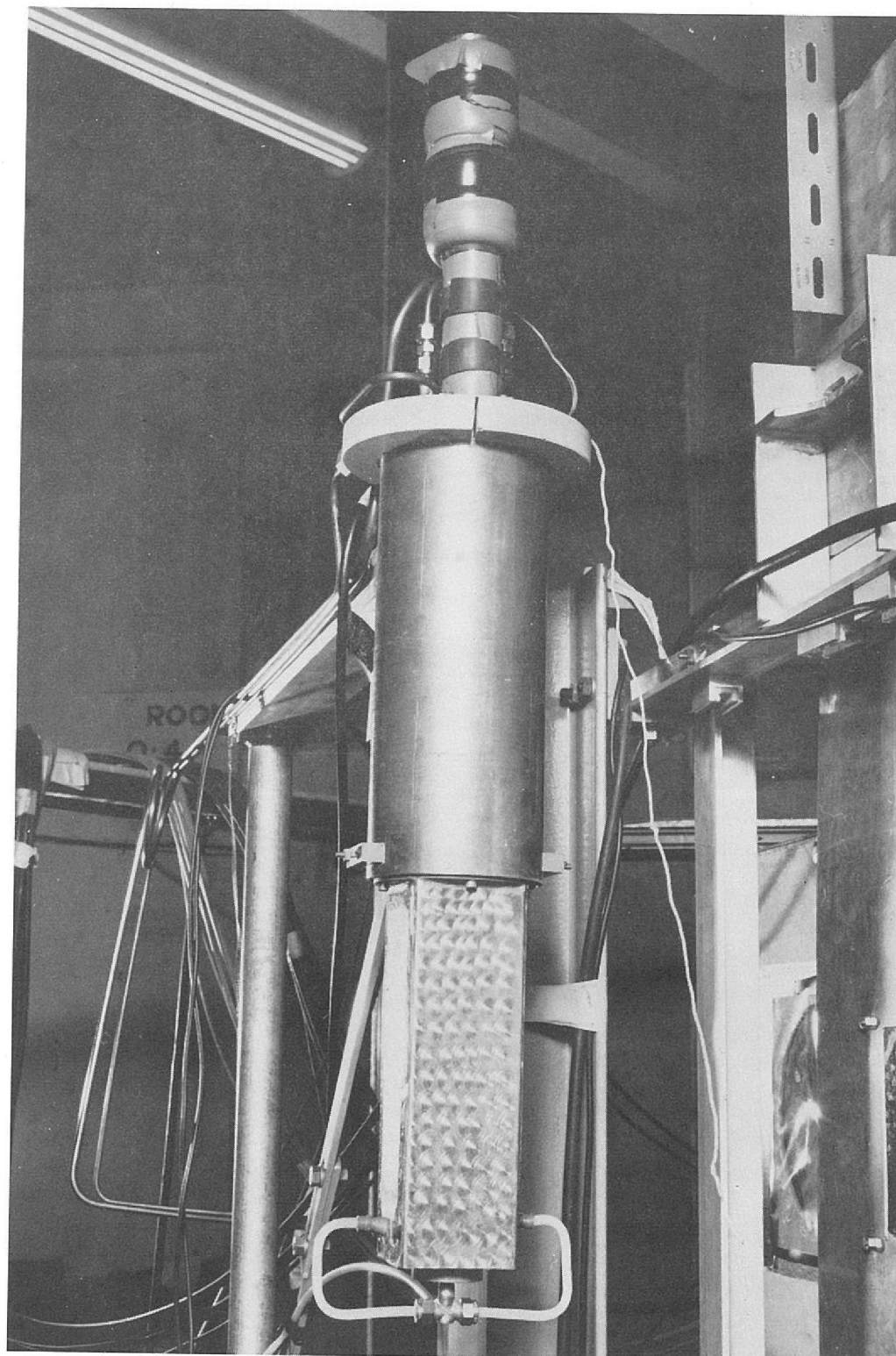
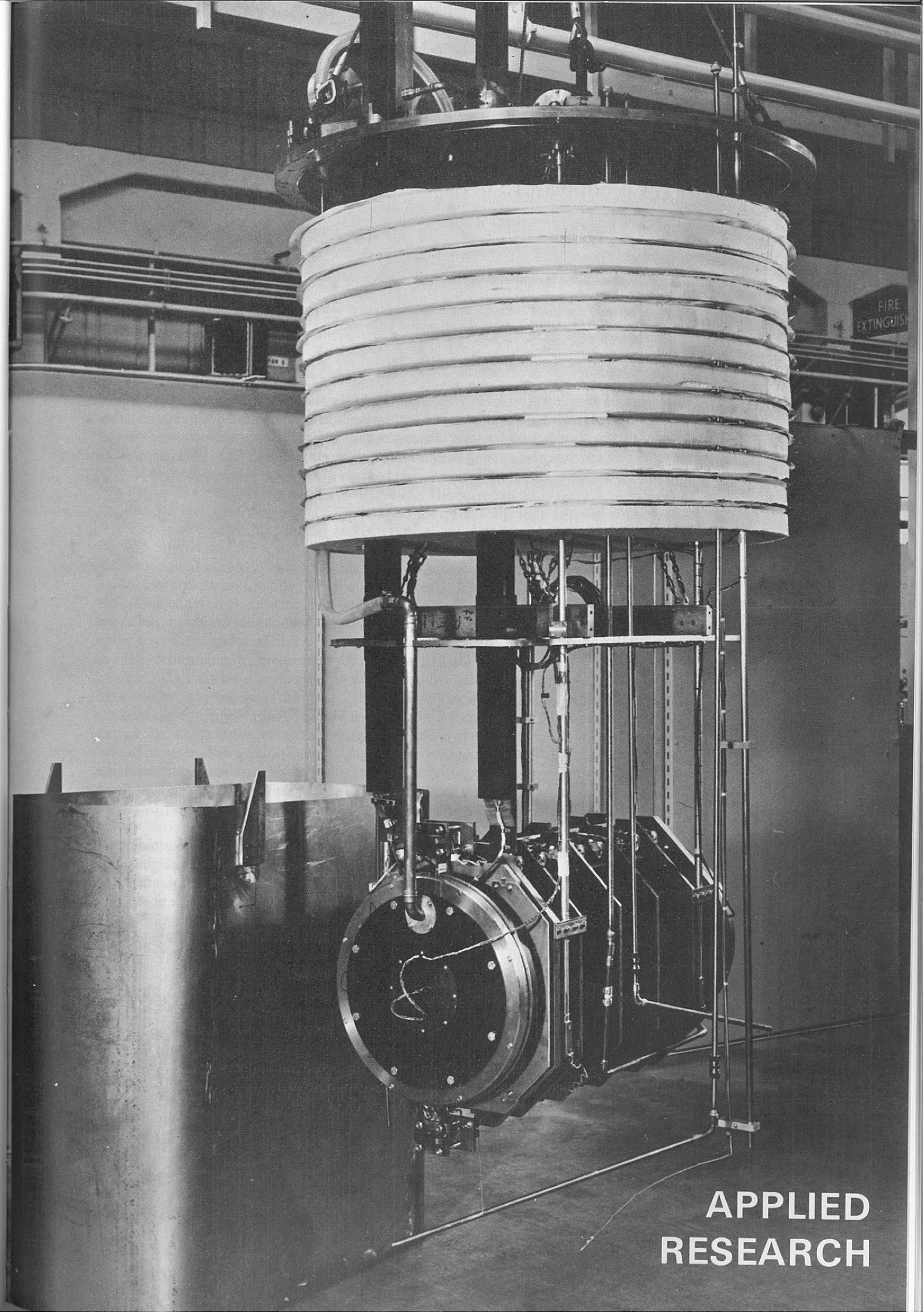


Figure 83. The liquid oxygen target: the actual target is enclosed in the box-shaped container in the lower part of the photograph.

The AC4 superconducting magnet ready to be lowered into its cryostat for cool-down to its operating temperature of 4.2 K. The magnet is pre-cooled to 77 K with liquid nitrogen and then cooled with liquid helium (11937)



**APPLIED  
RESEARCH**

# Applied Research

Progress towards a superconducting dipole magnet suitable for accelerators; superconducting cable and cryogenic materials development; a proposed superconducting energy transfer system; construction of a superconducting r.f. separator; polarized proton target development; rapid cycling bubble chamber development; a CO<sub>2</sub> laser; support of satellite mounted experiments.

## SUPERCONDUCTING MAGNET STUDIES

*Pulsed Dipole Magnets  
AC4 and AC5  
(ref. 21, 82, 136)*

Significant progress in the development of pulsed dipole magnets has been made during the year with the completion and testing of the magnet AC4, the design of which was described in the 1971 Annual Report. After cooling down to liquid helium temperature, a process which takes a few days for this 1200 kg magnet, the design value for the centre field of  $B_0 = 4.5$  T was reached on this first run after a few training steps from 4.0 T. The magnet could also be pulsed to 4.5 T for rise times as fast as 2 seconds. These early test results were reported to the Fourth International Conference on Magnet Technology together with the Fourier analyses of field measurements at different levels of excitation which follow very well in detail the predicted changes calculated by computer taking into account the increasing iron saturation. This agreement between theory and practice for fields in the useful aperture is very encouraging for the design of highly saturated iron magnets without recourse to scale models depending on Kelvin's theorem.

The magnet field quality was not as good as had been hoped for and indicated geometrical inaccuracies. Subsequently the coil clamping has been improved and the coil and iron assemblies re-clamped in a more symmetrical manner to give improved field quality. The special end windings have proved good with the result that at all excitations the uniformity of the overall field integral taken through the magnet is about  $\pm 3 \times 10^{-3}$  for paths within an aperture defined by 70% of the inner winding radius, or less than half this variation within 50% of the winding radius. If magnets are to be built for use in a high energy storage ring then an improvement of at least seven times is required.

Each successive cool down of the magnet, three to date, has been entirely trouble free and as with most superconducting windings the maximum field attained has steadily increased to  $B_0 = 5.1$  T which corresponds to the full short sample current of the conductor. Field plots clearly showing the effect of trapped fields within the windings have been obtained from  $B_0 = 0.1$  T to 4.9 T. Total losses due to pulsing, including those in the iron laminations, have been measured and are typically 83 joules/cycle of excitation 0→4.5 T→0 over 4 seconds, or 8.3 W for a 10 second cycle with a 6 second flat top.

All this experimental data and the experience gained in the design and manufacture of AC4 are currently being used in a revision of the design for a prototype synchrotron magnet, AC5.

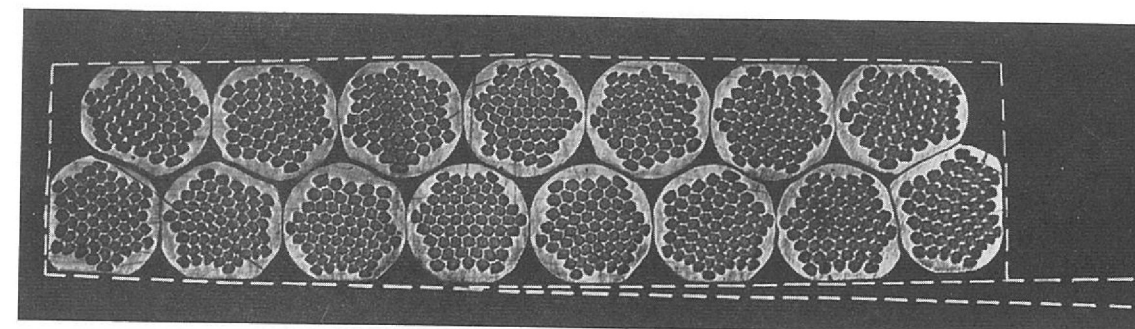


Figure 84. Cross section through superconducting cable containing 15 strands of composite wire. The superposed lines indicate the slight tapering at the edges to improve the packing of cables in circular aperture magnets (12627).

A new type of cable has been developed for use in high current pulsed magnets. The cable, which is fully transposed, consists of a hollow tube of helically twisted wires which has been flattened into a tape by rolling. It has proved possible to compact this cable until the wires fill more than 90% of the cable cross-section, without significantly damaging the superconducting properties of the wires; a marked improvement on previous cables which have only been able to reach filling factors of 40%–60%. The current density in a magnet winding can thus be increased accordingly. Techniques for producing long lengths of the cable have been perfected during the year and it is now planned to use this type of cable in both the AC5 magnet and the Energy Transfer Model. The cable for AC5, shown in Figure 84, has a specially shaped cross section, slightly tapered towards the edges, so that adjacent conductors will fit neatly together around the circular aperture.

*Superconducting Cable  
(ref. 330)*

Work has continued, in collaboration with Imperial Metal Industries Limited, on the development of improved composite superconductors for pulsed magnets. Because the new flat cables contain fewer wires than previously, each wire must now be of greater diameter if the current carrying capacity of the cable is to be maintained. For this reason, the work has concentrated on the development of larger composites containing greater numbers of filaments. Figure 85 shows a new 14,701 filament composite of niobium titanium, copper and cupro-nickel. The 'spider' of cupro-nickel alloy around the periphery of the composite and also around each cluster of filaments, is designed to minimise the additional magnetization currents which tend to flow between filaments through the copper matrix, in a changing magnetic field. These currents are undesirable because they increase the pulsed power loss and reduce the electromagnetic stability of the composite. They become stronger with increasing composite diameter and increasing rate of change of field. The 'spider' technique is needed to control such magnetization currents in composites of more than ~10,000 filaments, intended for use in pulsed magnets with rise times of ~1 second.

*Composites  
(ref. 108, 109, 113, 139)*

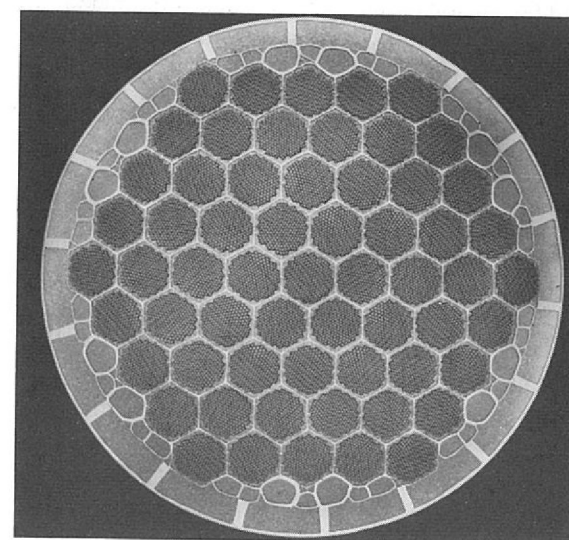


Figure 85. Superconducting composite containing 14,701 filaments of niobium-titanium alloy in copper with a resistive cupro-nickel 'spider' (mag.  $\times 100$ , filament diameter  $5 \mu\text{m}$ , etched to show niobium-titanium dark grey, copper light grey and cupro-nickel white).

#### Test Facility

A new facility for testing large cables and composites has been brought into operation during the year. It is one of the most powerful of its kind in existence. Samples of up to 9 cm diameter can be tested in fields of up to 6 Tesla while carrying currents of up to 10,000 A. The field can be swept at a rate of 7.5 Tesla/s; the sweep rate is accurately linear, and continuously variable; the field may be swept smoothly from positive values through zero to negative values and vice versa. A variable temperature sample enclosure will be added shortly.

#### AC3 Magnet (ref. 110)

An insert section of winding has been added to the magnet, raising its maximum field from 3.9 T to 4.6 T (with 5.2 T peak field on the winding). The critical current of the magnet, corresponding to this maximum field, is 4600 A which is only about 3% less than the critical current measured on short samples of cable. When the magnet is pulsed with a 2 second rise time the maximum field in the aperture is reduced from 4.6 T to 4.3 T. Rise times as short as  $\frac{1}{4}$  second have been achieved, but with greatly reduced maximum fields.

An improved technique has been developed for measuring hysteresis loss in pulsed magnets. This not only enables the superconductor loss to be measured more quickly and accurately than previously but also enables additional losses due to iron hysteresis, frictional movement of the winding, etc., to be detected and separated from the superconducting component.

#### 6 Tesla-Metre Solenoid

Work has started on the design of a 6 T solenoid magnet, 1 metre long with a 140 mm diameter bore, for use in a polarized proton beam at the TRIUMF accelerator in Canada. The magnet will be supplied as a complete operational system, in a cryostat with a horizontal bore 100 mm in diameter.

#### Cryogenic Materials Studies (ref. 112, 190, 192, 202)

The testing of epoxy resin systems for impregnation of superconducting windings has been continued. The work of fracture of a number of resins at low temperatures have been measured; values range from 100 to 3000 J/m<sup>2</sup> for the resin systems in use at the Rutherford Laboratory. Certain resins show useful increases in work of fracture when cooled to liquid helium temperature. Sufficient theoretical insight has been gained for the purpose of choosing a suitable impregnant for a magnet.

The Instron mechanical test equipment is being further extended by the addition of a data systems module. This unit will enable output from the test to be processed in punch tape form and permit a significant saving in data reduction time to be made.

In addition to the work on resins for encapsulating superconducting windings, studies have been made on the impregnation and potting of sub-assemblies and prototype magnet structures. Measurements on these has enabled some assessment of shrinkage strength criteria to be determined.

#### Heat Transfer

Thermal conductivities have been measured for several epoxy resin systems at liquid helium temperature. These results together with those obtained on our behalf by the Clarendon Laboratory, Oxford, have led to the conclusion that little can be done to improve thermal conductivity by adding particulate fillers. Therefore it will remain necessary to design pulsed superconducting magnets so as to minimise the thickness of any resin layers interposed between the superconductors and the liquid helium coolant. A programme of work on heat transfer in narrow vertical rectangular channels, cooled by naturally circulating liquid helium, has been begun. Widely varying temperature profiles have been measured along the channels, with temperature rises up to 0.25 K above bath temperatures.

#### Superconducting Energy Transfer System

The superconducting energy transfer system, described and illustrated in the 1969 and 1970 Annual Reports, consists of a system of coupled superconducting coils capable of storing and transferring electrical energy reversibly and without loss. Originally conceived as a possible synchrotron power supply, it may also find other applications requiring 10<sup>6</sup> to 10<sup>9</sup> Joules with pulse rise time in the region 0.01 to 10 seconds, (for example in fusion experiments) as an economic alternative to large capacitor banks or rotating machinery.

Design and construction of a superconducting model was initiated during 1972. The overall diameter will be about 1 metre, the nominal peak field 40 kG, and the system will be capable of transferring energies of up to about  $2 \times 10^5$  Joules, at 4,500 A, to an external load, with rise times down to about 1 second. This model is large enough for the engineering problems to be representative of those on future larger systems (10<sup>8</sup>-10<sup>9</sup> Joules), and in addition provides valuable experience on ancillary devices such as high current superconducting switches. During the period under review, the basic electrical and mechanical design was finalised and practical trials were carried out relating to coil windings, impregnation, low resistance joints, superconducting switches, bearings, and inductive correction schemes. Commissioning of the fully assembled system is scheduled for early 1975.

### SUPERCONDUCTING R.F. SEPARATORS

Steady progress towards building r.f. separator No. 1 has been made during the year. First operation of the completed separator is due early in 1973. All the mechanical components and systems are complete, and cryogenic tests are starting; development towards an eventual two-cavity r.f. control system continues.

The frequency stabilised r.f. source and klystron power amplifier are complete and operating satisfactorily. The klystron delivers 900 watts c.w., more than enough to cope with the eventual two cavities and transmission line losses. At present the output power is split by a T-section variable power divider between separator No. 1 and a matched load. Amplitude control is required to better than 1%, and is achieved in two stages: with automatic level control at the main amplifier, and with a variable power divider utilising a multiple r.f. bridge circuit at the cavity. The bridge circuit enables the main r.f. feed to the cavity to be varied by up to 15%, whilst its control varactor handles only 4% of the power.

Cavity phase must be maintained correct to within 2°, i.e. 0.45 Hz of the resonant frequency of 1.3 GHz. This is achieved by using the r.f. source as the frequency standard, and tuning the cavity to it by means of plungers driven by stepping motors (coarse) and reactive coupling to the cavity with varactor diodes (fine tuning). Phase stability to about 0.2° is expected.

Design and manufacture of the main r.f. feed, mechanical and varactor tuners, and r.f. monitors are complete. All components utilise choke joints to give effective r.f. contact with low thermal loss; the main r.f. feed gives an input VSWR of better than 1.03, r.f. lines are vacuum isolated with coaxial windows using ultra pure alumina.

The r.f. cavity is assembled in three units bolted together, each unit comprising four cells. A form of cantilever joint between the units has been developed to ensure an adequate seal for superfluid helium and to maintain good radio frequency contact.

A high temperature vacuum furnace brazing technique has been developed to braze together the four cells comprising a third of the full cavity. The four sections approximately 320 mm outside diameter and 100 mm deep have now been joined and have satisfied three important requirements. Firstly, the assembly should be concentric to a tolerance of  $\pm 0.005$  mm, secondly, there should be no spillage of braze metal on the inside of the cavity, and thirdly, the joint should be leak tight, maintaining a vacuum of  $1 \times 10^{-9}$  torr against superfluid helium. The brazing operation was carried out in a vacuum furnace at a temperature of 820°C under 0.2 torr of argon gas, the exact amounts of silver and copper eutectic braze filler wire being determined experimentally. Examination of the joints made under these conditions showed an extremely high degree of intergranular penetration of silver into the copper thereby ensuring a mechanically sound joint.

RF System

RF Cavity

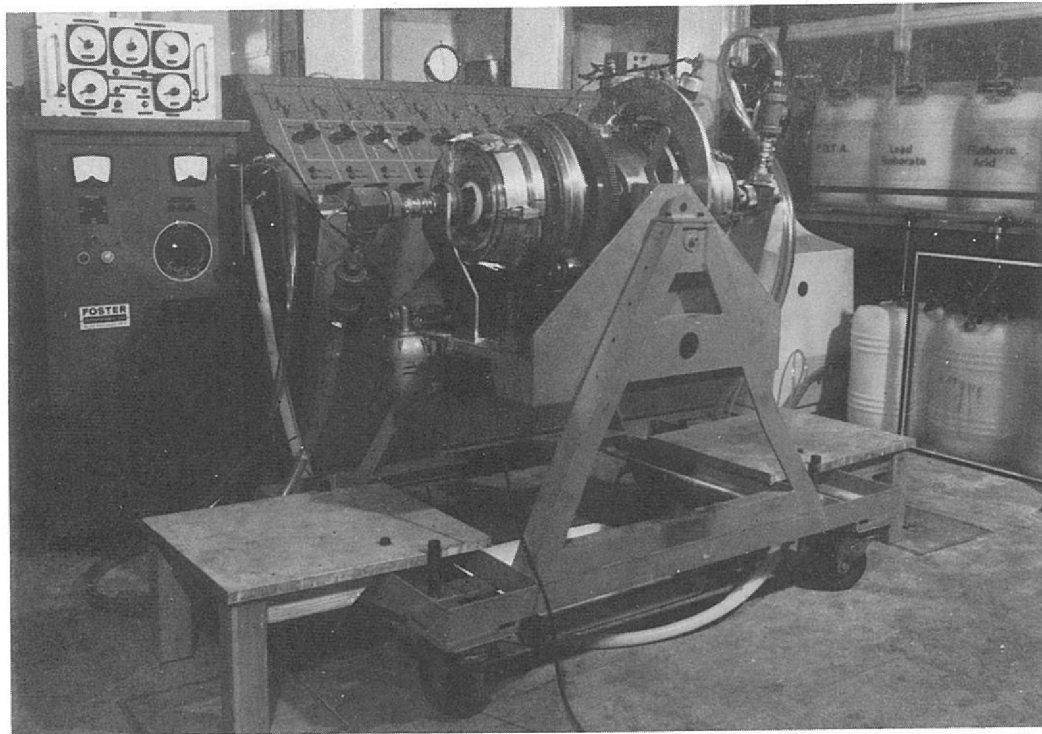


Figure 86. The rig for lead plating the internal surfaces of the r.f. cavity of the separator (12521).

#### Plating System

The internal surfaces of the cavity are plated with lead to provide a superconducting surface. A system has been built where the cleaning and plating fluids are separately pumped on a closed circuit through the cavity to be plated from appropriate storage vessels. The cavity is agitated to ensure that bubbles are dislodged from the inner cavity surfaces and complete wetting is achieved. This system provides close control on each operation and reduces considerably the time taken for plating compared with the more usual method of using open top tanks.

#### POLARIZED TARGET DEVELOPMENT

##### PT55—A Polarized Target for A and R Measurements

A polarized target for A and R measurements is being designed: Figure 87 shows a schematic representation of the system. The target is contained within a uniform field of 25 kG produced by a superconducting magnet with its axis horizontal, so that the beam enters the target along this axis, in the direction of polarization. A cone of half angle  $60^\circ$  is required on the downstream side of the magnet for particle detection. It is intended that the target material be butanol-water-porphyrin and that the target will be continuously polarized at 0.5 K, this temperature being maintained by a helium-3 refrigerator precooled to helium-4. The helium-4 for this cycle and the superconducting magnet will be provided by a closed circuit refrigerator-liquefier.

The programme of work so far has been concentrated mainly on optimising the design of the magnet to obtain a central field of 25 kG with a homogeneity of 2 parts in  $10^4$  over the target volume, which is 3 cm diameter  $\times$  5 cm long. The interactive graphics computer program GFUN was used extensively in this investigation.

##### Frozen Spin Polarized Target (ref. 223)

Work has continued on the development of a new type of polarized proton target of the separated function type in which the processes of polarization and use for data collection are separated in time and space. In this way conditions pertaining to polarization and data collection can be optimised separately.

The magnets for this target, consisting of a high homogeneity polarizing magnet and a low homogeneity magnet for holding the spins in the frozen target, have been examined, both electrically and cryogenically, in the target environment. Reliable operation at 4.2 K has been achieved and both magnets have been energised to their peak operational field strengths of 3.1 Tesla in the holding magnet and 5.0 Tesla in the polarizing magnet.

Assembly of the cavity holding the target material and the probe for moving the cavity from polarizing to holding positions has been completed. The cavity holds  $20 \text{ cm}^3$  of target material in the form of small spheres in a liquid He3 environment at an operating temperature of 0.3 K. To prevent unacceptably large temperature variations occurring, a pump has been developed and incorporated into the cavity to circulate the He3 liquid. The motive section of this pump is driven by an alternating electric current flowing in a filamentary superconducting wire which reacts upon the magnetic field produced by the holding magnet. During recent tests this pump has been operated successfully for 15,000 strokes. The fact that the cavity, the enclosed circulation pump and support structure must move through magnetic field gradients of 0.8 Tesla/cm complicates the design of this system, since the temperature of the target material within the cavity must not exceed 0.5 K during movement from the polarizing position to the beam target position.

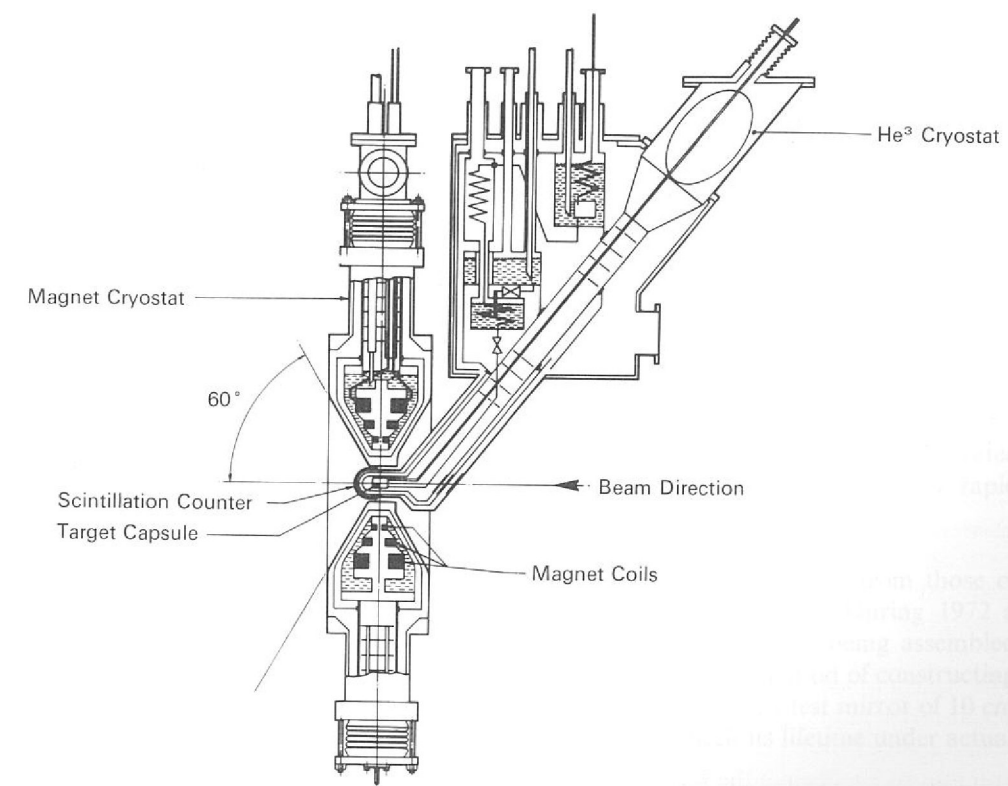
A feature of this target is the facility whereby a dummy target, similar to the actual target but devoid of hydrogen, rises into the beam path so as to replace the main target during the time the hydrogenous target material is being polarized.

Recently solid spheres of a water-glycerol-porphyrin mixture have been put into the cavity and polarization tests have been carried out successfully at 2.5 Tesla, enabling tests to be made on the NMR and microwave system.

Materials Development Facility

During the year a large capacity dilution refrigerator was received and commissioned. The refrigeration power at 100 K was measured to be 3000 ergs/sec. An important feature of this unit is the fast cooldown time from 0.5 K to 0.1 K, an essential characteristic since the refrigerator is to be used in materials research and in developing separated function type polarized targets. At present a 5 Tesla magnet is being incorporated into the system.

Figure 87. PT55, a horizontally polarized target system (13043).



RAPID CYCLING BUBBLE CHAMBER DEVELOPMENT

The design and development of a rapid cycling vertex detector has been continued and the specification established for an experiment.

The principal features of the detector are shown in Figure 88. Since it is designed to be part of a hybrid system employing other particle detectors, it is important that as large a solid angle as is possible should be available for viewing the target volume and that as little material as possible should impede this view. By combining the optical and expansion systems so that the expansion piston incorporates the window through which the chamber is viewed by retro-directive illumination and having a simple refrigeration system around the piston at the top of the chamber, a solid angle of more than  $3\pi$  steradians with respect to the mid point of the beam, has been achieved. The use of aluminium alloys for the chamber and vacuum tank alike has provided a high transparency for both nuclear particles and  $\gamma$ -rays. To avoid unnecessary use of material and to avoid high stresses at vital sections of these vessels, finite element stress analysis programmes have been used to compute the contours of these vessels.

Figure 88. Design for a rapid cycling vertex detector (12722).

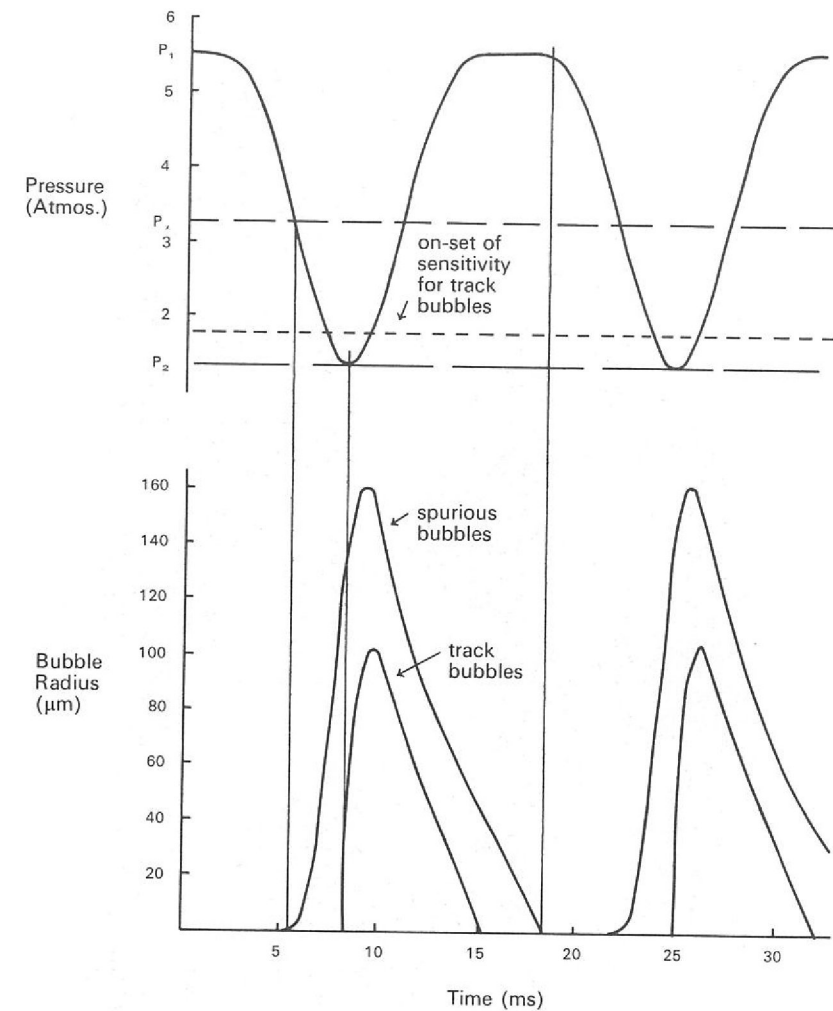
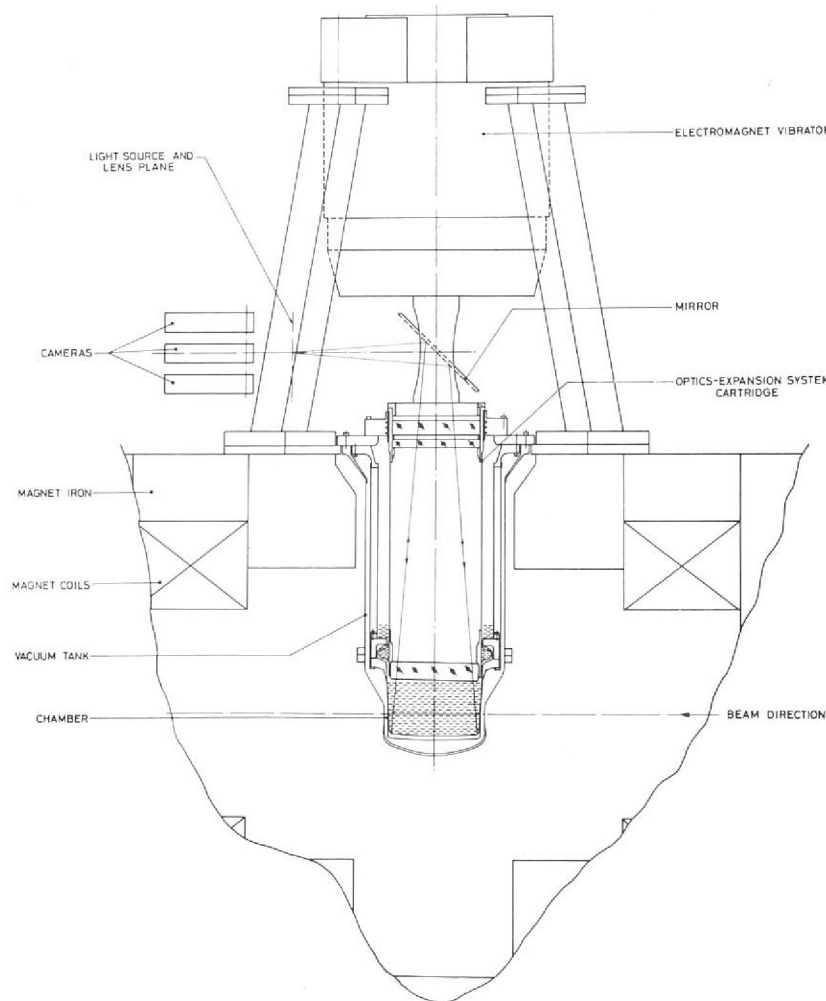


Figure 89. Pressure-time curve and the related bubble growth and recondensation conditions for a rapid cycling bubble chamber. ( $P_1 = 5.5$  atmos.,  $P_2 = 1.34$  atmos.,  $P_0 = 3.25$  atmos., temperature 25K).

An operating frequency of 60 Hz will be achieved by driving the expansion system with a powerful electromagnetic vibrator. To minimise the pressure swing per cycle and provide the necessary asymmetry in the pressure-time curve to accommodate the asymmetry in the bubble growth and recompression characteristics, the vibrator will be driven so as to provide a pressure variation of the following form:

$$P(t) = P (\cos \omega t - 0.27 \cos 2 \omega t)$$

Such a pressure time curve together with the growth and recompression curves for spurious and track bubbles is shown in Figure 89. The use of such a pressure time curve reduces the amplitude of the pressure swing by some 25% when compared to a simple sinusoidal pressure variation.

The triple camera system will have stereo angle of  $8^\circ$  and will use 35 mm unperforated film. The cameras will operate with pneumatically controlled storage loops for rapid transport and will have a dead time of less than 100 milliseconds.

The operating conditions and geometrical configuration are so different from those of normal bubble chambers that considerable development is necessary. During 1972 a complete optics-expansion system cartridge has been designed and is being assembled ready for vibration testing at low temperatures in a test rig. Also a method of constructing a mirror integral with the base of the chamber has been developed; a test mirror of 10 cm diameter has been installed in the Fast Cycling Test Rig to check its lifetime under actual operating conditions.

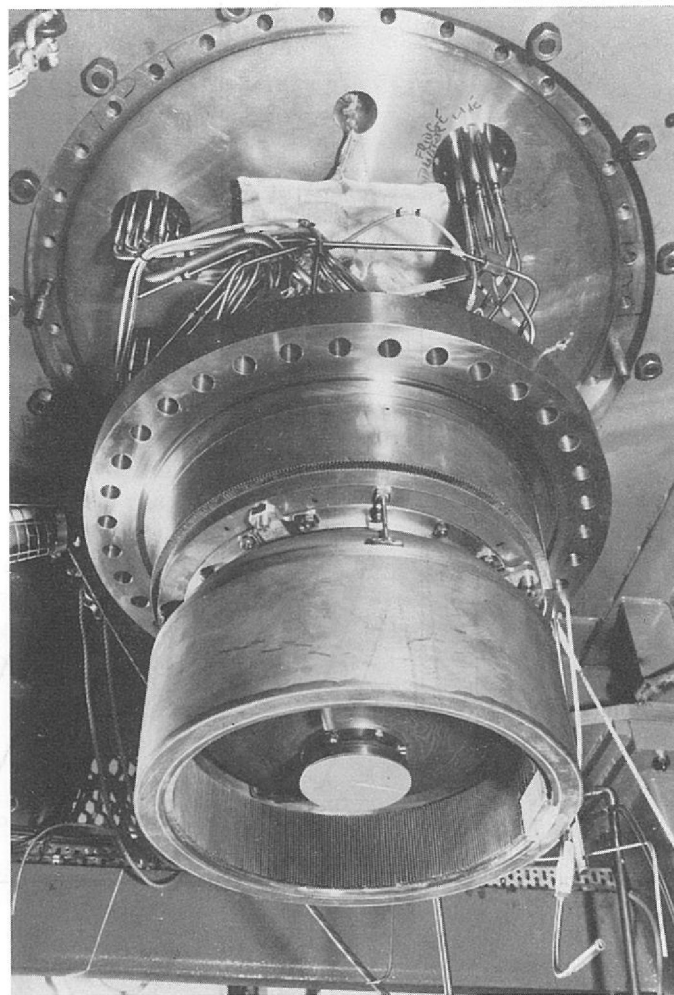


Figure 90. The fast-cycling bubble chamber test rig (the vacuum tank and chamber body have been removed) (12509).

*The Fast Cycling Bubble Chamber Test Rig*

The fast cycling test rig (see Figure 90) has been assembled and dynamically tested using liquid nitrogen at 92 K for 25,000 cycles. The pressures required for operation with hydrogen at 26 K were obtained. After establishing satisfactory operating conditions, the operating frequency was raised progressively from  $\frac{1}{2}$  Hz to 6 Hz and 10,000 cycles were completed at the highest frequency.

All systems performed satisfactorily including the integral Linde cycle refrigerator which was operated with nitrogen. The static heat load was measured to be 18.5 watts of which 2.5 watts was through the superinsulation which corresponds to an average value of  $<0.15$  mW/cm<sup>2</sup> which is well within the required value of 1 mW/cm<sup>2</sup>. The dynamic heat load was undetectable which was to be expected when operating with liquid nitrogen having little vapour content.

The measured damping losses were 20% for the first oscillation which is within the capability of the make-up energy actuator for resonant frequencies of up to 50 Hz. Photographs taken during the tests showed the clarity of the optical system to be good which was to be expected since the optics vacua were both  $<10^{-8}$  torr. After the tests the chamber was removed and the plastic piston and bellows assembly was inspected and found to be unaffected.

The system is being reassembled and prepared for operation with hydrogen. A new, lighter, mass carrier has been made to allow resonant frequencies as high as 40 Hz to be obtained when operating with hydrogen. This is to allow conditions as close as possible to those required by the Rapid Cycling Vertex Detector.

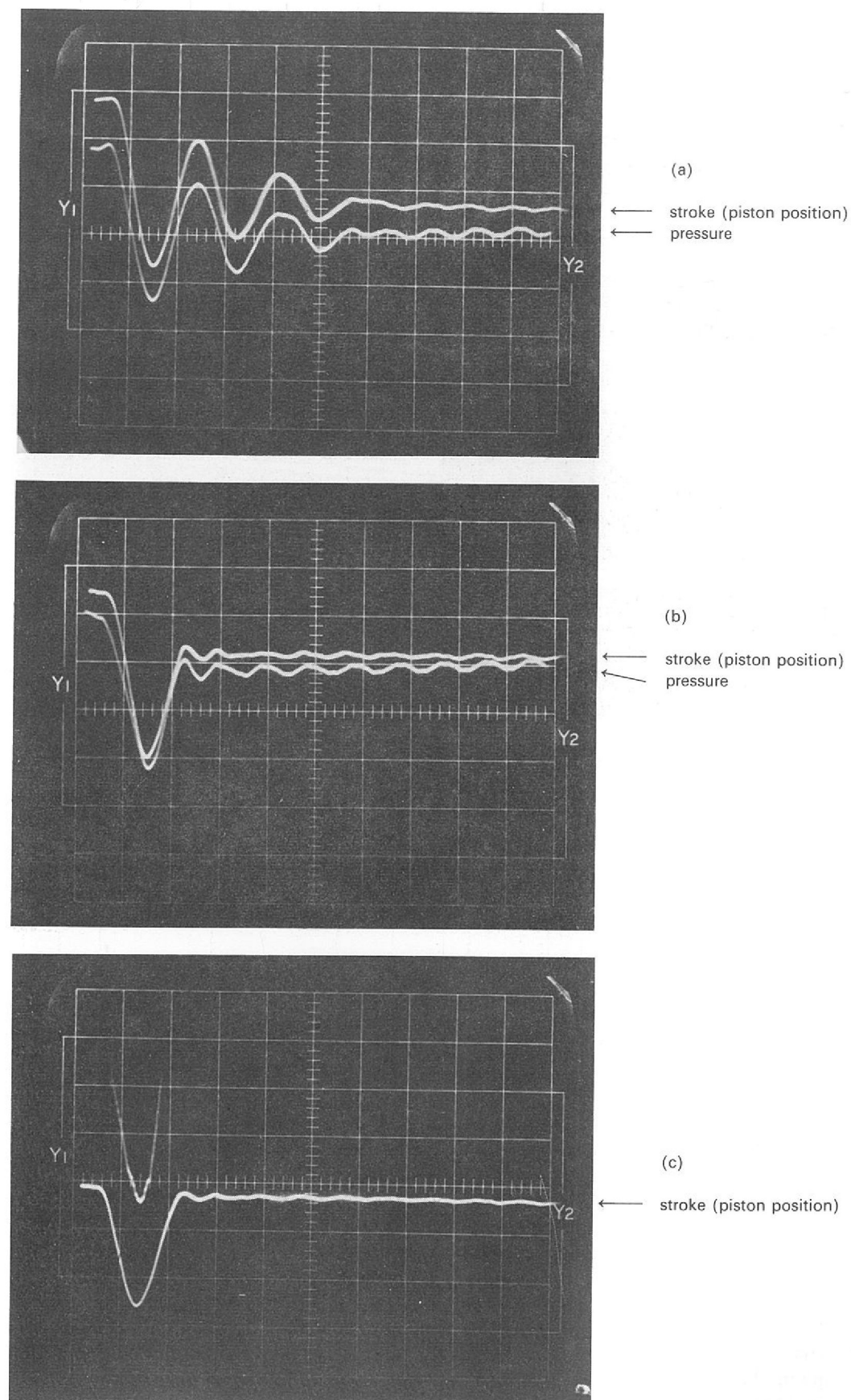


Figure 91. Expansion-recompression cycles of the fast cycling bubble chamber test rig: (a) under free oscillation (b) brakes applied at the end of the first oscillation (c) make-up energy added to bring the pressure and piston position back to the starting values (scale: pressure 10 psi, stroke 0.16 mm and time 20ms per large division).

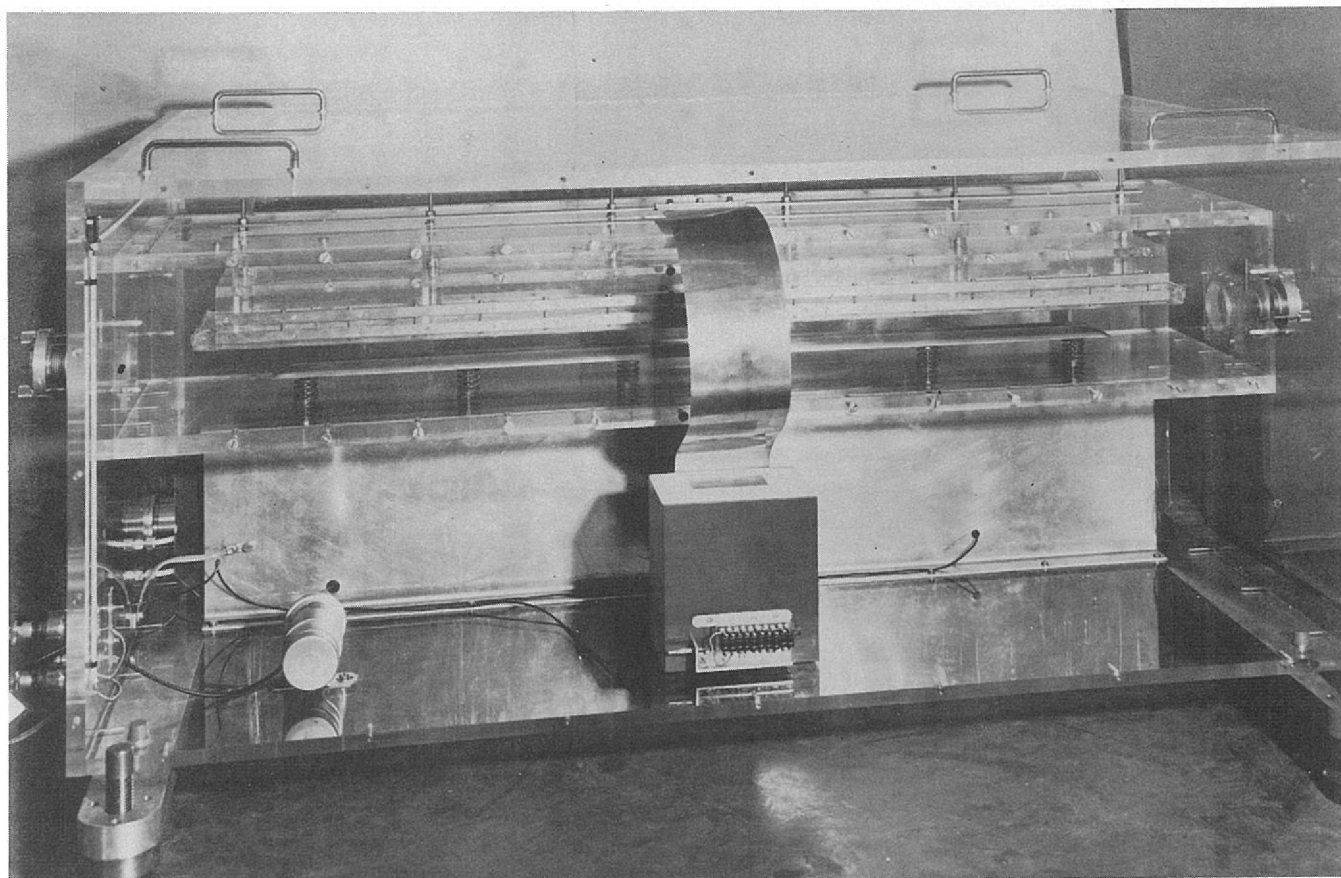


Figure 92. The pulsed carbon dioxide laser (10864).

### LASER-INDUCED BREAKDOWN

In collaboration with Swansea University work is in progress to investigate the feasibility of amplifying primary ionization using the energy of a laser beam. If successful, a new type of visual track detector could be built combining some of the advantages of both spark and streamer chambers. Interest is centred on carbon dioxide lasers which give power output at a wavelength of 10.6 micrometres with a pulse duration of 200 nanoseconds. Amplification should be achievable at low chamber pressures.

A pulsed carbon dioxide laser (see Figure 92) based on a design developed at the Services Electronic Research Laboratories at Baldock has been built. It uses a uniform glow discharge in a mixture of carbon dioxide, nitrogen and helium at atmospheric pressure to pump the laser. The device is self switching and produces a pulsed output of about 4 joules in a 200 nanosecond pulse every 10 seconds. The laser will be used to investigate breakdown phenomena in gases using a test chamber designed to permit studies at pressures up to 20 atmospheres. It is equipped with a radioactive source and a beta particle detection system which can be used to trigger the laser when an ionizing particle crosses the centre of the chamber. Any ionization tracks formed can be recorded photographically.

### MEASUREMENT OF THE ULTRA VIOLET FLUXES OF STARS

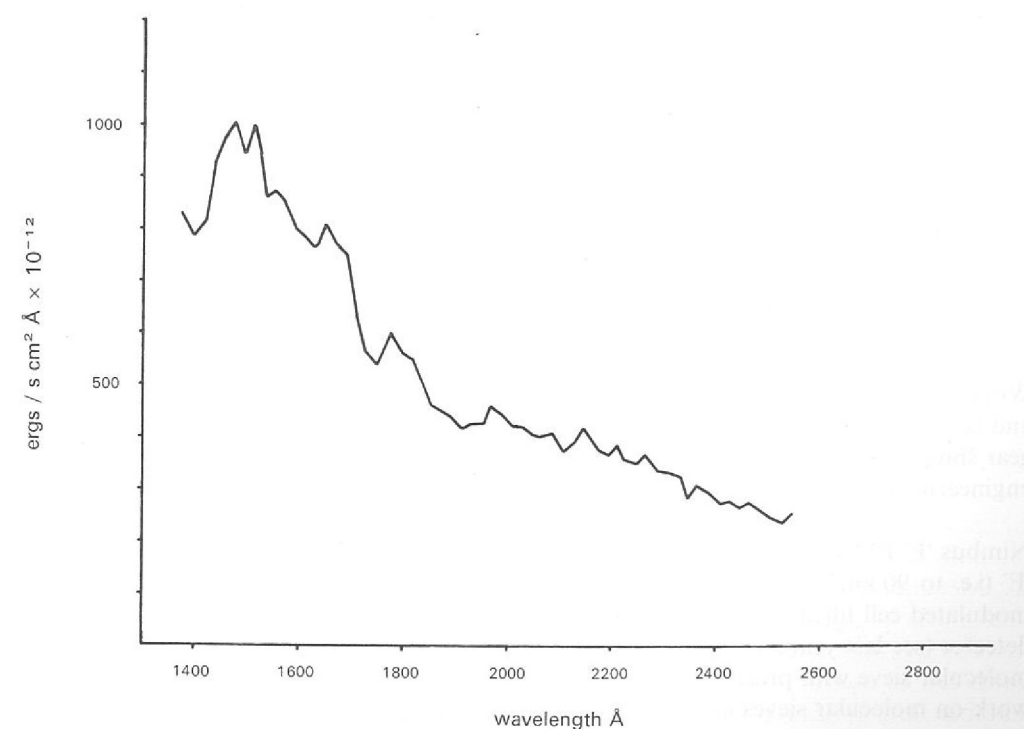
ASTROPHYSICS RESEARCH UNIT, CULHAM  
 ATLAS COMPUTING LABORATORY, CHILTON  
 DEPARTMENT OF MATHEMATICS, MONS  
 INSTITUTE OF ASTROPHYSICS, LIEGE  
 ROYAL OBSERVATORY, EDINBURGH  
 RUTHERFORD LABORATORY, CHILTON

The efforts of the collaborating institutions, including an SRC project team based at the Rutherford Laboratory, on the preparation of equipment to measure the ultra violet fluxes of stars, experiment S2/68 on the Thor-Delta 1A satellite, were rewarded by the successful launch of the satellite from the Western Test Range in California on 12 March 1972 and the initiation of routine operation of S2/68 on 19 March. Data recovery from the satellite was marred by the failure of the on-board tape recorders in May. This meant that data could only be recovered from the satellite during real time passes over ground stations. A rapid expansion, by ESRO, of the ground station network on an emergency basis was put in hand and by September about 50% of the data was being recovered.

Experiments were switched off on 25 October. In February 1973 the whole orbit emerges into full sunlight again and the experiments will be switched on for a second sky scan.

The data produced by S2/68 is of excellent quality, a sample of a spectral scan being shown in Figure 93. Work on computerised data reduction has continued throughout the year by a Royal Observatory Edinburgh/Atlas Computer Laboratory team and routine handling of data tapes provided by the Control Centre in Darmstadt was about to begin at the end of the year. In spite of the tape recorder failure it is expected that, for the first sky scan, 1500 bright stars giving good spectra are on record. Each will have been seen on average five times and recorded on average 3.5 times, giving 5000 useable spectra. In addition about 15,000 to 20,000 fainter stars will have useable data.

Figure 93. The u.v. spectrum of  $\gamma$  Columba [B3 IV,  $m_v = 4.35$ ]. Data from the first operational orbit, experiment S2/68, 19 March 1972.



Preliminary analysis of the in-flight data is being made using the calibration data obtained at the Royal Observatory, Edinburgh which, in turn, used a photomultiplier calibrated absolutely against a vacuum thermopile at the Rutherford Laboratory.

Some examples of the 'in-house' astronomical studies which have been prepared are given below:

- a. The determination of the UV interstellar extinction curve and its variation throughout the galactic plane. This will allow studies of the physics and chemistry of the solid interstellar particles responsible and enable corrections to be derived which will reduce all observations to intrinsic fluxes.
- b. The production of UV star catalogues on the basis of some colour system which will be derived from detailed studies of the spectrum.
- c. The study of a wide range of stellar types including "normal" absorption line stars for a comparison with theoretical model atmospheres, star clusters, the peculiar A stars and chemically anomalous objects together with a range of emission line stars which are characterised by gross non-thermal effects in their atmospheres. The latter include the Wolf-Rayet stars which have rapidly expanding atmospheres ( $\sim 10^3$  km/s) with apparent chemical anomalies represented by a carbon and nitrogen sequence.
- d. The study of the Magellanic Clouds—the nearest extra-galactic systems.
- e. The investigation of a UV emission effect which has been established as localised over a few thousand kilometres in the vicinity of the geo-magnetic equator.

#### INFRA-RED RADIOMETERS FOR ATMOSPHERIC TEMPERATURE SOUNDING

##### UNIVERSITY OF OXFORD RUTHERFORD LABORATORY

###### Selective Chopper Radiometer (SCR) (Nimbus 'E')

The selective chopper radiometer which has been described in previous Annual Reports was launched from Western Test Range, California, on 11 December 1972 on the Nimbus 'E' spacecraft. The instrument has now operated for six weeks, the period required for a successful experiment. It is hoped that it will operate for at least six months on its 16 channels providing synoptic information. After about a year or so the cage material in the 26 ball races in the mechanisms of the radiometer which provides the solid lubrication in space will be exhausted and so terminate the experiment.

The Laboratory designed the radiometer and manufactured the engineering model after a stringent programme of environmental tests on development models, components and then on the completed model. An extensive range of test gear was also designed and constructed in the Laboratory for use at the contractors' works, Oxford University and in the USA for spacecraft integration. The manufacturer for the flight models was Marconi Space and Defence Systems, Frimley.

###### Pressure Modulated Radiometer (PMR) (Nimbus 'F')

Work has continued during the year on a radiometer for Nimbus 'F' following the design and construction of a model at the Rutherford Laboratory in late 1971 and a range of test gear similar in content to that of Nimbus 'E' is now complete awaiting the delivery of the engineering model by industry to be followed by the two flight models.

Nimbus 'F' PMR makes possible temperature soundings to twice the altitude of Nimbus 'E' (i.e. to 90 km) and uses an elegant method of spectral selection by using a pressure modulated cell filled with  $\text{CO}_2$  between the earth viewing mirror and the light pipe and detector (see last year's report). The mean pressure in the cell can be varied by means of a molecular sieve with precise temperature control following a suggestion and development work on molecular sieves in the Rutherford Laboratory.

The arrangement of the radiometer is shown in Figure 94 with two pressure cells with path lengths in  $\text{CO}_2$  of 6 cm and 1 cm for measurement in the lower levels and upper levels of the atmosphere respectively. The field of view to earth is  $4^\circ$  along the satellite track and  $10^\circ$  each side of the track with a rotation of the view along the track (forwards and backwards) of  $15^\circ$  to give the required Doppler scan. Nimbus 'F' is scheduled for launch in May 1974.

The Laboratory is now working upon the engineering design for a radiometer for Nimbus 'G'. It will comprise a cluster of 8 radiometers filled with different gases and by selective absorption the concentration of various minor constituents of the atmosphere (including some pollutants) will be measured on a global scale.

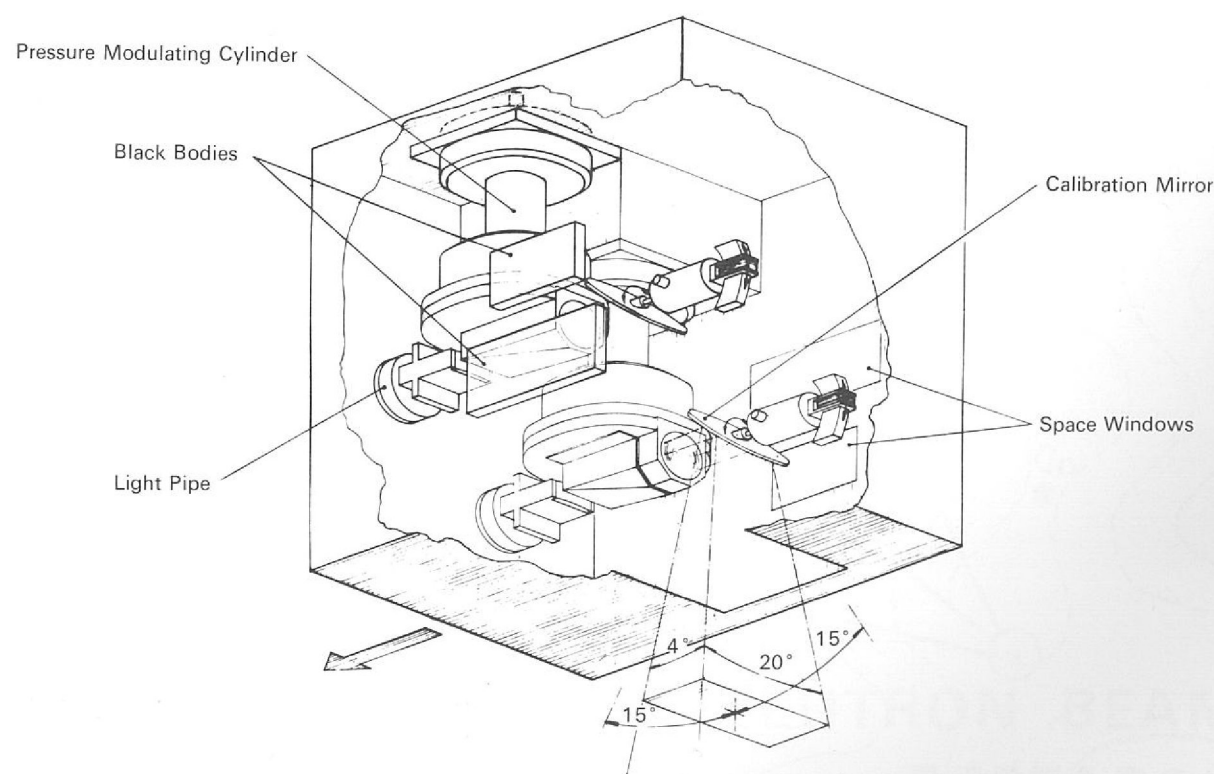
*Other Space Work*

The engineering model and the bench check and calibration equipment of the Nimbus 'E' SCR is being prepared for installation in a Canberra research aircraft of the Meteorological Office. This involves further electronics to interface with the data acquisition system on board the aircraft and a revised method of cooling the space calibration targets. The electronics units of the test equipment require repackaging and upgrading to flightworthy standards.

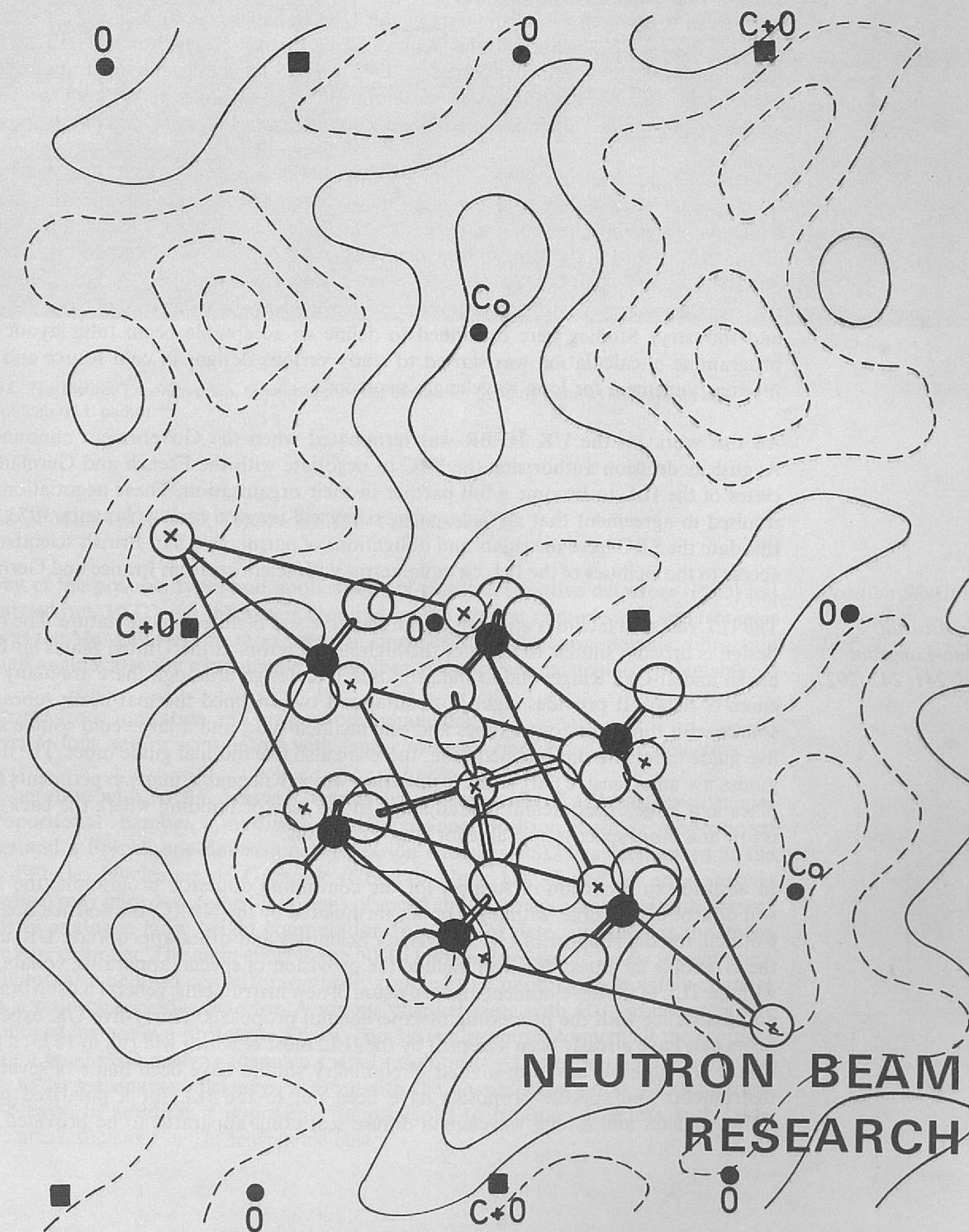
Three pressure modulated radiometers are being prepared for an experiment which will be carried aloft in a French balloon. This experiment is a forerunner of the possibilities proposed for Nimbus 'G' and will provide some information on pollutants from supersonic high flying aircraft.

A basic design and layout has been prepared for a preliminary proposal for a radiometer to be flown on a joint NASA/ESRO orbiter to probe the atmosphere of Venus. It is hoped to launch such a spacecraft in 1978.

Figure 94. The pressure modulated carbon dioxide radiometer for atmospheric temperature sounding from Nimbus 'F' satellite (10491).



The design shows the structure of the antiferromagnetic compound cobalt carbonate superimposed on a projection of a difference magnetisation density distribution as measured using polarized neutrons.



# Neutron Beam Research

During 1972 the direct strength of the Neutron Beam Research Unit (NBRU) increased to a total of 20. A widening range of activities was covered: preparatory work for the proposed UK High Flux Beam Reactor (HFBR); development studies for new instruments and techniques, technical support for the UK current neutron beam science programme; secretariat work for the Neutron Beam Research Committee (NBRC) of the Science Board and for the NBRC's Technical Sub Committee; general liaison with university scientists and relevant research establishments in the UK and overseas and preparation for the possible use by UK scientists of the facilities of the Institut Laue-Langevin (ILL) at Grenoble. The total direct effort involved in 1972 was 15 man years, divided about equally between HFBR preparatory work, development studies, current programme support and activities of general management and liaison.

## *The High Flux Beam Reactor*

The HFBR preparatory work continued in collaboration with the UKAEA, until the middle of the year. Safety analysis of the main design features was advanced to the stage which would enable the SRC to apply for a nuclear site licence for the proposed location at the Rutherford Laboratory. Two definitive reports were produced for this purpose (HFBR/72.5 and HFBR/72.6). The SRC's proposals were submitted for consideration by the Nuclear Safety Advisory Committee (which advises the Secretary of State for Trade and Industry). Studies were continued to define an acceptable beam tube layout and a programme of calculation was started to study various designs of cold source and guide tubes arrangement for long wavelength neutrons.

All this work on the UK HFBR was terminated when the Government announced in August its decision authorising the SRC to negotiate with the French and German associates of the ILL to become a full partner in their organisation. These negotiations have resulted in agreement that *de facto* partnership will operate from 1 January 1973. From this date the SRC have the rights and obligations of partnership and British scientists have access to the facilities of the ILL on equal terms with scientists from France and Germany.

## *The Institut Laue-Langevin (ref. 241, 242, 292)*

The ILL research facilities are both comprehensive and of an advanced nature. The reactor design is broadly similar to those of the high flux reactors in the United States (at Brookhaven and at Oak Ridge) and to the proposed UK design although there are many differences of detail. It provides eight horizontal and two inclined thermal beam tubes, a hot source with three horizontal tubes and one inclined tube, and a large cold source serving five guide tubes and one inclined tube; there are also five thermal guide tubes. The neutron guides are an extensive part of the installation which will enable many experiments to take place in a large experimental hall adjacent to the reactor building where the background is low and more space is available for large apparatus.

In addition to provision of support for the continuing domestic programme the NBRU will now be responsible, within the policy formulated by the NBRC, the Science Board and Council, for the support of UK University Scientists and other appropriate UK users of the Grenoble facilities. This will include the provision of special apparatus, collaboration with the ILL in the development and provision of new instruments, general liaison functions, and assistance with the processing of experimental proposals. Thirty-five UK experiment proposals have already been accepted by the ILL, most of which will run in 1973; a further round of proposals has been invited. Preliminary studies have been made of several new instruments and specific proposals have been put to the ILL for a polarized neutron diffractometer and a long wavelength diffuse scattering apparatus to be provided by the Unit.

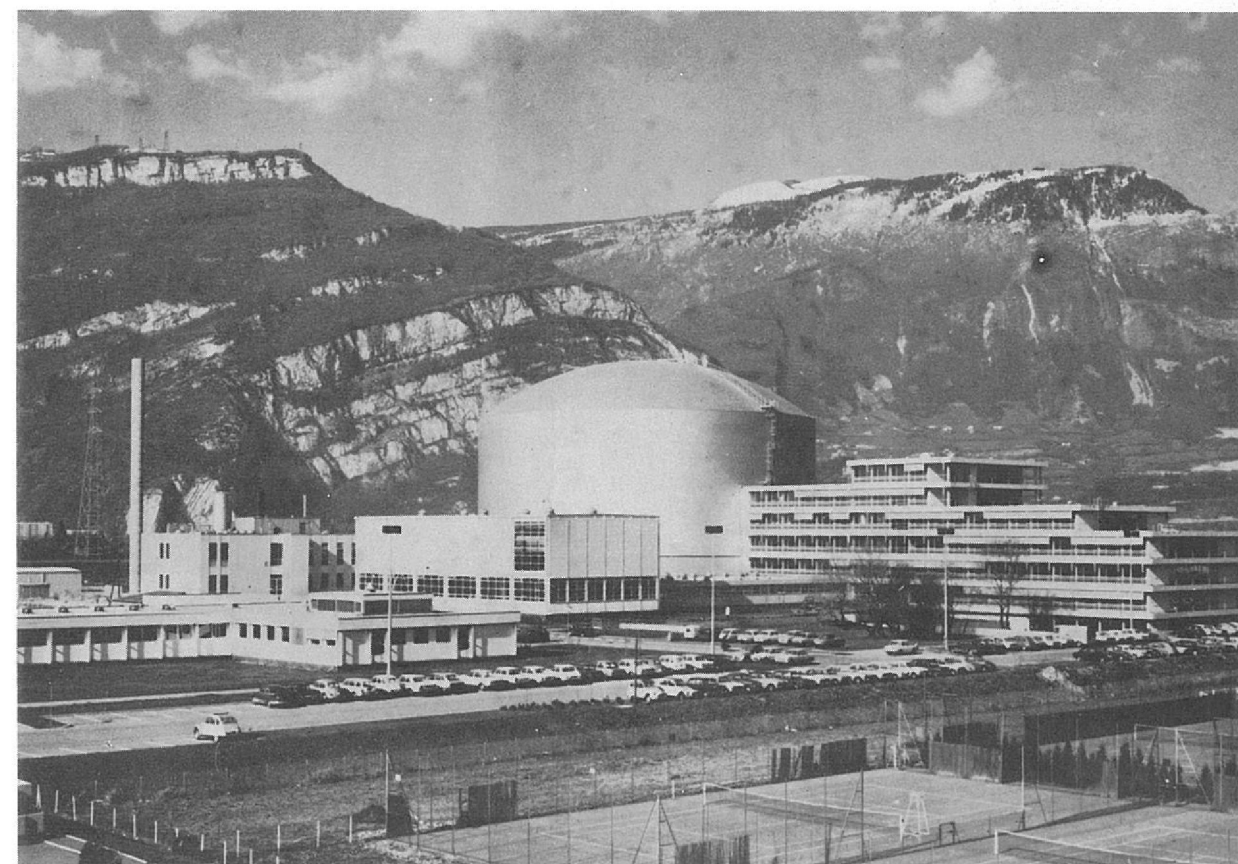


Figure 95. The Institut Laue-Langevin, Grenoble, showing the reactor building (centre), laboratories and office buildings (ILL photo).

## DEVELOPMENT OF NEUTRON BEAM TECHNIQUES

A survey of the possible types and applications of position sensitive detectors (PSD) has been carried out. PSD's are inherently required by the version of triple axis spectrometer known as the Marx and can be most useful in single crystal diffraction, powder diffraction and small angle scattering experiments. Two types of device are particularly promising:

*Position Sensitive Detectors (ref. 201)*

- multi-electrode ionisation and proportional chambers.
- converter foils and/or scintillators with semi-conductor or channel plate detectors.

In collaboration with AERE, Harwell, studies have been made of a linear resistive wire  $^3\text{He}$  proportional chamber, a multiwire two-dimensional position sensitive proportional chamber and a French one-dimensional ionisation chamber PSD has been tested at the Centre d'Etudes Nucleaires de Grenoble (CENG). Work has started on an electronic device which may improve on the limitations of speed and accuracy associated with present methods of analogue pulse height computation required for detectors such as the linear resistive wire chamber. The main effort in the NBRU is being applied to a new system using a scintillator, as a neutron converter, optically coupled to a photocathode with a channel plate as a position sensitive detector. A sample channel plate with  $100\ \mu\text{m}$  channels has been obtained for use in a prototype device. This system promises to meet all the requirements for a good PSD, such as adequate spatial resolution ( $\pm 1\ \text{mm}$ ), good pulse counting rates ( $> 10^4/\text{s}$ ) reasonable efficiency ( $> 30\%$ ) with the possibility of good discrimination against  $\gamma$  rays. In addition it is possible, in principle, to produce detectors with large sensitive areas, such as  $1\ \text{m}^2$ , at reasonable cost.

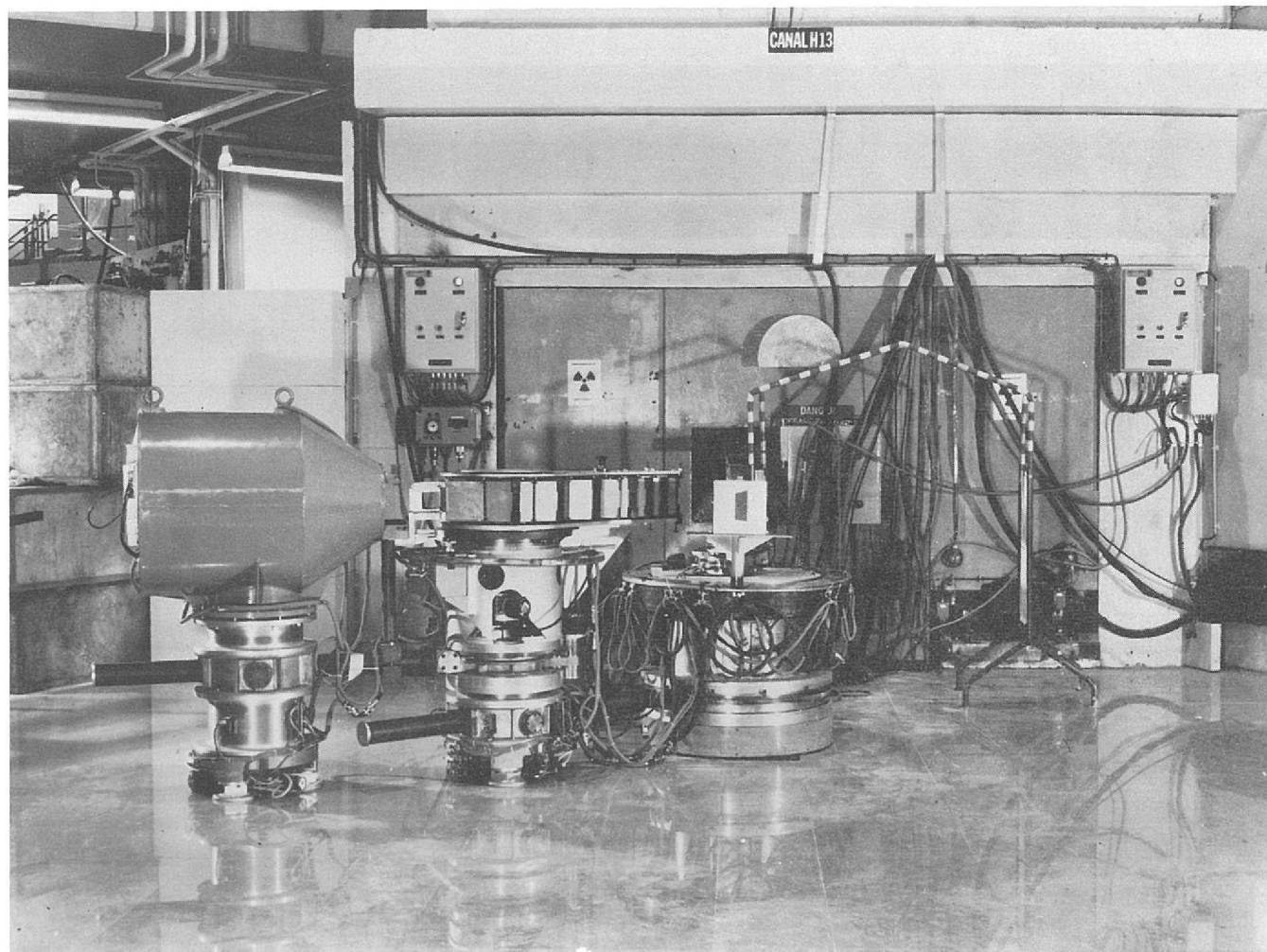


Figure 96. A triple axis spectrometer for measurements of dispersion curves, phase transitions etc. at medium to high resolution and with medium energy changes at the ILL reactor (ILL photo).

*Polarizing Monochromators*

Neutron beams can be polarized by Bragg reflection from certain magnetic crystals in which the magnetic and nuclear scattering effects are additive for one neutron spin direction but cancel out for the other. A collaborative programme is being operated on crystals of  $\text{Fe}_3\text{Si}$  and the Heusler alloy  $\text{Cu}_2\text{MnA}_1$  with AERE, Cambridge University, ILL and CENG. Initial experiments on an  $\text{Fe}_3\text{Si}$  crystal showed that a polarization of around 95% could be achieved, but that the crystal had a mosaic spread of some  $2.4^\circ$  at half maximum for the (111) reflection and consequently a poor reflectivity. A second crystal is currently being evaluated. It is anticipated that the mosaic spread will not exceed 20 arc minutes. The production of larger crystals and crystals at the composition for optimum polarizing efficiency are being investigated by Crystal-Tec (Grenoble).

*Polarizing Filters (ref. 141, 258, 326, 327, 328)*

An alternative way of polarizing neutrons is by nuclear scattering or absorption in crystals containing polarized nuclei. Several polarized nuclei including  $^1\text{H}$ ,  $^3\text{He}$ ,  $^{115}\text{In}$ ,  $^{149}\text{Sm}$ ,  $^{155}\text{Gd}$  and  $^{157}\text{Gd}$  have been investigated for feasibility as filters for polarizing thermal neutrons. Two filters, viz. (a) a single crystal of  $\text{La}_2\text{Mg}_3(\text{NO}_3)_{12}24\text{H}_2\text{O}$  (LMN) in which the protons of the water of crystallisation are dynamically polarized using the 'solid effect', and (b) a  $\text{Ce}_2\text{Mg}_3(\text{NO}_3)_{12}24\text{D}_2\text{O}$  single crystal containing approximately 5% polarized  $^{149}\text{Sm}$  (CSNM) have been shown to have suitably high polarizing efficiencies and transmittances for thermal neutrons. Special attention has been given to the use of polarizing filters as spin analysers in the polarization analysis of thermal neutron scattering by solids and liquids. In this context the CSMN filter offers several advantages over the LMN filter e.g. (i) the polarization of the  $^{149}\text{Sm}$  nuclei can be achieved statically by the 'Rose-Gorter' method, (ii) the filter polarizing efficiency is much less sensitive to changes in the nuclear polarization and (iii) the nuclear polarization achievable in the double nitrate is less critical on the crystal orientation in the applied magnetic field. The major

disadvantage of the SMN filter is that it requires to be cooled to approximately 15 to 20 mK before operating efficiency approaches that of the best LMN filter (proton polarization approximately 80%); however it is anticipated that cooling to such temperatures will be achievable by  $^3\text{He}$ - $^4\text{He}$  dilution refrigeration. The SMN filter is expected to be less expensive than one using LMN.

A design study with the aim of constructing a CSMN neutron polarizing filter for a polarized beam at the AERE PLUTO reactor is now well advanced. The scientific case for the filter is being investigated in collaboration with users at the University of Kent and Imperial College, London. Preliminary theoretical work has been carried out to estimate the accuracy with which spin-dependent cross-sections may be determined using this filter as the spin analyser. The effect of multiple scattering corrections in such experiments has also been studied.

A new type of thermal neutron spin flipper with high efficiency was recently described by F. Mezei (Central Research Institute for Physics, Budapest). The flipper depends on the principle that the neutron polarization direction changes in a well-known manner as it traverses a magnetic field (the neutron magnetic moment has a characteristic Larmor precession frequency proportional to this field), and for a monochromatic polarized beam it should be possible to control the polarization direction. The action of the flipper and the required magnetic fields are produced by d.c. coils which are easier to construct than those required for r.f. flippers.

The potential of the new flipper has been investigated in collaboration with AERE and the optimum performance was found to be equivalent to that of the r.f. flippers (flipping efficiency 0.995). The efficiency was limited in the present investigation by magnetic field inhomogeneities. Higher flipper efficiencies should be achievable in an improved apparatus.

Slow neutrons may undergo a process analogous to total internal reflection when they impinge at grazing incidence on a surface. For nickel, the critical grazing angle is only 1.7 mrad for neutrons of wavelength 1 Å. Using this effect, tubes with polished nickel surfaces can be made which conduct neutron beams over long distances by reflecting them back and forth between the walls. The tubes can be slightly curved with a radius of curvature about  $6 \times 10^5$  times the wall spacing for 1 Å neutrons. Studies have been concentrated on miniature guide tubes or 'micro-guides' (first investigated by Marx and Maier-Leibnitz) where the spacing is about 1 μm and the radius of curvature a few tens of centimetres. By stacking these curved micro-guides one on top of the other it would be possible to bend a neutron beam through several degrees in a short distance. This would greatly facilitate the layout of neutron beam experiments and enable better use to be made of inclined beam holes. By having the stack of micro-guides of gradually increasing length, a neutron beam could in principle be brought to a focus. Theoretical estimates of the efficiencies of stacked micro-guide lenses have been made, taking into account, in a crude way, losses due to stacking, absorption and multiple reflections. It is concluded that gains in neutron flux of up to ten (at the expense of increased beam divergence) might be possible in certain circumstances e.g. neutron wavelengths of a few Å and a beam convergence of a few degrees. Both stacked films and stacked fibres as microguide lenses have been examined theoretically. As a practical approach, for stacked films, vacuum deposition or electroplating of alternate layers of reflector and filler seems the most promising especially in combination with a new idea which is to use  $^{60}\text{Ni}$  as the filler material and  $^{58}\text{Ni}$  as the reflecting coating, thus avoiding difficulties due to differential expansion when different materials are used. For stacked fibres, drawing down a bundle of large diameter fibres until individual elements are a few microns in diameter seems to be the most profitable approach. Discussions have taken place with Imperial Metal Industries with a view to using the same techniques as are used in making filamentary superconducting cables. A trial extrusion of aluminium alloy inside a nickel sheath indicated however that the surface smoothness of the final fibres may not be good enough for the micro-guide application. A clear conclusion from the preliminary work is that stacked micro-guides will probably be difficult and costly to produce, especially if an application calls for a device to handle neutron beams of comparatively large dimension (several tens of  $\text{cm}^2$ ).

*Polarization Reversal Device (Spin Flipper)*

*Guide Tubes (ref. 332)*

The potential applications for straightforward beam benders seem clear cut and the development of a device for bending  $10 \text{ \AA}$  neutrons through about  $5^\circ$  is in hand. This consists of a stack of stretched films  $25 \mu\text{m}$  thick separated by air spaces of  $250 \mu\text{m}$  and bent to a radius of about 2 m. Various materials have been investigated for the films, optical quality Melinex being the most promising so far.

An important feature of all guide tubes is the finish of the reflecting surfaces, the most important parameter being the mean slope of the surface. In the absence of suitable standard instruments to measure this, a special device has been constructed in which laser light reflected from the specimen is measured by a quadrant diode. As the surface is traversed by the  $0.125 \text{ mm}$  diameter spot, an output proportional to the position of the light spot on the diode and therefore to the slope of the surface is obtained provided there are no significant surface features smaller than the spot diameter. This device has been used to assess the smoothness of stretched foils and also to measure surfaces of copper tube samples, polished in various ways. The latter measurements are in connection with an AERE development to use suitable polished standard metal tubing as a normal guide tube.

#### OTHER PROJECTS

*A Remote Job Entry Terminal to the Rutherford Laboratory IBM/370/195 Computer (ref. 207, 278, 279, 280)*

The major part of the raw data from neutron beam experiments on the DIDO and PLUTO reactors at AERE is written on Digital Equipment Corporation (DEC) magnetic tape, DECTape. In order to provide a data reduction service on the Rutherford Laboratory IBM 370/195 computer for SRC sponsored scientists, it was necessary to provide a DECTape input facility. This has now been done in the form of a Remote Job Entry Terminal consisting of a PDP-8E computer with Teletype, model ASR 33, Dual DECTape unit and 12 channel Buffered Digital I/O. The original scheme was for time of flight (Cassandra) data only. The system is being developed to allow data reduction from other neutron beam instruments.

*Neutron Gas Facility (ref. 259)*

When the neutron energy becomes very low, the critical angle for total reflection at a surface can become greater than  $90^\circ$ . This condition occurs at the highest neutron energy for a beryllium surface ( $25 \times 10^{-8} \text{ eV}$ ,  $\lambda \sim 60 \text{ \AA}$ ). These ultra cold neutrons (UCN) can thus be contained in a closed beryllium vessel and behave as a very low pressure ( $10^{-20} \text{ torr}$ ), low temperature ( $10^{-3} \text{ K}$ ) ideal gas of number density about  $1 \text{ cm}^{-3}$ . The Neutron Gas Facility is a proposal by Sussex University to study and exploit the unique properties of UCN at the DIDO reactor.

The ability to store UCN in a closed vessel means that the time available for measurements on each neutron is increased from less than one ms to more than 100 s, thus increasing the accuracy of several important measurements in nuclear physics. For example in the search for a possible neutron electric dipole moment the measurement accuracy could be increased ultimately by a factor  $5 \times 10^3$ . Also there is a good chance of improving the accuracy of the experimental value of the neutron lifetime and, by studying the decay of polarized UCN, of obtaining the weak interaction parameters with higher accuracy than at present. The sensitivity of reflection losses to the surface state of the UCN container should provide a novel method of surface characterization. Finally the ease of control of UCN should make possible neutron optical experiments using magnetic or material UCN lenses or a low resolution ( $1 \mu\text{m}$ ) UCN microscope.

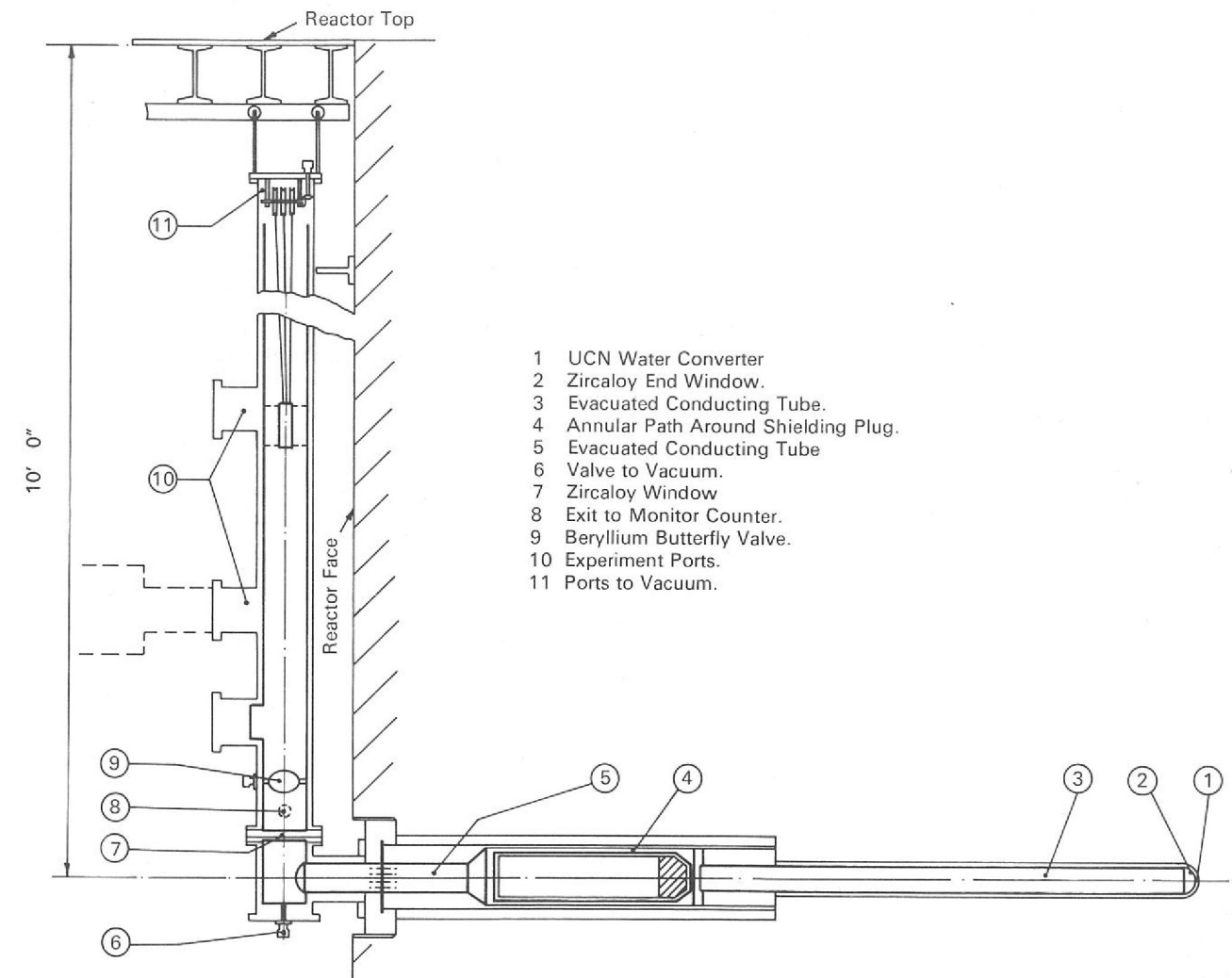


Figure 97. Design for an ultra-cold neutron source at the DIDO reactor.

The proposed facility consists essentially of two sections (see Figure 97), a horizontal in-pile section connected outside the reactor to a vertical out-pile section. The in-pile section is made up of concentric tubes in which the outer space forms a water jacket, the UCN being formed by inelastic collisions of thermal neutrons in the water between the hemispherical metal ends of the tubes. The inner tube is lined with beryllium and evacuated to a pressure of  $10^{-8} \text{ torr}$ , the UCN entering it via a thin zircaloy window and diffusing along it like a gas. A shielding plug prevents fast neutrons and  $\gamma$  rays from the reactor core escaping along the tube, the UCN diffusing through an annular gap between the plug and the inner tube. The out-pile section is essentially a vertical beryllium lined tube about 3 m high. Ports at various heights allow UCN of various energies to be tapped off for experiments.

During the year the NBRU, in collaboration with AERE and Sussex University, has been carrying out the project definition (due for completion early 1973) in order to confirm the final design and cost estimate. Lay-out work on the in-pile element, reactor face equipment including shielding, platform and the associated instrumentation has been completed. This has necessitated a development programme on electron beam and friction welding. A special test rig has been constructed in order to prove some high vacuum seals required for the in-pile element.

## PARTICIPATION IN NEUTRON BEAM RESEARCH PROGRAMMES

*Thorium-Caesium Alloy  
Magnetisation Studies  
(with Imperial College  
London)*

Diffuse magnetic neutron scattering provides an invaluable method for determining magnetic moment distributions, especially in alloys. The Th-Cs system shows anomalous behaviour between 4.2 K and 300 K which it is hoped to study by this method. Long wavelength experiments have been carried out using the elastic defect scattering instrument on PLUTO (the Gloppler). Room temperature measurements showed significant magnetic diffuse scattering, however, the isolation of the magnetic contribution by a new temperature switching technique failed due to poor mechanical stability of instruments. It is planned to repeat these experiments using the new Gloppler apparatus currently being installed.

*Magnetic Structure  
Studies (with various  
collaborators)*

The crystallographic distortion which takes place at 32 K in  $TbVO_4$  has been measured by X-rays in collaboration with the University of Bonn and AERE. A series of neutron experiments on single crystals of  $TbVO_4$  and  $DyVO_4$  in a magnetic field or under pressure are being planned in collaboration with the former. It is possible that some of these experiments will be conducted at the ILL. This work is complementary to the work on the Jahn-Teller effect in the rare earth materials by the Clarendon Laboratory, Oxford, and is a necessary preliminary to a single crystal investigation to obtain a complete description which takes place below the transition temperature.

The following measurements have been made on magnetisation density distribution on intermetallic compounds and ionic materials which can be used as a basis for a description of the materials in terms of their basic physical parameters such as ground state wavefunctions, covalency, conduction electron polarization and band structure:

- a. in collaboration with the Cavendish Laboratory, measurements on two samples of the intermetallic compound  $Mn_5Ge_3$  at a number of different wavelengths have been completed.

A full analysis has been made of both the antiferromagnetic and weak ferromagnetic components of the magnetic scattering from the ionic compound  $CoCO_3$ .

- b. In collaboration with Queen Elizabeth College, London, magnetic structure determinations are in progress on  $TbZn_{12}$  and on  $\delta$ -FeOOH with the Universities of Newcastle and Munich.
- c. Measurements on spinel structures have started in collaboration with the University of Portsmouth on nickel and lithium ferrites and with Queen Elizabeth College on  $Cu_3Ga_3Cr_2S_4$ .

*Dynamics of Fatty Acid  
Chains in Phospholipid  
Membranes (with  
King's College,  
London and AERE)*

With the aim of working towards an unambiguous and quantitative characterization of membrane 'fluidity', quasi-elastic experiments have been carried out for a series of dipalmitoyl bilayer systems as a function of conformation, hydration and certain added constituents. In the first instance these experiments give a direct measure of chain diffusional motions; work is continuing to provide a more quantitative interpretation of the results. Future work will aim at providing a complete picture of membrane dynamics, for example by studying headgroup motions in lipid samples with fully deuterated chains.



A computer-graphic display unit (9323)

COMPUTER SYSTEMS

# Computer Systems and Applications

The Computing Centre extended its service to all authorised users of the IBM 370/195 computer on 1st January 1972. During the early part of the year all the original 360/75 peripherals were replaced by 370 type peripherals—the Block Multiplexor, Fixed Head File, 3330 Disk Unit and fast tape drives (Figure 98). The final item, the control console, was added in September. (See Quarterly Reports, ref. 302, 303, 304, 305.)

There has been a marked increase in the number of Remote Job Entry work stations linked to the central computer and operating under HASP-RJE. Many of those now operating with rented equipment will be replaced by purchased GEC 2050 computers during the first quarter of 1973. The location of these stations will be at Imperial College, University College, Bristol, Westfield College, Durham, Queen Mary College, Oxford and CERN. In addition Glasgow and Birmingham have links to existing local IBM computers. Six ports have also been reserved for work stations for ATLAS users, of which one is occupied by the Radio and Space Research Station (RSRS), Slough. Remote work stations have proved remarkably successful and have come into operation with relatively few problems.

Another growth area during the year has been in the use of ELECTRIC—the Rutherford Laboratory data editing, file handling and remote job entry system with output retrieval through a variety of terminals (typewriters, VDU's and graphics displays). The organization of on-line equipment is shown in Figure 98.

The HPD1 and CYCLOPS film measuring machines have been joined by HPD2, which became fully operational on spark chamber film during the year. Film from two experiments (ISR and S104) was measured, and results from the former presented at an international conference in September.

## REMOTE JOB ENTRY WORK STATIONS

Many users of the Computing Centre are located at universities and one of the most interesting developments during the year has been an extensive programme of installing 'Work Stations' at remote centres. These are linked to the central computer and each comprises at least a card reader and line printer for submitting jobs and receiving output, based on a local computer or other device. At some stations an existing computer originally installed for other purposes has been utilised (e.g. an IBM 360/44 at Birmingham University) and in others a small computer specially purchased will be used. The location and status of all work stations now operating or currently planned are summarised in Table 8.

Information is transmitted to and from the Rutherford Laboratory via the Post Office Datel 2400 service. This offers a leased private telephone link between two points which is available to the renter 24 hours each day. This service is more economical for connect times of more than a few hours per day than the switched public telephone system alternative. Modems to operate at 2400 bits/second are also supplied, and can be attached to the slower switched public network as an insurance against failure of the private lines. This is a valuable diagnostic facility. Twelve Post Office private links have now been installed, and all use Post Office modems except for the link to CERN, Geneva, where it proved necessary to use privately manufactured modems.

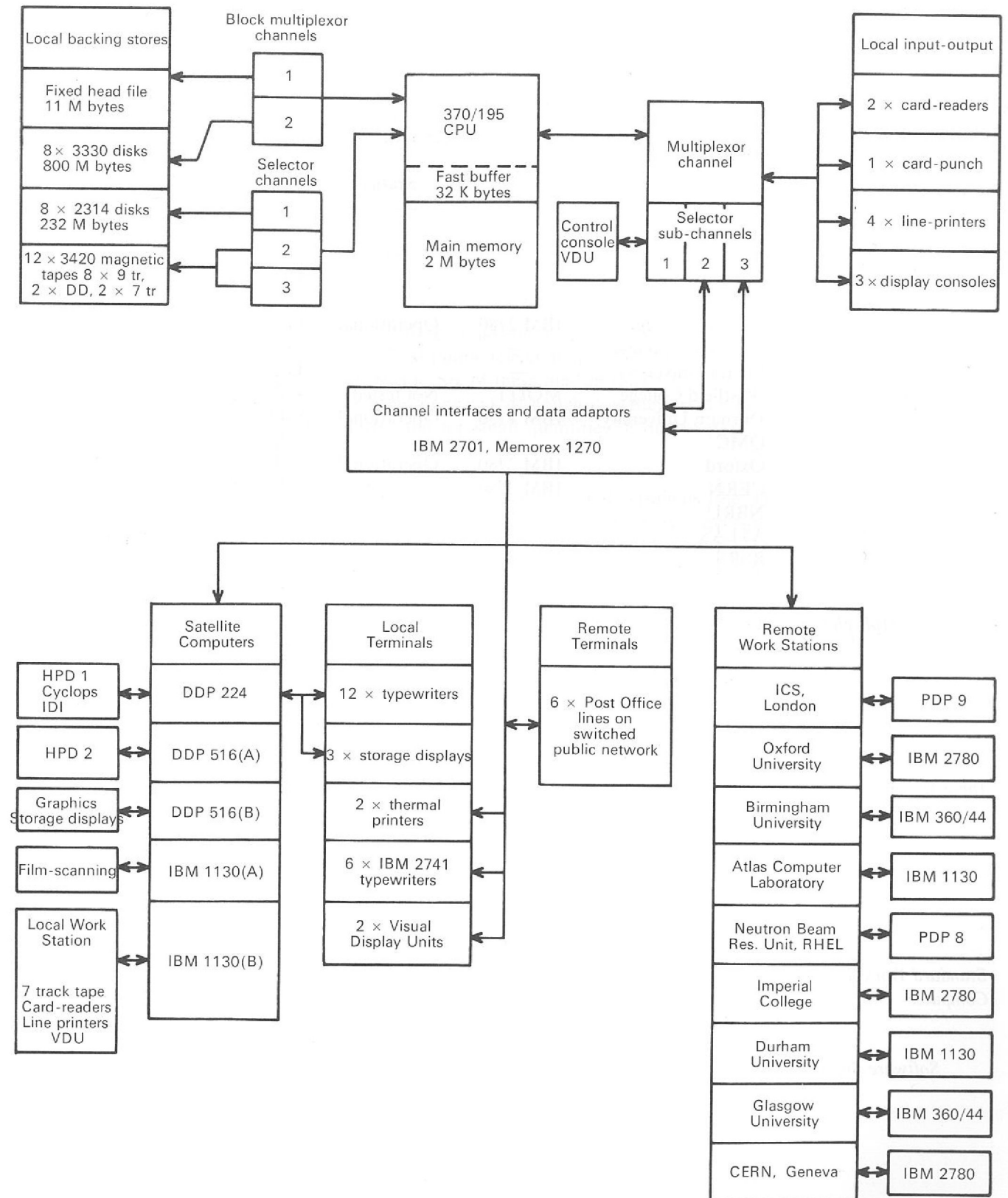


Figure 98. The central and satellite computer system.

**Table 8**

Status of Work Stations at the end of 1972

Location	Interim Equipment		Final Equipment	
	Type	Status	Type	Status
ICS, London	—	—	PDP9	Operational
RHEL (Hall 3)	—	—	IBM 1130	Operational
Glasgow	—	—	IBM 360/44	Operational
Birmingham	—	—	IBM 360/44	Operational
Imperial College	IBM 2780	Operational	GEC 2050	Not delivered
University College	—	—	GEC 2050	Not delivered
Bristol University	—	—	GEC 2050	Not delivered
Westfield College	MOD I	Not tested	GEC 2050	Not delivered
Durham University	IBM 1130	Operational	GEC 2050	Not delivered
QMC	—	—	GEC 2050	Not delivered
Oxford	IBM 2780	Operational	GEC 2050	Not delivered
CERN	IBM 2780	Not tested	GEC 2050	Not delivered
NBRU	—	—	PDP8E	Operational
ATLAS	—	—	IBM 1130	Operational
RSRS	IBM 2780	Operational	Undecided	—

*Multiplexor*

For the central computer end, a Memorex type 1270 communications multiplexor was bought. This makes provision for up to 24 synchronous data links of the Datel 2400 type operating at 2400 bits/second, and asynchronous connections to a further 72 terminals such as typewriters or visual display units, of varying speeds up to 1200 bits/second. All 96 devices can operate simultaneously. This Memorex multiplexor was successfully commissioned during July 1972, replacing the IBM type 2702 and 2703 interfaces.

*Input/Output Capacity*

In general, the remote job entry work station consists of a card reader and line printer connected to a data link (and thence to the central computer) via special purpose hardware or, more frequently, a smaller computer. A data transmission link operating at 2400 bits/second is capable of supporting a card reader of 200 cards/minute capacity or a line printer at 150 lines/minute in their simplest forms. If the card reader and line printer are attached via a computer (such as the GEC 2050) to the same link, these rates can be raised to 400 cards/minute and 300 lines/minute by interleaving.

*Standard Work Station Computer*

After a survey of existing installations the GEC 2050 computer with card reader and line printer was selected as the basis of new work stations at centres without an existing suitable local computer. Eight such stations will be provided by the Rutherford Laboratory.

*Software Support*

Remote job entry work stations are supported by the IBM 370/195 HASP-RJE system software. Each station must, however, appear to the system as one of several possible alternative IBM work stations, of which the simplest and slowest is an IBM 2780. So a station based on the GEC 2050 must meet IBM conventions, and this can be achieved by using a program (supplied by GEC) which makes a GEC 2050 simulate an IBM 2780. The GEC 2050 is, however, capable of simulating an IBM 1130, which has twice the performance of an IBM 2780. The simulator program is more complex and does not yet exist, but in collaboration with GEC, the Rutherford Laboratory will provide a suitable simulator program for each work station in the early part of 1973. In due course GEC will take responsibility for maintenance of the IBM 1130 simulator program.

Modifications to HASP and MAST have enabled some work station consoles to be used as ELECTRIC terminals, and further developments will allow auxiliary consoles (such as VDU's and graphics displays) attached to work stations to be similarly used.

Two of the remote job entry work stations are on the Rutherford Laboratory site. The terminal 1130 in Experimental Hall 3 offers card reader, line printer and 7-track magnetic tape drive facilities, and has had a 60 characters/second VDU added to it during the year. Secondly, the Neutron Beams Research Unit has a PDP8E computer intended primarily for transmitting DEC magnetic tapes to the central computer. A simulator program makes the PDP8E resemble an IBM 2780.

*On-Site Work Stations*  
(ref. 211, 265, 296, 297, 298)

**OTHER TERMINALS**

A number of slow speed (10 characters/second) terminals have been linked from various places to the central computer via the switched public telephone network and the asynchronous facilities of the Memorex multiplexor. Six of these dial-up lines are available, and teletypes and graphics terminals have been connected. Although slow they are valuable for remote job submission via ELECTRIC and for small quantities of output (text or graphics) and have functioned successfully.

*Public Telephone Links*

Within the Laboratory, tests have been made using faster lines and terminals (the 30 characters/second thermal printers and 120 characters/second VDU's). A successful demonstration of remote job submission and output retrieval was given during the 1972 SEAS annual conference in Gotenburg (Sweden), using a teletype in Gotenburg connected to the central computer via the switched public network.

In addition to the six IBM 2741 terminals available at the beginning of the year, two Telterm VDU's and two Texas thermal printers have been made available for public use in the data preparation area during the year.

*On-Site Terminals*

The new IBM 3270 console equipment including three VDU's was installed on the central computer during the year. These can communicate with ELECTRIC and system management operations for ELECTRIC are now directed from the main console.

Another terminal not publicly available is the T4002 display dedicated to the Bubble Chamber Research Group and used by them for graphics work and output retrieval. It is connected via the slow multiplexor and a 9600 bits/second serial interface to the DDP224 satellite computer.

**CENTRAL COMPUTER OPERATING SYSTEM**

During the year there has been no basic change in the operating system software for the 370/195. The current system in use is OS/MVT/HASP with some local additions which are described later. On-line activities are supported by Rutherford Laboratory software (MAST/DAEDALUS/ELECTRIC) which has been described in detail in previous reports. At the end of 1971, release 20.1 was introduced to support the IBM 2305 fixed head file and the 3330 large-capacity disk store. About mid-year release 21.0 was introduced to support the 3270 console equipment. IBM has announced that this is to be the final release of OS/360.

The version of HASP now used is HASP 2 Version 3.1. This version contains several operational improvements of which the most important is the ability to cancel a job with immediate resubmission. This facility is very convenient when, for example, a remotely submitted job is unable to proceed for some system reason such as a faulty tape drive.

Apart from minor teething troubles which arose with the introduction of new equipment the basic IBM software has been extremely reliable. The fixed head file is reserved mainly for system data sets (the job queue, the catalogue, etc.) but is also used as an overlay residence for the ELECTRIC file handling system and the HPD control program.

The 3330's are used for a very wide range of tasks—system support, HASP spooling, ELECTRIC, HPD's and a few users' data sets. With the growing use of the machine disk space is now under severe pressure. The IBM 3270 console equipment consists of three visual display units (3271's) and two printers (3286's). Hardware faults in the control unit (3272) and deficiencies in the software support produced a prolonged period of unsatisfactory performance of the machine during the last quarter. Nevertheless the 3270's have been very successful as aids to efficient operation. They permit instantaneous and simultaneous display of several types of information and command, for example, the states of the queues maintained by SETUP (see below). One of the VDU's is mostly used to give quick observation and control of the datalinks by which work stations are connected to the central machine, and to present the changing picture of main-memory occupancy by all jobs handled by it.

*HASP*  
(ref. 246, 247, 261)

Early in the year many changes were made to cope with the IBM 2702 and 2703 telecommunications control units which were then the main means of connection of terminals and work stations. Subsequently these control units were superseded by the Memorex 1270 unit and HASP has now been expanded to accommodate 24 work stations (the maximum the Memorex will handle). Alterations have also been made so that ELECTRIC facilities are available at any 370/195 console, or at any work station which is controlled by HASP multileaving Remote Job Entry.

Perhaps the most striking extensions to HASP made locally are the sub-tasks now attached to it. These are the modules which give the COPPER and SETUP facilities. Such a module need not only be a sub-task of HASP but can also appear to MAST as an on-line program and hence communicate with ELECTRIC.

*Software from the User's Angle*

During the year the collection of catalogued procedures was radically overhauled. Names of procedures are now systematic and mnemonic, there are far fewer to be remembered, and (for procedures containing a link-edit step) the same one may be used whether or not the user wishes to change the contents of one of the user-libraries. Each group of users now has an object-module library of its own, and designates a library manager who is responsible for clean-ups, listings, etc.

The Fortran compilers invoked by these procedures are still the G and H compilers of release 20.1 with some later corrections. They seem to give little trouble and there is no compelling reason to change to those of release 21 for the present, which are also available.

The class-structure has been altered only by the introduction of class X jobs, which must be short, small, produce little output and not require any magnetic tape or disk volumes to be mounted.

*MAST and DAEDALUS*

These are the original components of the Rutherford Laboratory on-line system, and only minor alterations in message buffering and some improvements in the bootstrap loader have been made to DAEDALUS. It has needed some human intervention to help locate hardware faults which have arisen from time to time during the year, but has stood up well to a regular and heavy operational load.

The code in the DDP516 which drives HPD2 was developed during the year and also conforms to the DAEDALUS conventions. It is now reliable enough for regular production use of HPD2 by computer operators.

MAST has been greatly extended this year. It now contains code to handle the various keyboards and display devices which were attached to the 370/195 during the year via the

Memorex 1270 and the byte multiplexor (instead of via a satellite computer). This was a new type of connection for MAST; the new code has been designed with a minimum of points of contact with the older MAST code. The new code was tested in independent programs outside MAST and subsequently in a new version of MAST during stand-alone test periods, before incorporating it into a production version. Modifications have made ELECTRIC facilities available at remote work station consoles.

Software support for two new kinds of Tektronix display (T4002 and T4010) has been added to the ELECTRIC system. It provides (for the T4002) smaller, more compact files for point plotting and thus faster output. One such display (linked to the DDP224 computer) has been used by the Bubble Chamber Research Group, and two more attached to the HEP DDP516 graphics computer have also been used for graphics and output retrieval. A T4010 at Reading University has communicated with ELECTRIC via the Post Office switched public telephone network.

*ELECTRIC*

Changes (including HASP and MAST) have enabled the consoles of multileaving remote job entry work stations to be used as ELECTRIC terminals and further developments will allow auxiliary consoles (such as VDU's and graphics displays) attached to work stations to be similarly used.

During the year it became necessary to double the size of the graphics filing system and implement automatic deletion of files unused for a month. There are at present 130 users of the graphics and output retrieval facilities.

These are additions to HASP written at the Rutherford Laboratory. They allow more control than OS/MVT and standard HASP in a large installation such as the 370/195, which serves several remote work stations as well as local users (who may submit jobs from terminals or through a card reader). The job request slip formerly handed in with local jobs had been abolished, and replaced with automated job validation and anticipatory volume fetching.

*COPPER and SETUP*

COPPER (Control of Priorities and Peripherals, Enquiries and Reports) is empowered firstly to check that the personal-identifier and account-number fields on the job card form a valid combination, i.e. that the account-number is that of a recognised user-group and that the person is a registered user within the group. This part has been running smoothly for some months. Secondly, COPPER can check that the group still has enough computer credit left to sustain the demands likely to be made by each job at its requested priority. COPPER will not reject a job if this is not so, but will run it at a reduced priority level. Users at a console or terminal can enquire about their credit position or about the status of any job. This second part is tested and ready to use, but it had not been thought necessary to introduce it by the end of the year.

SETUP concerns the fetching of tapes and disks from the storeroom, and mounting them on drives (two distinct stages) in advance of need. This too has been developed in two phases. By scanning the various queues of jobs as they await selection for being initiated, SETUP (phase 1) issues fetch commands. By keeping watch on the utilization of the various channels and drives, it can (in phase 2) take over from OS the duty of allocating devices to volumes. Phase 2 has not been implemented yet. It is an activity capable of considerable development in the light of operational experience.

A useful program was written which enables programmers to test that overlay programs have been constructed efficiently. Several extensions have been made to SMF (the System Management Function), for instance to record the use of data sets (except those qualified by SYS1 or ULIB) and several small programs have been written (often by students temporarily at the Laboratory) to perform statistical analyses on various aspects of system usage. OS itself and HASP have required a good deal of detailed attention during the year, but the present versions, at the present level of system activity, seem reliable.

*Miscellaneous Developments*

## CENTRAL COMPUTER OPERATIONS

This is the first year of operation of the IBM 370/195 and the first year with the present wide catchment area of users. The total number of jobs processed at 262,000 was a 60% increase on the previous year. These are summarised in various ways in the following tables and figures. Figure 99 shows the weekly number of jobs executed and Figure 100

the weekly averages of machine efficiency  $\frac{\text{scheduled-down time}}{\text{scheduled time}}$  and CPU utilisation

$$\frac{\text{CPU time used}}{\text{scheduled-down time}}$$

### Distribution of Jobs in 1972 by CPU Category

Category	Thousands of jobs	Average CPU time used
Short (<90 seconds CPU)	244	11 seconds
Medium (<5 minutes CPU)	10	3 minutes
Long (>5 minutes CPU)	8	15 minutes

### CPU Time and Number of Jobs Distribution by User Category

	CPU (Hours)	%	Number of Jobs	%
1. HEP—Counters and Nuclear Structure	1078	32	72,562	27
2. RHEL—Film Analysis	358	11	30,976	12
3. RHEL—Other Divisions (except C and A)	160	5	31,276	12
4. C and A Division	223	7	72,001	27
5. Theory	175	5	10,340	4
6. Univ.—Nuclear Structure	204	6	7,744	3
7. Univ.—Film Analysis	421	12	13,397	5
8. ATLAS	643	19	16,353	6
9. DNPL	16	1	379	—
10. Unaccountable (breaks, etc.)	80	2	10,363	4
	<u>3358</u>		<u>265,391</u>	

Table 9 shows how the available time was divided during each quarter of the year.

**Table 9**

### Distribution of elapsed time (in hours) for Computer Operations

	First Quarter	Second Quarter	Third Quarter	Fourth Quarter	Total for Year	Average per week
Job Processing	1073	1454	1539	1486	5552	115 $\frac{3}{4}$
Hardware Maintenance	64	84	67	53	268	5 $\frac{1}{2}$
Hardware Development	10	4	12	57	83	1 $\frac{3}{4}$
Software Development	29	34	55	27	145	3
Lost time attributed to Hardware	24	113	35	64	236	5
Lost time attributed to Software	6	4	10	9	29	$\frac{1}{2}$
Miscellaneous	3	4	11	5	23	$\frac{1}{2}$
Machine switched off	303	487	455	483	1728	36
Totals	<u>1512</u>	<u>2184</u>	<u>2184</u>	<u>2184</u>	<u>8064</u>	<u>168</u>

Time for the first quarter excludes four weeks written off to the National power strike and special installation work.

The on-line network, considerably extended this year, is shown in Figure 98. Apart from teething troubles with some new equipment the reliability of on-line terminals, both local and remote, was generally good.

The ELECTRIC system for remote job entry, output retrieval, file handling and graphics has continued to grow and now has 214 registered users, of whom over 100 use it frequently. By the end of the year over 30% of all batch jobs were being submitted via ELECTRIC. Figure 101 shows the weekly number of ELECTRIC users, and Figure 102 the weekly percentage of all jobs submitted this way, and the CPU time so utilised. It is not at present possible to appon these statistics between users within the Laboratory and outside it.

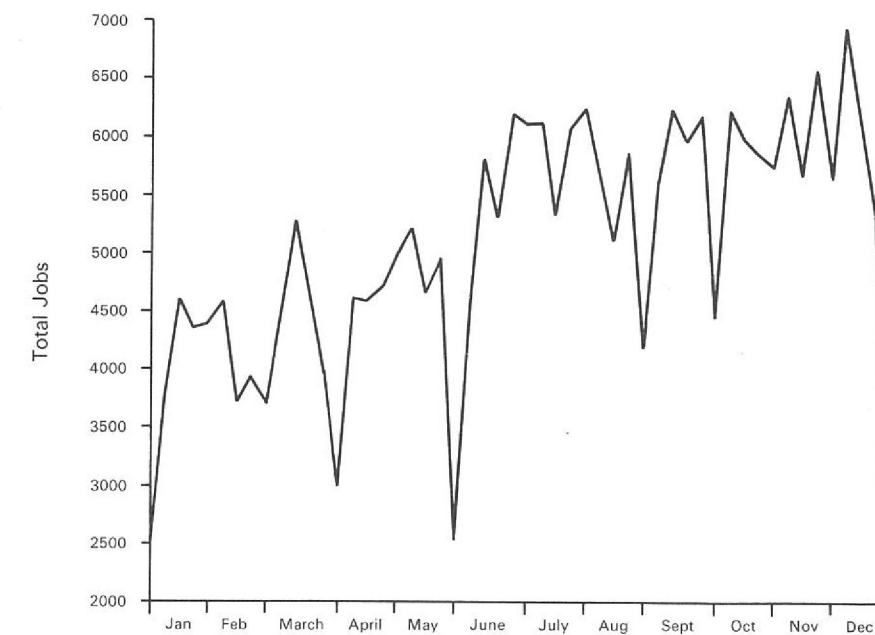


Figure 99. The number of jobs processed by the central computer for each week in 1972.

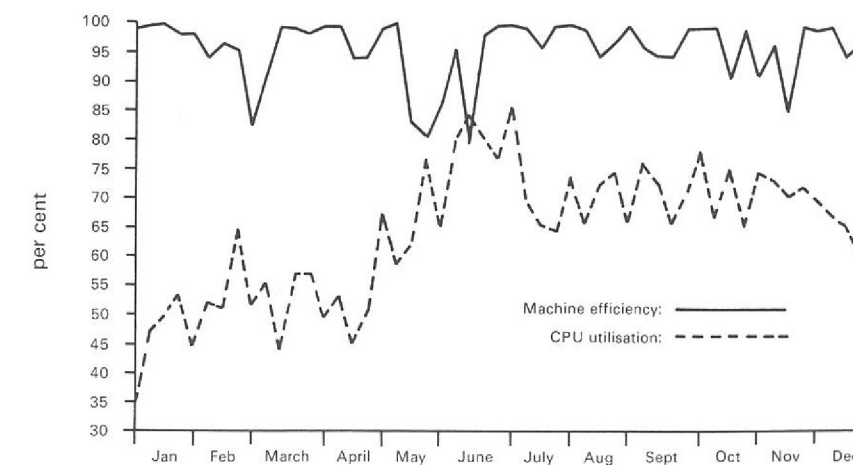


Figure 100. The weekly averages of machine efficiency and CPU utilisation.



Figure 101. Number of users of ELECTRIC terminals for each week in 1972.

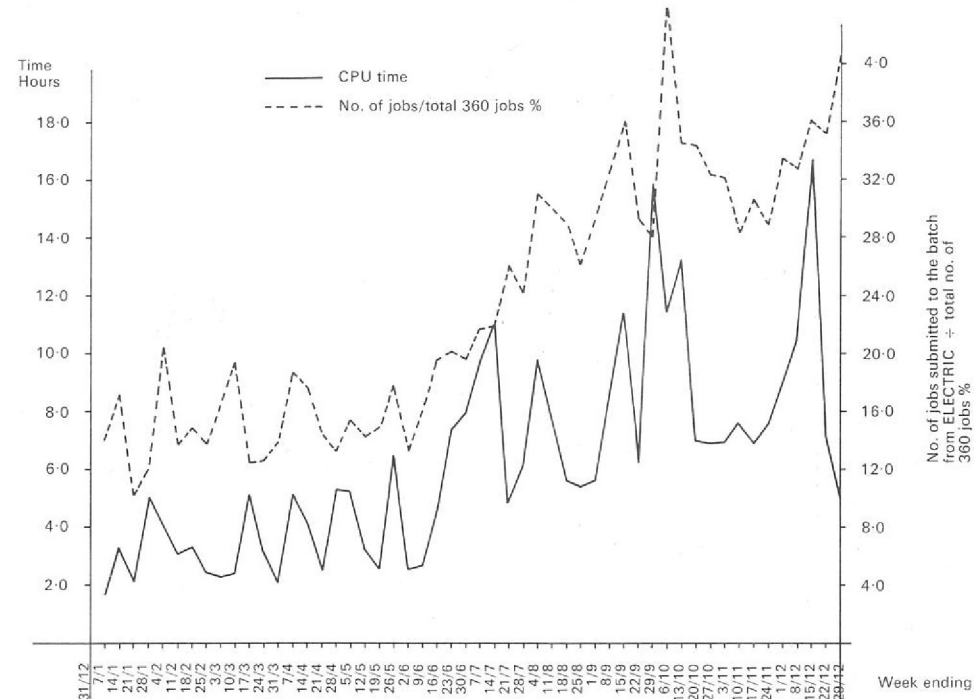


Figure 102. Number of jobs submitted to the batch from ELECTRIC and the CPU time used per week in 1972.

## USER SUPPORT

The year has seen the number of registered users rise from 250 to over 400, a large increase due primarily to the extension of the central computer facilities to the entire nuclear physics community in the country. Thirty-four research groups in other fields, selected by the Atlas Laboratory, also make extensive use of the machine.

Introducing this large number of new users to the system has been one of the main tasks of User Support this year. New administrative procedures have been introduced to cope with the increased job throughput.

Representatives within each User Group now act as focal points for all matters relating to the central computer. Informal contacts have usually enabled problems to be solved quickly, to the benefit of both users and operations staff, while quarterly meetings of Group Representatives and User Support provide a forum for ideas and developments to be discussed.

In view of the increasing number of work stations and remote terminals being linked to the central computer, a programme of visits to various Universities was arranged. These allowed an exchange of information of benefit to the new users and to User Support for future planning.

The larger and more widely spread band of users has meant that a more formal registration and accounting system was needed. Part of this need has been met by the introduction of COPPER during the year. It was also decided to write programs to gather more information about each job passing through the computer, particularly about usage of magnetic tapes and disks. This will be of considerable value in forward planning, spotting potential bottlenecks, etc. User Support also took on responsibility for allocating and controlling space available in the ELECTRIC file handling system and MUGWUMP graphics facilities.

Program Advisers are regularly available five hours daily and have dealt with an estimated 2500 queries about all aspects of computing on the IBM 370/195 system. Sometimes these show that further software facilities are needed, and several improvements (particularly of handling magnetic tapes) have been made in consequence.

A thorough overhaul of the Rutherford Subroutine Library is in progress. It is hoped to bring all subroutines up to date, and provide full documentation.

Documentation most important to users has been kept under continuing review. The nucleus of a reference library has been created in the computer area, to serve both users and systems or operations staff, and it is intended to extend this facility and keep it up to date.

A course of lectures was given at the Laboratory on Job Control Language, to help familiarise people with a rather awkward topic. The fortnightly series 'Seminars on Computing' continued throughout the year.

*Accounting*

*Program Advice and Technical Assistance*

*Information Dissemination (ref. 266)*

## FILM ANALYSIS

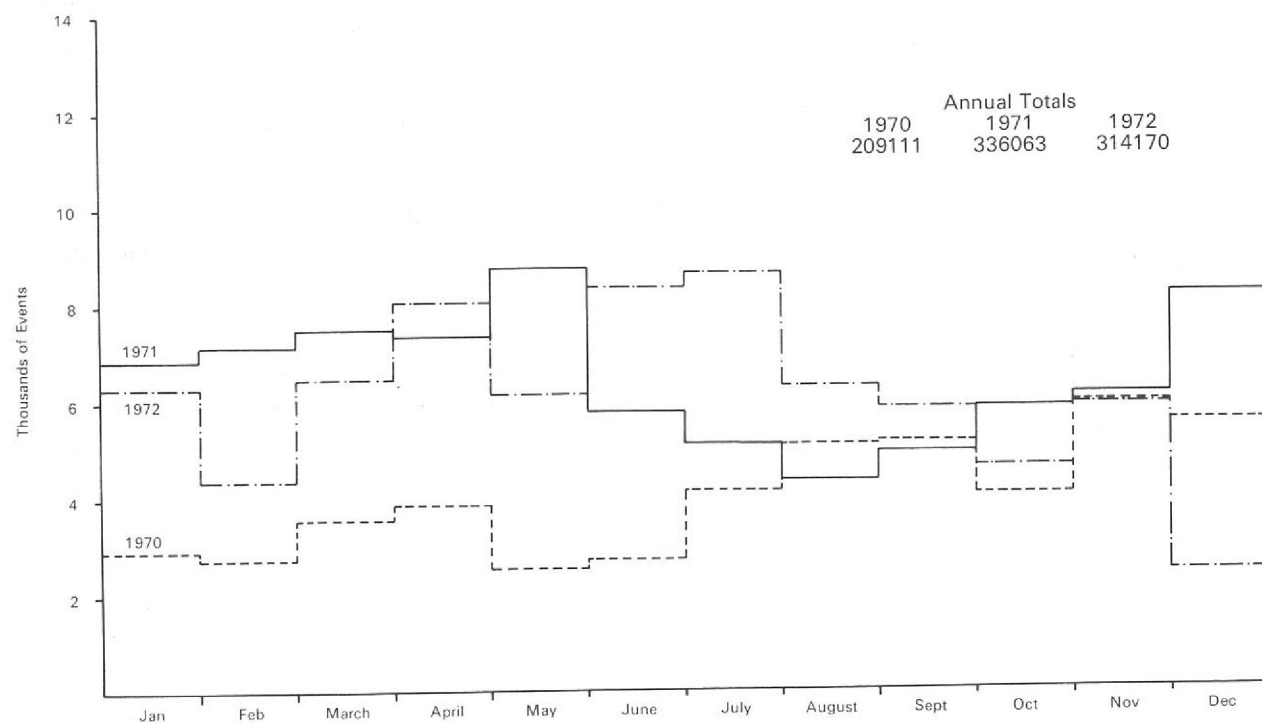
**HPD1** The machine was used exclusively for measuring film from the CERN 2-metre bubble chamber, though, with a view to more flexible scheduling, some tests were carried out on reverse-developed 35 mm film from the K13C spark chamber experiment. A total of 314,000 events was measured, from three experiments as follows:

High Energy $K^-p$ (14 GeV/c)	66,000
Low Energy $K^-p$ (1.0 to 1.4 GeV/c)	127,000
$\pi^+$ -deuterium (4 GeV/c)	121,000
	<u>314,000</u>

These figures are all for three-view events, and include remeasurements of some which failed GEOMETRY reconstruction tests. Nearly all of the film taken for these experiments before mid-1972 has now been measured and, where necessary, re-measured. However, in the second half of the year more film was taken for each experiment. There were periods when the machine was unused because no film was available, and the actual measuring time was practically the same as last year's, at 3700 hours or 42% of the year. The weekly average of events for each month of the year is shown in Figure 103, which includes corresponding information for 1970 and 1971.

The figure given for  $\pi^+$ -deuterium includes 4000 events pre-digitised at Durham University, where the Bubble Chamber Group is collaborating with Birmingham University and the Rutherford Laboratory on this experiment. It is expected that next year more film pre-digitised by groups outside will be measured on the Laboratory's HPD's.

Figure 103. Average weekly totals of events measured on HPD 1 during 1972 (1970 and 1971 results are shown for comparison).



Hardware developments include an improved film gate which holds the film flatter, and changes to the hydraulic system logic. The on-line control program has been modified in accordance with some of the new facilities available at the central computer. Thus advantage has been taken of the fast IBM 2305 Fixed Head File to decrease the core requirements by more extensive over-laying. This has cut the requirement from 186 K bytes to 136 K bytes, a valuable saving for this long-running program, and there is no significant deterioration in performance. The large type 3330 disk-packs have also proved useful, as they enable larger 'batches' of events to be measured before changing the disk or film.

Another short test was made for the Minimum Guidance system of pre-digitising, but a change of plan during this year has focused attention on Reduced Guidance (described under 'Data Analysis Software' below) for which some tests have been made.

A large part of the year was spent in bringing HPD2 up to a production standard for the ISR and S104 spark chamber experiments. By the end of the year nearly 70,000 events on ISR film had been measured, mostly by computer operations staff.

HPD2

**Film Transport.** A high performance universal film transport system was introduced, offering readily interchangeable spools and adaptors for 35, 50 and 70 mm perforated or unperforated film, wound on spark chamber, CERN 100m or CERN 300 m spools. The brenner mark frame indexing system was shown to have good tolerance to the range of mark irregularities in a sample of 100 rolls of film. The overall performance was optimized to position a frame within 1.2 seconds, a significant improvement over previous systems, and this has enabled HPD2 to achieve high measuring rates. This system is to be manufactured commercially for use by other HPD groups.

**Digitising Electronics.** The spot digitising hardware was improved by introducing 5 MHz bandwidth signal processing electronics, and further attention was devoted to some aspects of the logic. A start was made on the improved and additional electronics required for BEBC and other bubble chamber measuring.

**Laser.** The laser and optical system caused some problems in signal stability. These were overcome by a series of mechanical assembly improvements and, particularly, by changing the laser ion tube. This tube had supported the development work for over two years, and had aged.

**Software Changes for New Film.** As the experimental and operational program advanced, detailed software changes became necessary, and problems arose in introducing particular spark chamber requirements into established bubble chamber programs. For example, the use of a simple binary code for the picture number, and the introduction of track width information (in addition to the usual track centre coordinate) demanded some changes. Experimental problems at the ISR, for example in producing reliable binary numbers, further compounded these difficulties. However, as production measurement revealed the problems, they were solved and the system entered into high speed production.

**On Line Control System.** Improvements to the DAEDALUS 516 System continued, particularly as the work built up. Relatively little development was done on the DDP-516 control program, and together with DAEDALUS-516 the first operating control software (HPD OPS 1.0) was released. Although not entirely error-free, it has supported the production work with little modification.

**Measurement.** Work on the photographic techniques required to produce optimum film quality for an HPD was successfully concluded. A simple quantitative method of determining the exposure and development conditions was evolved and used in subsequent film preparation. Signal amplitudes at the HPD2 were generally increased by at least a factor of two, resulting in much improved track detection.

During the summer an initial sample of 4000 ISR events was measured semi-automatically (the scantape, from which the HPD control program derives basic control information, was not then available from the experiment). The measured frames were used to produce sample results, which were presented at the XVIth International Conference on High Energy Physics, Batavia, in September. This represented the first contribution of HPD2 to physics at the Rutherford Laboratory.

A break in the physics programme provided an opportunity for correcting a few hardware problems and for some minor developments and consolidation. This work was successfully carried out and, over the last three months of the year, the HPD2 was regularly scheduled for fully automatic production measurement of the ISR and S104 experiments. The resultant significant increase in measurement (see Figure 104), took the HPD2/DDP516 project from a predominantly system development phase to an operational status.

In total, approximately 70,000 events were measured during the year at an average rate of 200 events per scheduled hour. However, for individual rolls of 1500 events measuring rates of nearly 800 events/hour have been achieved. This is close to the theoretical limit for HPD2 with this experiment (and is between two and three times the speed of HPD1). The lower average figure shows the effect of various machine and software problems, and problems arising from the new film.

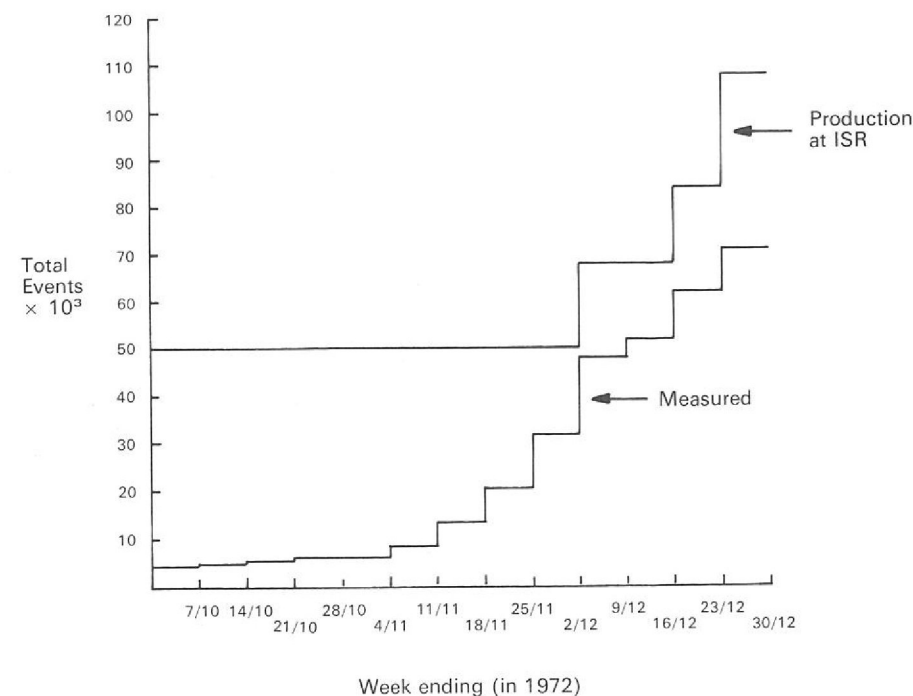
#### Tandem HPD Complex

Towards the end of the year, plans were made to upgrade HPD1 to the standard of HPD2 and to operate it in tandem with HPD2 on the DDP516. A modest start to this programme of work was made.

#### CYCLOPS

Testing and pre-production measuring has been carried out for two spark chamber experiments during the year. It was decided to adopt a common output format for digitising from CYCLOPS and the HPD's, to facilitate measuring and subsequent off-line processing. This has been achieved by modifying the CYCLOPS on-line control program to find fiducial mark centres during measurement, which is desirable for its own sake, and extending the operator commands to allow greater control over automatic measurement and provide improved testing facilities and automatic recovery from various fault conditions.

Figure 104. Initial performance of HPD2



A few thousand events from the Oxford University experiment (K10S) were measured in the first half of the year, enabling the on-line control program to be 'tuned' for the experiment, but pre-scanned film was not available in quantity for production measuring this year. Similar testing and development of the on-line control program for measurement of film from the Cambridge University/Rutherford Laboratory experiment (K13C) was carried out during the first half of the year and an extended pre-production run made in the Autumn. This was intended to train or re-train operators (after eighteen months during which CYCLOPS had been largely idle) and feed back measurement information, both for deciding on film density and contrast and for checking measurement quality.

Detailed checking revealed some hardware faults, in particular that measured widths and even coordinates were occasionally wrong, and difficulties in automatic running showed that the machine needed overhauling. With a lot of measuring in prospect, it was decided to change the cathode ray tube, which had served for six years but had become seriously burnt, and check out the whole machine. This programme of work should be completed early next year.

This display was again used exclusively for 'patching-up' faulty tracks in bubble chamber film measurements made with the HPD road guidance system. In all, tracks from some 80,000 events were examined during the year, of which just over 55,000 were successfully treated and subsequently satisfied geometrical reconstruction criteria.

IDI Display and Light Pen

At the beginning of the year the IDI control program resident in the central computer occupied 116 K bytes of core. As the program may be in use for up to 40 hours per week (actually 1400 hours were used in the year) any possible reduction of this was to be welcomed. With the arrival of the fast type 3330 disks the data structure in the program was re-arranged and it proved possible to reduce the program to 72 K bytes of core, without significantly degrading its performance.

#### DATA ANALYSIS SOFTWARE

**Road Guidance.** Nearly one million events have now been measured on HPD1 in the Road Guidance mode, and little work in the programming chain is now required for the analysis of these events. Some modifications have been made in the treatment of short tracks and tracks with points in both HPD scans. Improvements have also been made to the method of fitting ionisation calculated for each kinematic hypothesis to the HPD bubble density measurements.

Bubble Chambers

**Minimum and Reduced Guidance.** Work on the Minimum Guidance system of measurement began three or four years ago using the filter program developed in collaboration with CERN. Although initial results seemed promising, with a pass rate of 60-70%, the results from later samples revealed problems, e.g. in a high energy experiment the outgoing tracks may not separate until a considerable distance from vertex, and in some samples the pass rate dropped to 40-45%. Thus it was decided to concentrate on a reduced guidance form of pre-measurement in which one fiducial, each vertex, and a point in a clear region on each track are digitised by the operator. Tests show that there is a 50% increase over road guidance in digitising rate for this form of measurement. It is intended that reduced guidance will be the system used in HPD measurement of film from large bubble chambers.

The minimum guidance filter program is being adapted to establish tracks at clear points instead of the vertex, and preliminary results show that few unwanted tracks are picked up by the program. Also, the CPU time per event is about two-thirds that of the basic minimum guidance program.

**Track Sensitive Target.** The Rutherford Laboratory geometry program has been modified to reconstruct events from experiments using the track sensitive target in the 1.5 metre bubble chamber. This work is almost complete, and events can be successfully identified by the kinematics program.

**Spark Chambers.** A common output format has been established for digitisings from HPD and CYCLOPS, so that either machine can be used to measure film from spark chamber experiments, and the off-line analysis programs can then process the data irrespective of which was used.

**Spark and Track Reconstruction.** The program which reads output tapes from the measuring machines and converts the digitisings to spark images on the film is now operational. Subsequent processing depends on the experiment and type of film produced: in some cases the spark images are well separated, while in others they are close to each other or even run together. The ISR experiment is of the first type, with well separated sparks, and the processing program can link the sparks in two dimensions and thereby follow tracks in two dimensions, finally combining the stereoscopic views to give three-dimensional geometrical information. Events from the K13C experiment are of more complicated topology, with the sparks often very close together. In view of the ambiguities in track-following in two dimensions, it is planned to use the stereoscopic views to establish sparks in three dimensions, and then link the sparks to form three-dimensional tracks.

**Programs for Omega.** The CERN off-line program suite ('ROMEO') for experiments at the Omega magnet facility has been adapted to run on the IBM 370/195 central computer. The suite comprises event simulation, pattern (i.e. spark and track) recognition and geometry sections, and the new version will allow the bulk of the data taken in the Glasgow University and Birmingham University/Rutherford Laboratory/Westfield College Omega experiments to be analysed at the Rutherford Laboratory.

A version of the Rutherford Laboratory bubble chamber kinematics program has been prepared for experiments on Omega. It is available for general use on the CII 10070 computer at CERN.



A party of visitors in the Exhibition Area (12978)

TECHNICAL AND

# Technical Services and Administration

## RADIATION PROTECTION

*Personal Dosimetry*  
(ref. 253)

The total number of persons at the Laboratory issued regularly with some kind of personal dosimeter was 730 in 1972 compared with 780 in 1971. The personnel engaged in the maintenance and repair of Nimrod are the most heavily exposed group at the Laboratory although none are expected to exceed the annual permitted limit. Proposed increases in Nimrod's beam intensity will clearly aggravate this problem which will need close co-operation between health physics staff, designers and the maintenance staff themselves if acceptable exposure levels are to be maintained.

There have been no significant technical developments in this field but a preliminary investigation has been made of the possible application of the effect of radiation on thermoelectrets ("permanent" electrostatic dipoles). In principle, inexpensive plastic film could make a sensitive tissue-equivalent dosimeter suitable for mixed radiation fields such as accelerator prompt leakage radiation, but it is not yet clear whether this technique is capable of achieving the reliability and accuracy required for practical use.

*Shielding*  
(ref. 281, 282)

The Group continues to give advice on all aspects of shielding; in particular, specifications have been produced for the 70 MeV injector.

There are indications that in some areas the quantity of shielding required around extracted beam blockhouses may be dictated by experimental background counting rates rather than health physics considerations.

*Investigations*  
(ref. 254)

A comprehensive survey has been made of the responses of a number of standard survey instruments to low activities of typical mixtures of accelerator induced nuclides. Because many instruments have a low counting efficiency for these nuclides (which mainly decay by electron capture) great care is needed to detect loose surface contamination and airborne dust activities at levels around the maximum permitted.

Comparisons have been made between measured and predicted levels of induced activity for a number of irradiation conditions. Good agreement has been found between experimental measurements and fairly simple methods of prediction developed at CERN.

Both the above investigations have been facilitated by further improvements in methods of data processing for gamma-ray analysis of the complex mixtures of nuclides arising from high energy irradiation.

## GENERAL SAFETY

The prevention of accidents depends upon several factors which include the awareness of individuals to possible hazards associated with their work and how to avoid them. A continuous and significant function of the Safety Group is to communicate appropriate information.

The work of the Laboratory involves new and sophisticated apparatus and techniques, occasionally with unknown hazards. Established safety arrangements may be inappropriate and discussion and involvement from the design stage through to commissioning and operation are essential in order to minimise risks. A particular instance of this was the successful liquid oxygen target for the  $\pi 10$  Beam Line.

Considerable effort was given during the first half of the year to the Basic Safety Training Course. About 90% of staff have now attended one of the 24 sessions given since its introduction in 1971. An illustrated booklet summarising the course was produced in conjunction with the Radiation Protection Group and issued to all who attended. The course programme of synchronised slides and pre-recorded commentary on the subjects of Manual Handling, First Aid and Radiation Protection may be of interest to other establishments. A large majority of those who attended have also received supplementary practical training.

Safety Tours continued on a regular basis as an executive responsibility under the overall direction of the Safety Committee. These covered the entire Laboratory twice during the year. In addition to professional safety staff, one member of the Safety Committee attended each tour on a rota basis. The Tours have resulted in improved housekeeping and the spotting of potential hazards which have been rectified with the minimum of delay.

The number of items registered for periodic inspection increased during 1972 to a total of 4738. The rate of increase was 2.4% against the 1971 increase of 5%. During the year the Group acquired a Crane Weighing Machine with a capacity of 45,000 kg; this has been put to good use particularly for verifying the design weight of assembled equipment and for weighing apparatus for transit to CERN. The total of registered items is as follows with the 1971 total in brackets: Lifting tackle 2600 (2508), Pressure Vessels 890 (892), High Voltage Equipment 385 (408), Lifting Machines 396 (387), Safety Valves 268 (239), Breathing Apparatus and Safety Equipment 147 (147) and Fire Prevention 52 (51). The total number of inspections of registered items carried out during 1972 was 7524 (1971 total 8091).

Several new Safety Codes were published during the year. One of these specified formal authorisation of persons concerned with mechanical lifting operations and the Group carries this out in conjunction with local supervision. Publicity of existing and new hazards continued to be given by means of displays and "Safety News" sheets.

During 1972 a total of 94 (1971-107) injuries involving Laboratory staff were reported, 13 (10) of these resulted in lost time, the average absence of the latter being 10.2 (43.8) days. There were no significant trends compared with previous years and causes of the injuries were in the following categories:

Handling goods	24
Stepping on or striking against objects	11
Falls of persons	22
Use of hand tools	8
Machinery	11
Falls of objects	8
Electric shock	0
Miscellaneous	10

Accident Frequency Rates: expressed as the number of injuries per 100,000 man hours worked (100,000 man hours is an approximate working lifetime), these were: all-injury frequency rate 3.5 (3.9), lost-time frequency rate 0.49 (0.36).

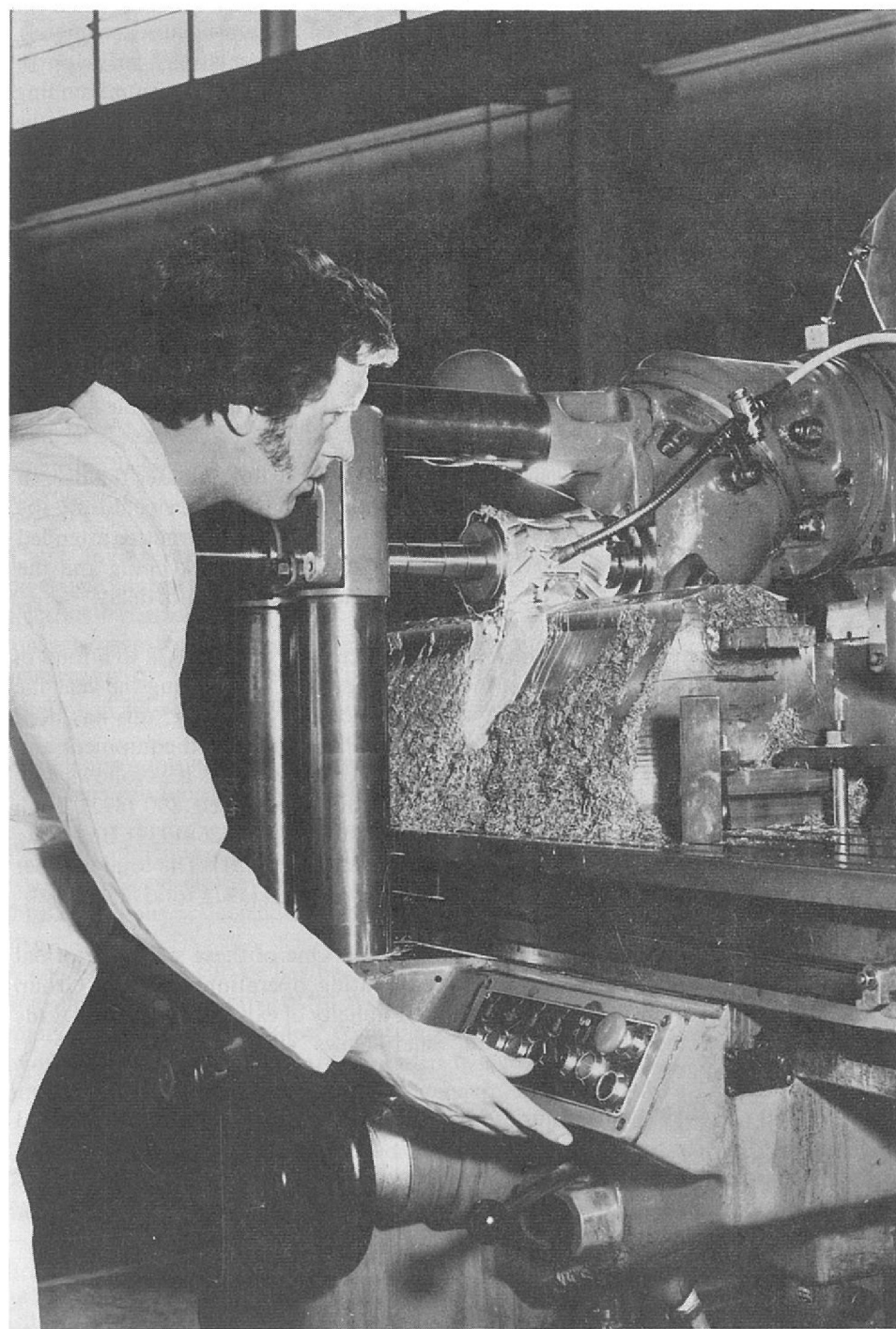


Figure 105. Milling the profile of a pole piece for a quadrupole magnet (12965).

#### ENGINEERING SERVICES

##### *Mechanical Manufacture*

During 1972 over 1000 jobs were placed on outside contractors to a value of over £200,000. R9 workshop was involved in approximately 800 jobs including the manufacture of a Low Temperature Bearing Test Rig and the manufacture and installation (at CERN) of High Flux Pulsed Magnets.

Track analysis machine section had an increasingly busy year with operational improvements to the 30 machines in use, including the design, manufacture and commissioning of interface units to prepare spark chamber digitisers for on line operation on the DDP 516 computer and the establishment of a new 3 machine scanning laboratory to be used initially on the ISR experiment spark chamber film. Two "BESSY" machines designed specifically for use with 70 mm film from the Big European Bubble Chamber (BEBC) have been installed in an extension to the scanning laboratory suite. The digitisers have been installed and the interface units are complete and connection to the IBM 1130 computer will follow shortly. This section has also undertaken increasing responsibility for the production, running and maintenance of the HPD1 machine.

##### *Track Analysis Machines*

During the year 101 new designs of printed circuit boards were produced, involving 412 drawings, including the artwork, with the trend to increasing complexity continuing. Electronics manufacturing section has completed work to the value of £160,000 during the year including component costs, 50% being done off site. A quarter of the in-house work has been done by the printed circuit board assembly line with ladies working part-time; over 150 jobs ranging from single boards to 100-off and including several using wire-wrap terminations were completed. The prototype workshop completed 212 jobs ranging from a few man hours to 6 man months. Much of the work has been directed to the supply of equipment for use on Nimrod and beam line experiments. Six racks of electronics were made for the Nimbus radiometer test and calibration equipment.

##### *Electronic Design and Manufacture*

The Electronic Instrument Loan Pool continued to function as a site service with 540 issues from the 500 instruments in the Pool. Electronic and Instrument repair section handled over 2500 items for repair, calibration, first line servicing and "on call" breakdown investigations; 20% of this total was repaired by specialist firms.

#### SCIENCE RESEARCH COUNCIL WORKS UNIT

On 1 April 1972 the Council Works Unit (CWU) was set up to provide a consulting engineering service and undertake new works, alterations and additions to general service plant and buildings. The Establishments covered are as follows:

- Atlas Computer Laboratory
- London Office
- RGO, Slough
- RSRS, Herstmonceux
- Rutherford Laboratory

The following major works were progressed from initial proposals to the stage where tenders had been invited for the main Building and Civil contract:

**Library Building—Rutherford Laboratory** Comprising a Reading Room built as a single storey on a re-inforced concrete bridge with supporting pillars, and a two storey block to contain a Library Stock Room, Offices, Conference Room and ventilating plant room, the whole built between and forming a connecting link to two existing buildings. The building will form an architectural feature in the Laboratory. The total floor area is approximately 820 m<sup>2</sup>.

**A4 Building—Atlas** An extension linking two main buildings together at first and second floor level with a single storey small Lecture Theatre on the ground floor and an associated entrance hall. Total floor area is approximate 600 m<sup>2</sup>.

**Injector Building—Rutherford Laboratory** A single storey building to be built alongside and integral with an existing reinforced concrete building which at present is covered by a chalk mound. A preparatory contract will be placed separately to remove the bulk of the unwanted mounding. The work involves construction of a reinforced concrete retaining wall and a tunnel in open cut, and the subsequent remounding of this part of the works. The single storey building will be of steel frame construction with provision for overhead travelling cranes on a concrete floor slab with service trenches, brick or asbestos sheet infill panels and metal deck roofing suitably covered. The work also includes the necessary service roads and drains. The total floor area is approximately 900 m<sup>2</sup>.

The following works each costing over £10,000 were proceeding:

**A8 Stores Extension—Atlas Computer Laboratory** This extension is of load bearing brick walls with structural steel roof covered with wood wool slabs and felt. Heating is provided by hot water radiators. The total floor area is approximately 280 m<sup>2</sup>.

**Oxford Street Premises—London Office** Renovations and alterations to existing premises for office accommodation.

The number of jobs, each over £1,000 in value, handled for each of the Establishments served in addition to the above, was:

Atlas Computer Laboratory	4
RGO, Herstmonceux	2
RSRS, Slough	6
Rutherford Laboratory	20

There were also a large number of small jobs at the various Establishments under £1000 in value in which the CWU was involved.

#### ADMINISTRATION

**CERN** An Administration Office has been set up in CERN, staffed by a member of General Administration Group, to assist the Rutherford and Daresbury experimental teams working there.

**Office Services** The increased volume and quality of work undertaken by the inplant Reprographic Section since its re-organisation in 1970 has been maintained in the current year and all target dates have been met. There has been a greater changeover than usual in typing and secretarial staff during the year but the resultant difficulties have been overcome.

**Finance** The Laboratory expenditure (financial year 1972/73) was £8.35 million, of which £0.90 million was for capital items (including final payments on the new IBM 370/195 computer amounting to nearly £0.25 million) and £7.45 million was recurrent. Corresponding figures for 1971/72 were £10.5 million, £3.7 million and £6.8 million. Purchase and usage of the 370/195 computer led to a reduction of expenditure on computer rental of more than £200,000 for this year compared with 1971/72.

A brief analysis of the net expenditure is given below, with corresponding figures for the previous year shown in brackets.

	£ million	
Staff expenditure (salaries and wages, insurance, superannuation, etc.)	3.60	(3.26)
Research and development (see below)	3.85	(3.80)
Plant and equipment	0.82	(3.30)
Building works	0.08	(0.14)
<b>Total</b>	<b>8.35</b>	<b>(10.50)</b>

A proportional representation of the breakdown of the R and D expenditure into divisional and the other main components is shown in the pie chart (Figure 106).

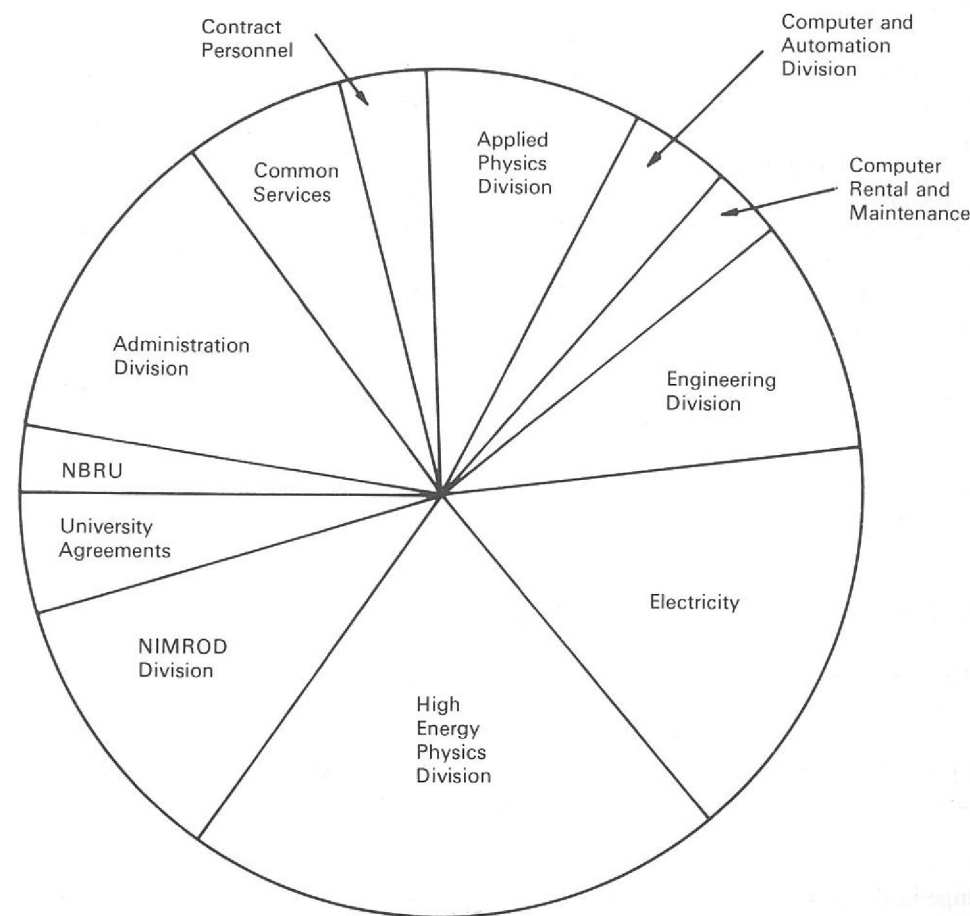


Figure 106. Breakdown of the £3.85 million R and D expenditure.

**Table 10**

Staff Numbers 1972

The staff position at the beginning and end of the year.

	Opening Strength 1.1.72	Changes during 1972		Closing Strength 31.12.72
		Gains	Losses	
<b>PROFESSIONAL</b>				
Senior and Banded Staff	25	0	0	25
Science Group	242.5	20	15	247.5
Research Associates	56	25	27	54
*Engineers I, II, III	104	0	4	100
*ADE	4	0	0	4
<b>Total Professional</b>	<b>431.5</b>	<b>45</b>	<b>46</b>	<b>430.5</b>
<b>ANCILLARY</b>				
*Draughtsmen	42	4	2	44
*Technical class	189	4	4	189
Non-Techs. and Stores	42	1	1	42
Administrative	29	2	1	30
Librarian	1	0	0	1
Clerical	44	11	9	46
Secretarial and Typing	28.5	9.5	11	27
Photographers	4	0	1	3
Photoprinters	5	0	0	5
Machine Operators	62.5	12.5	11.5	63.5
Hostel Manageress	2	0	0	2
Telephone Operators	2	1	1	2
<b>Total Ancillary</b>	<b>451</b>	<b>45</b>	<b>41.5</b>	<b>454.5</b>
<b>INDUSTRIAL</b>				
Craft	181.5	8	17	172.5
Non-craft	128	13	24	117
Apprentices	29	5	11	23
<b>Total Industrial</b>	<b>338.5</b>	<b>26</b>	<b>52</b>	<b>312.5</b>
<b>GRAND TOTALS</b>	<b>1221</b>	<b>116</b>	<b>139.5</b>	<b>1197.5</b>

The figures listed under "changes" include new entrants, resignations and promotions. Staff on sandwich courses, and those working part-time are counted as half.

Staff Structure

A change in the staff structure resulted in the merger, as from 1 January, of the Engineer, Chemist, Draughtsman and Technical Classes into the Professional and Technology Group. For comparison purposes they are shown asterisked under their former titles in the above table.

The Local Joint Consultative Committee continued to meet at regular intervals and to provide effective communications between management and Industrial staff.

Staff Relations

The Joint Consultative Productivity Committee met twice in the early part of the year; the local divisional productivity committees continued to meet regularly and to provide a forum for an exchange of ideas between staff and divisional management.

The Local Whitley Committee met regularly during the year. Four full meetings were held including the Annual Meeting chaired by the Director in June; in addition special meetings of the full Committee and its sub-committees were held to discuss in detail problems affecting staff conditions. The most important topic discussed was the current work and future programme of the Laboratory, particularly the consequences of the Government's decision not to proceed with the construction of the proposed High Flux Beam Reactor but instead to participate on equal terms with the Franco-German reactor collaboration at the Institut Laue-Langevin, Grenoble. Useful and constructive discussions were also held on a wide variety of matters including accommodation standards, safety, staff training and suggestion schemes.

Day-release and evening training in the Rutherford Laboratory has continued to decline during the academic year 1971-72 as a result of the continuing low recruitment rate, but the examination pass-rate has remained very high. Attendance at short courses increased by about 30% compared with 1970-71, largely as a result of a series of three internal metrication courses for engineers and designers. Full-time training also declined but the overall level of apprentice training was maintained.

Training

The total number of part-time concessions awarded was 99, about 8% of the total staff of the Laboratory compared with 11% last year. The 84 students who sat examinations achieved an overall pass-rate of 87%, compared with 77% last year and with the national average of 60-70% for this kind of examination.

The main source of internal short courses used by Laboratory staff has been the AERE Education and Training Department, but the proportion has fallen somewhat to about 60% of the total. As in previous years the Laboratory provided a number of specialist lecturers for some of the technical courses run by AERE. The Laboratory has made extensive use of the SRC management courses and staff attended other short courses run by a wide range of Universities, Polytechnics, Technical Colleges, Research Associations, professional bodies and commercial organisations.

The Laboratory has continued its collaboration with AERE in the Apprentice Training Scheme. There were 28 Craft Apprentices, Student Engineers and Graduate Engineers in the scheme at the beginning of the academic year and this number had fallen to 23 by August 1972. Three Graduate Engineers and two Craft Apprentices completed their "time" during the year.

The major internal training activity was the provision of three two-day Metrication Courses attended by about 150 members of staff engaged in engineering design. These courses were held during the Spring in readiness for design work in the Laboratory "going metric" on 1 May 1972. The Laboratory again acted as host establishment for two SRC Central Induction Courses which were held in December 1971.

The Laboratory provided industrial training during the academic year for 52 college-based sandwich course students, the highest annual total to date. The overall number of such students trained in the Laboratory during the last twelve years is now 367. The majority of the students this year were studying Applied Physics, but some were studying Applied Mathematics, Computer Science, Electrical Engineering (Electronics) or Applied Chemistry and one was studying Mechanical Engineering.

*Conferences* The Laboratory was responsible for the organisation of the 4th International Conference on High Energy Collisions (Stony Brook Series). It took place at St Catherine's College, Oxford, 5-7 April. Participants numbered 237, of whom the vast majority were accommodated at the College. The Proceedings have been published by the Laboratory.

The annual Theoretical High Energy Physics gathering took place from 5-7 January. Two Summer Schools were organised, both dealing with HEP theory. The first (3-14 July) was for postgraduate students of experimental physics, while the second (4-22 September) was for budding theoreticians. There were also two Cosener's House weekend meetings during the year, on Proportional Wire Chambers (3-4 June) and on Gauge Theories of Unified Weak and Electromagnetic Interactions (11-12 November).

*Visits* The Nuclear Physics Board held its November meeting at the Laboratory, and were shown examples of the Laboratory's work on the preceding afternoon. Parties of visitors during the year totalled 540, substantially fewer than usual due to the overriding demand for manpower made by the Stony Brook Conference and other commitments.

*Physics Exhibition* The Laboratory showed six items at the Physics Exhibition in London, 13-16 March. Data acquisition from spark chambers by means of television cameras (vidicons) was demonstrated, and there were two exhibits connected with particle beams—the wire electrode d.c. separator and the superconducting r.f. separator. Magnet technology was once again well represented, with displays on thin septa, mineral insulation and epoxy resins for superconducting coils.

The Rutherford Laboratory stand was one of those visited by Mrs Margaret Thatcher MP, Secretary of State for Education and Science, during her tour of the Exhibition.



Figure 107. Mrs. Margaret Thatcher, MP, Secretary of State for Education and Science talking to Laboratory personnel at the Physics Exhibition (10900).

PUBLICATIONS  
AND LECTURES



Using a reader-printer for microfilms (12979)

PUBLICATIONS  
AND LECTURES

## List of Publications

### JOURNAL ARTICLES

- 1 ALLARDYCE B. W., BATTY C. J., BAUGH D. J., FRIEDMAN E., HEYMANN G., WEIL J. L., CAGE M. E., PYLE G. J., SQUIER G. T. A., CLOUGH A. S., COX J., JACKSON D. F., MURUGESU S., RAJARATNAM V.  
Ratio of pion-nucleus reaction cross-sections and the neutron density distribution for lead.  
Phys. Lett., **41B** (5) 577 (October 1972), preprinted as RPP/NS8.
- 2 ANSORGE R. E., BAKER R. D., KRZESINSKI A. E. S., NEALE W. W., RUSHBROOKE J. G., STREET G. S. B.  
A study of electromagnetic processes at 1 GeV/c in a hydrogen bubble chamber and production rate limits for new low-mass particles.  
Phys. Rev., **D7** (1) 26 (January 1973).
- 3 AYRES J. F., COLEMAN T. G., DAMERELL A. R., FISHER C. M., FITZHARRIS E. W., FOSTER J. H., GOTTFELDT P., MACK B., MORTIMER A. R., SEAGER P., STOKOE J. R., WILLIAMS P. R., LEUTZ H., TISCHHAUSER J., WENNIGER H.  
The operation of a track sensitive hydrogen target in a 500 litre hydrogen bubble chamber.  
Nucl. Instrum. Meth., **107** (1) 131 (February 1973), preprinted as RPP/N26.
- 4 BAKER S. L., DORNAN P. J., GOPAL G. P., STARK J., WEBSTER G. J., BUCKLEY T. S., BULL V. A., TAYLER V., TOWNSEND D. W., WHITE A.  
Single pion production in  $\pi^+p$  interactions at 895, 945, 995 and 1040 MeV/c  
Nucl. Phys., **B41** (1) 91 (May 1972).
- 5 BARGER V., PHILLIPS R. J. N.  
Rival models for total cross-sections.  
Nucl. Phys., **B40**, 205 (April 1972).
- 6 BARGER V., PHILLIPS R. J. N.  
Shackles on linear absorption models.  
Phys. Lett., **42B** (4) 479 (December 1972), preprinted as RPP/T23.
- 7 BARGER V., PHILLIPS R. J. N., GEER K.  
pp slope break and the Pomeron periphery.  
Nucl. Phys., **B47** (1) 29 (October 1972), preprinted as RPP/T12.
- 8 BEILLIERE P., MAYEUR C., PEETERS P., WILQUET G., GUY J. G., KNIGHT W. L., TOVEY S. N.  
The  $\Lambda^0 p$  invariant mass spectrum in  $K^-$  - nucleus interactions.  
Phys. Lett.,
- 9 BEILLIERE P., MAYEUR C., WILQUET G., FLIAGINE V. B., GUY J. G., KNIGHT W. L., TOVEY S. N., ARMENIAN H. K., GOVAN M., SCHNEPS J., WOLSKY G., AZEMOON T., MILLER D. J., NASSALSKI J.  
An enhancement in the  $\Lambda\Lambda$  invariant mass spectrum.  
Phys. Lett., **39B** (5) 671 (May 1972).
- 10 BELLAMY E. H., ANDERSON J., CRAWFORD J. F., OSMON P. E., STRONG J. A., VICKERY R. P., WALKER R. N. F., LIPMAN N. H., UTO H., WALKER T. G., MONTGOMERY T. A., SOLOMONIDES C. M.  
Polarization in the reaction  $\pi^+p \rightarrow K^+\Sigma^+$  at 1.11 GeV/c.  
Phys. Lett., **39B** (2) 299 (April 1972), preprinted as RPP/H 88.
- 11 BENTLEY K. R., DAVIES J. D., DOWELL J. D., McLEOD C., McMAHON T. J., VAN DER RAAY H. B., RHOADES T. G., WICKENS F. J., DAMERELL C. J. S., HOTCHKISS M. J.  
An automatic spark chamber system with sonic and magnetostrictive read-out.  
Nucl. Instrum. Meth., **104** (2) 299 (October 1972), preprinted as RPP/H84.
- 12 BINNIE D. M., CAMILLERI L., DUANE A., GAR BUTT D. A., HOLMES J. R., JONES W. G., KEYNE J., LEWIS M., SIOTIS I., UPADHYAY P. N., BURTON I. F., McEWAN J. G.,  
Meson mass spectrum near the  $X^0$  (958).  
Phys. Lett., **39B** (2) 275 (April 1972), preprinted as RPP/H91.
- 13 CHAN H. M., MIETTINEN H. I., LAM W. S.  
Factorisation and inclusive photoproduction.  
Phys. Lett., **40B** (1) 112 (June 1972), preprinted as RPP/C42.
- 14 CHAN H. M., MIETTINEN H. I., ROY D. P., HOYER P.  
Regge phenomenology of inclusive spectra in the central region.  
Phys. Lett., **40B** (3) 406 (July 1972), preprinted as RPP/T15.
- 15 CHARLES B. J., COWAN I. M., EDWARDS T. R. M., GIBSON W. M., GILLMAN A. R., GILMORE R. G., GLEDHILL M. H., HUGHES C. M., MALOS J., SMITH V. J., TAPPER R. J., McCARTNEY B., OADES C. G., WARD D. L., WROATH P. D., BECK G. A., COUPLAND M., FRANK S. G. F.  
Differential cross-sections for elastic scattering of positive Kaons on protons in the momentum range 0.9 to 1.9 GeV/c.  
Phys. Lett., **40B** (2) 289 (June 1972), preprinted as RPP/H94.
- 16 CHARLESWORTH J. A., INTIZAR N., NEALE W. W., RUSHBROOKE J. G.  
Isospin analysis of exchange mechanisms and  $(\Sigma K) -$  systems in  $NN \rightarrow (\Sigma K)N$  at 6 GeV/c.  
Nucl. Phys., **B48** (1) 225 (November 1972).
- 17 CHARLESWORTH J. A., INTIZAR N., NEALE W. W., RUSHBROOKE J. G.  
Isospin analysis of  $NN \rightarrow (\Lambda K)N$  and comparison of isoscalar and isovector exchange in  $NN \rightarrow (YK)N$  at 6 GeV/c  
Nucl. Phys., **B51**, 488 (January 1973).
- 18 COHEN-TANNOUJJI G., LACAZE R., HENYEV F. S., RICHARDS D., ZAKRZEWSKI W. J., KANE G. L.  
Unitarity, duality and absorption - a general discussion and a definite model.  
Nucl. Phys., **B45** (1) 109 (August 1972), preprinted as DPh-T/72-6 (Saclay).
- 19 COLEMAN T. G., FISHER C. M., FITZHARRIS E. W., FOSTER J. H., GUY J. G. V., WILLIAMS P. R., LEUTZ H., WENNIGER H.  
First physics run with a track sensitive target.  
Nucl. Instrum. Meth., **107** (2) 399 (March 1973), preprinted as RPP/N27.
- 20 CONNOLLY J. F., GILBY A. S.  
A compact EHT power supply for use with high pulse rate spark chambers.  
Nucl. Instrum. Meth., **106** (2) 213 (January 1973), preprinted as RPP/H101.

- 21 COUPLAND J. H., SIMKIN J., RANDLE T. C.  
Very high field synchrotron magnets with iron yokes.  
Nucl. Instrum. Meth., **106** (3) 595 (February 1973), preprinted as RPP/A90.
- 22 CULLIFORD D. R.  
Stabilised power supplies at the Rutherford Laboratory.  
Electron. Power, **18** (4) 133 (April 1972).
- 23 DANYZ J. A., PENNEY B. K., STEWART B. C., THOMPSON G., BRUNET J. M.,  
NARJOUX J. L., ALLEN J. E., JACOBS N. J. D., LEWIS P. H., MARCH P. V.  
 $K^+p$  elastic scattering between 2.11 and 2.72 GeV/c.  
Nucl. Phys., **B42**, 29 (June 1972), preprinted as RPP/H83.
- 24 DAVIDSON R. C., LAWSON J. D.  
Self-consistent Vlasov description of relativistic electron ring equilibria.  
Particle Accel., **4** (1) 1 (October 1972).
- 25 DICK L., JANOUT Z., AOI H., CAVERZASIO C., GONIDEC A., KURODA K.,  
MICHALOWICZ A., POULET M., SILLOU D., ASCHMAN D. G., BOOTH N. E.,  
GREEN K., SPENCER C. M.  
Measurement of the polarization parameter in  $\pi^+p$  backward elastic scattering  
at 6 GeV/c.  
Nucl. Phys., **B43**, 522 (June 1972).
- 26 DRUMMOND I. T., KANE G. L.  
On the interest of polarization in multiparticle processes.  
Nucl. Phys., **B45** (1) 157 (August 1972), preprinted as DAMTP 72/2 (Cambridge).
- 27 ELLIS R. J., BLAIR I. M., TAYLOR A. E., ASTBURY A., AXEN D., KALMUS  
P.I.P., SHERMAN H. J., WILLIAMS D. T., GIBSON W. R., BLOODWORTH I. J.,  
GOUANERE M., MEYER S. L., EFREMENKO V.  
Measurement of the electron asymmetry parameter in the decay of polarized  
 $\Sigma^-$  hyperons  
Nucl. Phys., **B39**, 77 (April 1972), preprinted as RPP/H79.
- 28 ELVEKJAER F.  
Short-range  $\pi N$  P-wave interactions. Comparison with high energy backward  
Regge models.  
Nucl. Phys., **B47** (1) 253 (October 1972), preprinted as RPP/T16.
- 29 ELVEKJAER F., PIETARINEN E.  
An optimised FESR.  
Nucl. Phys., **B45** (2) 621 (August 1972).
- 30 FIALKOWSKI K.  
A simple explanation of correlation data in inclusive pp interactions at high  
energy.  
Phys. Lett., **41B** (3) 379 (October 1972), preprinted as RPP/T28.
- 31 FIALKOWSKI K., MIETTINEN H. I.  
High energy multiplicity distributions and the two component picture of  
particle production.  
Phys. Lett., **43B** (1) 61 (January 1973), preprinted as RPP/T37.
- 32 FROGGATT C. D., MORGAN D.  
Model amplitude analysis of  $\pi^-p \rightarrow \pi^+\pi^-n$ .  
Phys. Lett., **40B** (6) 655 (August 1972), preprinted as CERN-TH-1507.
- 33 FRY J. R., MATTHEWS R., MUIRHEAD H., BRANKIN C., ANGELOPOULOS  
A., APOSTOLAKIS A., THEOCHAROPOULOS P., VASILIADES G., FILIPPAS  
T. A., SIMOPOULOU E., TSILIMIGRAS P., VAYAKI A., BUSCHBECK B.,  
DALLMAN D., OTTER G., SCHMID P., MIETTINEN H. I.  
Differential cross-sections for the reaction  $K^- + p \rightarrow \pi^- + \text{anything}$  and  
predictions of  $\gamma + p \rightarrow \pi^- + \text{anything}$  and  $\pi^- + p \rightarrow \pi^- + \text{anything}$ , based on  
factorisation.  
Nucl. Phys.,
- 34 GABATHULER K., ROHLIN J., DOMINGO J. J., INGRAM C. H. Q., ROHLIN  
S., TANNER N. W.  
Pion production in the reactions  $d(p, \pi^+)t$ ,  ${}^3\text{He}(p, \pi^+){}^4\text{He}$  and  ${}^4\text{He}(p, \pi^+){}^5\text{He}$ .  
Nucl. Phys., **B40**, 32 (April 1972).
- 35 GRESHAM A. T., SHELDON R., STAPLETON G.  
Magnets for radiation-resistant accelerators.  
Particle Accel., **4** (1) 43 (October 1972).
- 36 HARTLEY B. J., KANE G. L.  
An interpretation of the high energy  $\pi N$  scattering amplitudes and data.  
Phys. Lett., **39B** (4) 531 (May 1972), preprinted as ICTP/71/18.
- 37 KAMAL A. N.  
A calculation of the charge radius of the pion.  
Lett. Nuovo Cim., **3** (6) 248 (February 1972), preprinted as RPP/C 32.
- 38 KAMAL A. N.  
On the construction of Fourier-Bessel transforms of scattering amplitudes.  
Lett. Nuovo Cim., **3** (13) 529 (March 1972) and **4** (7) 288 (June 1972) (erratum),  
preprinted as RPP/C 33.
- 39 KANE G. L.  
A simple description of high energy scattering.  
Phys. Lett., **40B** (3) 363 (July 1972), preprinted as RPP/T 14.
- 40 LEVINE G. S., SQUIER D. M., STAPLETON G. B., STEVENSON G. R.,  
GOEBEL K., RANFT J.  
The angular dependence of dose and hadron yields from targets in 8 GeV/c  
and 24 GeV/c extracted proton beams.  
Particle Accel., **3** (2) 91 (April 1972).
- 41 LIPMAN N. H., UTO H., WALKER T. G., MONTGOMERY T. A.,  
SOLOMONIDES C. M., BELLAMY E. H., ANDERSON J., CRAWFORD J. F.,  
OSMON P. E., STRONG J. A., VICKERY R. P., WALKER R. N. F.  
A test of the  $\Delta I = \frac{1}{2}$  rule and the Lee-Sugawara relation in the decay  $\Sigma^+ \rightarrow p\pi^0$ .  
Phys. Lett., **B43** (1) 89 (January 1973), preprinted as RPP/H90.
- 42 LOVE A.  
Testing weak interaction models in  $e^+e^- \rightarrow \mu^+\mu^-$ .  
Lett. Nuovo Cim., **5** (2) 113 (September 1972), preprinted as RPP/T11.
- 43 LOVE A., ROSS G. G., NANOPOULOS D. V.  
Muon-proton scattering and the effect of neutral currents in the scaling region.  
Nucl. Phys., **B49**, 513 (December 1972), preprinted as RPP/T 26.

- 44 MADEN D., ROSNER R. A.  
A multi-terminal interactive graphics system using a small computer.  
Nucl. Instrum. Meth., **104** (2) 375 (October 1972), preprinted as RPP/H93.
- 45 MARCHESI C. J., CLARKE N. M., GRIFFITHS R. J.  
Energy dependence of the  $^3\text{He}$  optical potential.  
Phys. Rev. Lett., **29** (10) 660 (September 1972).
- 46 MARCHESI C. J., GRIFFITHS R. J., CLARKE N. M., PYLE G. J., SQUIER G. T. A., CAGE M. E.  
Optical model analysis of elastic scattering of 53.4 MeV helions from  $^{56}\text{Fe}$ .  
Nucl. Phys., **A191** (3) 627 (September 1972).
- 47 MARTIN A. D., MICHAEL C., PHILLIPS R. J. N.  
Polarization relations in charge and hypercharge exchange reactions.  
Nucl. Phys., **B43**, 13 (June 1972), preprinted as CERN-TH-1436.
- 48 MAYEUR C., VAN BINST P., WILQUET G., FLIAGINE V. B., GUY J. G., KNIGHT W. L., TOVEY S. N., DOWD R. M., GOVAN M., SANDERS A. J., SCHNEPS J., WOLSKY G., AZEMOON T., BARTLEY J., MILLER D. J., STANNARD F. R.  
A measurement of the  $\Xi$  hyperon lifetimes and  $\alpha$  parameters.  
Nucl. Phys., **B47** (2) 333 (October 1972), preprinted as RPP/H99.
- 49 MIETTINEN H. I.  
Factorisation and exchange degeneracy of secondary trajectories in inclusive reactions.  
Phys. Lett., **38B** (6) 431 (March 1972), preprinted as RPP/C 35.
- 50 MIETTINEN H. I., PIRILA P.  
Momentum transfer dependence in diffraction dissociation.  
Phys. Lett., **40B** (1) 127 (June 1972), preprinted as RPP/T9.
- 51 MORGAN D., SHAW G.  
Low energy pion-pion scattering from current algebra; unitarity corrections.  
Nucl. Phys., **B43**, 365 (June 1972), preprinted as DNPL/P 108.
- 52 NIELSEN H., OADES G. C.  
Pion-nucleon partial wave amplitudes in the low energy region and below threshold.  
Nucl. Phys., **B49**, 573 (December 1972)
- 53 NIELSEN H., OADES G. C.  
Consistency between the low energy pion - pion interaction and pion - nucleon scattering.  
Nucl. Phys., **B49**, 586 (December 1972)
- 54 NIELSEN H., OADES G. C.  
 $K^+p$  backward dispersion relations.  
Nucl. Phys., **B41** (2) 525 (May 1972), preprinted as RPP/C 31
- 55 PHILLIPS R. J. N., RINGLAND G. A.  
Regge phenomenology.  
High Energy Physics (Burhop E. H. S., ed.)V, 187 (Academic Press, 1972), preprinted as RPP/C25.
- 56 PHILLIPS R. J. N., RINGLAND G. A., WORDEN R. P.  
Polarization effects in inclusive reactions.  
Phys. Lett., **40B** (2) 239 (June 1972), preprinted as RPP/T13.

- 57 RINGLAND G. A., ROBERTS R. G., ROY D. P., TRAN THANH VAN J.  
A phenomenological prescription for Regge cuts.  
Nucl. Phys., **B44** (2) 395 (July 1972), preprinted as RPP/C39.
- 58 ROBERTS R. G., ROY D. P.  
Nucleon exchange mechanism in the inclusive reaction  $p \rightarrow \pi^+$ .  
Phys. Lett., **38B** (7) 507 (April 1972), preprinted as RPP/C37.
- 59 ROHLIN J., GABATHULER K., TANNER N. W., COX C. R., DOMINGO J. J.  
Pionic proton stripping and  $\pi^-$  production.  
Phys. Lett., **40B** (5) 539 (August 1972).
- 60 ROSS G. G.  
Optimised integral continuation methods.  
Nucl. Phys., **B41** (1) 272 (May 1972), preprinted as RPP/C29.
- 61 ROY D. P., ROBERTS R. G.  
An estimate of Regge cuts from inclusive finite mass sum rules.  
Phys. Lett., **40B** (5) 555 (August 1972), preprinted as RPP/T18.
- 62 ROY D. P., ROBERTS R. G., PHILLIPS R. J. N., MIETTINEN H. I.  
Backward scattering extrapolations and baryon couplings.  
Phys. Rev., **D6** (5) 1317 (September 1972), preprinted as RPP/C 36.
- 63 SACHARIDIS E. J.  
Plastic threshold Cerenkov detectors with wavelength shifter and quencher.  
Nucl. Instrum. Meth., **101** (2) 327 (June 1972) preprinted as RPP/H 89.
- 64 SINHA B. C., EDWARDS V. R. W., BURGE E. J., TAIT W. H.  
Optical model analysis of  $^{92, 94, 96, 100}\text{Mo}$  (p, p) for 20, 30 and 50 MeV incident proton energies.  
Nucl. Phys., **A183** (2) 401 (March 1972).
- 65 STAPLETON G. B., THOMAS R. H.  
Estimation of the induced radioactivity of the ground water system in the neighbourhood of a proposed 300 GeV high energy accelerator situated on a chalk site.  
Health Phys., **23** (5) 689 (November 1972), preprinted as RPP/A83.
- 66 STEWART N. M., GIBSON W. R.  
Triple scattering measurements for the proton deuteron system.  
Nucl. Phys., **A188** (1) 205 (June 1972).
- 67 TROTMAN J. V.  
A program for closed orbit minimisation by analytic technique.  
Comput. Phys. Commun., **5** (1) 56 (January 1973).
- 68 WILLIAMS D. T., BLOODWORTH I. J., EISENHANDLER E., GIBSON W. R., KALMUS P. I. P., LEE CHI KWONG L. C. Y., ARNISON G. T. J., ASTBURY A., GJESDAL S., LILLETHUN E., STAVE B., ULLALAND O., WATKINS I. L.  
Wide angle proton-proton elastic scattering from 1.3 to 3.0 GeV/c.  
Nuovo Cim., **8A** (2) 447 (March 1972), preprinted as RPP/H77.
- 69 WILQUET G., FLIAGINE V. B., GUY J. G., KNIGHT W. L., TOVEY S. N., DOWD R. M., GOVAN M., SANDERS A. J., SCHNEPS J., WOLSKY G., AZEMOON T., BARTLEY J., MILLER D. J., STANNARD F. R.  
The masses of the  $\Xi$  hyperons.  
Phys. Lett., **42B** (3) 372 (December 1972)

- 70 WINSBORROW L. A., THOMAS G. L., COLEMAN C. F., CONLON T. W.  
Deuteron elastic scattering from the tin isotopes at 20 and 27 MeV.  
Nucl. Phys., **A180** (1) 19 (January 1972).
- 71 WOOLLAM P. B., GRIFFITHS R. J., CLARKE N. M.  
Elastic and inelastic scattering of 53.4 MeV helions from  $^{144}\text{Sm}$ .  
Nucl. Phys., **A189** (2) 321 (July 1972).
- 72 WOOLLAM P. B., GRIFFITHS R. J., KINGSTON F. G., FULMER C. B.,  
HAFELE J. C., SCOTT A.  
Analysis of 50.8 MeV proton scattering from the samarium isotopes.  
Nucl. Phys., **A179** (3) 657 (February 1972)
- 73 WORDEN R. P.  
Symmetries of Regge-Regge cuts.  
Phys. Lett., **40B** (2) 260 (June 1972), preprinted as RPP/T8.

#### UNPUBLISHED PREPRINTS

- 74 ASTBURY A.  
A possible explanation for the structures seen in antiproton-proton, nucleon-nucleon and  $\text{K}^+$ -proton total cross-sections.  
RPP/H103.
- 75 BACON T. C., BUTTERWORTH I., MILLER R. J., PHELAN J. J., DONALD  
R. A., EDWARDS D. N., HOWARD D., MOORE R. S.  
 $\bar{p}p$  annihilations into two charged particles near centre-of-mass energy  
2200 MeV.  
RPP/H 86.
- 76 BANDER M.  
Inclusive production off nuclear targets.  
RPP/T 22.
- 77 BARGER V., PHILLIPS R. J. N., GEER K.  
Rising  $d\sigma/dt$  probes pp diffraction mechanisms.  
RPP/T 38.
- 78 BRACHER B. H., MACEWAN J. F., ABBOTT A. G.  
An on-line data collection system for film measurement.  
RPP/H92.
- 79 CHAN H. M., MIETTINEN H. I., ROBERTS R. G.  
Dual properties of inclusive spectra.  
RPP/T40.
- 80 CHARLES B. J., COWAN I. M., EDWARDS T. R. M., GIBSON W. M.,  
GILLMAN A. R., GILMORE R. S., GLEDHILL M. H., HUGHES C. M.,  
MALOS J., SMITH V. J., TAPPER R. J., McCARTNEY B., WARD D. L.,  
WROATH P. D., BECK G. A., COUPLAND M., FRANK S. G. F.  
Measurements of  $\text{K}^+p$  elastic differential cross-sections for Kaon momenta  
between 0.9 and 1.9 GeV/c.  
RPP/H 95.

- 81 CLOUGH A. S., TURNER G. K., ALLARDYCE B. W., BATTY C. J.,  
BAUGH D. J., McDONALD J. D., RIDDLE R. A. J., WATSON L. H.,  
CAGE M. E., PYLE G. J., SQUIER G. T. A.  
Coulomb effects in  $\pi^\pm - \text{C}$  total cross-sections.  
RPP/NS 9.
- 82 COUPLAND J. H.  
Towards the design of superconducting magnets for a proton synchrotron.  
RPP/A 88.
- 83 ELVEKJAER F., INAMI T., RINGLAND G. A.  
Amplitude analysis of  $\pi\text{N}$  charge exchange to large momentum transfers.  
RPP/T 42.
- 84 ELVEKJAER F., PIETARINEN E.  
Optimised FESR applied to  $\pi\text{N}$  charge exchange amplitudes.  
RPP/T 36.
- 85 FIALKOWSKI K.  
Correlation integrals for charged and neutral pions in inclusive production and  
the two-component picture.  
RPP/T 34.
- 86 FIELD J. H.  
Tests of the  $\Delta I \leq 1$  rule in backward photoproduction processes.  
RPP/H 87.
- 87 FUKUGITA M., INAMI T.  
Impact parameter analysis of  $\bar{\text{K}}\text{N}$  and  $\pi\text{N}$  scattering in the intermediate energy  
region.  
RPP/T 32.
- 88 GROOT E. H. de, ZALEWSKI K.  
Uncorrelated jet model predictions for the multiplicity distribution of  $\pi^-$  mesons  
produced in high energy annihilations  $p\bar{p} \rightarrow$  pions.  
RPP/T 24.
- 89 HOYER P., ROBERTS R. G., ROY D. P.  
Duality in Reggeon-particle scattering; baryon-antibaryon and meson-  
baryon channels.  
RPP/T 43.
- 90 HOYER P., ROBERTS R. G., ROY D. P.  
New relations for two-body reactions from inclusive finite mass sum rules.  
RPP/T 35.
- 91 LAM C. S.  
Diffractive models in non-diffractive regions.  
RPP/T 25.
- 92 LEWIS P. H., ALLEN J. E., JACOBS N. J. D., DANYSZ J. A., ISLAM A. K. M. A.,  
MILLER D. B., PENNEY B. K., STEWART B. C., THOMPSON G., BORG A.,  
BRUNET J. M., NARJOUX J. L.  
Four and five body  $\text{K}^+p$  interactions at 2.11, 2.31, 2.53 and 2.72 GeV/c.  
RPP/H 96.

- 93 LITCHFIELD P. J.  
An experimental demonstration of duality in  $K^-p \rightarrow \Lambda\pi, \Lambda\eta$ .  
RPP/H 100.
- 94 LOVE A., NANOPOULOS D. V., ROSS G. G.  
Three triplet realisations of gauge models and deep inelastic scattering.  
RPP/T 39.
- 95 LOVE A., ROSS G. G.  
Neutral weak currents and the proton-neutron mass difference.  
RPP/T 19.
- 96 LOVE A., ROSS G. G.  
Three triplet realisations of gauge models and electromagnetic mass differences.  
RPP/T 33.
- 97 OADES G. C., ZIMMERMANN H.  
KN interactions in the low energy region and below threshold.  
Aarhus University preprint (un-numbered).
- 98 ROY D. P.  
Duality and Regge approach to the inclusive reaction.  
RPP/T 41.
- 99 TAYLOR J. C.  
An introduction to gauge-fields and renormalisable theories of charged vector mesons.  
RPP/T 29.
- 100 ULEHLA I.  
Finite nuclei in many body theory.  
RPP/T 30.
- 101 ULEHLA I.  
Relativistic two-nucleon potential.  
RPP/C 41
- 102 ULEHLA I., FRANEK B.  
The  ${}^4\text{He}$  nucleus and soft core potentials.  
RPP/T 31.
- 103 WHITEHEAD C., WEST D., BIRD L., AULD E. G., CRABB D. G., OTT R., McEWEN J. G., AITKEN D. K., BENNETT G., HAGUE J. F., JENNINGS R. E., PARSONS A. S. L.  
A spark chamber experiment on the reaction  $\pi^- + p \rightarrow n + \pi^+ + \pi^-$  at 3.1–3.6 GeV/c.  
RPP/H 85.

CONFERENCE PAPERS (alphabetically by conference title, then by author).

- 104 BAKER S. L., DANYSZ J. A., HALL G., ISLAM A. K. M. A., MAY G., MILLER D. B., ORR R. S., ALLEN J. E., MARCH P. V., O'BRIEN K.  
The reaction  $K^+n \rightarrow Kp$  at 2.2 and 2.45 GeV/c.  
**American Physical Society Spring Meeting**, Washington, 24–27 April 1972.
- 105 BAKER S. L., DANYSZ J. A., HALL G., ISLAM A. K. M. A., MAY G., MILLER D. B., ORR R. S., ALLEN J. E., MARCH P. V., O'BRIEN K.  
Single pion production in 2.2 GeV/c  $K^+d$  interactions.  
Ibid.
- 106 GOPAL G. P., BAKER S. L., DORNAN P. J., STARK J., WEBSTER G. J., BUCKLEY T., BULL V. A., TAYLER V., TOWNSEND D. W.  
Angular momentum analysis of the Dalitz plot distributions of the  $\pi^+\pi^0p$  and  $\pi^+\pi^+n$  final states from  $\pi^+p$  interactions in the centre of mass range from 1610 to 1690 MeV.  
Ibid.
- 107 LEWIS P. H., ALLEN J. E., JACOBS N. H. D., DANYSZ J. A., ISLAM A. K. M. A., MILLER D. B., PENNEY B. K., STEWART B. C., THOMPSON G., BORG A., BRUNET J. M., NARJOUX J. L.  
4 and 5 body  $K^+p$  interactions at 2.11, 2.31, 2.53 and 2.72 GeV/c.  
Ibid.
- 108 POPLEY R. A., SAMBROOK D. J., WALTERS C. R., WILSON M. N.  
A new superconducting composite with low hysteresis loss.  
**Applied Superconductivity Conference**, Annapolis, 1–3 May 1972. Proceedings p. 516.
- 109 WILSON M. N.  
Filamentary composite superconductors for pulsed magnets.  
Ibid., p. 385, preprinted as RPP/A 89.
- 110 WILSON M. N., HOPES R. B., STOVOLD R. V., GALLAGHER-DAGGITT G. E., TOLCHER R., LAWLER J. V., BROWN J., EDWARDS V. W.  
AC3—A prototype superconducting synchrotron magnet.  
Ibid., p. 277.
- 111 MORTIMER A. R.  
The cryogenic heat pipe—a review of work at the Rutherford Laboratory.  
**Chemical Equipment Design and Automation, 4th International Congress of Chemical Engineering on, (CHISA 72)**, Prague, 11–15 September 1972, preprinted as RPP/E 19.
- 112 EVANS D., SIMMONDS G. E., STAPLETON G. B.  
Improved facility for the determination of mechanical properties of materials in liquid helium.  
**Cryogenic Engineering Conference, 4th International (ICEC IV)**, Eindhoven, 24–26 May 1972. Proceedings, p. 331, preprinted as RPP/E 17.

- 113 POPLEY R. A., SAMBROOK D. J., WALTERS C. R., WILSON M. N.  
A new 13255 filament superconducting composite.  
Ibid., p. 165.
- 114 CHAN H. M.  
Diffractive dissociation in inclusive reactions.  
**Diffractive Processes at High Energies**, XII School of Theoretical Physics, Cracow, 8-18 June 1972. Proceedings (Acta. Phys. Polon., **B3** (6) November 1972) p. 879.
- 115 KANE G. L.  
Phenomenology of diffractive reactions.  
Ibid., p. 845, preprinted as RPP/T 20.
- 116 BUGG D. V.  
Coulomb corrections to  $\pi N$  scattering below 300 MeV.  
**Elementary Particle Physics, IOP Conference on**, Southampton, 12-14 September 1972.
- 117 LEE CHI KWONG L. C. Y.  
Cross-over values for elastic  $\bar{p}p$  and  $pp$  scattering.  
Ibid.
- 118 BINNIE D. M., CAMILLERI L., DUANE A., GARBUTT D. A., HOLMES J. R., JONES W. G., KEYNE J., LEWIS M., SIOTIS I., UPADHYAY P. D., BURTON I. F., McEWAN J. G.  
Meson mass spectrum near the  $X^0$  (958).  
**Experimental Meson Spectroscopy, 3rd International Conference on**, Philadelphia, 28-29 April 1972.
- 119 RUTHERFORD/SACLAY/ECOLE POLYTECHNIQUE COLLABORATION.  
 $K^- \pi^-$  elastic scattering cross-section measured in 14.3 GeV/c  $K^- p$  interactions.  
Ibid.
- 120 EDGINGTON J. A.  
Low energy parameters.  
**Few Particle Problems in Nuclear Interactions International Conference on**, Los Angeles, 28 August-1 September 1972.
- 121 EDGINGTON J. A., HOWARD V. J., BLAIR I. M., BAKER A. C., McNAUGHTON M. N., BONNER B. E., BRADY F. P.  
Evidence for large off-shell effects in n-p bremsstrahlung.  
Ibid.
- 122 DAS GUPTA S. S., EDGINGTON J. A., BLAIR I. M., McNAUGHTON M. W., BONNER B. E., STEWART N. M.  
Measurement of the differential cross-section for n-d elastic scattering at 128 MeV.  
Ibid.
- 123 McNAUGHTON M. W., GRIFFITHS R. J., STEWART N. M., EDGINGTON J. A., MAY M. P., BLAIR I. M., BONNER B. E.  
A determination of the neutron-neutron scattering length from a kinematically complete experiment on the  $d(n, np)n$  reaction at 130 MeV.  
Ibid.

- 124 CHAN H. M.  
The many body problem in hadron reactions.  
**High Energy Collisions, 4th International Conference on, (Stony Brook series)**, Oxford, 5-7 April 1972, Proceedings (RHEL-72-001, Smith J. R. (ed.)), **1**, 499 preprinted as RPP/T 17.
- 125 SHARP P. H.  
A search for the large transverse momentum muons at the ISR.  
Ibid., **2**, 214.
- 126 TONER, W. T.  
Lepton-hadron interactions.  
Ibid., **1**, 1.
- 127 ADAMS, C. J., COX G. F., DAVIES J. D., DOWELL J. D., GRAYER G. H., HATTERSLEY P. M., HOMER R. J., HOWELLS R. J., McLEOD C., McMAHON T. J., VAN DER RAAJ H. B., ROB L., DAMERELL C. J. S., HOTCHKISS M. J.  
Measurement of  $K^+ p$  elastic scattering between 432 MeV/c and 939 MeV/c and phase shift analysis.  
**High Energy Physics, XVI International Conference on**, Chicago and NAL, 6-13 September 1972.
- 128 BAKER R. D.  
Low energy  $\pi\pi$  scattering phases.  
Ibid.
- 129 CHARLES B. J., COWAN I. M., EDWARDS T. R. M., GIBSON W. M., GILLMAN A. R., GILMORE R. S., GLEDHILL M. H., HUGHES C. M., MALOS J., SMITH V. J., TAPPER R. J., McCARTNEY B., OADES G. C., WARD D. L., WROATH P. D., BECK G. A., COUPLAND M., FRANK S. G. F.  
Differential cross-sections for elastic scattering of positive kaons on protons in the momentum range 0.7 to 1.9 GeV/c.  
Ibid.
- 130 LEA A. R., OADES G. C., MARTIN B. R., MOORHOUSE R. G.  
Multichannel analysis of  $\bar{K}N$  data 0.4-1.2 GeV/c.  
Ibid.
- 131 RUTHERFORD/SACLAY/ECOLE POLYTECHNIQUE COLLABORATION.  
Two-body final states in  $K^- p$  interactions at 14.3 GeV/c.  
Ibid., preprinted as RPP/H 102.
- 132 RUTHERFORD/SACLAY/ECOLE POLYTECHNIQUE COLLABORATION.  
Test of helicity conservation for the  $(K\pi\pi)^-$  system diffractively produced in  $K^- p$  interactions at 14.3 GeV/c.  
Ibid.
- 133 RUTHERFORD/SACLAY/ECOLE POLYTECHNIQUE COLLABORATION.  
Evidence for a  $\pi$ -exchange contribution to the production of diffractive  $K\pi\pi$  systems.  
Ibid.
- 134 RUTHERFORD/SACLAY/ECOLE POLYTECHNIQUE COLLABORATION.  
 $K^- \pi^-$  elastic scattering cross-section measured in 14.3 GeV/c  $K^- p$  interactions.  
Ibid.

- 135 MIETTINEN H. I.  
Inclusive reactions and the Regge model.  
**High Energy Physics, Symposium on**, Copenhagen, 7-11 August 1972.
- 136 COUPLAND J. H., BAYNHAM D. E.  
Measurements of pulsed superconducting dipole magnets.  
**Magnet Technology, 4th International Conference on**, Brookhaven, 19-22 September 1972.
- 137 MORTIMER A. R., GRESHAM A. T.  
An ultra-thin septum magnet.  
Ibid., preprinted as RPP/E 18.
- 138 NEWMAN M. J., TROWBRIDGE C. W., TURNER L. R.  
GFUN: An interactive program as an aid to magnet design.  
Ibid., preprinted as RPP/A 94.
- 139 THOMAS D. B., WILSON M. N.  
Filamentary superconductors for pulsed magnets.  
Ibid., preprinted as RPP/A 93.
- 140 TROWBRIDGE C. W.  
Progress in magnet design by computer.  
Ibid., preprinted as RPP/A 92.
- 141 WILLIAMS W. G.  
Polarizing filters for thermal neutrons.  
**Neutron Beam Research, Conference on Recent Developments in**, Oxford, 13-15 September 1972.
- 142 SINHA B. C., DUGGAN F.  
A three parameter nucleon-nucleus optical model on the energy shell.  
**Nuclear Many Body Problem, International Symposium on present status and novel developments in**, Rome, 19-23 September 1972.
- 143 BATTY C. J.  
High energy particles and nuclear sizes.  
**Nuclear physics, nuclear structure and nuclear reactions, IOP Conference on**, Birmingham, 18-20 April 1972.
- 144 BATTY C. J., WATSON L. H.  
Shape of the real optical potential for elastic alpha-particle scattering.  
Ibid.
- 145 EDWARDS V. R. W., SINHA B. C., WEBB C. J.  
The form factor of the deformed imaginary potential for the scattering of nucleons from collective nuclei.  
Ibid.
- 146 MARCHESI C. J., CLARKE N. M., GRIFFITHS R. J.  
Collective model analysis of the inelastic scattering of 53 and 33 MeV helions by  $^{56}\text{Fe}$ .  
Ibid.

- 147 TAIT W. H., EDWARDS V. R. W.  
Inelastic scattering of 30.5 MeV protons from  $^{64,66,68}\text{Zn}$  and  $^{92,96,100}\text{Mo}$ .  
Ibid.
- 148 THOMAS G. L., SINHA B. C., DUGGAN F.  
A proton optical potential generated from effective nucleon-nucleon force.  
Ibid.
- 149 WOOLLAM P. B., GRIFFITHS R. J., CLARKE N. M.  
Elastic and inelastic scattering of protons and helions from Samarium.  
Ibid.
- 150 CHAN H. M.  
Regge Phenomenology of inclusive reactions.  
**Physics, 1972 CERN School of**, Grado, 15-31 May 1972. Proceedings (CERN 72-17) p. 1, preprinted as RPP/T 21.
- 151 PHILLIPS R. J. N.  
High-energy two-body phenomenology.  
Ibid., p. 541, preprinted as RHEL/M/THEORY 1.
- 152 MORGAN D.  
Questions in  $\pi\pi$  scattering and related processes.  
**Physics, 7th Finnish Summer School in**, Loma-Koli, 26 June-7 July 1972. Proceedings (Pellinen R. (ed.)) p. 9, preprinted as RPP/T 27.
- 153 ROBERTS R. G.  
Phenomenology of inclusive reactions.  
Ibid., p. 119, preprinted as RHEL/M/THEORY 2.
- 154 ELLIS R. E., MILL A. J., PERRY D. R.  
Comparative dosimetry of 14 MeV electrons, neutrons and negative pi mesons as relevant to applied biology.  
**Radiobiology, British Institute of Radiology meeting on**, London, 21 January 1972.
- 155 HOLT P. D., PERRY D. R.  
Dose and LET measurements on the Nimrod low energy negative pion beam, and comparison with theory.  
Ibid.
- 156 SHEWELL J., LINDOP P. J., PROUKAKIS C., ELLIS R. E., PERRY D. R.  
Thymic weight and thymocyte changes in the immature mouse as a measure of RBE of 14 MeV electrons, 14 MeV neutrons and negative pi mesons.  
Ibid.
- 157 WINSTON B. M., BERRY R. J., PERRY D. R.  
Response of Vicia Faba to irradiation under aerobic and hypoxic conditions with a negative pion beam from Nimrod in the "plateau" and "peak" ionisation regions.  
Ibid.
- 158 PHILLIPS R. J. N.  
Regge poles and duality.  
**Subnuclear Physics, International School in**, Erice, 7-29 July 1972, preprinted as RHEL/M/THEORY 3.

159 FORSYTH J. B.  
Automation of neutron intensity measurements using on-line computers.  
**X-ray and Neutron Single Crystal Diffraction Methods, Advanced Study Institute on Experimental Aspects of**, Aarhus, 31 July–11 August 1972.

160 FORSYTH J. B.  
Data processing and assessment using on-line graphical facilities.  
Ibid.

#### THESES FOR HIGHER DEGREES

(i) PhD and D. Phil.

161 BAKER R. D. (University of Cambridge).  
Low energy  $\pi\pi$  and  $\pi N$  interactions.  
Reprinted as HEP/T/31.

162 BUCKINGHAM I. D. (University of Oxford).  
A spark chamber study of  $K^-p \rightarrow$  neutral final state from 0.690–1.0 GeV/c.

163 DAINTY J. C. (Imperial College, University of London).  
Speckle statistics and the detection of images in hologram reconstructions of bubble chamber tracks and other objects.

164 HANNA A. M. (Queen's University, Belfast).  
The direct interaction of protons with light nuclei.

165 HART J. C. (University of Cambridge).  
An experiment to study the leptonic decay of neutral K-mesons.

166 HOLMES J. R. (Imperial College, University of London).  
Single pion production with forward going nucleons in  $\pi p$  interactions in the range 670–1300 MeV/c.

167 HOWARD V. J. (Queen Mary College, University of London).  
A study of the neutron-proton interaction over the energy range 100–160 MeV.

168 HUGHES C. M. (University of Bristol).  
 $\pi^+p$  elastic scattering differential cross sections for 18 pion laboratory momenta between 0.8 and 1.6 GeV/c.  
Reprinted as HEP/T/34.

169 HUTTON J. S. (University of Cambridge).  
An experimental test of the weak interaction selection rule  $\Delta S = \Delta Q$ .  
Reprinted as HEP/T/32.

170 ISLAM A. K. M. A. (Imperial College, University of London).  
Single pion production in intermediate energy  $K^+d$  interactions.  
Reprinted as HEP/T/39.

171 KAY M. E. (Imperial College, University of London).  
A decay detection system and its application to the omega meson.

172 KRZESINSKI A. E. S. (University of Cambridge).  
A study of electromagnetic processes in a hydrogen bubble chamber.  
Reprinted as HEP/T/28.

173 LEE CHI KWONG L. C. Y. (Queen Mary College, University of London).  
Small angle elastic proton-proton and antiproton-proton scattering between 1 and 2 GeV/c.  
Reprinted as HEP/T/33.

174 LEWIS P. H. (Westfield College, University of London).  
A study of multi-body final states in  $K^+p$  reactions between 2 and 3 GeV/c.  
Reprinted as HEP/T/29.

175 McCARTNEY B. (University of Bristol).  
Elastic scattering of positive kaons by protons.  
Reprinted as HEP/T/30.

176 McNAUGHTON M. W. (King's College, University of London).  
The  $d(n,np)$  reaction at 50–150 MeV.  
Reprinted as AERE-R-71 51.

177 MARTIN J. F. (University of Oxford).  
A study of polarization effects in  $\pi^+p$  elastic scattering.  
Reprinted as HEP/T/35.

178 NORTON P. R. (University of Oxford).  
A study of neutral  $Y^*$  resonance formation.

179 SHARP P. H. (University of London (external)).  
An experimental study of weak interactions using  $\Lambda^0$  and  $K^0$  decays.

180 SLEEMAN J. C. (University of Oxford).  
An experiment to study polarization effects in  $\pi^+p$  elastic scattering in the momentum range 600 to 2700 MeV/c.

181 SPENCER C. M. (University of Oxford).  
The measurement of the polarization in pion-nucleon backward elastic scattering.

182 STARK J. W. (Imperial College, University of London).  
Isobar production in low energy  $\pi^+p$  interactions and the use of a small computer in the control of measuring machines.

183 STEWART B. C. (Imperial College, University of London).  
Two and three pion production in a  $K^+p$  experiment between 2.11 and 2.72 GeV/c.  
Reprinted as HEP/T/36.

184 VICKERY R. P. (Westfield College, University of London).  
A measurement of decay parameters of the sigma plus hyperon.  
Reprinted as HEP/T/25.

(ii) M.Sc.—

185 PITTS P. R. (London Polytechnic).  
Spark chambers, multiwire proportional chambers and streamer chambers in high energy physics.  
Reprinted as HEP/T/27.

## REPORTS

- 186 ADAMS P.  
K9 computer software system.  
RHEL/R 240.
- 187 BARLOW J., FRANEK B.  
Graphic representation of functions of two variables.  
RHEL/R 259.
- 188 BRYDEN A. D.  
A computer program for matching track images from three views in a bubble chamber.  
RHEL/R 235.
- 189 CAWTHRAW M. J.  
The system crate—a modular method of controlling CAMAC systems.  
RHEL/R 246.
- 190 COLYER B.  
The impregnation of superconducting windings with epoxy resins. Part 1: Theoretical considerations.  
RHEL/R 264.
- 191 EVANS D., MORGAN J. T., STAPLETON G. B.  
Irradiation damage studies of some epoxy resin systems of reduced viscosity.  
RHEL/R 249.
- 192 EVANS D., MORGAN J. T., STAPLETON G. B.  
Epoxy resins for superconducting magnet encapsulation.  
RHEL/R 251.
- 193 GRAY D. A. (ed.).  
Proceedings of the meeting of the Daresbury-Rutherford Accelerator Working Party held at the Cosener's House, Abingdon, 16-17 December 1971.  
RHEL/R 252.
- 194 GRAY D. E. (ed.).  
Nimrod operation and development, quarterly report—October 1 to December 31, 1971.  
RHEL/R 239.
- 195 GRAY D. E. (ed.).  
Nimrod operation and development, quarterly report—January 1 to March 31, 1972.  
RHEL/R 253.
- 196 GRAY D. E. (ed.).  
Nimrod operation and development, quarterly report—April 1 to June 30, 1972.  
RHEL/R 260.
- 197 GRAY D. E. (ed.).  
Nimrod operation and development, quarterly report—July 1 to September 20, 1972.  
RHEL/R 263.
- 198 HALLOWELL P. J.  
A track detection program for a Hough-Powell device.  
RHEL/R 241.
- 199 JAROSLAWSKI S.  
The analysis of the 100 kW reactor regulator set with the magnet load type Q425.  
RHEL/R 254.
- 200 LAWES R. A.  
Optimising the photographic variables of spark chamber film for automatic measurement.  
RHEL/R 247.
- 201 MEARDON B. H., SALTER D. C.  
A survey of position sensitive detectors and multi-counter arrays with particular reference to thermal neutron scattering.  
RHEL/R 262.
- 202 MIDDLETON A. J., HEY P. D., COLYER B.  
The impregnation of superconducting windings with epoxy resins. Part 2: Resin Data.  
RHEL/R 265.
- 203 MORGAN J. T., STAPLETON G. B.  
A technique for controlling the pressure of CO<sub>2</sub> in the Nimbus F radiometer.  
RHEL/R 216.
- 204 MORTIMER A. R., STOKOE J. R.  
A liquid hydrogen or deuterium target system with closed cycle refrigeration.  
RHEL/R 237.
- 205 MOTT E. M.  
A transparent touch-screen device for interactive computer graphics displays.  
RHEL/R 248.
- 206 OADES G. C. (ed.).  
K-meson physics below 5 GeV/c.  
RHEL/R 245.
- 207 PENFOLD J., FORSYTH J. B.  
A remote job entry terminal to the Rutherford Laboratory IBM 360/195 computer.  
RHEL/R 261.
- 208 SMITH J. R. (ed.).  
Proceedings of the 4th International Conference on High Energy Collisions (Stony Brook series), Oxford, 5-7 April 1972.  
RHEL-72-001 (2 vols).

- 209 SMITH J. R., TELLING F. M. (eds.).  
The work of the Rutherford Laboratory in 1971.  
RHEL/R 243.
- 210 SWALES F. J., REASON C. J.  
The  $\pi$ 10 beam line for nuclear structure experiments on Nimrod.  
RHEL/R 257.

#### MEMORANDA

- 211 ABBOTT G., ADAMS C., KNIGHT K., McEWAN J., TAYLOR K.  
Terminal 1130 Computer.  
RHEL/M/C 21.
- 212 ANONYMOUS.  
Design office guide.  
RHEL/M/E 5.
- 213 ARNISON G. T. J.  
Some characteristics of a capacity read-out spark chamber.  
RHEL/M/H 13.
- 214 ATCHISON F.  
Notes on the program RANGE.  
NIMROD 72-7.
- 215 ATKINSON R. W.  
70 MeV injector; Electrical supplies, etc.  
NIMROD/INJ/12.
- 216 ATKINSON R. W.  
Control cabling and equipment, standardisation of.  
NIMROD/INJ/22.
- 217 BATTY C. J. (ed.).  
Stopping kaons and nuclear structure—some notes on an informal meeting  
at the Rutherford Laboratory—7 October 1971.  
RHEL/M/H9.
- 218 BRACHER B. H.  
RHEL rough digitising system: principles of operation and IBM 360 files.  
RHEL/M/H 15.
- 219 BRACHER B. H.  
RHEL rough digitising system: IBM 360 file information programs  
DD LATEST, DD POPSI.  
RHEL/M/H 16.
- 220 BRACHER B. H.  
RHEL rough digitising system: File modification programs DD BODGE 3,  
DD ELETE.  
RHEL/M/H 17.

- 221 BRACHER B. H., GOPAL G. P.  
RHEL rough digitising system: Remote job entry and file loading programs:  
DD RJSL, DD RJS and KGF15AP.  
RHEL/M/H 20.
- 222 BUTTERWORTH J.  
Some modifications to the program LURCH.  
RHEL/M/NIM 13.
- 223 CLEE P. T.  
The superconducting holding magnet for the frozen target experiment.  
RHEL/M/E4.
- 224 COATES J. A., JESSETT A.  
To show that the proportion of  ${}^6\text{Li}$  in the  ${}^6\text{Li}$  F disc batches in current use at  
the Rutherford Laboratory is constant.  
RP/PN/60.
- 225 COLEMAN T. G., FITZHARRIS E. W.  
1.5 m cryogenic bubble chamber operation July–October 1972.  
NIMROD 72-19.
- 226 COUPLAND J. H.  
The 'S' bend—a new concept in smooth ends for dipole magnets.  
RHEL/M/A 21.
- 227 DEAN J. W.  
The cryogenic aspects of the proposed European 1000 GeV superconducting  
synchrotron.  
RHEL/M/A 22.
- 228 DONALD M. H. R.  
Effective thickness of thin ejection septa.  
RHEL/M/NIM 12.
- 229 DONALD M. H. R.  
MUGWUMP package CCGMUG: a graphics package for the Computek  
display.  
RHEL/M/NIM 11.
- 230 DONALD M. H. R.  
Some non-linear resonances in the SPS.  
CERN/LAB II-DI-PA/INT 72-11.
- 231 DONALD M. H. R., KING N. M.  
Choice of the SPS working point.  
CERN/LAB II-DI-PA/INT 72-10.
- 232 EASTWOOD A. W., GOTTFELDT P., MORRISSEY M.  
Proposal for the computerisation of the frozen target.  
NIMROD 72-12.
- 233 ELLIOTT R. T., FLOWER P. S.  
Pulsed magnets for a  $\Sigma^-$  experiment in the CERN 2 m hydrogen bubble  
chamber.  
NIMROD 72-4.

- 234 EUSTACE J. G.  
Compilation of  $\pi$ 11 beam line data.  
RP/PN/61.
- 235 EVANS W. H. (ed.).  
Multiwire proportional chambers—proceedings of the meeting at Cosener's  
House, Abingdon, 3-4 June 1972.  
RHEL/M/H 21.
- 236 FERGUSON N. W.  
Recommendation for the installation of vacuum isolating valve in Straight 4.  
NIMROD 72-10.
- 237 FERGUSON N. W.  
Test results—pre-cooling the air cooling system to Straight 8 r.f. amplifier.  
NIMROD 72-14.
- 238 FISHER CM., LAWES R. A., POWELL B.  
A vidicon trigger and data processing system for a rapid cycling bubble  
chamber.  
RHEL/M/H 14.
- 239 FITZHARRIS E. W.  
1.5 m cryogenic bubble chamber operating conditions.  
NIMROD 72-13.
- 240 FORSYTH J. B.  
NBGEO—a program for calculating single crystal setting angles for  
diffraction using normal beam geometry.  
NBRU 72-2.
- 241 FORSYTH J. B.  
Neutron beam instrumentation at Grenoble.  
NBRU 72-5.
- 242 FORSYTH J. B.  
Automatic control of experiments at ILL.  
NBRU 72-6.
- 243 FORSYTH J. B.  
UBCALC—a program which calculates the orientation matrix giving the best  
least-squares fit to a set of observed single crystal reflection angles.  
NBRU 72-14.
- 244 GILL P.  
The DCF interface in the DDP 224 and diagnostic aids for the DCF channel.  
RHEL/M/C 29.
- 245 GILL P., WATSON J. G.  
The interfaces for the IBM Golfball typewriters attached to the DDP 224.  
RHEL/M/C 28.
- 246 GIRARD P. M.  
An introduction to HASP.  
RHEL/M/C 23.

- 247 GIRARD P. M.  
The extension of on-line facilities to 'consoles'.  
RHEL/M/C 48.
- 248 GOODYER P. T. J.  
Tanks 2-3-4 power supplies (including specification).  
NIMROD/INJ/18.
- 249 GRAY D. A.  
Final inflector element, choice of.  
NIMROD/INJ/2.
- 250 GRAY D. A.  
Pole face winding experiment to investigate the reason for inside steering.  
NIMROD 72-18.
- 251 GRAY D. A.  
Future beam layout for Exp. Hall 1.  
NIMROD 72-20.
- 252 GRAY D. A.  
Literature search—storage rings.  
EPIC/MC/2.
- 253 HACK R. C.  
Radiation Protection Group (Operations) Progress Report for 1971.  
RHEL/M/R9.
- 254 HACK R. C.  
The estimation of low levels of accelerator induced nuclides.  
RHEL/M/NIM 16.
- 255 HAROLD M. R.  
Ejection from a 500 GeV 'missing-magnet' superconducting synchrotron.  
GESSS/MD/23.
- 256 HEMMINGS P. J.  
ENPLOT—A program package for the production of histograms and scatter  
plots.  
RHEL/M/C 50.
- 257 HEMMINGS P. J., HURST H.  
Access to the Rutherford Laboratory Central Computing System via the  
switched public network.  
RHEL/M/C 25.
- 258 HEY P. D.  
Polarizing filter for thermal neutrons—a preliminary engineering design note.  
NBRU 72-9.
- 259 HOBBS L. C. W.  
The proposed ultra-cold neutron gas facility on DIDO.  
NBRU 72-1.

- 260 HODGES A. R.  
The effects of neutron radiation on the electrical characteristics of selected silicon diodes.  
NIMROD 72-16.
- 261 HURST H., TUCKER A. W.  
Instructions for HASP RJE Workstation operation on the system 195.  
RHEL/M/C 35.
- 262 KING N. M., MAIDMENT J. R. M.  
Calculations relevant to the superconducting 'missing-magnet' option.  
GESS/MD/20.
- 263 KNIGHT K. M.  
The interface connecting a SAC multiplexor sub-channel to an IBM 2701 PDA and the DCF multiplexor (hardware information).  
RHEL/M/C 24.
- 264 KNIGHT K. M.  
The IBM 1130 computer storage access channel multiplexor. The SAC multiplexor sub-channel test box (hardware descriptions).  
RHEL/M/C 36.
- 265 KNIGHT K. M.  
The transmission of data from the terminal 1130 computer to the IBM 360/195 computer via the high speed serial data link (hardware notes).  
RHEL/M/C 44.
- 266 LEA A. T.  
An introduction to the central computing facilities.  
RHEL/M/C 20.
- 267 LIDBURY J. A.  
A helium heat pipe.  
NIMROD 72-11.
- 268 MAIDMENT J. R. M., PLANNER C. W.  
Notes on beam instabilities.  
EPIC/MC/6.
- 269 MARTIN C. S., SQUIER D. M.  
Investigation into the measurement of high energy radiation using spallation products of calcium.  
NIMROD 72-17.
- 270 MASKELL S. C., SERGEANT D. J.  
A cathode ray tube decimal display unit for CAMAC (RL 199).  
RHEL/M/H 12.
- 271 MORGAN R. H. C.  
70 MeV injector control system.  
NIMROD/INJ/5.
- 272 MORGAN R. H. C.  
70 MeV injector. Proposals for interfacing to CAMAC control system.  
NIMROD/INJ/7.

- 273 MORGAN R. H. C.  
Commissioning 70 MeV injector (with special reference to inflector system).  
NIMROD/INJ/20.
- 274 MURRELL C. N. E.  
Minimisation routines for non-linear functions.  
RHEL/M/C 32.
- 275 NEWMAN M. J.  
A message decoding system for use with the interactive graphics package LDMPX.  
RHEL/M/A 19.
- 276 NORRIS S.  
Daedalus Version 2 DDP 224 Users guide.  
RHEL/M/C 30.
- 277 O'CONNELL M. J.  
Multidimensional least squares orthogonal polynomial approximation (with users' guide to the surface fitting program PSI 2).  
RHEL/M/C 17.
- 278 PENFOLD J.  
Notes on running the Dido Triple Axis Spectrometer control tape generation program at RHEL.  
NBRU 72-12.
- 279 PENFOLD J.  
Notes on the electric file handling and job submission facilities for the RHEL IBM 360/195.  
NBRU 72-13.
- 280 PENFOLD J.  
Operators Guide to the NBRU remote job entry terminal.  
NBRU 72-16.
- 281 PERRY D. R.  
Radiation shielding.  
NIMROD/INJ/14.
- 282 PERRY D. R.  
X-ray hazard from pre-injector.  
NIMROD/INJ/16.
- 283 PLANNER C. W.  
The 70 MeV beam transfer line and injection system.  
NIMROD/INJ/15.
- 284 REES G. H.  
The effect of noise on bunch compression in an e-p storage ring.  
RHEL/M/NIM 15.
- 285 REES G. H.  
Initial design aspects of storage rings for a possible future UK facility.  
EPIC/MC/1 (formerly DRAG/SR/1).

- 286 REES G. H.  
Useful formulae for luminosity estimates of colliding beams.  
EPIC/MC/3.
- 287 REES G. H.  
Suggested initial list of storage ring machine topics for detailed study.  
EPIC/MC/4. (formerly DRAG/SR/2).
- 288 REES G. H.  
The effect of noise on bunch compression in an e-p storage ring.  
EPIC/MC/5.
- 289 RUSSELL F. M.  
Design criteria for a new RHEL polarized target.  
RHEL/M/A 18.
- 290 RUSSELL R. G.  
Injector beam requirements.  
NIMROD/INJ/6.
- 291 SMITH P. F.  
The possibility of quark production by multistage excitation in collisions  
between heavy nuclei.  
RHEL/M/A 20.
- 292 STIRLING G.  
ILL instrumentation.  
NBRU 72-8.
- 293 STIRLING G.  
Neutron beam instruments in UK.  
NBRU 72-10.
- 294 SWALES F. J.  
Momentum measurement in the HEDS.  
NIMROD/INJ/19.
- 295 SWALES F. J.  
Diagnostics equipment.  
NIMROD/INJ/21.
- 296 TAYLOR K. W.  
A simulated storage access channel for the IBM 1130 computer.  
RHEL/M/C 39.
- 297 TAYLOR K. W.  
A hardware timing monitor for the IBM 1130 computer.  
RHEL/M/C 40.
- 298 TAYLOR K. W.  
A multichannel character multiplexor for attaching devices to the IBM 1130  
computer.  
RHEL/M/C 41.
- 299 TAYLOR K. W.  
A BSI interface for a Texas thermal printer.  
RHEL/M/C 42.

- 300 THORNE A.  
Computer controlled interactive graphics: description of hardware.  
RHEL/M/C 34.
- 301 TROTMAN J. V.  
Some notes on Nimrod stores programs.  
RHEL/M/NIM 14.
- 302 WALKINSHAW W., LEA A. T. (eds.).  
Computing and Automation Division quarterly report: 1 January-31 March  
1972.  
RHEL/M/C 22.
- 303 WALKINSHAW W., LEA A. T. (eds.).  
Computing and Automation Division quarterly report: 1 April-30 June 1972.  
RHEL/M/C 31.
- 304 WALKINSHAW W., LEA A. T. (eds.).  
Computing and Automation Division quarterly report: 1 July-29 September  
1972.  
RHEL/M/C 45.
- 305 WALKINSHAW W., LEA A. T. (eds.).  
Computing and Automation Division quarterly report 30 September-29  
December 1972.  
RHEL/M/C 47.
- 306 WALLIS E. W. G. (ed.).  
Technical information and installation guide for experimental apparatus.  
RHEL/M/H 18.
- 307 WALLIS E. W. G., SIMMONS J. E.  
NAL Chicago cyclotron magnet field measuring probe survey bar. Operators  
handbook.  
RHEL/M/H19.
- 308 WARD B. C. W.  
Modulator characteristics, design parameters.  
NIMROD/INJ/10.
- 309 WATSON J. G.  
16 way multiplexor (DDP 224).  
RHEL/M/C 27.
- 310 WATSON J. G.  
Customer bus interface for the DDP 224.  
RHEL/M/C 37.
- 311 WATSON J. G.  
The Computek interface.  
RHEL/M/C 38.
- 312 WEST N. D.  
Some parameters of the 70 MeV injector.  
NIMROD/INJ/1.

- 313 WEST N. D.  
Some 70 MeV Injector design figures relating to the longitudinal motion of the beam.  
NIMROD/INJ/3.
- 314 WEST N. D.  
Specification of the drift tube positions in Tank 4.  
NIMROD/INJ/4.
- 315 WEST N. D.  
70 MeV Injector. Dimensions of Tank 1 built to the NAL design.  
NIMROD/INJ/8.
- 316 WEST N. D.  
70 MeV injector. Dimensions of Tank 4.  
NIMROD/INJ/9.
- 317 WEST N. D.  
Choice of diameters for tanks 1 and 4.  
NIMROD/INJ/13.
- 318 WEST N. D., PLANNER C. W.  
Notes on visit to BNL and NAL, July 1972.  
NIMROD/INJ/11.
- 319 WHELDON A. G.  
EHT area earthing and earthing interlocks.  
NIMROD/INJ/17.
- 320 WILLIAMS J. A.  
Measurements of coupling variations between spheres approximated by cylindrical coils.  
RHEL/M/A 23.
- 321 WILLIAMS P. R.  
The Rutherford Laboratory/CERN track sensitive target programme.  
NIMROD 72-1
- 322 WILLIAMS P. R.  
Hydrogen bubble chamber operating conditions: the foam limit.  
NIMROD 72-3.
- 323 WILLIAMS P. R.  
Properties of Ne/H<sub>2</sub> mixtures at 29 K  
NIMROD 72-5.
- 324 WILLIAMS P. R.  
A possible form of stack for a charged particle detector based on X-ray transition radiation.  
NIMROD 72-15.
- 325 WILLIAMS P. R., BATEMAN J. E.  
Hydrogen X-ray transition radiation detectors.  
NIMROD 72-21.
- 326 WILLIAMS W. G.  
Preliminary report on a new polarizing filter for thermal neutrons.  
NBRU 72-3.

- 327 WILLIAMS W. G.  
Studies on the use of polarized protons and polarized Samarium 149 filters on spin analysers in thermal neutron scattering.  
NBRU 72-11.
- 328 WILLIAMS W. G.  
Separation of the spin-dependent partial cross-sections in the polarization analysis of thermal neutron scattering.  
NBRU 72-15.
- 329 WILSON M. N.  
Design curves for dipole magnets of elliptical cross-section.  
RHEL/M/A 17.
- 330 WILSON M. N.  
Rate dependent magnetisation in flat twisted superconducting cables.  
RHEL/M/A 26.
- 331 WIMBLETT R. W.  
Estimate of cost of liquid helium using the helium B.C. refrigerator as liquifier.  
NIMROD 72-9.
- 332 WROE H.  
Focussing neutrons using stacked microguides.  
NBRU 72-4.

#### HFBR MEMORANDA

The following memoranda were prepared by SRC and UKAEA staff as part of the UK HFBR preparatory work.

- DENT K. H. (UKAEA)  
Precis of major accidents on the BNL HFBR, ORNL HFIR and Grenoble RHF.  
HFBR/72-1.
- Reactor Group Risley (UKAEA)  
High flux beam reactor: parameters for use in safety analysis.  
HFBR/72-2.
- HUNT D. L. (UKAEA)  
Decay heat removal by natural circulation in the core.  
HFBR/72-3
- Systems Reliability Service, Risley (UKAEA)  
An assessment of alternative cooling arrangements.  
HFBR/72-4.
- HFBR Project Office, RL  
HFBR application for nuclear site licence: Part 1: Siting and emergency procedures.  
HFBR/72-5.

HFBR Project Office, RL

HFBR application for nuclear site licence: Part 2: Reactor design and safety.  
HFBR/72-6.

BELL G. D. (UKAEA)

HFBR dose calculations for accidental releases of activity.  
HFBR/72-7.

DENT, K. H. (UKAEA)

Over pressurizing of secondary containers.  
HFBR/72-8.

DENT, K. H. (UKAEA)

Use of the International System of Units.  
HFBR/72-9.

CARTER P. (UKAEA)

Calculations of the efficiency of various cylinder shaped cold sources for the HFBR.  
HFBR/72-10.

HOBBIS L. C. W. (NBRU) STIRLING G. C. (NBRU)

Preliminary note on neutron attenuation by primary containment barriers  
HFBR/72-11.

BAKER L. J. (UKAEA)

Nuclear heating in beam tube windows.  
HFBR/72-12.

McBRIDE C. (UKAEA) DENT K. H. (UKAEA)

HFBR provisional, technical and engineering parameters  
HFBR/72-15

HEY P. D. (RL) STIRLING G. C. (NBRU)

Notes on data used in HFBR/72-11 Neutron beam attenuation by primary  
containment barriers.  
HFBR/72-16.

HEY P. D. (RL) STIRLING G. C. (NBRU)

HFBR: proposed beam tube layout.  
HFBR/72-17.

DENT K. H. (UKAEA)

The proposed programme of Authority work during Phase 1. (draft only).  
HFBR/72-18.

DENT K. H. (UKAEA)

Total cost of Authority design and construction work (draft only).  
HFBR/72-19.

DENT K. H. (UKAEA)

HFBR provisional nomenclature  
HFBR/72-20

ROBERTS H. A. (UKAEA) COURSE A. (UKAEA)

Thermal performance of HFBR.  
HFBR/72-21.

CARTER P. (UKAEA)

Further calculations of cold source efficiency  
HFBR/72-22.

## Lectures

### RUTHERFORD LABORATORY LECTURES

A series of lectures in which eminent people are invited to the Laboratory to address the staff on subjects of general scientific importance.

MITCHELL J. (Social Sciences Research Council, 13 January): The Social Sciences – are they human?

FOWLER P. H. (University of Bristol, 9 March): Ultra-heavy elements in the cosmic rays.

COOMBS A. W. (Post Office Research Station, 25 May): The advent of the intelligent machine.

ISAACS M. D. J. (Home Counties Forensic Science Laboratory, 13 July): The work of the Home Counties Forensic Science Laboratory.

KORNBERG H. L. (University of Leicester, 5 October): The regulation of life processes.

FREEMAN C. (University of Sussex, 2 November): Technical progress and limits of growth.

HUNT R. W. G. (Kodak Ltd, 14 December): The strange journey from retina to brain.

### NIMROD LECTURES

A weekly series in which physicists active in high energy physics talk about their research programmes, or on topics related to particle physics.

RANFT G. (Leipzig, 10 January): Inclusive reactions.

KLEINKNECHT K. (CERN, 17 January): Lambda-proton total cross-sections.

BARSHAY S. (Copenhagen, 24 and 25 January): Do muons interact anomalously with hadrons? Longitudinal mass and proton-proton interactions at the ISR.

KLANNER R. (CERN, 31 January): Analysis of the  $3\pi$  system of the reaction  $\pi^- p \rightarrow 2\pi^- \pi^+ p$  at Serpukhov.

KITTEL W. (CERN, 7 February): How one can look at data without being led by a model.

BLOCK M (Northwestern University and CERN, 14 February): Coherent effects in deuterium collisions at high energy.

BARLOUTAUD R. (Saclay, 28 February): The experimental situation for the line reversed reactions.

PETERSON J. L. (CERN, 6 March): Meson-meson interactions.

DASS G. V. (DESY, 13 March): CP-, T- and CPT- invariances in neutral K-decay.

VELTMAN M. (Utrecht, 20 March): Recent developments in the theory of weak interactions.

SALVINI G. (Frascati, 27 March): The reactions  $e^+ + e^- \rightarrow$  hadrons, leptons. Recent results and future perspectives.

BARGER V. (Wisconsin, 17 April): Systematic features of particle exchange amplitudes.

TONER W. T. (RHEL, 24 April): Inelastic electron scattering.

PHILLIPS R. N. J., KANE G. L. (RHEL, 1 May): Various interpretations of elastic scattering including ISR data.

BLAND R. (Ecole Polytechnique, 8 May): Results from CERN hyperon beam.

JANE M., SHAH T. P., BROWN R. (RHEL, 15 May) Report on Philadelphia meeting on mesons and Washington APS meeting.

ROBERTS R. (RHEL, 22 May): Phenomenological model for meson-baryon scattering.

STEINBERGER J. (CERN, 2 June): Recent results in  $K^0$  decay.

HANSEN K. (Copenhagen, 5 June): Some features of inelastic pp collisions.

EBERHARD P. (CERN and Berkeley, 12 June): Search for magnetic monopoles.

BELLETTINI G. (CERN and Pisa, 19 June): Total proton-proton cross-sections at ISR energies.

TURLEY R. (Saclay, 26 June):  $K_{e4}$  decay.

PEREZ-MENDEZ V. (Berkeley, 6 July): Bio-medical application of Xenon-filled wire chambers.

OLIVE D. (CERN, 10 July): Dual resonance models.

KANE G. L. (RHEL, 14 July): How we should view diffractive scattering.

ZALEWISKI K. (Cracow, 17 July): Correlations in inclusive reactions.

BLANKENBECKER R. (SLAC, 14 August): Deep scattering.

FUBINI S. (MIT, 21 August): Recent progress in dual models.

MAOR U. (Tel Aviv, 30 August): Absorptive corrections to OPE amplitudes in inclusive reactions.

MURPHY P. (Manchester, 4 September): New results on inclusive reactions from the CERN Intersecting Storage Rings.

ROY D. P. (RHEL, 11 September): Finite mass sum rules and inclusive reactions.

MILLER R. J. (RHEL, 18 September): Two body final states from 14 GeV  $K^-p$ .

VENEZIANO G. (CERN, 25 September): A dual model of inclusive reactions.

CANESCHI L. (CERN, 9 October): Absorbed multiperipheralism.

RINGLAND G. A., MANNING G. (RHEL, 16 October): Report on Batavia conference.

LE BELLAC M. (Nice, 23 October): Inclusive spectra in single and double excitation models.

PIRILA P. (CERN, 25 October): Recent results on fragmentation models.

GABATHULER E. (DNPL, 30 October): Lepton physics at 300 GeV.

NEFKENS B. (UCLA, 6 November): Unexpected results in radiative pion scattering or 'Lower than Low'.

POUNDS K. (Leicester, 13 November): Recent developments in X-ray astronomy.

TONER, W. T. (RHEL, 20 November): Hadron production in deep inelastic scattering.

KIRZ J. (Stony Brook, 27 November): Small angle elastic scattering of high energy particles from nuclei.

JACOB M. (CERN, 4 December): Correlations in inclusive reactions.

MOORHOUSE G. (Glasgow, 11 December): Resonance couplings and the quark model.

KERNAN A. (CERN, 18 December): Recent results on  $\pi^+p \rightarrow \Delta^{++}\pi^0$ ,  $p\rho$  in the resonance region.

#### SEMINARS ON COMPUTING

GENERAL MEETING (14 January).

DOWN H. J. (ULCC, London, 28 January): Recent trends in computing at CERN.

KIRSTEIN P. T. (ICS, London, 11 February): Developments in Data Networks.

ROBINSON C. (Glasgow, 25 February): "POLLY"

GIRARD P. (10 March): An Introduction to HASP

HALLOWELL P. (24 March): Computer Control of the HPD Flying Spot Digitizer.

MAYBURY P. (7 April): The computing involved in a typical HEP experiment.

CHESHIRE I. M. (AERE, 21 April): Fleet Scheduling.

GENERAL MEETING (5 May).

HURST H. (16 June): The Operational Environment.

TROWBRIDGE C. W. (30 June): Interactive programming as an aid to magnet design.

STORMER A. (14 July): Compiler Design and Techniques.

GENERAL MEETING (20 October).

OSLAND C. D. (3 November): Other programming languages available at RHEL.

STEGGLE R. A. (IBM(UK), 17 November): The IBM Virtual Storage Operating System.

ROSNER R., MADEN D. and HUTTON J. (1 December): The work of the HEP Data Handling Group.

BARLOW J. and FRANEK B. (15 December): Some programs of the RHEL Film Analysis Group.

**PATENTS FILED DURING 1972**

Patent Application	Inventor	Invention
C7741	Adams T. C.	Running Puddle (Specialised Soldering Technique)
P25975	Lonsdale B. F.	Liquid Scintillation Light Source
P54479	Gallagher-Daggitt G. E.	Manufacture of Non-circular Stranded Cable by Velocity Transition
P54480	Gallagher-Daggitt G. E.	Manufacture of Non-circular Stranded Cable by Distortion using a Compacting Die.



Figure 108. Beam lines in the Experimental Halls during 1972 (13482).